

**INVESTIGATIONS IN LIGHT CONTROLLED REACTIVITY
USING DITHIENYLETHENES**

by

David Sud
B.Sc., McGill University, 2002

THESIS SUBMITTED IN PARTIAL FULFILLMENT OF
THE REQUIREMENTS FOR THE DEGREE OF

DOCTOR OF PHILOSOPHY

In the
Department of Chemistry

© David Sud 2008

SIMON FRASER UNIVERSITY

Spring 2008

All rights reserved. This work may not be
reproduced in whole or in part, by photocopy
or other means, without permission of the author.

APPROVAL

Name: David Sud
Degree: Doctor of Philosophy
Title of Thesis: Investigations in Light Controlled Reactivity Using Dithienylethenes

Examining Committee:

Chair Dr. David J. Vocadlo
Assistant Professor, Department of Chemistry

Dr. Neil R. Branda
Senior Supervisor
Professor, Department of Chemistry

Dr. Andrew J. Bennet
Supervisor
Professor, Department of Chemistry

Dr. Robert A. Britton
Supervisor
Assistant Professor, Department of Chemistry

Dr. Peter D. Wilson
Internal Examiner
Associate Professor, Department of Chemistry

Dr. Robert P. Lemieux
External Examiner
Professor, Department of Chemistry
Queen's University

Date Defended/Approved: March 14, 2008



SIMON FRASER UNIVERSITY
LIBRARY

Declaration of Partial Copyright Licence

The author, whose copyright is declared on the title page of this work, has granted to Simon Fraser University the right to lend this thesis, project or extended essay to users of the Simon Fraser University Library, and to make partial or single copies only for such users or in response to a request from the library of any other university, or other educational institution, on its own behalf or for one of its users.

The author has further granted permission to Simon Fraser University to keep or make a digital copy for use in its circulating collection (currently available to the public at the "Institutional Repository" link of the SFU Library website <www.lib.sfu.ca> at: <<http://ir.lib.sfu.ca/handle/1892/112>>) and, without changing the content, to translate the thesis/project or extended essays, if technically possible, to any medium or format for the purpose of preservation of the digital work.

The author has further agreed that permission for multiple copying of this work for scholarly purposes may be granted by either the author or the Dean of Graduate Studies.

It is understood that copying or publication of this work for financial gain shall not be allowed without the author's written permission.

Permission for public performance, or limited permission for private scholarly use, of any multimedia materials forming part of this work, may have been granted by the author. This information may be found on the separately catalogued multimedia material and in the signed Partial Copyright Licence.

While licensing SFU to permit the above uses, the author retains copyright in the thesis, project or extended essays, including the right to change the work for subsequent purposes, including editing and publishing the work in whole or in part, and licensing other parties, as the author may desire.

The original Partial Copyright Licence attesting to these terms, and signed by this author, may be found in the original bound copy of this work, retained in the Simon Fraser University Archive.

Simon Fraser University Library
Burnaby, BC, Canada

Abstract

Compounds that undergo reversible photochemical transformations have been investigated for use in optoelectronic technologies, molecular devices and to a lesser extent, in influencing chemical reactivity. Photoresponsive 1,2-dithienylethenes (DTEs) represent a significant improvement over azobenzenes, used in previous research, primarily because they undergo thermally irreversible photochemical ring-closing and ring-opening reactions. The light-induced isomerization between *ring-open* and *ring-closed* isomers results in steric, electronic and localized π -bond arrangement changes. This makes DTEs appealing in the design of systems controlling the chemical reactivity of photoresponsive catalysts and reagents. The research presented in this thesis demonstrates control of reactivity using the DTE architecture.

The initial approach of modulating reactivity used the flexible-to-rigid changes of the DTE backbone to control the stereochemical outcome of a catalytic reaction. The results showed that only the flexible *ring-open* form of a bis(oxazoline) DTE ligand, where the metal-binding groups could converge towards each other and chelate copper(I). With this binding geometry, the cyclopropanation reaction of styrene with ethyldiazoacetate afforded stereoselectivity in the product distribution. Irradiation with UV light generated the rigid *ring-closed* isomer, rendering it ineffective towards metal-chelation by forcing the metal-binding groups to diverge away from one another.

In a second study, a DTE bearing bis(phosphine) groups was prepared, representing a new class of photoresponsive ligands with steric and electronic differences between the two photogenerated isomers. It was also shown that DTE-metal complexes remained photochromic, albeit with decreased photoconversion. Results also indicated that the extended conjugation in the *ring-closed* isomer resulted in greater electron-withdrawing effects on the phosphine compared to the *ring-open* isomer.

In a third study, the localized π -bond rearrangement accompanying the ring-opening/ring-closing isomerization reactions of a DTE were used to activate/deactivate an enediyne towards Bergman cyclization. This was done by installing/removing a localized π -bond shared between an enediyne and the DTE backbone. Only the *ring-open* isomer contained the enediyne structure required to produce a diradical, which is responsible for the potent antitumor activity of enediyne derivatives. The *ring-open* isomer was created by irradiating the thermally stable *ring-closed* isomer with visible light, thus unmasking an enediyne, which could subsequently undergo a Bergman cyclization.

Keywords: photochromism, dithienylethene, modulation of reactivity, oxazoline, triarylphosphine, enediyne

Dedication

À mes parents, Irène Loiselle et Satish Sud.

Acknowledgements

I would first like to thank the members of my supervisory committee, Neil Branda, Jason Clyburne, Andrew Bennet and Robert Britton for supporting me all along my research program from the very beginning with helpful advice and guidance. In addition, I would like to extend my thanks to the faculty members who shared their laboratory equipment or chemicals, and for making the department a welcoming work environment.

There are also several technicians and specialists I would like to acknowledge including: M.K Yang for elemental analyses; Hongwen Chen for mass spectrometry; Andrew Lewis, Marcy Tracey and Collin Zhang for NMR services; and Robert McDonald from the University of Alberta, for X-Ray crystallography. Much of my characterization would not have been possible without the training they provided or their dedicated work.

I am also grateful to the members of the Branda group, past and present, for sharing their experience and knowledge. I would especially like to thank Brian Gorodetsky and Jeremy Finden for proofreading my thesis.

Finally, I would like to thank all my family and friends who have provided invaluable moral support and encouragement, with a very special mention for Maria I. Lavis who found pleasure in proofreading my thesis.

Table of Contents

Approval	ii
Abstract	iii
Dedication	v
Acknowledgements	vi
Table of Contents	vii
List of Equations	x
List of Figures	xii
List of Schemes	xvii
List of Tables	xviii
List of Abbreviations	xix
1 Introduction	1
1.1 Regulation of reactivity with light	1
1.2 Using photochromic molecules to modulate reactivity	2
1.3 The dithienylethenes	6
1.3.1 Synthetic reactions with DTEs	10
1.3.2 Steric changes for dithienylethenes	11
1.3.3 Electronic changes of the DTE	13
1.3.4 Localized π -bond rearrangements of DTE derivatives	16
1.4 Thesis preview	19
2 Photoswitching of Stereoselectivity in Catalysis Using a Copper Dithienylethene Complex	22
2.1 Using light to control catalysis	22
2.1.1 Flexibility change of DTE	23

2.1.2	Design for photocontrol of a DTE ligand	23
2.1.3	Catalytic reaction with bis(oxazoline) ligands	25
2.2	C5 bis(oxazoline) DTE 2.2o	27
2.2.1	Synthesis of the C5 bis(oxazoline) DTE	29
2.2.2	Photochromic behaviour of the C5 bis(oxazoline) DTE	30
2.2.3	Metal complexation of C5 bis(oxazoline) DTE with copper	33
2.2.4	Photocontrol of catalysis with C5 bis(oxazoline) DTE	35
2.3	C2 bis(oxazoline) DTE 2.3o	37
2.3.1	Synthesis of the C2 bis(oxazoline) DTE	38
2.3.2	Photochromic behaviour of the C2 bis(oxazoline) DTE	40
2.3.3	Metal complexation of C2 bis(oxazoline) DTE with copper	42
2.3.4	Photocontrol of catalysis with C2 bis(oxazoline) DTE	45
2.4	Conclusion	48
2.5	Future work	49
2.6	Experimental	51
2.6.1	General	51
2.6.2	Methods	51
2.6.3	Syntheses and experiments	53
3	Synthesis and Coordination Chemistry of a Photoswitchable Bis(phosphine) Ligand	63
3.1	Dithienylethene ligands	63
3.2	Triarylphosphine DTE derivative	64
3.3	Synthesis of DTE diphenylphosphine derivatives	65
3.3.1	Photochromism of bis(phosphine) DTE 3.1o	66
3.4	Bis(phosphine) DTE gold complex 3.2o	69
3.4.1	Crystal structure of complex 3.2o	69
3.4.2	Photochromism of bis(phosphine) DTE gold complex 3.2o	71
3.5	Bis(phosphine) DTE selenide 3.3o	73
3.5.1	Photochromism of bis(phosphine) selenide 3.3o	74
3.5.2	Electronic effects of the backbone conjugation differences	76
3.6	Conclusion	78
3.7	Future work	79
3.8	Experimental	84
3.8.1	General	84
3.8.2	Methods	84
3.8.3	Syntheses and experiments	86
4	Creating a Reactive Eneidyne by Using Visible Light: Photocontrol of the Bergman Cyclization	92

4.1	Generating more reactive structures with light	92
4.1.1	Previous systems used for controlling an enediyne with light	94
4.1.2	Design for the control of a Bergman cyclization with DTE	97
4.2	Phenyl-substituted enediyne DTE 4.3o	99
4.2.1	Synthesis of the phenyl-substituted enediyne DTE 4.3o	100
4.2.2	Photochromism of the phenyl-substituted enediyne DTE 4.3o	102
4.2.3	Thermal studies of the phenyl-substituted enediyne DTE 4.3o	104
4.3	10-membered ring enediyne DTE 4.4o	106
4.3.1	Synthesis of the 10-membered ring enediyne DTE 4.4o	107
4.3.2	Photochromism of the 10-membered ring enediyne DTE 4.4o	108
4.3.3	Thermal studies of the 10-membered ring enediyne DTE 4.4o	110
4.4	Conclusion	115
4.5	Future work	115
4.6	Experimental	119
4.6.1	General	119
4.6.2	Methods	120
4.7	Syntheses and experiments	121
5	Conclusions	134
6	Appendix	138
6.1	NMR Characterization of new compounds from Chapter 2	138
6.2	Synthesis and characterization of previously known compounds for Chapter 2	144
6.3	Characterization of new compounds from Chapter 3	149
6.3.1	Future work experiments from Chapter 3	158
6.4	NMR characterization of new compounds from Chapter 4	160
6.5	Synthesis and characterization of previously known compounds and unsuccessful reactions in Chapter 4	172
6.5.1	Future work experiments from Chapter 4	176
	Reference List	181

List of Equations

- Equation 1.2.1** The isomerization of azobenzene between *cis* and *trans* isomers exemplifies T-type photochromism where the isomerization induced by UV light can be reversed either with light (VIS) or heating (Δ). **3**
- Equation 1.2.2** Ester hydrolysis with β -cyclodextrin was modulated with light using azobenzene as the photoresponsive unit, where the azobenzene acted as a competitive inhibitor inside the β -cyclodextrin cavity. The *cis* isomer generated with UV light resulted in increased reaction catalysis. **3**
- Equation 1.2.3** Ester hydrolysis with an azobenzene functionalized β -cyclodextrin was modulated with light using azobenzene as the photoresponsive unit, where the the azobenzene influenced the β -cyclodextrin cavity depth. **4**
- Equation 1.2.4** Binding groups appended on azobenzenes that were remote in the *trans* isomer could be brought into proximity to each other in the *cis* isomer with UV-light irradiation, thus enhancing catalysis by templating an amide formation reaction. **5**
- Equation 1.2.5** Crown ethers binding barium appended on azobenzene that were remote in the *trans* isomer could be brought into proximity to each other in the *cis* isomer with UV-light irradiation, thus enhancing amide hydrolysis by providing a favourable geometry. **5**
- Equation 1.3.1** The photochromic dithienylethenes (DTEs) can be toggled between the thermally stable "colourless" *ring-open* isomer containing a 1,3,5-hexatriene (bold) and "coloured" *ring-closed* isomer containing a cyclohexadiene (bold) using UV light for the ring-closing reaction and visible wavelengths of light for the ring-opening reaction. **6**
- Equation 1.3.2** Each DTE isomer has a distinct set of ^1H NMR resonance signals. The thiophene proton and the methyl in the C2 position of the thiophene are attached to an aromatic thiophene in the *ring-open* isomer and to an alkene or no longer to a thiophene, for the proton and methyl groups, respectively in the *ring-closed* isomer. **9**
- Equation 1.3.3** The photostationary state calculated from ^1H NMR peak integrations. **10**
- Equation 1.3.4** The isomerization of the DTE is accompanied by a change in the conjugation along the backbone. In the *ring-open* isomer, functional groups on separate thiophene rings are independent electronically from each other, whereas in the *ring-closed* isomer these same functional groups are conjugated to each other along the backbone **14**
- Equation 1.3.5** The $\text{p}K_{\text{a}}$ of phenol appended on DTE derivatives can be modulated with light. The differences between the *ring-open* and *ring-closed* isomers provide conjugation (bold) between remote groups on separate thiophene rings. **14**
- Equation 1.3.6** The $\text{p}K_{\text{a}}$ of phenol appended on DTE derivatives can be modulated with light. The differences between the *ring-open* and *ring-closed* isomers provide conjugation (bold) between remote groups on the same thiophene ring, in the *ring-open* isomer or separate thiophene rings, in the *ring-closed* isomer. **15**
- Equation 1.3.7** DTE could be used to modulate the Lewis basicity and nucleophilicity of a pyridine. The lone pair on the pyridine in the *ring-open* isomer **1.1o** was more reactive than that in the *ring-closed* isomer **1.1c** because the pyridine in the latter was electronically conjugated to an electron-withdrawing pyridinium group through the backbone. **16**

- Equation 1.3.8** The ring-closing isomerization of DTEs using UV light is accompanied by the “removal” of the localized π -bond (shaded area) from the *ring-open* isomer, where the *ring-closed* isomer does not have a localized π -bond in the central position (circled area). The localized π -bond can be “created” from the *ring-closed* isomer using visible wavelengths of light, regenerating the *ring-open* isomer. **17**
- Equation 1.3.9** The Diels-Alder adduct, only present in the *ring-open* isomer **1.2o** with a localized π -bond (shaded area) generated with visible light, could “release” a dienophile **1.4** by the *retro* Diels-Alder equilibrium. The same dienophile was “locked” within the *ring-closed* isomer **1.2c** due to the absence (circled area) of a localized π -bond. **18**
- Equation 2.1.1** Enantiomeric excess. **27**
- Equation 2.1.2** Diastereomeric excess. **27**
- Equation 3.2.1** A triaryl phosphine DTE derivative **3.1o** can be isomerized with UV light into its corresponding *ring-closed* isomer **3.1c**. The *ring-open* isomer **3.1o** can be regenerated with visible wavelengths of light. **64**
- Equation 3.4.1** Diphenylphosphine gold chloride DTE **3.2o** can be converted into the *ring-closed* isomer **3.2c** using UV light. Irradiation of the *ring-closed* isomer **3.2c** with visible wavelengths of light regenerates the *ring-open* isomer **3.2o**. **69**
- Equation 3.5.1** Diphenylphosphine selenide DTE **3.3o** is converted to the *ring-closed* isomer **3.3c** with UV light. Visible wavelengths of light regenerate the *ring-open* isomer **3.3o**. **74**
- Equation 3.7.1** Electronic communication between a diphenyl phosphine and an electron-donating group (EDG) or electron-withdrawing group (EWG) can be turned “on” using UV light or “off” using light of visible wavelengths. The conjugation is highlighted in both structures in bold. **80**
- Equation 3.7.2** The reactivity-gated photochromism is based on the Diels-Alder reaction of a non-photochromic diene precursor with a dienophile “analyte” creating a colourless DTE containing a 1,3,5-hexatriene (bold), and thus generating a photochromic Diels-Alder adduct. UV light is then used to generate the coloured isomer, indicating that the analyte was detected. **81**
- Equation 4.2.1** Phenyl-substituted enediyne DTE derivative **4.3o** can isomerize with UV light into its corresponding *ring-closed* isomer **4.3c**. The *ring-open* isomer **4.3o** can be regenerated with visible wavelengths of light. **100**
- Equation 4.3.1** First-order rate equation. **113**
- Equation 4.3.2** Normalized rate equation. **113**
- Equation 4.3.3** Apparent rate of product formation. **113**

List of Figures

- Figure 1.3.1** Illustrative example of the UV-VIS absorption profile of a dithienylethene derivative. The dithienylethene molecules are typically converted from a colourless isomer (solid line) using UV light into a coloured isomer, which has an absorption band in the visible range (broken line). The colourless isomer can be regenerated by irradiating the coloured isomer with light of visible wavelengths (VIS). **8**
- Figure 1.3.2** Functional groups can be attached at the C5 “external” and/or the C2 “internal” positions on the thiophene rings. **10**
- Figure 1.3.3** The *ring-open* one exists as two conformers in solution, the antiparallel one, with C₂ symmetry, and the parallel with a mirror plane. The ring-closing reaction can only occur from the antiparallel conformation. Isomerization of DTE is accompanied with a flexibility change in the backbone where the *ring-closed* isomer is rigid due to restricted free rotation in the tricyclic system compared to the relatively free rotation (curled arrows) about the σ-bonds in the *ring-open* isomer. **11**
- Figure 1.3.4** A DTE switch with metal-binding groups can be toggled between the flexible *ring-open* isomer, which can possibly chelate a metal, and the rigid *ring-closed* isomer, where the binding groups are held apart at a distance preventing chelation. **13**
- Figure 1.4.1** Two different bis(oxazoline) DTE derivatives prepared to illustrate how the differences in flexibility between the *ring-open* and *ring-closed* isomers could be applied to control the binding geometry in a metal complex. **19**
- Figure 1.4.2** A bis(phosphine) DTE used in demonstrating how the changes in electronic communication between the *ring-open* and the *ring-closed* isomers could affect the reactivity of the phosphine. **20**
- Figure 1.4.3** Eneidyne DTE derivatives where only the *ring-open* isomers contain an enediyne moiety illustrate how reactions requiring a precise arrangement of π-bonds, such as the Bergman cyclization, could be regulated with light. **21**
- Figure 2.1.1** Two bis(oxazoline) DTEs prepared and studied. **24**
- Figure 2.2.1** Different metal-binding possibilities for C5 bis(oxazoline) DTE **2.2o** and **2.2c**. Arrows on **2.2o** represent the possibility for free rotation, unlike the rigid compound **2.2c**. Molecular model representations, generated using Spartan™ '02 for Macintosh, highlight geometrical arrangements for metal-binding pockets or lack thereof. **28**
- Figure 2.2.2** The UV-VIS absorption spectra of a 1.6×10^{-5} M solution of compound **2.2o** in CH₂Cl₂ upon irradiation with 313-nm light. (a) Total irradiation periods are 0, 10, 20, 30 and 40 sec. (b) Modulated absorbance at 251 nm (○) and 581 nm (■) during alternate irradiations with 313-nm light for 40 sec, then > 434 nm for 40 sec. **31**
- Figure 2.2.3** Selected region in the ¹H NMR spectrum obtained after irradiation of a CD₂Cl₂ solution of **2.2o** (2.3×10^{-3} M) with 313-nm light, highlighting the thiophene proton singlet used in determining the extent of photoconversion. **32**
- Figure 2.2.4** ¹H NMR study of the complex formation of a CDCl₃ solution of compound **2.2o** (1.3×10^{-2} M) with increasing equivalents of Cu(CH₃CN)₄PF₆ monitoring the oxazolinyl protons. **33**

- Figure 2.2.5** The two possible diastereoisomeric products **2.2c** of the ring-closing reaction. (a) geometry of the diastereoisomers, highlighting the C2 methyl producing distinct signals for the two diastereoisomers and (b) the ^1H NMR signals of the C2 methyl protons generated with 313-nm light in the absence of copper(I). **35**
- Figure 2.3.1** Different conformational possibilities for C2 bis(oxazoline) DTE **2.3o** and **2.3c**. The perfluorinated portion of the cyclopentene ring is hidden in **2.3c** for clarity. Molecular model representations, generated using SpartanTM '02 for Macintosh, highlight the geometrical arrangements for the metal-binding possibilities. **37**
- Figure 2.3.2** Changes in the UV-VIS absorption spectra of solutions of **2.3o** in CH_2Cl_2 upon irradiation with 313-nm light. (a) Total irradiation periods are 0, 1, 2, 5, 10, 20, 30 and 60 sec for a 9.9×10^{-6} M solution. (b) Modulated absorbance at 258 nm (●) and 505 nm (■) during alternate irradiation with 313-nm light for 30 sec, and > 434-nm light for 30 sec for a 1.7×10^{-5} M solution. **40**
- Figure 2.3.3** Selected region in the ^1H NMR spectrum obtained after irradiation of a CD_2Cl_2 solution of **2.3o** (3.1×10^{-3} M) with 313-nm light, highlighting the thiophene-C5 methyl singlet used in determining the extent of photoconversion. The perfluorinated portion of the cyclopentene ring is hidden from **2.3c** for clarity. **42**
- Figure 2.3.4** ^1H NMR study of the complex formation of **2.3o** (1.4×10^{-2} M) with increasing equivalents of $\text{Cu}(\text{CH}_3\text{CN})_4\text{PF}_6$ in CDCl_3 . A new distinct set of peaks appears as soon as the copper salt is added. **43**
- Figure 2.3.5** The two possible diastereoisomeric products **2.3c** of the ring-closing reaction, where the thiophene proton producing distinct signals for the two diastereoisomers is highlighted. (a) geometry of the diastereoisomers and (b) the ^1H NMR signal of the thienyl proton generated with 313-nm light in the absence of copper. **44**
- Figure 2.5.1** Different metal-binding possibilities for the proposed DTE **2.12o** and **2.12c**. The perfluorinated portion of the cyclopentene ring is hidden from **2.12c** for clarity. Molecular model representations, generated using SpartanTM '02 for Macintosh, highlight the geometrical arrangements for the metal-binding geometries. **50**
- Figure 3.3.1** Changes in the UV-VIS absorption spectra of a 9.9×10^{-6} M solution of bis(diphenylphosphine) **3.1o** in CH_3CN upon irradiation with 313-nm light. (a) Total irradiation periods are 0, 5, 10, 30, 45, 60, 75 and 90 sec. (b) Modulated absorbance at 253 nm (●) and 570 nm (■) during alternate irradiation of with 313-nm light for 90 sec, then > 434 nm for 120 sec. **67**
- Figure 3.3.2** Selected region in the ^1H NMR spectrum obtained after irradiation of a CD_2Cl_2 solution of **3.1o** (4.4×10^{-3} M) with 313-nm light, highlighting the thiophene-C2 methyl singlet used in determining the extent of photoconversion. **68**
- Figure 3.4.1** Molecular structure of complex **3.2o**. Ellipsoids are shown at the 20% probability level. The hydrogen atoms were omitted for clarity. **70**
- Figure 3.4.2** Changes in the UV-VIS absorption spectra of a 9.6×10^{-6} M solution of bis(diphenylphosphine) gold chloride **3.2o** in CH_3CN upon irradiation with 313-nm light. (a) Total irradiation periods are 0, 5, 10, 30, and 60 sec. (b) Modulated absorbance at 246 nm (●) and 565 nm (■) during alternate irradiation with 313-nm light for 20 sec, then > 434 nm for 30 sec. **72**
- Figure 3.4.3** Selected region in the ^1H NMR spectrum obtained after irradiation of a CD_2Cl_2 solution of **3.2o** (2.1×10^{-3} M) with 313-nm light, highlighting the thiophene-C2 methyl singlet used in determining the extent of photoconversion. **73**

- Figure 3.5.1** Changes in the UV-VIS absorption spectra of a 5.4×10^{-6} M solution of bis(diphenylphosphine) selenide **3.3o** in CH_3CN upon irradiation with 313-nm light. (a) Total irradiation periods are 0, 10, 20, 30, 40, 50 and 60 sec. (b) Modulated absorbance at 245 nm (○) and 574 nm (■) during alternate irradiation of with 313-nm light for 60 sec, then > 434 nm for 60 sec. **75**
- Figure 3.5.2** Selected region in the ^1H NMR spectrum obtained after irradiation of a CDCl_3 solution of compound **3.3o** (2.2×10^{-3} M) with 313-nm light, highlighting the thiophene-C2 methyl singlet used in determining the extent of photoconversion. **76**
- Figure 3.5.3** ^{31}P NMR of a photostationary state CDCl_3 solution of compounds **3.3o** and **3.3c** generated using 313-nm light where the coupling constants are indicated below the corresponding resonance signal peak. The central peak is a coincidental overlap of the splitting of both peaks. **77**
- Figure 4.1.1** Natural products containing enediyne moieties. **93**
- Figure 4.1.2** Examples of enediynes and their respective cyclization temperatures. **94**
- Figure 4.1.3** Literature examples where light induces a change in the ring strain of an enediyne macrocycle. **95**
- Figure 4.1.4** Literature examples that generate the enediyne substructure from a thermally stable precursor. **96**
- Figure 4.1.5** DTE enediyne derivatives, prepared and analyzed. **99**
- Figure 4.2.1** Changes in the UV-VIS absorption spectra of a 2.65×10^{-5} M solution of enediyne **4.3o** in C_6H_6 upon irradiation with 365-nm light. (a) Total irradiation periods are 0, 10, 20, 30, 40, 50, 60, 70, 80 and 90 sec. (b) Modulated absorbance at 369 nm (○), 393 nm (◆) and 575 nm (■) during alternate irradiation of with 365-nm light for 90 sec, then > 490 nm for 90 sec. **103**
- Figure 4.2.2** Selected region in the ^1H NMR spectrum obtained after irradiation of a C_6D_6 solution of compound **4.3o** (3.8×10^{-3} M) with 313-nm light, highlighting the thiophene-C5 methyl singlet used in determining the extent of photoconversion. **104**
- Figure 4.2.3** DSC thermograph with a heating rate of $10^\circ\text{C}/\text{min}$ for *ring-open* isomer **4.3o** (broken line) and *ring-closed* isomer **4.3c** (bold line) phenyl-substituted enediyne **105**
- Figure 4.3.1** Changes in the UV-VIS absorption spectra of a 8.22×10^{-5} M solution of enediyne **4.4o** in C_6H_6 upon irradiation with 365-nm light. (a) Total irradiation periods are for 10 sec intervals until 120 sec is reached. (b) Modulated absorbance at 301 nm (○), 373 nm (◆) and 550 nm (■) during alternate irradiation of with 365-nm light for 120 sec, then > 490 nm for 90 sec. **109**
- Figure 4.3.2** Selected region in the ^1H NMR spectrum obtained after irradiation of a C_6D_6 solution of compound **4.4o** (2.1×10^{-2} M) with 313-nm light, highlighting the thiophene proton singlet used in determining the extent of photoconversion. **110**
- Figure 4.3.3** Selected ^1H NMR signals in C_6D_6 for *p*-nitroanisole, 1,4-cyclohexadiene, *ring-open* isomer **4.4o**, *ring-closed* isomer **4.4c** and cyclized product **4.10** as monitored for the thermal reaction progress. **111**
- Figure 4.3.4** Concentration of the *ring-open* isomer **4.4o** (○) and the cyclized product **4.10** (◆) obtained by integration, normalized against the internal standard in thermal study in C_6D_6 . Initial concentrations were of 4.2×10^{-3} M for **4.4o**, of 1.9×10^{-3} M for *p*-nitroanisole and of 2.8×10^{-1} M for 1,4-cyclohexadiene. **112**
- Figure 4.3.5** Changes in concentration of *ring-open* isomer **4.4o** (○) (4.2×10^{-3} M), *ring-closed* isomer **4.4c** (■) (2.4×10^{-3} M) and cyclized product **4.10** (◆). **114**

Figure 4.5.1 Possible modification sites on an enediyne DTE derivative for DNA targeting and biologically soluble groups.	119
Figure 6.1.1 ¹ H NMR (500 MHz) spectrum of compound 2.7 in CDCl ₃ .	138
Figure 6.1.2 ¹³ C NMR (125 MHz) spectrum of compound 2.7 in CDCl ₃ .	139
Figure 6.1.3 ¹ H NMR (400 MHz) spectrum of compound 2.2o in CD ₂ Cl ₂ .	139
Figure 6.1.4 ¹³ C NMR (100 MHz) spectrum of compound 2.2o in CD ₂ Cl ₂ .	140
Figure 6.1.5 ¹ H NMR (500 MHz) spectrum in CD ₂ Cl ₂ of compound 2.2c after 5 min irradiation with 313-nm light containing 87% compound 2.2c and 13% compound 2.2o , highlighted (*) by the C2 methyl and thienyl peaks.	140
Figure 6.1.6 ¹ H NMR (500 MHz) spectrum of compound 2.10 in CDCl ₃ .	141
Figure 6.1.7 ¹³ C NMR (125 MHz) spectrum of compound 2.10 in CDCl ₃ .	141
Figure 6.1.8 ¹ H NMR (500 MHz) spectrum of compound 2.11 in CDCl ₃ .	142
Figure 6.1.9 ¹³ C NMR (125 MHz) spectrum of compound 2.11 in CDCl ₃ .	142
Figure 6.1.10 ¹ H NMR (500 MHz) spectrum of compound 2.3o in CD ₂ Cl ₂ .	143
Figure 6.1.11 ¹³ C NMR (125 MHz) spectrum of compound 2.3o in CD ₂ Cl ₂ .	143
Figure 6.1.12 ¹ H NMR (500 MHz) spectrum in CD ₂ Cl ₂ of compound 2.3c after 5 min irradiation with 313-nm light containing 59% compound 2.3c and 41% compound 2.3o , highlighted (*) by the C5 methyl and thienyl peaks.	144
Figure 6.2.1 ¹ H NMR (500 MHz) spectrum of compound 2.5 in CDCl ₃ .	146
Figure 6.2.2 ¹ H NMR (400 MHz) spectrum of compound 2.6 in CD ₃ OD.	147
Figure 6.2.3 ¹ H NMR (500 MHz) spectrum of compound 2.9 in CDCl ₃ .	149
Figure 6.3.1 ¹ H NMR (500 MHz) spectrum of compound 3.1o in CD ₂ Cl ₂ .	149
Figure 6.3.2 ¹³ C NMR (100 MHz) spectrum of compound 3.1o in CD ₂ Cl ₂ .	150
Figure 6.3.3 ¹ H NMR (500 MHz) spectrum in CD ₂ Cl ₂ of compound 3.1c after 10 min irradiation with 313-nm light containing 80% compound 3.1c and 20% compound 3.1o , highlighted (*) by the C2 methyl and thienyl peaks.	150
Figure 6.3.4 ³¹ P NMR (162 MHz) spectrum in CD ₂ Cl ₂ of a mixture of compound 3.1o and compound 3.1c generated with 313-nm light.	151
Figure 6.3.5 ¹ H NMR (500 MHz) spectrum of compound 3.2o in CD ₂ Cl ₂ .	151
Figure 6.3.6 ¹³ C NMR (150 MHz) spectrum of compound 3.2o in CDCl ₃ .	152
Figure 6.3.7 ³¹ P NMR (162 MHz) spectrum of compound 3.2o in CDCl ₃ .	152
Figure 6.3.8 ¹ H NMR (400 MHz) spectrum in CD ₂ Cl ₂ of compound 3.2c after 10 min irradiation with 313-nm light containing 60% compound 3.2c and 40% compound 3.2o , highlighted (*) by the C2 methyl and thienyl peaks.	153
Figure 6.3.9. Molecular structure of complex 3.2o . Thermal ellipsoids are shown at 20% probability. The hydrogen atoms are omitted for clarity.	153
Figure 6.3.10 ¹ H NMR spectrum (500 MHz) of compound 3.3o in CDCl ₃ .	155
Figure 6.3.11 ¹³ C NMR (100 MHz) spectrum of compound 3.3o in CDCl ₃ .	155
Figure 6.3.12 ¹ H NMR (500 MHz) spectrum in CDCl ₃ of compound 3.3c after 3 min irradiation with 313-nm light containing 55% compound 3.3c and 45% compound 3.3o , highlighted (*) by the C2 methyl and thienyl peaks.	156

Figure 6.3.13 ^1H NMR (500 MHz) spectrum of compound 3.4o in CD_2Cl_2 .	156
Figure 6.3.14 ^{13}C NMR (150 MHz) spectrum of compound 3.4o in CDCl_3 .	157
Figure 6.3.15 ^{31}P NMR (243 MHz) spectrum of compound 3.4o in CDCl_3 .	157
Figure 6.3.16 ^1H NMR (500 MHz) spectrum in CD_2Cl_2 of compound 3.4c after 3 min irradiation with 313-nm light containing 59% compound 3.4c and 41% compound 3.4o , highlighted (*) by the C2 methyl and thienyl peaks.	158
Figure 6.4.1 ^1H NMR (500 MHz) spectrum of compound 4.6 in CDCl_3 .	160
Figure 6.4.2 ^{13}C NMR (100 MHz) spectrum of compound 4.6 in CDCl_3 .	160
Figure 6.4.3 ^1H NMR (500 MHz) spectrum of compound 4.7 in CDCl_3 .	161
Figure 6.4.4 ^1H NMR (100 MHz) spectrum of compound 4.7 in CDCl_3 .	161
Figure 6.4.5 ^1H NMR (400 MHz) spectrum of compound 4.8 in CDCl_3 .	162
Figure 6.4.6 ^1H NMR (500 MHz) spectrum of compound 4.9 in CDCl_3 .	162
Figure 6.4.7 ^{13}C NMR (100 MHz) spectrum of compound 4.9 in CDCl_3 .	163
Figure 6.4.8 ^1H NMR (500 MHz) spectrum of compound 4.3o in CD_2Cl_2 .	163
Figure 6.4.9 ^{13}C NMR (100 MHz) spectrum of compound 4.3o in CDCl_3 .	164
Figure 6.4.10 ^1H NMR (500 MHz) spectrum in C_6D_6 of compound 4.3o after 4 min irradiation with 313-nm light containing 92% compound 4.3c and 8% compound 4.3o , highlighted (*) by the C2 methyl peak.	164
Figure 6.4.11 ^1H NMR (500 MHz) spectrum of compound 4.11 in CDCl_3 .	165
Figure 6.4.12 ^{13}C NMR (100 MHz) spectrum of compound 4.11 in CDCl_3 .	165
Figure 6.4.13 ^1H NMR (400 MHz) spectrum of compound 4.12 in CDCl_3 .	166
Figure 6.4.14 ^{13}C NMR (100 MHz) spectrum of compound 4.12 in CDCl_3 .	166
Figure 6.4.15 ^1H NMR (500 MHz) spectrum of compound 4.4o in CDCl_3 .	167
Figure 6.4.16 ^{13}C NMR (150 MHz) spectrum of compound 4.4o in CDCl_3 .	167
Figure 6.4.17 ^1H NMR (500 MHz) spectrum of compound 4.4c in C_6D_6 .	168
Figure 6.4.18 ^{13}C NMR (150 MHz) spectrum of compound 4.4c in C_6D_6 .	168
Figure 6.4.19 ^1H NMR (500 MHz) spectrum of compound 4.10 in C_6D_6 .	169
Figure 6.4.20 ^{13}C NMR (150 MHz) spectrum of compound 4.10 in C_6D_6 .	169
Figure 6.4.21 ^1H NMR (500 MHz) spectrum of compound 4.13 in CDCl_3 .	170
Figure 6.4.22 ^{13}C NMR (100 MHz) spectrum of compound 4.13 in CDCl_3 .	170
Figure 6.4.23 ^1H NMR (500 MHz) spectrum of compound 4.15 in CDCl_3 .	171
Figure 6.4.24 ^{13}C NMR (150 MHz) spectrum of compound 4.15 in CDCl_3 .	171
Figure 6.5.1 ^1H NMR (400 MHz) spectrum of compound 4.5 in CDCl_3 .	173
Figure 6.5.2 ^1H NMR (400 MHz) spectrum of 1-(2-chloroethyl)benzene in CDCl_3 .	174
Figure 6.5.3 ^1H NMR (400 MHz) spectrum of 1-(2-bromoethyl)benzene in CDCl_3 .	175
Figure 6.5.4 ^1H NMR (400 MHz) spectrum of 1-(2-bromoethyl)trimethylsilane in CDCl_3 .	176
Figure 6.5.5 ^1H NMR (500 MHz) spectrum of compound 4.16 in CDCl_3 .	179

List of Schemes

- Scheme 2.1.1** Two non-fluorinated bis(oxazoline) DTEs in **2.1** assembled into a copper double helicate. **23**
- Scheme 2.1.2** Cyclopropanation of styrene with ethyldiazoacetate using a bidentate bis(oxazoline) ligand with Cu(I)OTf affords four stereoisomeric products. **26**
- Scheme 2.2.1** Synthesis of C5 bis(oxazoline) DTE **2.2o**. **29**
- Scheme 2.3.1** Synthesis of C2 bis(oxazoline) DTE **2.3o**. **39**
- Scheme 2.3.2** *In situ* photocontrol of the ligands **2.3o** and **2.3c** used in the catalytic cyclopropanation of styrene with ethyldiazoacetate. The perfluorinated portion of the cyclopentene ring is hidden in **2.3c** for clarity. The *ring-closed* isomer **2.3c** was converted into the *ring-open* isomer **2.3o** *in situ* using light of wavelengths greater than 434 nm. **48**
- Scheme 3.3.1** Synthesis of bis(diphenylphosphine) **3.1o**, gold chloride complex **3.2o** and selenide **3.3o** derivatives. **65**
- Scheme 3.7.1** Two different synthetic routes for the phosphine derivatives starting either from a preassembled DTE or from derivatized thiophene groups. **80**
- Scheme 3.7.2** The POP reagent, prepared in two steps from compound **3.1o**, should be locked in a non-photochromic parallel conformation. The reaction with a primary alcohol is the slow step, which “unlocks” the photochromism followed by the esterification, which is the fast step. The reactivity gated photochromism of a DTE could be used to monitor the progress of the esterification reaction. **83**
- Scheme 4.1.1** The Bergman cyclization of an enediyne **4.1e** is a thermal process that produces a benzenoid diradical **4.1r**, which can be trapped with a radical hydrogen source to afford the cyclized product **4.1p**. **93**
- Scheme 4.1.2** An enediyne **4.2o** is generated using visible light from compound **4.2c** by taking advantage of the photoisomerization of a DTE. The enediyne could then undergo a Bergman cyclization to yield the benzenoid diradical **4.2r**. **98**
- Scheme 4.2.1** Synthesis of the phenyl-substituted enediyne DTE **4.3o**. **101**
- Scheme 4.3.1** Visible light isomerizes the *ring-closed* **4.4c** into the *ring-open* isomer **4.4o**, which thermally forms the benzenoid diradical that can be trapped, using a radical quencher, as the cyclized product **4.10**. **106**
- Scheme 4.3.2** Synthesis of the 10-membered ring enediyne DTE **4.4o** and its corresponding *ring-closed* isomer **4.4c**. **107**
- Scheme 4.3.3** Unsuccessful synthetic route to make the compound **4.4o** in one pot from compound **4.9** using bis(alkyne) **4.13**. **108**
- Scheme 4.5.1** Unsuccessful synthetic route to make the *ring-closed* isomer of a 9-membered ring enediyne DTE **4.14c** by quenching the lithiated product of **4.12** with diiodopropane. **116**
- Scheme 4.5.2** Alkyne metathesis route starting with methyl-terminated enediyne DTE **4.15**. **117**

List of Tables

Table 2.3.1 Cyclopropanation product distribution.	46
Table 3.5.1 ^{31}P NMR characterizations for a series of phosphine selenide derivatives.	78
Table 6.3.1 Crystallographic data for complex 3.2o .	154
Table 6.3.2 Selected bond lengths and angles for complex 3.2o .	154

List of Abbreviations

P_{∞}	product concentration at reaction completion
$[\alpha]_D^{20}$	specific optical rotation at 20 °C with irradiation at the sodium- <i>D</i> line (589 nm)
Δ	heating
δ	chemical shift
λ	wavelength
μL	microlitre
λ_{max}	wavelength at the absorption maximum in a given region
$^1J(^{77}\text{Se}-^{31}\text{P})$	Selenium-77 to Phosphine-31 spin-spin coupling constant
Å	Ångstrom
AcOH	acetic acid
Anal. Calcd.	analytically calculated
Au(tht)	gold tetrahydrothiophene
Bn	benzyl
br	broad
C	concentration at time <i>t</i>
C_0	initial concentration
CI	chemical ionization
cm	centimetre
cm^{-1}	wavenumber
Cp	cyclopentadienyl
CuOTf	coppertrifluoromethylsulfonate
d	doublet
d.e.	diastereomeric excess
d.r.	diastereomeric ratio
dd	doublet of doublets
dec.	decomposed
DMF	dimethylformamide
DNA	deoxyribonucleic acid
DSC	differential scanning calorimetry
dt	doublet of triplets
DTE	1,2-dithienylethene
e.e.	enantiomeric excess
EDG	electron-donating group
EI	electron impact
equiv	equivalents
Et_2O	diethyl ether

NEt ₃	triethylamine
EtMgCl	ethyl magnesium chloride
EtOAc	ethyl acetate
EWG	electron-withdrawing group
FT-IR	Fourrier transform infrared
g	gram
H	proton
h	hours
hν	irradiation with light
HMPA	hexamethylphosphoramide
HPLC	high performance liquid chromatography
Hz	Hertz
<i>in situ</i>	in the reaction mixture
<i>in vacuo</i>	under vacuum
<i>i</i> Pr	<i>iso</i> -propyl
<i>J</i>	coupling constant
<i>k_{eff}</i>	apparent reaction rate, or effective reaction rate
LRMS	low-resolution mass spectrometry
m	multiplet
M	mole/litre
m.p.	melting point
<i>m/z</i>	mass-to-charge ratio
MALDI	matrix-assisted laser desorption ionization
Me	methyl
MsCl	methanesulfonyl chloride
mg	milligram
MHz	megahertz
min	minutes
mL	millilitre
mm Hg	millimetres of mercury
mmol	millimole
mol	mole
mol%	mole percent
mW	milliwatts
NBS	<i>N</i> -bromosuccinimide
NCS	<i>N</i> -chlorosuccinimide
<i>n</i> -BuLi	<i>n</i> -butyllithium
nm	nanometer
NMR	nuclear magnetic resonance
°	degree
°C	degree Celcius
<i>p</i>	para
Ph	phenyl
PhCl	chlorobenzene

pK_a	acid dissociation constant
POP	phosphine-oxygen-phosphine
ppm	parts per million
PSS	photostationary state
s	singlet
sec	second
<i>t</i>	time
t	triplet
<i>t</i> -BuLi	<i>tert</i> -butyllithium
<i>t</i> BuO	<i>tert</i> -butoxy
TFAA	trifluoromethanesulfonic anhydride
THF	tetrahydrofuran
tht	tetrahydrothiophene
TLC	thin layer chromatography
TMS	trimethylsilyl
UV-VIS	ultraviolet-visible
<i>via</i>	by way of
vol%	volume percentage
W	Watt

1 Introduction

1.1 Regulation of reactivity with light

Chemical processes can be optimized through improving methods to activate and terminate reactions. Within industrial settings, enhanced reaction regulation provides not only safety, but also increases reaction efficiency while decreasing the amount of unwanted side-reactions. In the medical field, the ability to control drug releasing and triggering would decrease the amount of drug required for treatment as well as lowering patient-associated side effects. However, in order to completely regulate a chemical reaction, it is necessary to be able to both switch a reaction “on” and “off” reversibly. In synthetic organic chemistry, chemical reactions are typically initiated by applying thermal energy to the reagents in order to overcome an energy barrier for the formation of products. While heat provides a simple initiation method, there are several instances in which heating a reaction is either not possible, in the case of biological applications *in vivo*, or not economically efficient, in the case of industrial synthesis.

The first law of photochemistry states that light must be absorbed by a molecule for a photochemical reaction to take place¹ and offers an alternative to temperature-controlled reactions. Light provides not only the necessary energy to overcome the energy barrier, but also the possibility of controlling the nature and amount of photochemical reaction products to a considerable degree by fine-

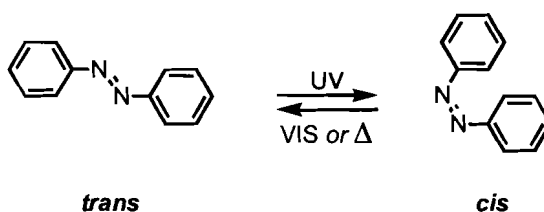
tuning the wavelength and intensity of irradiation. By supplying the activation energy only to compounds that absorb the light, photochemistry can give greater reaction specificity in a complex medium. Light can also be used to spatially and temporally regulate reactions due to the fast response of reagents to light excitation. Simply switching off the light results in the immediate removal of the energy source, instantaneously halting the reaction, whereas a thermal reaction can only be heated or cooled in bulk. Hence, the application of light can provide an efficient mechanism of “on” and “off” control over reactions.

Photochromism is the light-induced reversible transformation of a chemical species between two forms that have different absorption spectra.² There are two main categories of photochromic compounds:² 1) T-type molecules, which can either photochemically or thermally revert back to their original form; and 2) P-type molecules, which have increased thermal stability and require light to interconvert between isomeric forms, hence giving full “photocontrol” over the isomerism of the molecule. Photochromic compounds are also referred to as “switches” since they can be toggled between two isomers using light.

1.2 Using photochromic molecules to modulate reactivity

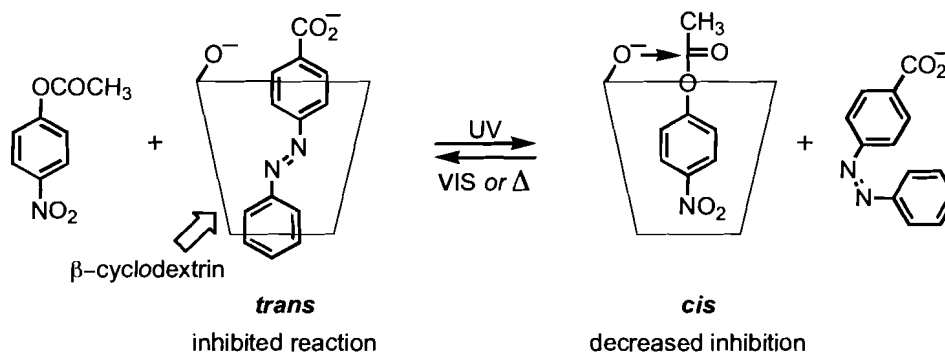
Properties such as colour, fluorescence, optical rotation, oxidation/reduction potentials and conformational flexibility may vary between two isomers of a given photochromic molecule.^{3,4} Changes in these properties accompanying the reversible isomerization could be applied to modulating chemical reactivity. The concept of taking advantage of the geometric changes

that accompany a photoreaction to regulate chemical reactivity was introduced over 20 years ago; however, there exist only four examples⁵⁻⁹ in the literature, all of which rely on an azobenzene as the photoresponsive structure shown in Equation 1.2.1.



Equation 1.2.1 The isomerization of azobenzene between *cis* and *trans* isomers exemplifies T-type photochromism where the isomerization induced by UV light can be reversed either with light (VIS) or heating (Δ).

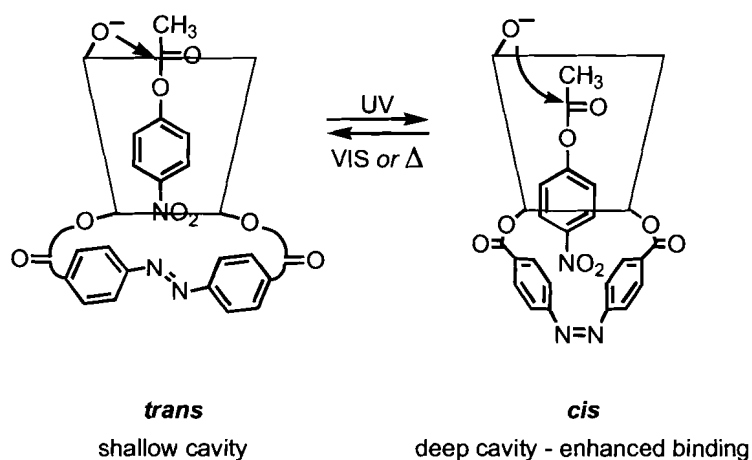
Differences in catalytic reactivity could arise from the shape change resulting from the *trans*→*cis* isomerization of the azobenzene using UV light. These conformational changes can be reverted using visible light or thermally, and examples are illustrated in Equations 1.2.2 and 1.2.3.



Equation 1.2.2 Ester hydrolysis with β -cyclodextrin was modulated with light using azobenzene as the photoresponsive unit, where the azobenzene acted as a competitive inhibitor inside the β -cyclodextrin cavity. The *cis* isomer generated with UV light resulted in increased reaction catalysis.

Ueno *et al.* were the first to apply the photoisomerization of an azobenzene to regulate the rates of ester hydrolysis. In one instance, the *trans*

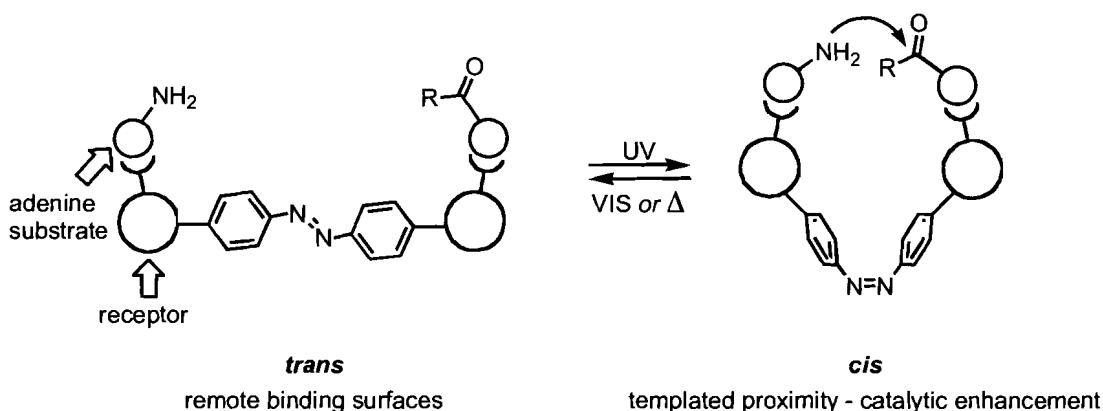
isomer of azobenzene acted as an inhibitor by fitting inside a functionalized β -cyclodextrin (Equation 1.2.2).⁵ The catalytic activity was restored following photoconversion using UV light, releasing from the β -cyclodextrin cavity. the corresponding *cis* azobenzene, which did not fit as well as the *trans* isomer.



Equation 1.2.3 Ester hydrolysis with an azobenzene functionalized β -cyclodextrin was modulated with light using azobenzene as the photoresponsive unit, where the the azobenzene influenced the β -cyclodextrin cavity depth.

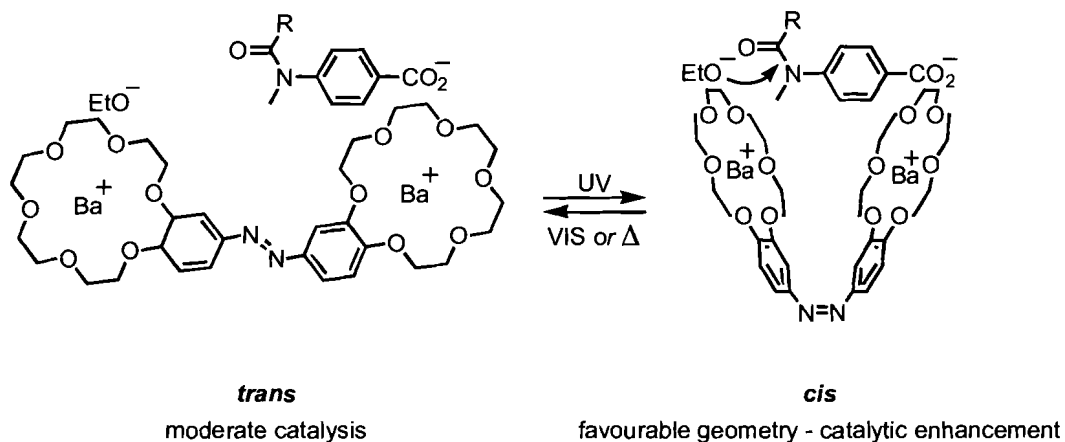
In a second example,⁶ the rate of ester hydrolysis by an azobenzene-capped β -cyclodextrin (Equation 1.2.3) was accelerated by photoirradiation with UV light, mainly due to the increased binding ability of the *cis* isomer. While the *trans* azobenzene resulted in a shallow cavity, the *cis* isomer provided a deeper cavity which enhanced the binding of the substrate and subsequently led to an increase in the hydrolysis reaction.

In later examples,⁷⁻⁹ catalytic activity was modulated using an azobenzene backbone functionalized with binding groups, which could be brought into proximity in the *cis* isomer or held apart in the *trans* isomer. The two examples illustrating this strategy are shown in Equations 1.2.4 and 1.2.5.



Equation 1.2.4 Binding groups appended on azobenzenes that were remote in the *trans* isomer could be brought into proximity to each other in the *cis* isomer with UV-light irradiation, thus enhancing catalysis by templating an amide formation reaction.

Würthner and Rebek^{7,8} regulated amide formation by linking two adenine-binding surfaces by an azobenzenes (Equation 1.2.4), where only the *cis* isomer allowed the geometrical proximity required for the templated reaction to be catalyzed. In the *trans* isomer, the remote binding surfaces did not provide a favourable geometry.



Equation 1.2.5 Crown ethers binding barium appended on azobenzene that were remote in the *trans* isomer could be brought into proximity to each other in the *cis* isomer with UV-light irradiation, thus enhancing amide hydrolysis by providing a favourable geometry.

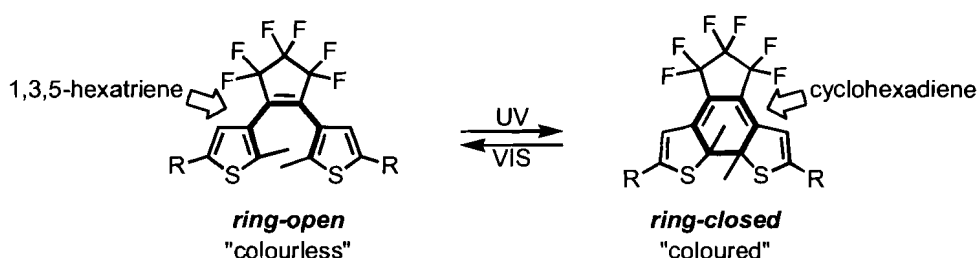
In a more recent example by Cacciapaglia *et al.*,⁹ the catalytic efficiency of a bis-barium complex (Equation 1.2.5) was regulated. The geometrical changes

induced by the photoisomerization of an azobenzene on which crown ethers were attached could affect the catalyst since the *cis* conformation was more productive towards ethanolysis of anilide derivatives than the *trans* conformation.

While the previously mentioned systems demonstrated the concept of photocontrolling catalysis, photoresponsive azobenzene derivatives are plagued by thermal reversibility¹⁰ to their *trans* isomers, making them less productive in these catalytic reactions. This is a major drawback that significantly limits the practical use of azobenzenes if the goal is to have full control over the reactivity using light under a wide range of temperatures.

1.3 The dithienylethenes

Photoresponsive 1,2-dithienylethenes (DTEs), illustrated in Equation 1.3.1, represent a significant improvement over the azobenzene photochromic compounds primarily because they undergo thermally irreversible photochemical ring-closing and ring-opening reactions, thus P-type photochromism.¹¹⁻¹³



Equation 1.3.1 The photochromic dithienylethenes (DTEs) can be toggled between the thermally stable "colourless" *ring-open* isomer containing a 1,3,5-hexatriene (bold) and "coloured" *ring-closed* isomer containing a cyclohexadiene (bold) using UV light for the ring-closing reaction and visible wavelengths of light for the ring-opening reaction.

Most published derivatives include a perfluorinated cyclopentene ring, which prevents the *E-Z* isomerization of the central alkene bond and increases

the photochromic performance by decreasing photodegradation.¹³ The *ring-open* isomer of DTE derivatives contains a 1,3,5-hexatriene backbone (bold in Equation 1.3.1), which, according to the Woodward-Hoffman rules based on the π -orbital symmetries, undergoes a conrotatory electrocyclization reaction with UV light. This reaction converts a *ring-open* starting material into a product that contains a cyclohexadiene (bold in Equation 1.3.1), referred to as the *ring-closed* form because of the newly formed cycle. Light of visible wavelengths can be used to regenerate the *ring-open* isomer from the *ring-closed* isomer. The photochemical transformation using UV light is referred to as the “ring-closing reaction” and the reverse is termed the “ring-opening reaction”. The *ring-open* and *ring-closed* isomers are described as being thermally stable because they do not interconvert when kept in the dark, even at elevated temperatures for certain derivatives.¹³ This enhanced thermal stability is of particular significance in the modulation of chemical reactivity since it enables predictably controlling the isomeric form of the photochromic molecule without having competing thermal reversion.

Several detection methods can be employed to determine the state of a given DTE. UV-VIS absorption spectroscopy is most commonly utilized to study the photochromic properties of dithienylethenes since there is a dramatic difference in colour between the *ring-open* and *ring-closed* isomers, determined by their respective UV-VIS absorption profiles. Dithienylethene derivatives typically have a colourless (solid line) and coloured isomer (broken line), as illustrated in Figure 1.3.1.

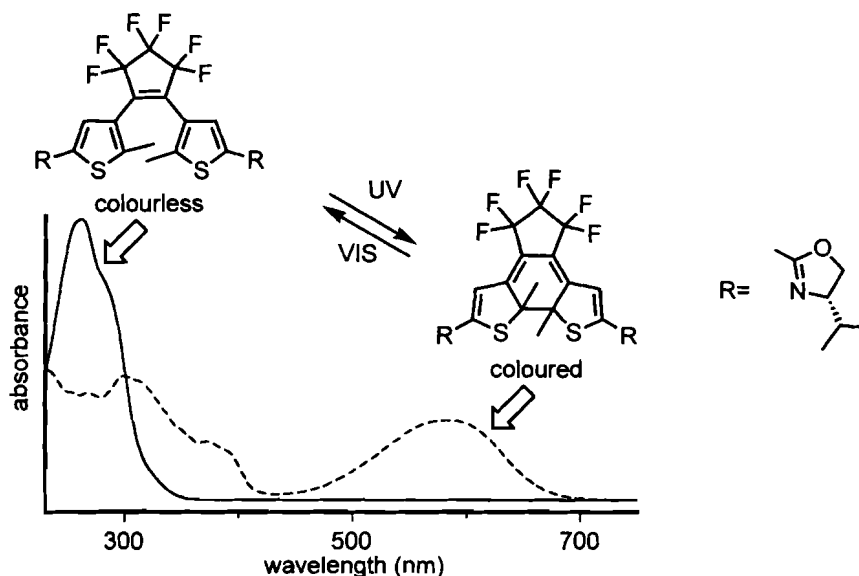
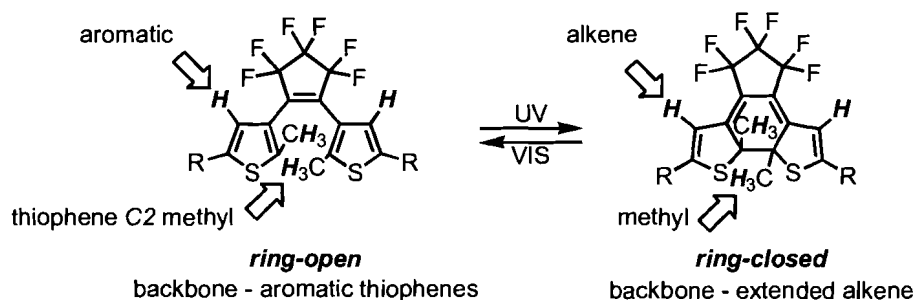


Figure 1.3.1 Illustrative example of the UV-VIS absorption profile of a dithienylethene derivative. The dithienylethene molecules are typically converted from a colourless isomer (solid line) using UV light into a coloured isomer, which has an absorption band in the visible range (broken line). The colourless isomer can be regenerated by irradiating the coloured isomer with light of visible wavelengths (VIS).

Irradiation of the colourless isomer a dithienylethene derivative with UV light generates the corresponding coloured isomer and this process can be reversed using visible wavelengths of light. In the *ring-open* form, the π -systems are localized on the thiophene heterocycles and the two ends of the molecule are cross-conjugated to each other through the backbone of the molecule. Therefore, the *ring-open* isomers are usually colourless and have absorption bands only in the UV-region of the absorption spectrum (solid line in Figure 1.3.1). Upon irradiation with UV light, a new absorption band appears at longer wavelengths in the spectrum (broken line where $\lambda_{\text{max}} = 575 \text{ nm}$ in Figure 1.3.1) due to the production of the coloured *ring-closed* isomer.

^1H NMR spectroscopy is also very useful for monitoring the progress of the photochemical interconversion processes. Previous work has shown that the

resonances of the protons on the thiophene heterocycles shift upfield upon ring-closure of DTEs.¹⁴ This is due to the loss of aromaticity of the heterocycles when the ring-closing reaction takes place, illustrated in Equation 1.3.2.



Equation 1.3.2 Each DTE isomer has a distinct set of ^1H NMR resonance signals. The thiophene proton and the methyl in the C2 position of the thiophene are attached to an aromatic thiophene in the *ring-open* isomer and to an alkene or no longer to a thiophene, for the proton and methyl groups, respectively in the *ring-closed* isomer.

In the *ring-open* form, the protons attached to the aromatic thiophene ring are more downfield in the ^1H NMR spectrum than in the *ring-closed* form, where these protons are attached to a conjugated polyene and thus appear more upfield (in the alkene region). Additionally, the extent of ring-cyclization can be obtained by measuring the relative integrals of the areas under the peaks for the corresponding pairs of signals for the two isomers. In practice, any set of protons giving distinct well-resolved resonances for both photoisomers can be used to measure the extent of photocyclization. In this thesis, the resonance signals arising from other protons, such as the C2 methyl protons on the thiophene highlighted in Equation 1.3.2, are used in instances where the thiophene protons are not clearly resolved from other signals in the ^1H NMR spectra.

The percentage of conversion reached following irradiation at a given wavelength of light when additional irradiation does not result in any change in

the relative amounts of photoisomers is defined as a photostationary state, calculated in Equation 1.3.3.

$$PSS = \frac{\text{one photoisomer}}{\text{total photoisomers}} \times 100\%$$

Equation 1.3.3 The photostationary state calculated from ^1H NMR peak integrations.

1.3.1 Synthetic reactions with DTEs

The DTE architecture is amenable to a variety of synthetic modifications based on thiophene chemistry while maintaining photochromic activity. Two common strategies for preparing derivatives include functional group transformation on a DTE compound or synthetic functionalization of the thiophenes groups prior to the assembly into a DTE photochromic molecule. A number of reviews^{13,15,16} describing DTE derivatives attest to this synthetic versatility. The most common modification sites are highlighted in Figure 1.3.2.

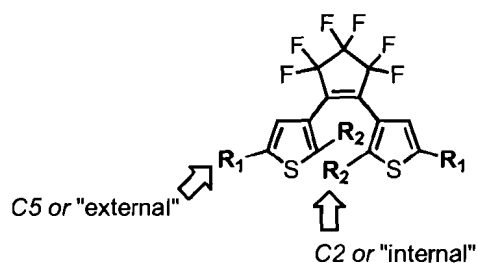


Figure 1.3.2 Functional groups can be attached at the C5 “external” and/or the C2 “internal” positions on the thiophene rings.

The thiophene-C5 and -C2 positions, ‘R₁’ and ‘R₂’ in Figure 1.3.2, respectively are also referred to as the “external” and “internal” positions in this thesis.

1.3.2 Steric changes for dithienylethenes

The concept of taking advantage of the geometric changes between photoisomers to modulate reactivity was discussed for examples incorporating azobenzenes. The DTE derivatives also display significant steric differences between photoisomers. The *ring-open* isomer has more conformational flexibility allowing the molecule to reorganize spatially due to the relatively free rotation about the σ -bond joining the thiophene to the central alkene, as illustrated in Figure 1.3.3.

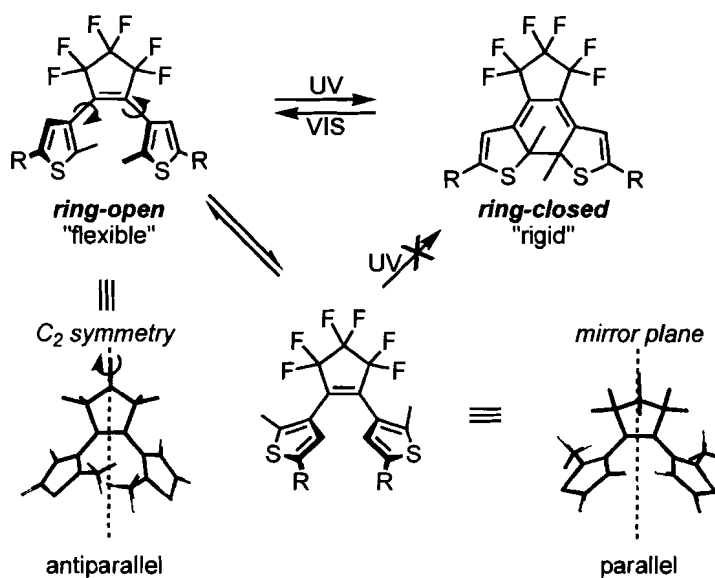


Figure 1.3.3 The *ring-open* one exists as two conformers in solution, the antiparallel one, with C_2 symmetry, and the parallel with a mirror plane. The ring-closing reaction can only occur from the antiparallel conformation. Isomerization of DTE is accompanied with a flexibility change in the backbone where the *ring-closed* isomer is rigid due to restricted free rotation in the tricyclic system compared to the relatively free rotation (curled arrows) about the σ -bonds in the *ring-open* isomer.

Two *ring-open* conformers coexist in solution, referred to as the “parallel” conformer, with the two thiophene rings arranged in mirror symmetry, and the “antiparallel” conformer, where the molecule has C_2 symmetry.¹⁷ Figure 1.3.3 demonstrates how ‘R’ groups can converge towards each other (parallel) or

diverge from one another (antiparallel). The ring-closing reaction generates a rigid tricyclic structure, which forces the 'R' groups to diverge from each other. However, flexibility can be regenerated using light of visible wavelengths. Photocyclization can only occur from the antiparallel conformation having consequences on the photoconversion extent in examples where molecular movement is restricted, for instance in single crystals,¹⁸ where parallel assembled crystals are not photochromic; or host-guest interactions with systems locked in the parallel conformation such as complexation to a saccharide,¹⁹ to a metal ion²⁰ or to itself¹⁷ exhibit limited photochromism.

The photoregulation of metal-binding geometries in turn could be used to affect reactivity and catalytic properties of metal complexes. If the thiophene substituents were metal-binding groups, it would be possible to control the chelation to a metal center. In the *ring-open* isomer, the binding groups could chelate a metal center, while in the *ring-closed* isomer the two binding groups would be separated, as shown in Figure 1.3.4.

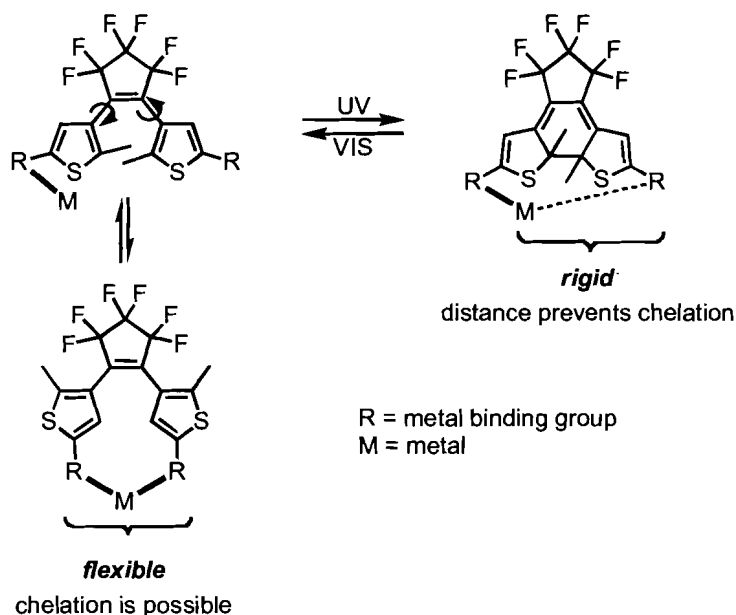
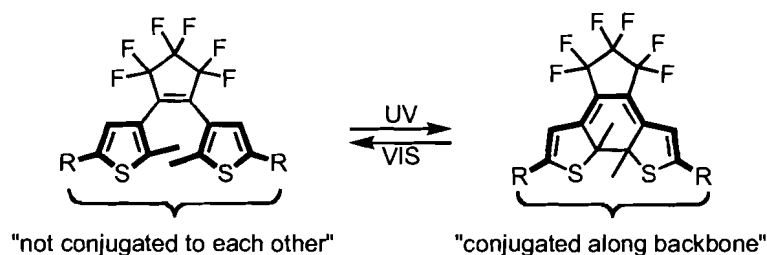


Figure 1.3.4 A DTE switch with metal-binding groups can be toggled between the flexible *ring-open* isomer, which can possibly chelate a metal, and the rigid *ring-closed* isomer, where the binding groups are held apart at a distance preventing chelation.

The concept of regulating metal-chelation in Figure 1.3.4 will be illustrated in *Chapter 2* for a DTE designed such that the *ring-open* isomer could chelate copper(I), but the *ring-closed* isomer could not. Furthermore, the photoregulation of the metal-complex applied to controlling the outcome of a catalytic reaction will be demonstrated.

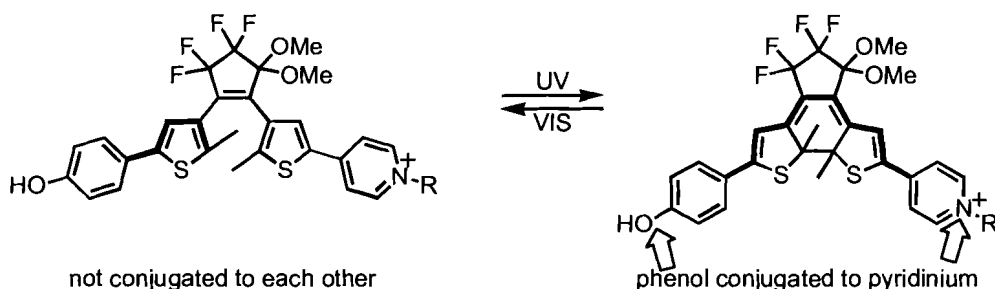
1.3.3 Electronic changes of the DTE

In the *ring-open* isomer of a DTE, the two thiophene rings are electronically isolated from one another. The two π -systems are localized on either thiophene ring and functional groups attached to separate thiophene rings are electronically independent because the thiophene rings are not coplanar due to steric repulsions at the internal positions. Upon ring-closing, extended conjugation is generated along the backbone, as shown in Equation 1.3.4.



Equation 1.3.4 The isomerization of the DTE is accompanied by a change in the conjugation along the backbone. In the *ring-open* isomer, functional groups on separate thiophene rings are independent electronically from each other, whereas in the *ring-closed* isomer these same functional groups are conjugated to each other along the backbone

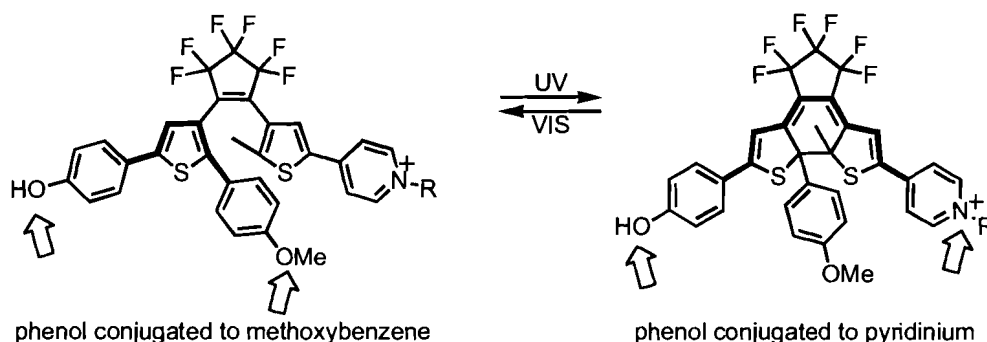
Functional groups on the C5 external positions are insulated electronically from one another in the *ring-open* isomer, but conjugated, and hence electronically connected, in the *ring-closed* isomer. Toggling between isomers provides a means to control the electronic influences of functional groups that are remote to one another in the *ring-open* isomer, but conjugated in the *ring-closed* isomer. A few reports^{21,22} have demonstrated that differences in reactivity arising from the changes in conjugation can be modulated with light, as illustrated in Equations 1.3.5 and 1.3.6.



Equation 1.3.5 The pK_a of phenol appended on DTE derivatives can be modulated with light. The differences between the *ring-open* and *ring-closed* isomers provide conjugation (bold) between remote groups on separate thiophene rings.

Kawai *et al.*²¹ described a DTE system (Equation 1.3.5) in which the phenol pK_a decreased upon the light induced generation of a conjugation

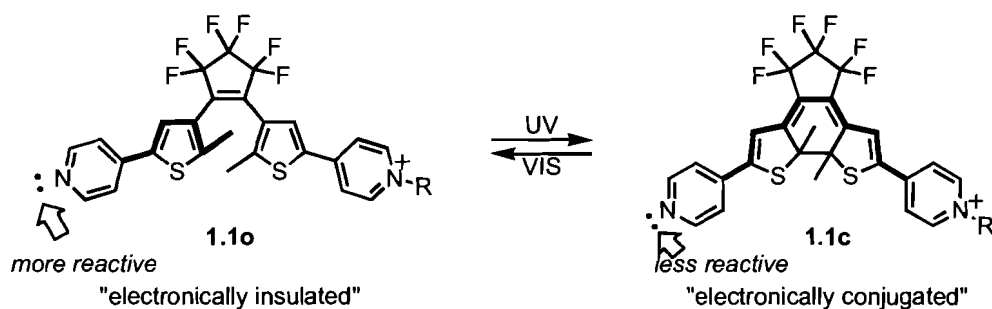
pathway between the acidic phenol and an electron-withdrawing pyridinium moiety.



Equation 1.3.6 The pK_a of phenol appended on DTE derivatives can be modulated with light. The differences between the *ring-open* and *ring-closed* isomers provide conjugation (bold) between remote groups on the same thiophene ring, in the *ring-open* isomer or separate thiophene rings, in the *ring-closed* isomer.

More recently, Odo *et al.*²² designed another phenol-based DTE system (Equation 1.3.6) that combined both electron-donating effects from a *p*-methoxybenzene, and electron-withdrawing effects from a pyridinium. In the *ring-open* isomer, the phenol was conjugated to the electron-donating group located on the same thiophene. However, in the *ring-closed* isomer the phenol was conjugated to the electron-withdrawing pyridinium, and thus a larger pK_a difference was expected compared to the previous example (Equation 1.3.5).

Conjugation differences between *ring-open* and *ring-closed* isomers also have an effect on the reactivity of a pyridine-functionalized DTE reported by Samachetty *et al.*,²³ illustrated in Equation 1.3.7.



Equation 1.3.7 DTE could be used to modulate the Lewis basicity and nucleophilicity of a pyridine. The lone pair on the pyridine in the *ring-open* isomer **1.1o** was more reactive than that in the *ring-closed* isomer **1.1c** because the pyridine in the latter was electronically conjugated to an electron-withdrawing pyridinium group through the backbone.

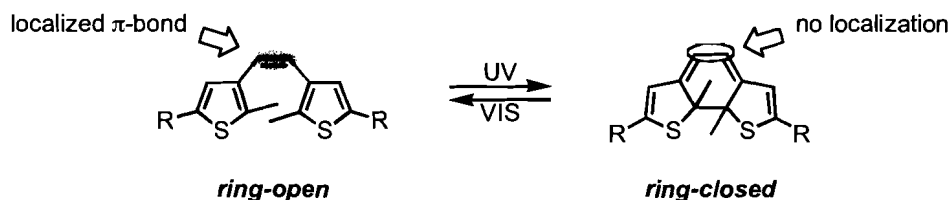
The electron-withdrawing properties of a pyridinium group could directly affect the Lewis basicity²³ and nucleophilicity²⁴ of a pyridine in the *ring-closed* **1.1c** conjugated state, while the effects were minimized in the electronically insulated *ring-open* isomer **1.1o** resulting in a more Lewis basic and more nucleophilic pyridine. Throughout this thesis, the isomers of a given dithienylethene compound will be referred to using the same numbering labels, denoting the *ring-open* isomer with an “o” and the *ring-closed* isomer with a “c” after the number.

A photoresponsive DTE ligand in *Chapter 3* will be used to demonstrate that the differences in conjugation between the *ring-open* and *ring-closed* isomers can also be applied to affect the reactivity of a metal-ligand complex.

1.3.4 Localized π -bond rearrangements of DTE derivatives

The ring-closing isomerization of the DTEs, induced by UV light, leads to a rearrangement of the π -system. The hexatriene moiety electrocyclizes into a cyclohexadiene with UV light and the localized central π -bond in the *ring-open*

isomer becomes delocalized in the *ring-closed* isomer, as depicted in Equation 1.3.8.

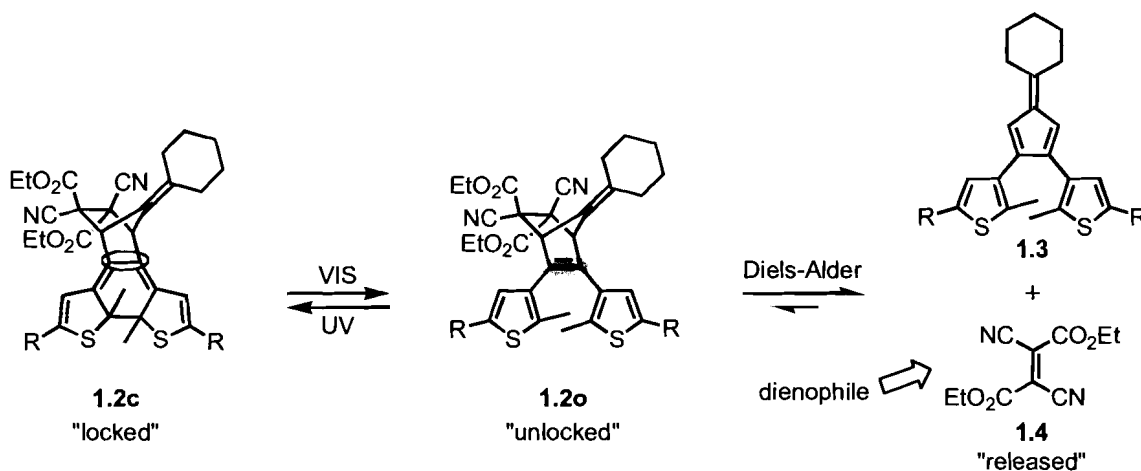


Equation 1.3.8 The ring-closing isomerization of DTEs using UV light is accompanied by the “removal” of the localized π -bond (shaded area) from the *ring-open* isomer, where the *ring-closed* isomer does not have a localized π -bond in the central position (circled area). The localized π -bond can be “created” from the *ring-closed* isomer using visible wavelengths of light, regenerating the *ring-open* isomer.

UV light converts a hexatriene-containing *ring-open* DTE into a corresponding cyclohexadiene-containing *ring-closed* isomer. This rearrangement of π -bonds can also be thought of as the “creation” and “removal” of double bonds in specific locations. In Equation 1.3.8, the shaded area highlights a localized π -bond that is present only in the *ring-open* isomer, but absent in the circled area of the *ring-closed* isomer where the π -bonds are delocalized along the backbone. Visible wavelengths of light can be used to restore the *ring-open* isomer, thus “creating” a π -bond in a specific location.

By employing the discussed changes, wherein π -bond rearrangements can be photoregulated, it would be possible to design a system in which reactions requiring specific arrangements of localized π -bonds could be efficiently and reversibly switched from an “on” to an “off” state with light. In spite of the potential benefits of such a system, such as the complete “on/off” control applicable to the wide-range of localized π -bond dependent reactions, only one

report of this approach has been published to date by Lemieux *et al.*,²⁵ with their system depicted in Equation 1.3.9.



Equation 1.3.9 The Diels-Alder adduct, only present in the *ring-open* isomer **1.2o** with a localized π -bond (shaded area) generated with visible light, could “release” a dienophile **1.4** by the *retro* Diels-Alder equilibrium. The same dienophile was “locked” within the *ring-closed* isomer **1.2c** due to the absence (circled area) of a localized π -bond.

A *retro* Diels-Alder reaction could only proceed from the *ring-open* isomer **1.2o** of the DTE because the *ring-closed* isomer **1.2c** lacked the cyclohexene required for the fragmentation reaction with the localized π -bond (circled where it is absent or shaded where it is present in Equation 1.3.9). The ring-opening reaction from the “locked” *ring-closed* isomer **1.2c** with visible light could be considered a phototrigger since it subsequently lead to the release of a dienophile **1.4** in the thermal *retro* Diels-Alder equilibrium from the *ring-open* isomer **1.2o**.

The Bergman cyclization of an enediyne is another notable reaction requiring a precise arrangement of localized π -bonds. The reactivity modulation of an enediyne DTE derivative will be discussed in *Chapter 4*.

1.4 Thesis preview

In light of the different approaches available for the photoregulation of reactivity using DTEs, a series of systems were designed to address specifically the steric changes in *Chapter 2*; the electronic changes in *Chapter 3*; and the π -bond creation/removal in *Chapter 4*.

In *Chapter 2* the synthesis and photochromic properties of DTE bis(oxazoline) derivatives (**2.2o** and **2.3o** in Figure 1.4.1) are described. The changes in flexibility between *ring-open* and *ring-closed* isomers allow for different metal-binding geometries, where the more flexible *ring-open* isomers could chelate copper, while the rigid *ring-closed* isomers could not. The differences in the metal complexation could directly affect the stereoselectivity in the product distribution of the cyclopropanation of styrene with ethyldiazoacetate.

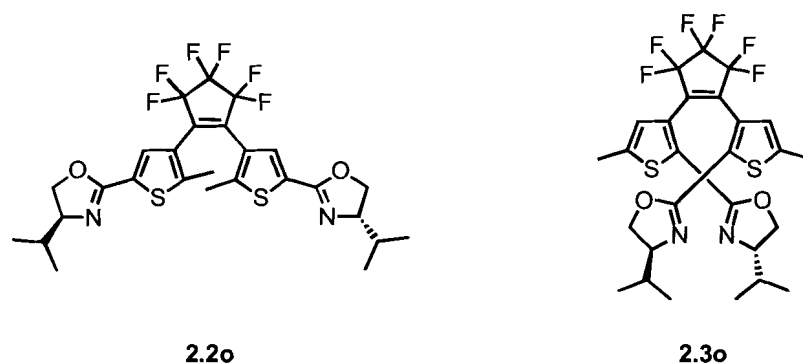
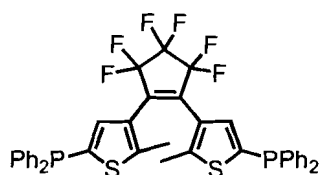


Figure 1.4.1 Two different bis(oxazoline) DTE derivatives prepared to illustrate how the differences in flexibility between the *ring-open* and *ring-closed* isomers could be applied to control the binding geometry in a metal complex.

In *Chapter 3*, the synthesis and photochromic properties of DTE bis(phosphine) derivatives of (**3.1o** in Figure 1.4.2) are described. The wide range of potential applications that could benefit from the photoregulation of the phosphine derivatives stems from the ubiquitous nature of tertiary phosphines in

chemical reactions and catalytic processes. Through selected examples, reactivity differences accompanying the photoinduced changes in electronic communication between the *ring-open* and *ring-closed* isomers and metal complexes are demonstrated. Functional groups on separate thiophene rings should not affect each other in the electronically insulated *ring-open* isomer, whereas electronic communication could take place along the backbone in the *ring-closed* isomer.



3.1o

Figure 1.4.2 A bis(phosphine) DTE used in demonstrating how the changes in electronic communication between the *ring-open* and the *ring-closed* isomers could affect the reactivity of the phosphine.

In *Chapter 4*, an example highlighting how the presence/absence of localized π -bonds could be used to photoregulate a reaction requiring a precise arrangement of π -bonds is discussed. An enediyne substructure could be created/removed from DTE derivatives (**4.3o** and **4.4o** in Figure 1.4.3) using appropriate wavelengths of light, where the enediyne structure was essential for the Bergman cyclization to proceed. This design illustrates a useful strategy of drug activation/deactivation using light.

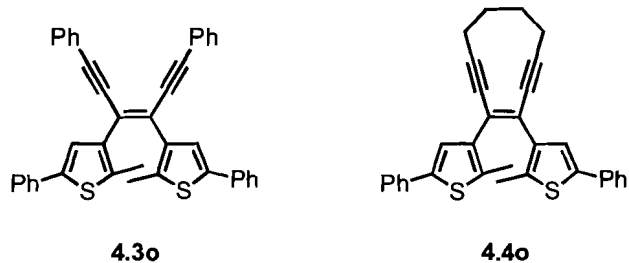


Figure 1.4.3 Enediyne DTE derivatives where only the *ring-open* isomers contain an enediyne moiety illustrate how reactions requiring a precise arrangement of π -bonds, such as the Bergman cyclization, could be regulated with light.

This thesis concludes with a summary of the results of the research presented and identifies the potential problems encountered when designing photoresponsive systems. Finally, directions for future work will be discussed.

2 Photoswitching of Stereoselectivity in Catalysis Using a Copper Dithienylethene Complex

The research presented in Section 2.3 of this chapter was published as a communication in: Sud, D.; Norsten, T. B.; Branda, N. R. "Photoswitching of Stereoselectivity in Catalysis Using a Copper Dithienylethene Complex" *Angew. Chem. Int. Ed.* **2005**, *44*, 2019-2021.

2.1 Using light to control catalysis

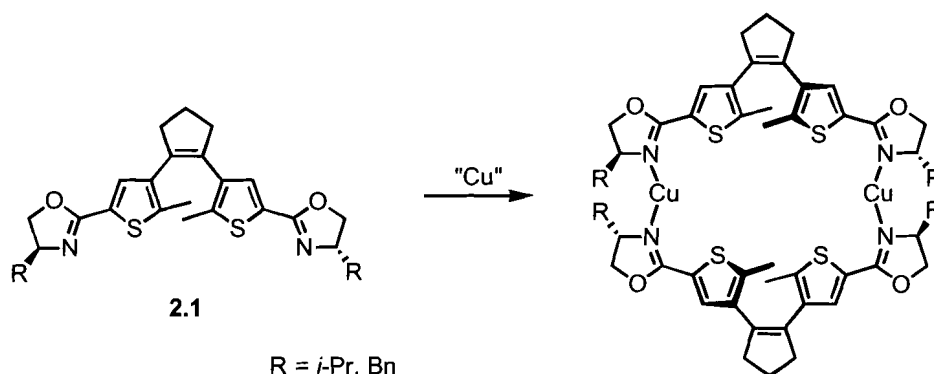
There are few examples of research that describe systems in which light is used as a stimulus to control catalytic reactivity.⁵⁻⁹ A more detailed description of these systems was given in the *Introduction*. Their common element was the use of an azobenzene moiety for their photoregulation. As previously mentioned, azobenzenes exhibit some disadvantages in photoswitching performance when compared to that of dithienylethenes. The major advantage of DTE switches is the improved thermal stability of the photoisomerization reaction for both DTE isomers.¹³ In the context of reaction catalysis, thermal reversibility limits the useful temperature range for such control systems due the inability to predetermine the state of the catalyst and therefore the reactivity. Full photocontrol over the catalyst requires that no isomerization by non-photochemical pathways take place. Therefore, the DTE switches provide an improved means to control catalysts that could be used with a greater range of reaction temperature conditions than azobenzene derivatives.

2.1.1 Flexibility change of DTE

DTE switches undergo a flexible-to-rigid change in their backbone when isomerized from their *ring-open* to *ring-closed* isomer. Substituents in the external and internal thiophene positions can converge closer to one another in the flexible *ring-open* isomer, unlike in the rigid *ring-closed* isomer where these same substituents are forced to diverge. This concept was applied to metal-ligand complexes in this chapter and is described in the following sections.

2.1.2 Design for photocontrol of a DTE ligand

Murguly et al.²⁶ have demonstrated the synthesis of bis(oxazoline) DTEs and their binding to copper, resulting in double helicates, where two ligands were wrapped around two metals in a stereospecific manner, as illustrated in Scheme 2.1.1.



Scheme 2.1.1 Two non-fluorinated bis(oxazoline) DTEs in **2.1** assembled into a copper double helicate.

Both *i*-Pr and Bn derivatives were prepared, but the double helicate structure was only shown directly by X-ray crystallographic analysis for the Bn derivative. The assembly of the double helicate templated a diastereoselective

ring-closing reaction. This was proven for both the *i*-Pr and Bn derivative, thus suggesting that the *i*-Pr derivative also assembled into a double helicate.

Bis(oxazoline) DTE ligands could also potentially chelate with a single metal center where this chelation was photoregulated. With a flexible *ring-open* isomer, the oxazoline groups could converge creating a metal-binding pocket and for a complex in a bidentate fashion. The rigid *ring-closed* isomer should restrict the bond rotation and distort the binding pocket in such a way that a bidentate complex could not form.

In this chapter, the regulation of metal-catalyzed reactions is demonstrated by taking advantage of the geometrical changes accompanying the photoisomerization of bis(oxazoline) DTEs. Two bis(oxazoline) DTEs were prepared, **2.2o** and **2.3o** shown in Figure 2.1.1, and their metal-binding behaviours were investigated by using them as ligands in a catalytic reaction. It is shown that the metal-chelation of these ligands has a significant influence on the outcome of the reaction.

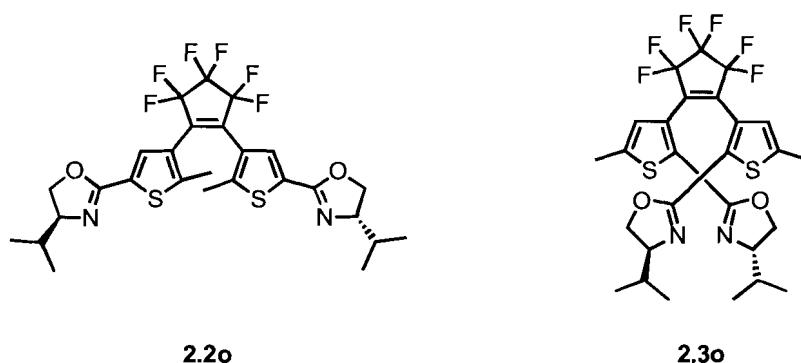


Figure 2.1.1 Two bis(oxazoline) DTEs prepared and studied.

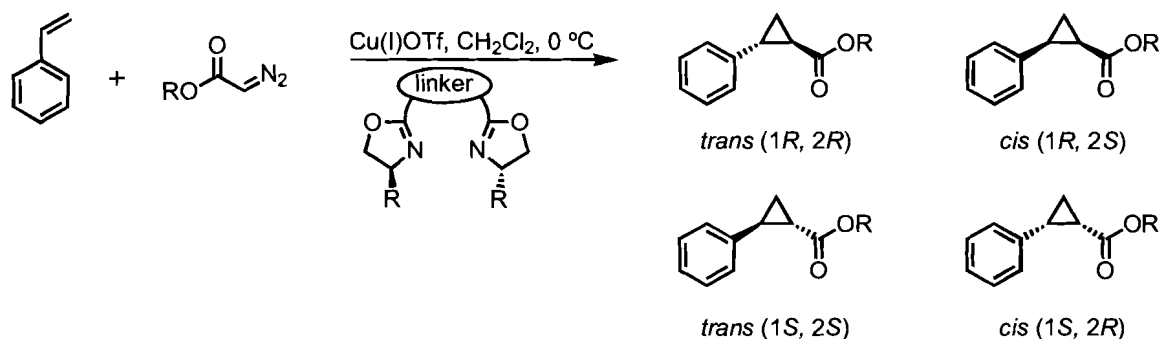
This chapter will describe how compounds **2.2o** and **2.3o** in Figure 2.1.1 provided geometrically different chelating possibilities. In both cases the *ring-*

open isomers were expected to chelate a metal due to their flexibility, while the corresponding *ring-closed* isomers were not expected to, because of their rigidity. Instead, it was expected that the *ring-closed* isomers would form dimers or polymers. The bis(oxazoline) DTE **2.2o**, with its oxazoline substituents in the thiophene C5 positions, inspired directly from the non-fluorinated derivative **2.1** (Scheme 2.1.1) was the first one to be investigated. However, it could only provide low stereoselectivity within error limits. The DTE **2.3o** was then prepared as an alternative bis(oxazoline) DTE and its *ring-open* and *ring-closed* isomers displayed the predicted differences in catalytic reactivity.

2.1.3 Catalytic reaction with bis(oxazoline) ligands

Bidentate bis(oxazoline) ligands are commonly used in catalysis. In asymmetric synthesis, their chirality results in a stereoselective distribution of reaction products.²⁷ For example, bis(oxazoline)-copper complexes catalyze the cyclopropanation of olefins with diazoesters. This was a good reaction to illustrate the photocontrol of a catalyst concept because it provided a simple model reaction that was easy to analyze and had a well-characterized product distribution.²⁸ Subtle changes in the ligand sterics and geometrical arrangements have large effects on the product distribution and it was expected that the geometrical differences accompanying the photoisomerization of a bis(oxazoline) DTE would have a measurable effect in the product distribution. Thus, toggling between the *ring-open* and *ring-closed* isomer would provide a way of controlling the catalytic reaction's outcome. The cyclopropanation of styrene with ethyldiazoacetate using a bis(oxazoline) ligand with copper(I), as shown in

Scheme 2.1.2, gives a distribution of four products that can be monitored by chiral HPLC since all four products display different retention times.



Scheme 2.1.2 Cyclopropanation of styrene with ethyldiazoacetate using a bidentate bis(oxazoline) ligand with Cu(I)OTf affords four stereoisomeric products.

The major products from the cyclopropanation of styrene with ethyldiazoacetate using bis(oxazoline) ligands are the *trans* stereoisomers based on steric effects and geometry of the binding pocket.²⁸⁻³⁰ The bite angle, defined as the ligand-metal-ligand angle formed in a bidentate complex, the relative conformation and rigidity of the linker between the oxazolines have an important effect on the product distribution.^{31,32} Previous reports have shown that the proximity to the metal and orientation towards the binding pocket of the oxazolines' chiral alkyl groups can be fine-tuned to give different distributions. The highest stereoselectivities were demonstrated for systems where the oxazoline 'R' groups were in closer proximity to the metal ion and rigid framework of the metal-chelate, and thus provided a well-ordered environment at the catalytic site. The product distribution is commonly described as an enantiomeric excess (e.e.) or a diastereomeric excess (d.e.), calculated using Equations 2.1.1 and 2.1.2.

$$e.e. = \frac{(\text{moles of major enantiomer} - \text{moles of minor enantiomer})}{\text{total moles of both enantiomers}} \times 100\%$$

Equation 2.1.1 Enantiomeric excess.

$$d.e. = \frac{(\text{moles of major diastereoisomers} - \text{moles of minor diastereoisomers})}{\text{moles of other diastereoisomers}} \times 100\%$$

Equation 2.1.2 Diastereomeric excess.

2.2 C5 bis(oxazoline) DTE 2.2o

In the first studied bis(oxazoline) DTE, the oxazoline groups were attached in the C5 position, also referred to as the external position, based on the bis(oxazoline) DTE **2.1** shown in Scheme 2.1.1. The fluorinated derivative was prepared for its improved photochromic performance properties (less degradation from photoreactions, higher photostationary state (PSS)) over those of the non-fluorinated derivative.¹³ The *ring-open* isomer **2.2o** could be rigidified by conversion to the *ring-closed* isomer **2.2c** using UV light, and this change could be reversed using visible light, as shown in Figure 2.2.1.

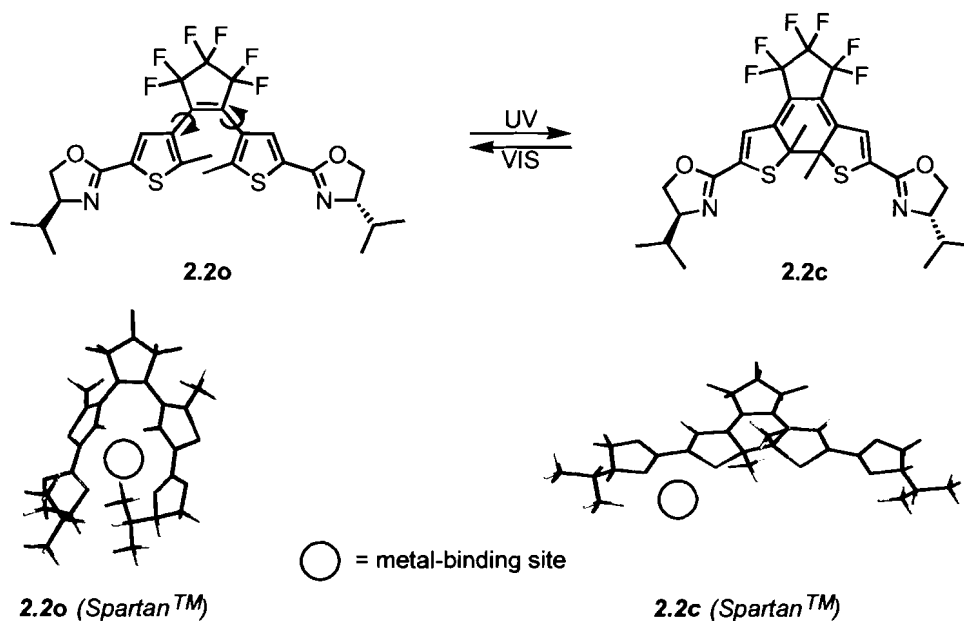
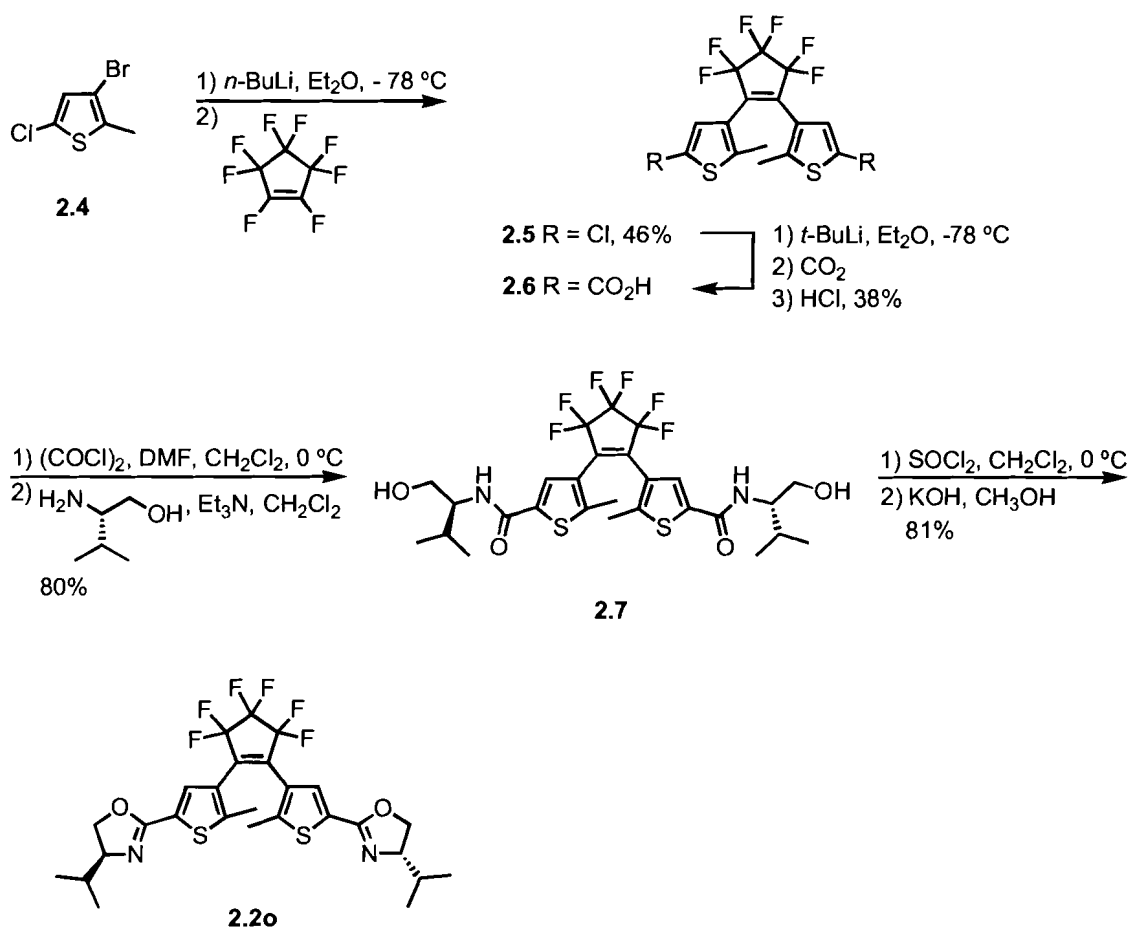


Figure 2.2.1 Different metal-binding possibilities for C5 bis(oxazoline) DTE **2.2o** and **2.2c**. Arrows on **2.2o** represent the possibility for free rotation, unlike the rigid compound **2.2c**. Molecular model representations, generated using Spartan™ '02 for Macintosh, highlight geometrical arrangements for metal-binding pockets or lack thereof.

In the flexible *ring-open* isomer **2.2o**, the two oxazoline groups could converge towards each other as shown by the Spartan™ model in Figure 2.2.1. In contrast, these same oxazoline groups were rigidly held apart from each other in the case of the *ring-closed* isomer **2.2c** due to restricted bond rotation in the tricyclic structure. The spatial proximity of the two oxazolines is essential for any bidentate complexation to take place and would thus directly influence whether the metal would be in a restricted chiral environment.³² Preliminary product distribution results,³³ using the non-fluorinated derivative *ring-open* isomer **2.1** as a ligand in the cyclopropanation of styrene with ethyldiazocacetate, indicated that there might be limited stereoselectivity.

2.2.1 Synthesis of the C5 bis(oxazoline) DTE 2.2o

DTE **2.2o** was prepared by first making a diacid DTE **2.6**, which was subsequently transformed into a bis(oxazoline) following the procedure developed for the non-fluorinated derivative,³⁴ as shown in Scheme 2.2.1.



Scheme 2.2.1 Synthesis of C5 bis(oxazoline) DTE **2.2o**.

The starting material, 3-bromo-5-chloro-2-methylthiophene **2.4**, prepared according to established procedure,³⁵ underwent a lithium-halogen exchange and was then quenched with 0.5 equivalents of octafluorocyclopentene, affording compound **2.5** in 46% yield. Conversion of the chloro substituents in compound **2.5** into the carboxylic acid in compound **2.6** was achieved by a lithium-halogen

exchange followed by a quenching with carbon dioxide and an acid workup in 38% yield. The stereocenters were installed on the DTE by first converting the diacid to a diacid chloride, and then forming diamide **2.7** by coupling it with (*S*)-2-amino-3-methyl-1-butanol (L-valinol).³⁶ The conversion to the bis(oxazoline) **2.2o** was done in two steps using thionyl chloride and basic workup conditions with an overall yield of 11% from compound **2.4**.

2.2.2 Photochromic behaviour of the C5 bis(oxazoline) DTE

The photochromic properties of dithienylethene derivatives are typically studied using UV-VIS spectroscopy, which monitors the absorption changes accompanying the light-induced electrocyclization reaction. The photochemical interconversion between the *ring-open* isomer **2.2o** and the *ring-closed* isomer **2.2c** isomers of the C5 bis(oxazoline) DTE resulted in a colour change, from colourless to purple, and the differences in the UV-VIS absorption profiles are shown Figure 2.2.2.

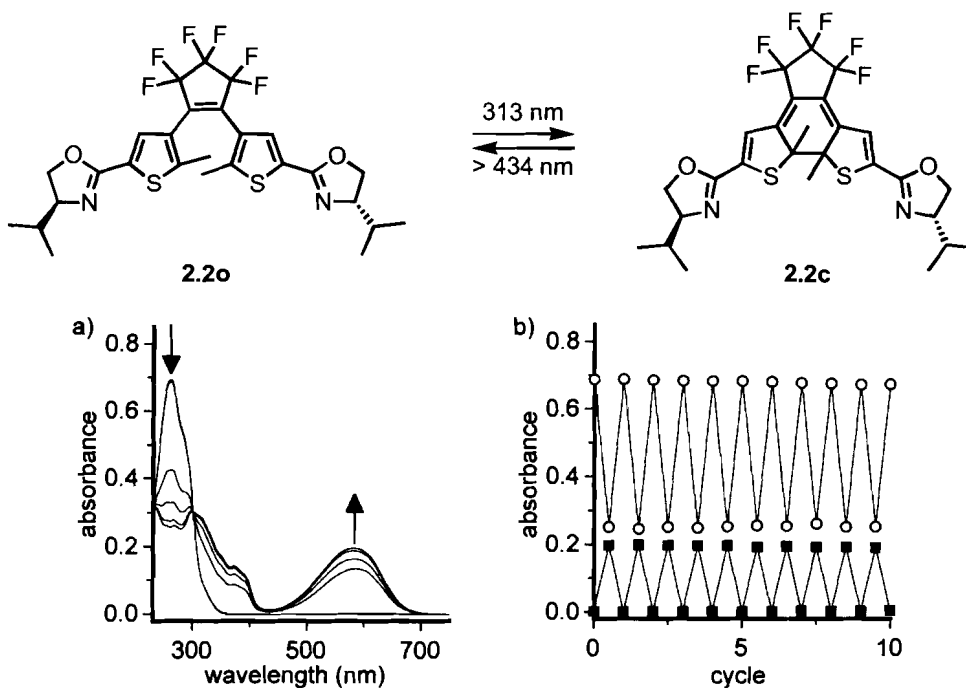


Figure 2.2.2 The UV-VIS absorption spectra of a 1.6×10^{-5} M solution of compound **2.2o** in CH_2Cl_2 upon irradiation with 313-nm light. (a) Total irradiation periods are 0, 10, 20, 30 and 40 sec. (b) Modulated absorbance at 251 nm (○) and 581 nm (■) during alternate irradiations with 313-nm light for 40 sec, then > 434 nm for 40 sec.

Irradiation of a CH_2Cl_2 solution of compound **2.2o** (1.6×10^{-5} M) with 313-nm light, using a hand-held UV lamp, induced a rapid colour change as indicated by the growth of a visible region absorption ($\lambda_{\text{max}} = 581$ nm), with a concomitant decrease in the UV absorptions ($\lambda_{\text{max}} = 251$ nm). The solution was irradiated with 313-nm light for 40 sec, at which time subsequent irradiation with the UV-light source did not result in changes in the absorption profile, indicating that a photostationary state was reached (Figure 2.2.2a). The original absorption spectrum was regenerated using the light of a 150-W tungsten source that was passed through a 434-nm cutoff filter to eliminate higher energy light. The ring-closing and ring-opening isomerization reactions were repeated several times in order to determine the photochromic performance of compound **2.2o**. No

significant degradation to side-products from the photoreactions occurred after ten cycles of ring-closing/ring-opening, as indicated by the lack of a decrease in the modulated absorbance values in Figure 2.2.2b.

The photochemical interconversion between the *ring-open* isomer **2.2o** and the *ring-closed* isomer **2.2c** was also monitored by ^1H NMR spectroscopy. Irradiation of a CD_2Cl_2 solution of compound **2.2o** (2.3×10^{-3} M) with 313-nm light resulted in the appearance of a new set of signals for compound **2.2c** (the presence of two diastereomeric products is discussed in Section 2.2.3) including a singlet at 6.70 ppm, while the corresponding thiophene proton singlet was at 7.50 ppm for compound **2.2o**, as shown in Figure 2.2.3.

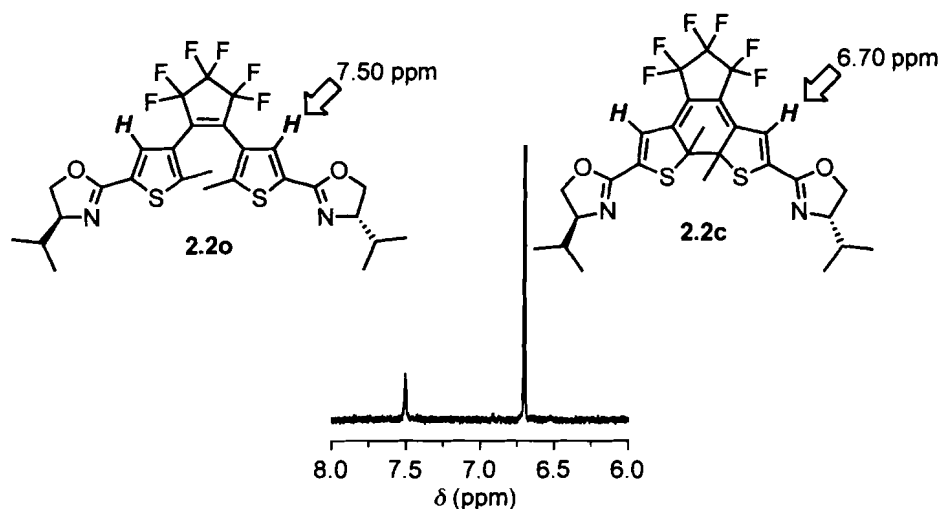


Figure 2.2.3 Selected region in the ^1H NMR spectrum obtained after irradiation of a CD_2Cl_2 solution of **2.2o** (2.3×10^{-3} M) with 313-nm light, highlighting the thiophene proton singlet used in determining the extent of photoconversion.

When additional irradiation of the solution with 313-nm light resulted in no further changes in the relative integration between the signals assigned to compounds **2.2o** and **2.2c**, the photostationary state was determined to be a mixture of 87% of *ring-closed* isomer **2.2c** as a mixture of diastereoisomers, with

the remaining 13% assigned to the *ring-open* isomer **2.2o**. Since the T_1 values were not measured for any of the photostationary state experiments described throughout this thesis, the relative integration data was used as an estimate.

2.2.3 Metal complexation of C5 bis(oxazoline) DTE with copper

It was necessary to determine if a metal complex was formed in solution, since this bis(oxazoline)-metal complex is required for the catalytic reaction to occur stereoselectively. Due to the air sensitivity of the copper(I) trifluoromethanesulfonate (CuOTf) required for the catalytic reaction, tetrakis(acetonitrile) copper(I) hexafluorophosphate (Cu(CH₃CN)₄PF₆) was used to investigate the complexation in CDCl₃ solutions, following previously established methodology.³² A solution of compound **2.2o** (1.3×10^{-2} M) in CDCl₃ was titrated with increasing amounts of copper salt until 1 molar equiv. was reached and the complexation was monitored by ¹H NMR spectroscopy and is shown in Figure 2.2.4.

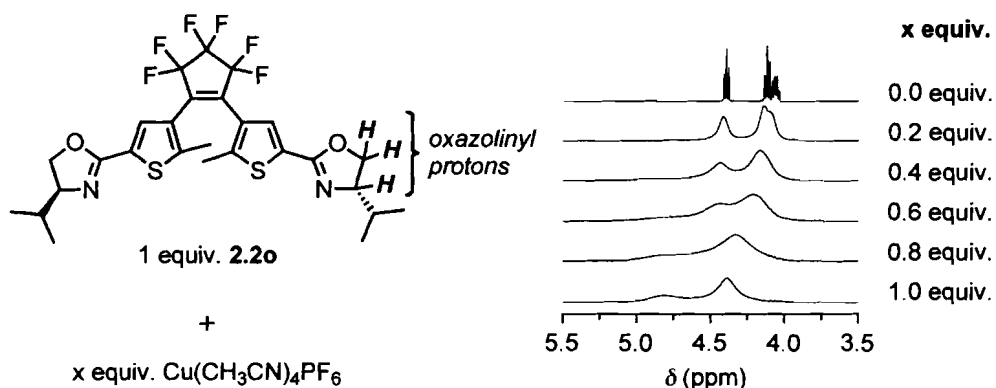


Figure 2.2.4 ¹H NMR study of the complex formation of a CDCl₃ solution of compound **2.2o** (1.3×10^{-2} M) with increasing equivalents of Cu(CH₃CN)₄PF₆ monitoring the oxazolinylyl protons.

Since the oxazolinylyl peaks, which are closest to the metal-binding, were shifted and there was only one set of peaks at any point of the titration, this trend

indicated a uniform rapid complex formation where the proton resonance signals were an average of the free ligand and complex in solution. These results were in accordance to literature precedents where a single set of peaks demonstrated the presence of one complex, whereas multiple sets of peaks indicated the presence of a mixture of cuprous complexes.³² The peak broadening observed by ¹H NMR spectroscopy in Figure 2.2.4 was a result of the partial oxidation of copper into the Cu(II), which is paramagnetic. Several crystallization attempts with different metal salts and solvent mixtures remained unsuccessful, which meant that the geometry of this complex could not be fully determined.

The next experiment to investigate the nature of the complex in solution focused on the outcome of the ring-closing isomerization of compound **2.2o** in the presence of copper. A CH₂Cl₂ solution of compound **2.2o** (1.3×10^{-2} M) and 1.0 molar equiv of CuOTf was irradiated with 313-nm light for 15 min at which point the copper was removed using an excess of NH₄OH.²⁶ The d.e. of the ring-closed products **2.2c**, determined by ¹H NMR spectroscopy, showed an increase from 0% to 31% in the presence of copper. The two diastereoisomers and the ¹H NMR resonances are shown in Figure 2.2.5.

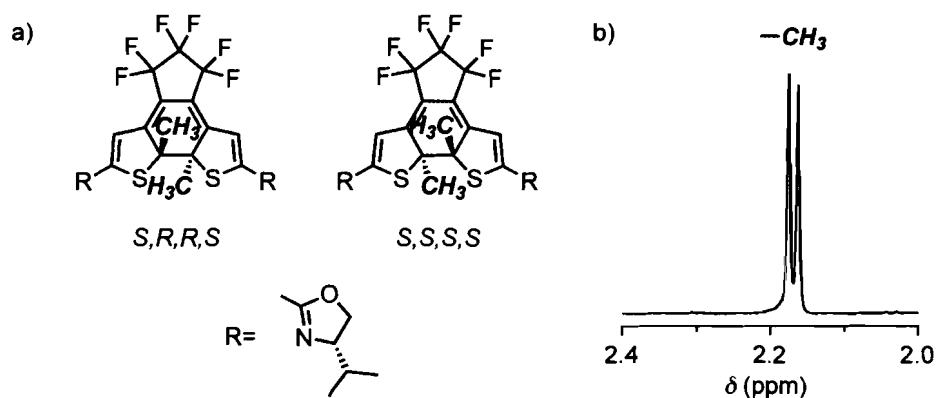


Figure 2.2.5 The two possible diastereoisomeric products **2.2c** of the ring-closing reaction. (a) geometry of the diastereoisomers, highlighting the C2 methyl producing distinct signals for the two diastereoisomers and (b) the ^1H NMR signals of the C2 methyl protons generated with 313-nm light in the absence of copper(I).

The d.e. was measured from the integration of the areas under the peaks assigned to the C2 methyl protons, which showed separate peaks for either diastereoisomer of **2.2c** with distinct resonances at $\delta = 2.16$ and 2.18 ppm. A similar effect on the ring-closing diastereoselectivity was previously shown with compound **2.1** providing a d.e. of 49-55% for the ring-closing reaction in the presence of copper. This effect was attributed to the geometry in the double helicate complex illustrated in Scheme 2.1.1 templating the stereoselective ring-closure.²⁶ Similarly, the stereoselectivity of the ring-closure of compound **2.2o** suggested that its complexation with copper might result in a double helicate rather than in a bidentate.

2.2.4 Photocontrol of catalysis with C5 bis(oxazoline) DTE

The chelation of the *ring-open* DTE **2.2o** was studied by verifying whether catalytic reaction conditions provided a chiral environment that could dictate the diastereoselectivity of the reaction. Both the *ring-open* and the *ring-closed* isomers are chiral, but their flexibility change should result in a change in the

chiral environment around the metal leading to differences in the product distribution. The product distribution was monitored by HPLC using a chiral column (CHIRACEL-OD). Samples of the racemic *cis* and *trans* products were used to determine the specific retention times, and were found to be consistent with literature reports.³⁷ The peaks corresponding to the *trans* enantiomers were fully resolved, while those for the *cis* enantiomers overlapped, but could be resolved using the HPLC software (*Breeze*TM) provided by Waters.

Catalytic experiments were performed using the conditions summarized previously in Scheme 2.1.2. After mixing 1 molar equiv. of CuOTf with 1.05 molar equiv. of bis(oxazoline) ligand **2.2o** at 0 °C, styrene was added, followed by the slow addition of a solution of ethyldiazoacetate over 6 h using an injection pump to prevent decomposition of the ethyldiazoacetate,³⁸ at which point the reaction was stirred overnight at 22 °C. No reproducible enantiomeric excess could be measured using 10-25 mol% of **2.2o** ligand-metal complex to styrene/ethyldiazoacetate. The obtained stereoselectivities fell within the 5-10% error range of the experiment. This lack of stereoselectivity could occur only if the geometry around the metal did not allow proximity of the oxazolyl groups around the catalytic site, perhaps by forming a dimer or polymer, hence not providing the chiral environment necessary for stereoselectivity. Considering it was assumed that the stereoselectivity was to arise from the *ring-open* isomer **2.2o**, experiments using the *ring-closed* isomer **2.2c** were not performed. Instead, the DTE was redesigned to provide different chelating possibilities.

2.3 C2 bis(oxazoline) DTE 2.3o

The material discussed in this section has been published.³⁹ Following the lack of stereoselectivity in catalysis using the C5 bis(oxazoline) DTE in a metal complex, the system was redesigned such that the oxazoline substituents were located at the C2 position on the thiophene rings, providing the potential for different complexation geometries, as shown for **2.3o** and **2.3c** in Figure 2.3.1.

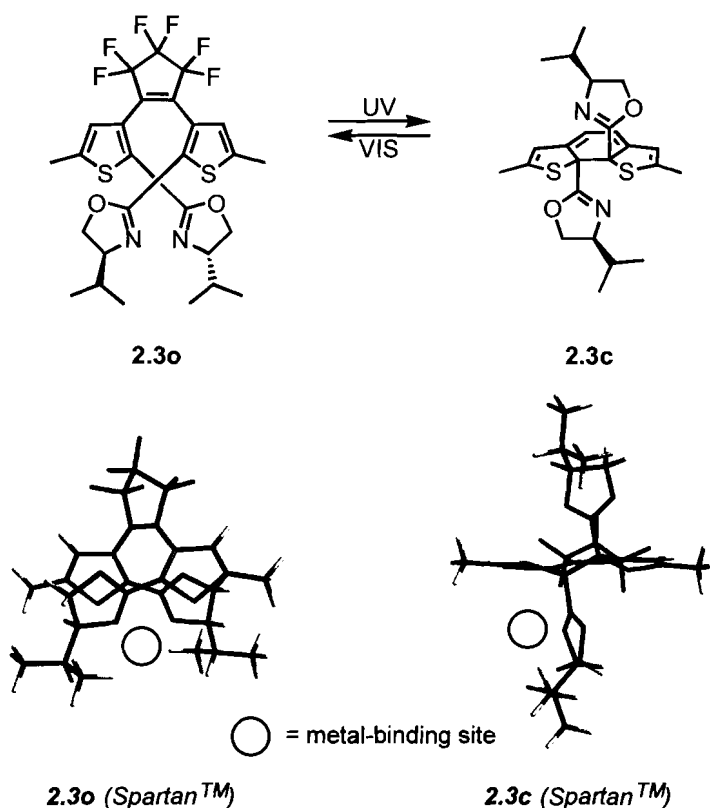


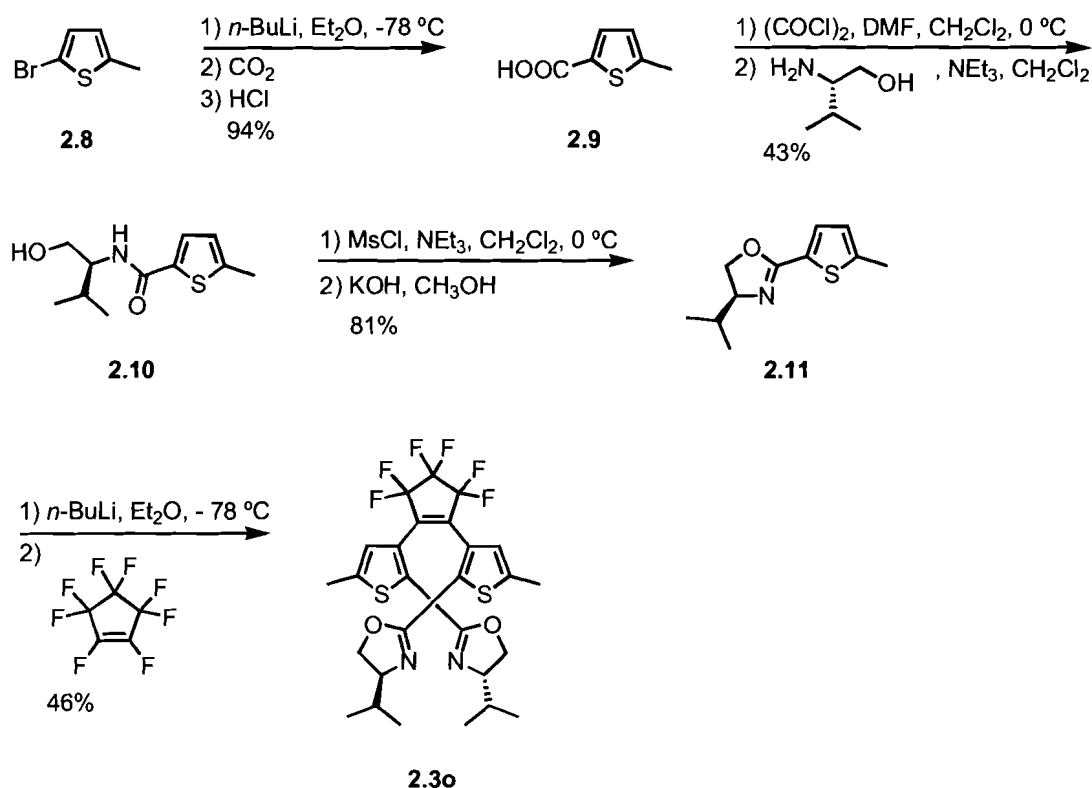
Figure 2.3.1 Different conformational possibilities for C2 bis(oxazoline) DTE **2.3o** and **2.3c**. The perfluorinated portion of the cyclopentene ring is hidden in **2.3c** for clarity. Molecular model representations, generated using SpartanTM '02 for Macintosh, highlight the geometrical arrangements for the metal-binding possibilities.

Using UV light, a flexible *ring-open* **2.3o** should isomerize to a rigid *ring-closed* **2.3c**, and this change can be reversed using visible light. Free rotation in **2.3o** should allow the two oxazoline groups to converge towards each other, providing a chiral metal-binding pocket where the bis(oxazoline) could chelate

the metal center. The (*Spartan*TM) model representation of **2.3o** in Figure 2.3.1 shows the oxazoline groups in a convergent geometry where the potential metal-binding site is surrounded by the chiral *iso*-propyl side chains. Once ring-closed to **2.3c**, the oxazoline groups should be rigidly held apart. In addition, the (*Spartan*TM) modelling of the rigid *ring-closed* isomer **2.3c** shows that even if a bidentate complex were to be formed, the chiral substituents on the oxazoline groups would not have a large influence on the metal center due to their spatial orientation diverging away from the possible binding center.

2.3.1 Synthesis of the C2 bis(oxazoline) DTE

The C2 bis(oxazoline) DTE **2.3o** was prepared by taking advantage of the *ortho*-directing reactivity of oxazolines on thiophenes to lithiation,⁴⁰ as shown in Scheme 2.3.1.



Scheme 2.3.1 Synthesis of C2 bis(oxazoline) DTE **2.3o**.

The oxazoline substituted thiophene **2.11** was prepared from 2-bromo-5-methylthiophene **2.8** in 33% overall yield. Following a lithium-halogen exchange of compound **2.8** quenched by CO_2 with acid workup yielding compound **2.9**, an acid-chloride coupling with L-valinol provided amide **2.10**, which was converted into thiophene oxazoline **2.11** using methanesulfonyl chloride (MsCl), triethylamine and a basic workup.⁴¹ Ligand **2.3o** was prepared in 46% yield in two steps from the thiophene oxazoline **2.11**, in a similar fashion to that described previously for compound **2.5** (Scheme 2.2.1), by trapping the lithiated product with octafluorocyclopentene.

2.3.2 Photochromic behaviour of the C2 bis(oxazoline) DTE

The changes in the absorption spectra accompanying the ring-closing reaction **2.3o**→**2.3c** were best monitored using UV-VIS spectroscopy. Irradiation of a CH₂Cl₂ solution of compound **2.3o** (9.9×10^{-6} M) with 313-nm light, using a hand-held UV lamp, resulted in a spontaneous colour change from colourless to deep red, as indicated by a decrease of high energy absorptions ($\lambda_{\text{max}} = 258$ nm) accompanied by an increase in the visible region absorptions ($\lambda_{\text{max}} = 505$ nm), as shown in Figure 2.3.2a.

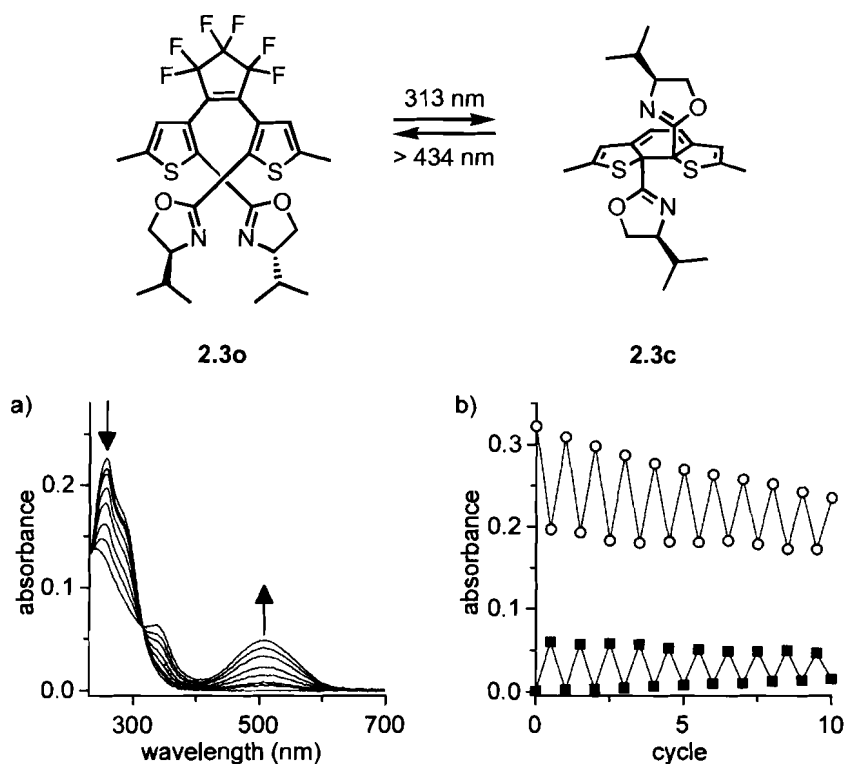


Figure 2.3.2 Changes in the UV-VIS absorption spectra of solutions of **2.3o** in CH₂Cl₂ upon irradiation with 313-nm light. (a) Total irradiation periods are 0, 1, 2, 5, 10, 20, 30 and 60 sec for a 9.9×10^{-6} M solution. (b) Modulated absorbance at 258 nm (○) and 505 nm (■) during alternate irradiation with 313-nm light for 30 sec, and > 434-nm light for 30 sec for a 1.7×10^{-5} M solution.

Irradiation for longer than 1 min did not result in additional changes in the absorption spectra of the solution, indicating that a photostationary state had

been reached. The original spectrum of **2.3o** could be regenerated by irradiating the solution with light of wavelengths greater than 434 nm from a 150-W tungsten source passed through a cutoff filter that removed higher energy light. Figure 2.3.2b illustrates the fatigue resistance of a CH₂Cl₂ solution of **2.3o** (1.7×10^{-5} M) to photochemical cycling. After ten cycles of ring-closing/ring-opening, the absorbance of **2.3o** had decreased to 73% of its initial value. While degradation is never desirable, a catalyst would not be required to cycle many times during a single reaction.

The photochemical interconversion between the *ring-open* isomer **2.3o** and the *ring-closed* isomer **2.3c** was also monitored by ¹H NMR spectroscopy. Irradiation of a CD₂Cl₂ solution of compound **2.3o** (3.1×10^{-3} M) with 313-nm light resulted in the appearance of a new set of signals for compound **2.3c** (the presence of two diastereomeric products is discussed in *Section 2.3.3*) including a singlet at 2.16 ppm, while the corresponding thiophene-C5 methyl singlet was at 2.43 ppm for compound **2.3o**, as illustrated in Figure 2.3.3.

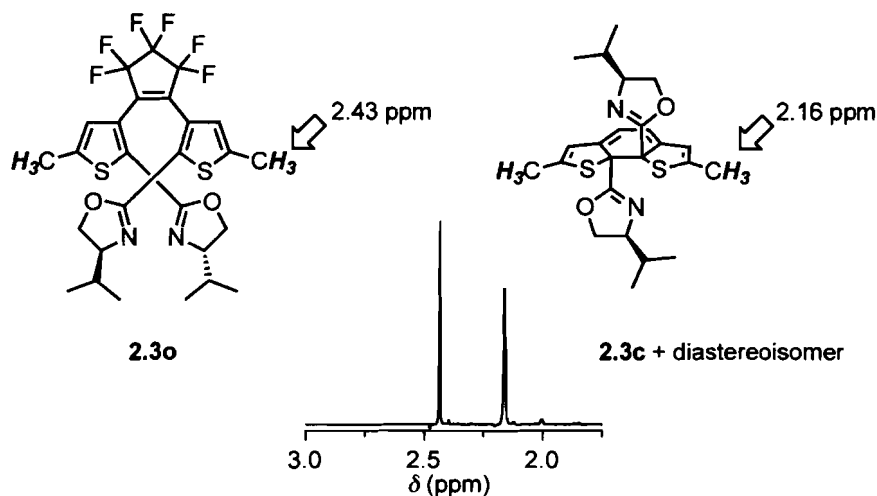


Figure 2.3.3 Selected region in the ^1H NMR spectrum obtained after irradiation of a CD_2Cl_2 solution of **2.3o** (3.1×10^{-3} M) with 313-nm light, highlighting the thiophene-C5 methyl singlet used in determining the extent of photoconversion. The perfluorinated portion of the cyclopentene ring is hidden from **2.3c** for clarity.

When additional irradiation of the solution with 313-nm light resulted in no further changes in the relative integration between the signals assigned to **2.3o** and **2.3c**, the photostationary state was determined to be a mixture of 59% of *ring-closed* isomer **2.3c** with the remaining 41% assigned to the *ring-open* isomer **2.3o**.

2.3.3 Metal complexation of C2 bis(oxazoline) DTE with copper

The copper(I) metal binding was studied by monitoring a titration of a solution of compound **2.3o** (1.4×10^{-2} M) with $\text{Cu}(\text{CH}_3\text{CN})_4\text{PF}_6$ using ^1H NMR spectroscopy. An addition of increasing amounts of copper until 1.0 molar equiv. was reached revealed that **2.3o** did not form a uniform bidentate complex as anticipated. Instead, ^1H NMR spectroscopy indicated the formation of a mixture of cuprous complexes, as could be seen from the multiple new signals illustrated in Figure 2.3.4. However, it did seem that a major component was formed since one set of peaks was quite larger than the other. Irradiation with 313-nm light did

not result in a spontaneous change in the colour of the solution. Only an extended irradiation of 20 min afforded a slight colouration, which was estimated to be 5% of the *ring-closed* isomer by integration of the peaks assigned to the resonance signals of this isomer.

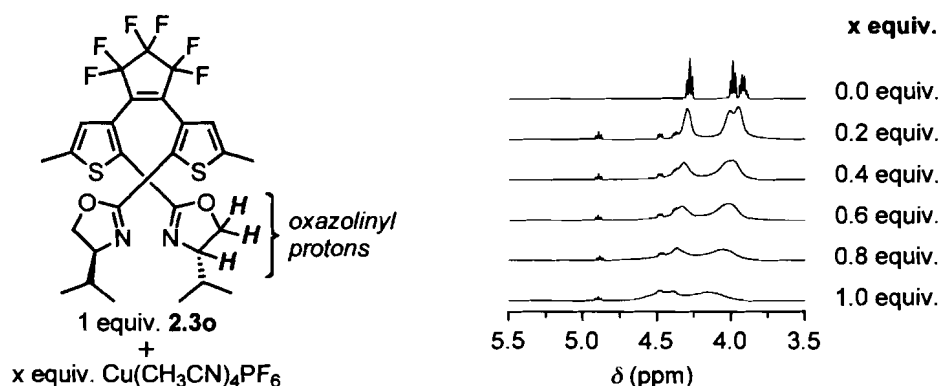


Figure 2.3.4 ^1H NMR study of the complex formation of **2.3o** (1.4×10^{-2} M) with increasing equivalents of $\text{Cu}(\text{CH}_3\text{CN})_4\text{PF}_6$ in CDCl_3 . A new distinct set of peaks appears as soon as the copper salt is added.

The inhibition of the ring-closing reaction could have been caused by the copper being too tightly bound within the ligand's chelation site to allow for photoswitching. The presence of the copper center would thus prevent the ligand from undergoing the necessary geometric changes required for the ring-closing reaction to proceed. Several unsuccessful attempts were made at crystallizing **2.3o** with metal salts to elucidate the nature of the complex formed in solution.

As discussed previously for compound **2.2o**, the copper(I) complexation might predispose the bis(oxazoline) geometrically for diastereoselectivity in the ring-closing reaction. Figure 2.3.5 describes the two diastereoisomers and the characteristic separate peaks observed for the thiophene proton.

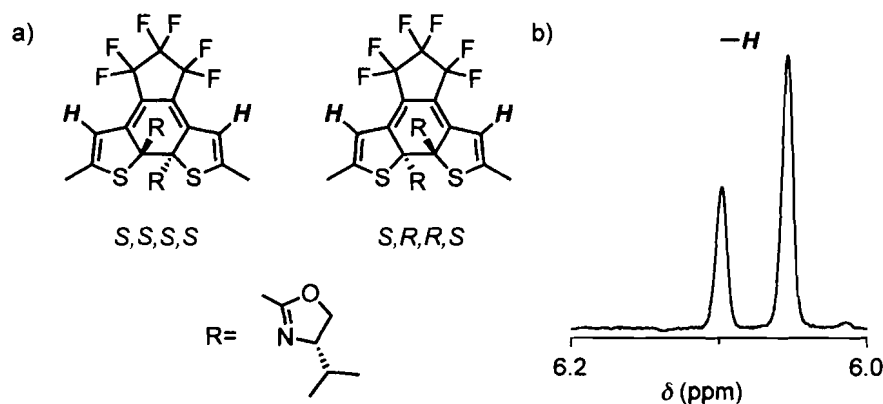


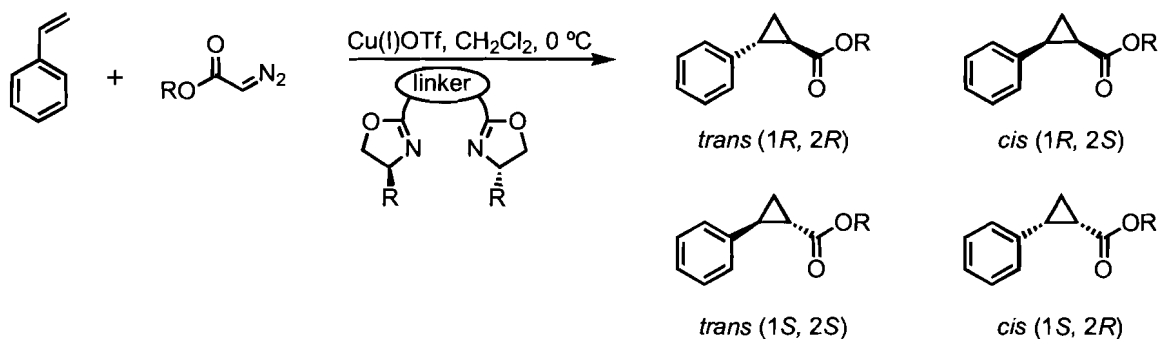
Figure 2.3.5 The two possible diastereoisomeric products **2.3c** of the ring-closing reaction, where the thiophene proton producing distinct signals for the two diastereoisomers is highlighted. (a) geometry of the diastereoisomers and (b) the ^1H NMR signal of the thienyl proton generated with 313-nm light in the absence of copper.

A CH_2Cl_2 solution of compound **2.3o** (1.3×10^{-2} M) and 1.0 molar equiv of $\text{Cu}(\text{I})\text{OTf}$ was irradiated with 313-nm light for 15 min. The ring closure was only possible by adding a small amount (5-10%) of the more competitive coordinating solvent, CH_3CN , to the solution providing a conversion to compound **2.3c** of 6-8%. Once the copper was removed, using an excess of ammonium hydroxide, the d.e. of the ring-closed products **2.3c** showed a decrease from 30% without copper to 0% with copper. This result indicated that while the ring-closing of the free ligand displayed a certain diastereoselectivity, the copper(I) complex possibly favoured the opposite diastereoselectivity, thus coincidentally cancelling the net effect of both. Since the stereoselectivity was only 30% in the absence of a metal, the difference in energy is relatively small between the two possible diastereoisomers and might be due to slightly differing energies in the geometries approaching the transition state of the ring-closing reaction.⁴² The internal chiral oxazolines are adjacent to the new bond being formed from the electrocyclozation and could influence the stereoselectivity of its formation by steric effects.

2.3.4 Photocontrol of catalysis with C2 bis(oxazoline) DTE

At the ligand concentrations used in the catalysis experiments, 1.3×10^{-2} M in CH_2Cl_2 , irradiation with 313-nm light for 15 min resulted in a 23% conversion from compound **2.3o** to compound **2.3c** in the absence of copper. As described in the previous section, this ring-closing reaction was only possible either without copper or with copper and the addition of small amounts of CH_3CN (5 vol%). It was expected that the diastereoselectivity of the reaction would be diminished if CH_3CN displaced the ligand from the metal center. Purification of the *ring-closed* isomer **2.3c**, determined to be up to 97% by ^1H NMR spectroscopy, was performed by centrifugal chromatography and allowed for comparison between the *ring-open* isomer **2.3o** and *ring-closed* isomer **2.3c**. In order to verify the hypothesis that the chelation of the *ring-open* bis(oxazoline) **2.3o** provided diastereoselectivity, reactions were set up with the same conditions reported previously for **2.2o** (results included in Table 2.3.1): slow addition of ethyldiazoacetate over 6 h, using an injection pump, to a mixture of 10 mol% $\text{Cu}(\text{I})\text{OTf}$ and 11 mol% of bis(oxazoline) **2.3o** or a mixture of **2.3o** and **2.3c**. The ratio of *trans* to *cis* products was determined by ^1H NMR spectroscopy from the crude mixture, whereas the mixture had to be purified by using a short plug (SiO_2) to remove the catalyst and the excess of styrene in order to have a suitable for HPLC. The results of the stereoselective cyclopropanation reactions are listed in Table 2.3.1.

Table 2.3.1 Cyclopropanation product distribution.



ligand ^a	area (%) ^b				ee(%)		d.r. ^c trans:cis
	trans 1R, 2R ^d	trans 1S, 2S ^d	cis 1R, 2S ^d	cis 1S, 2R ^d	trans	cis	
2.2o	37	39	13	11	2	8	n/o ^e
2.3o	45	26	22	7	27	50	55:45
2.3o/2.3c^f	37	29	24	10	11	39	70:30
2.3c^g	36	32	17	15	5	5	63:37
2.3o/CH₃CN^h	36	22	32	10	23	51	n/o ^e
2.3o/2.3c/CH₃CNⁱ	34	28	29	9	10	53	n/o ^e

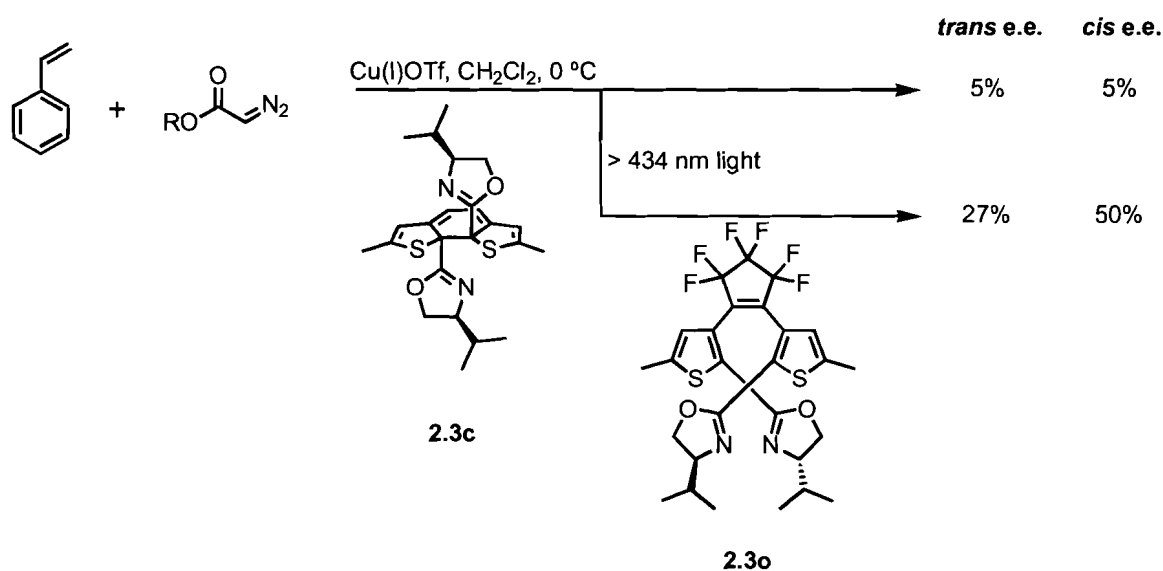
^aThe ligand indicates which bis(oxazoline) was used in the cyclopropanation reaction. ^bThese values were normalized to include only the four cyclopropanation products from a purified sample. ^cThe diastereomeric ratio was determined from a crude reaction mixture using ¹H NMR spectroscopy. ^dMajor products determined by comparing to literature precedent.³⁷ ^en/o indicates that the diastereomeric ratio was not obtained from the crude mixture. ^fThe ligand used was a mixture of 77% *ring-open* isomer **2.3o** and 23% *ring-closed* isomer **2.3c**, as determined from ¹H NMR spectroscopy, resulting from irradiating compound **2.3o** in dichloromethane for 15 min prior to adding copper and styrene. ^gThe *ring-closed* isomer **2.3c** was purified by centrifugal chromatography. ^hAcetonitrile (5 vol%) was added as a binding competitor solvent. ⁱThe ligand used was a mixture of 94% *ring-open* isomer **2.3o** and 6% *ring-closed* isomer **2.3c**, as determined from ¹H NMR spectroscopy, resulting from irradiating compound **2.3o** in dichloromethane with acetonitrile (5 vol%) for 15 min prior to adding copper and styrene.

While the complexation studies indicated that the metal complex of ligand **2.3o** with copper was tightly bound, it appeared that the geometry present in solution provided only limited low stereoselectivities (Table 2.3.1). However, there were obvious changes in the stereoselectivity of the products depending on the extent of conversion of **2.3o** to **2.3c** obtained by irradiation with 313-nm light. When pure *ring-open* ligand **2.3o** was used, the enantiomeric excess (e.e.) for

the *trans* products was 30% and 50% for the *cis* products. Irradiating the solution with 313-nm light for 15 min, before the addition of copper, provided a conversion to the *ring-closed* isomer **2.3c** of 23%. This mixture of **2.3o** and **2.3c** decreased the *trans* e.e. to 11% and the *cis* e.e. to 39%. When a sample of one of the diastereoisomers of the *ring-closed* isomer **2.3c** (97% with the remaining 3% assigned to the *ring-open* isomer **2.3o**) was used as a ligand, both the *trans* and *cis* e.e. dropped to 5%, which was about the same as the error range for the detector. This low percentage indicated that the reaction was catalyzed by either the free or monocoordinated copper(I), thus resulting in a racemic product mixture. There seemed to be no clear correlation between the ligand and the diastereomeric ratio obtained. Addition of a small amount of CH₃CN (5 vol%) was essential for the ring closure to take place in the presence of copper. With pure *ring-open* **2.3o**, the *trans* e.e. decreased to 23%. This effect could be attributed to the more labile complex formed because of the binding competition provided by CH₃CN. After a 15-min irradiation with 313-nm light in the presence of copper, the resulting ligand solution, containing 6% of **2.3c**, resulted in a *trans* e.e. of 10%. These results clearly demonstrated that the product distribution was directly affected by the isomeric state of the bis(oxazoline).

The next experiment verified the possibility of controlling the catalyst's reactivity reversibly with light *in situ*. Proceeding with the same reaction conditions as described above for a solution of 97% **2.3c**, an aliquot (0.5 mL) was extracted and analyzed after 3 h, at which point half of the ethyldiazoacetate had been added. At the same time, the solution mixture was irradiated with >

434-nm light for 15 min to ring-open compound **2.3c** to compound **2.3o**, illustrated in Scheme 2.3.2.



Scheme 2.3.2 *In situ* photocontrol of the ligands **2.3o** and **2.3c** used in the catalytic cyclopropanation of styrene with ethyldiazoacetate. The perfluorinated portion of the cyclopentene ring is hidden in **2.3c** for clarity. The *ring-closed* isomer **2.3c** was converted into the *ring-open* isomer **2.3o** *in situ* using light of wavelengths greater than 434 nm.

As expected, minimal stereoselectivity, 5% e.e. for both the *cis* and *trans* products, was obtained in the presence of 97% **2.3c** after the initial 3 h. Ring opening the ligand to compound **2.3o** did regenerate the stereoselectivity, 50% and 27%, for the *cis* and the *trans* products, respectively. These results were very consistent with those presented above in Table 2.3.1, indicating that the metal-ligand complex could be controlled *in situ*.

2.4 Conclusion

When trying to find a photoresponsive chelating chiral ligand to affect the stereoselective outcome of a catalytic reaction, it was demonstrated that the very design of the ligand could strongly influence the nature of the complexation to the

metal. With a bis(oxazoline) DTE having C5 substitution, **2.2o**, the possibility of forming a double helicate and the arrangement of the oxazolyl groups around the metal center in such a complex provided no stereoselectivity in the catalysis. A different bis(oxazoline) DTE derivative, **2.3o** having the oxazoline groups in the C2 positions on the thiophene ring, provided different metal-chelation geometry, resulting in a restricted chiral environment about the metal center, thus influenced the stereochemical outcome of a catalytic cyclopropanation of styrene with ethyldiazoacetate. The complex formed between compound **2.3o** and copper was tightly bound, hence preventing the photoconversion to compound **2.3c**. The addition of a binding competitor solvent, CH₃CN in this case, restored the photochromism of compound **2.3o** in the presence of copper, but decreased the stereoselectivity in the product distribution of the catalytic reaction. A significant difference in the stereoselectivity in the products was observed between the *ring-open* and *ring-closed* isomers, and controlling the isomeric form was achieved *in situ* with light.

2.5 Future work

A first improvement for the bis(oxazoline) ligands presented above would be to prepare *t*-butyl substituted oxazoline derivatives, which are known to provide higher e.e. than *iso*-propyl in most studies.²⁸⁻³⁰ This increased stereoselectivity is attributed to the larger steric bulk provided by a *t*-butyl group compared to that of an *iso*-propyl group.

Another variation for a bis(oxazoline) DTE would be to attach both oxazoline groups on the same thiophene ring as depicted below in Figure 2.5.1.

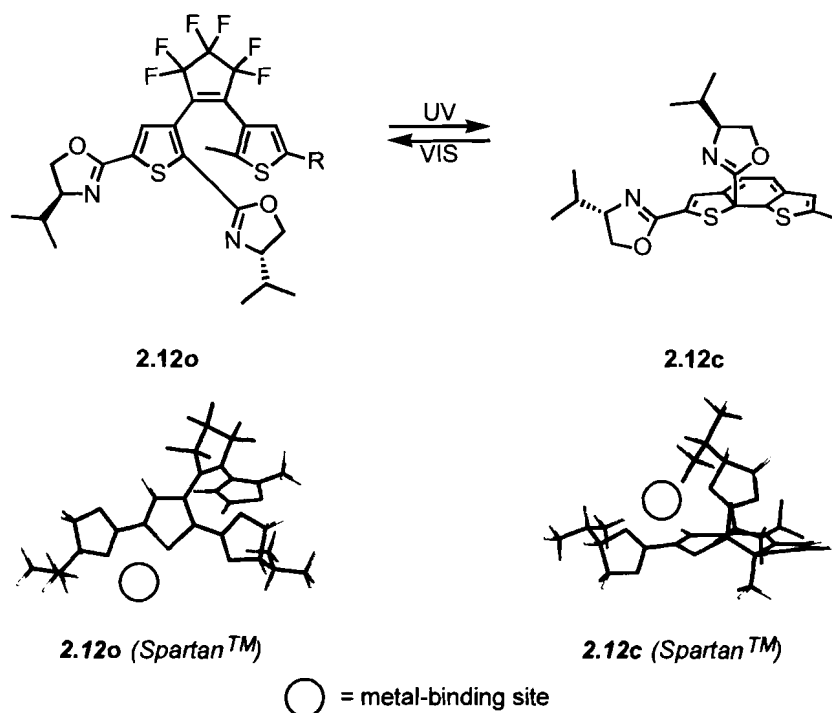


Figure 2.5.1 Different metal-binding possibilities for the proposed DTE **2.12o** and **2.12c**. The perfluorinated portion of the cyclopentene ring is hidden from **2.12c** for clarity. Molecular model representations, generated using Spartan™ '02 for Macintosh, highlight the geometrical arrangements for the metal-binding geometries.

A system incorporating C2 and C5 oxazolines on the same thiophene provides a rigid-to-rigid control over chelation. Implementing such a system would decrease the extent of rearrangement required between the two photoisomers due to a limited free rotation in either isomer. The Spartan™ modelling suggests that the bite angle, or the geometrical orientation of the *iso*-propyl groups relative to the binding pocket would be smaller for compound **2.12c**, where the oxazoline groups are closer to the binding site, compared to compound **2.12o**. This steric difference could affect the stereoselective outcome of a catalytic reaction using this photoresponsive catalyst depending on the isomeric form of the ligand.

2.6 Experimental

2.6.1 General

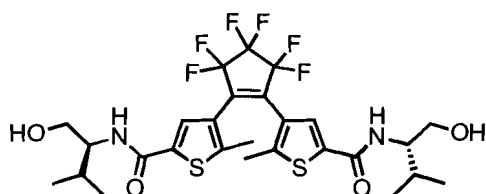
All solvents used for synthesis and characterization were dried and degassed by passing them through steel columns containing activated alumina under nitrogen using an MBraun solvent purification system. Solvents for NMR analysis (Cambridge Isotope Laboratories) were used as received. All reagents were purchased from Aldrich with the exception of octafluorocyclopentene, which was provided by Nippon Zeon Corporation. The starting materials, 3-bromo-2-methyl-5-chlorothiophene **2.4**,³⁵ was prepared according to the literature procedure.

2.6.2 Methods

¹H NMR and ¹³C NMR characterizations were performed on a Bruker AMX 400 instrument with a 5 mm inverse probe operating at 400.13 MHz for ¹H NMR and 100.6 MHz for ¹³C NMR; a Varian 400 MercuryPlus instrument with a 5 mm ATB probe equipped with a shielded gradient operating at 400.10 MHz for ¹H NMR and 100.60 MHz for ¹³C NMR; or a Varian Inova 500 instrument with a 5 mm inverse probe equipped with a shielded gradient operating at 499.8 MHz for ¹H NMR and 125.7 MHz for ¹³C NMR. Chemical shifts (δ) are reported in parts per million relative to tetramethylsilane using the residual solvent peak as a reference standard. Coupling constants (J) are reported in Hertz. FT-IR spectroscopy was performed using a Nicolet Nexus 670 instrument. UV-VIS absorption spectroscopy was performed using a Varian Cary 300 Bio spectrophotometer. Low resolution mass spectrometry (LRMS) measurements

were performed using a HP5985 mass spectrometer with isobutane as the chemical ionization source, a Varian 4000 GC/MS/MS with electron impact operating at 10 mamp as the ionization source or chemical ionization (CI) with methanol or a PerSeptive Biosystems Voyager-DE Biospectrometry Workstation MALDI spectrometer using a 2,4-dihydroxybenzoic acid matrix. Melting points were measured using a Fisher-Johns melting point apparatus. Flash chromatography was performed using silica gel 60 (230–400 mesh) from Silicycle Inc. Centrifugal chromatography was performed using a Harrison Research Inc. Chromatotron, model 8924 using TLC grade 7749 silica gel from Merck. HPLC analyses were performed using a Waters 1515 HPLC pump connected in series with a Waters 2487 Absorbance detector and equipped with a CHIRACEL-OD chiral column. Standard hand-held lamps used for visualizing TLC plates (Spectroline E-series, 470 mW/cm²) were used to carry out the ring-closing reactions at 313 nm. The ring-opening reactions were carried out using the light of a 150-W tungsten source that was passed through a 434-nm cutoff filter to eliminate higher energy light. Microanalyses were performed on a Carlo Erba Model 1106 CHN analyser. Optical rotations measurements were performed at room temperature using a Perkin Elmer 341 polarimeter.

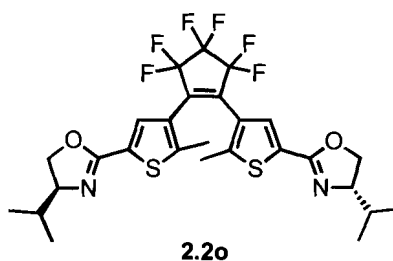
2.6.3 Syntheses and experiments



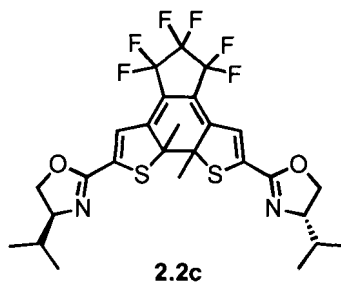
2.7

Synthesis of (S,S)-1,2-bis(5'-((1-hydroxy-3-methylbutan-2-yl)carbamoyl)-2-methylthiophen-3-yl)perfluorocyclopent-1-ene (2.7).³⁴ A suspension of compound **2.6** (200 mg, 0.44 mmol) in anhydrous DMF (150 μ L) and anhydrous CH_2Cl_2 (40 mL) was treated dropwise with a solution of oxalyl chloride (3.0 mL, 2 M in CH_2Cl_2 , 6.1 mmol) at 0 $^\circ\text{C}$ over 5 min under an N_2 atmosphere. The cooling bath was removed and the reaction mixture was allowed to slowly warm to room temperature and stirred there for 16 h, at which time it was evaporated to dryness *in vacuo* and dried under high vacuum (10 mm Hg) for 18 h. The crude acid chloride was taken up in anhydrous CH_2Cl_2 (10 mL) and was added dropwise over 30 min to a 0 $^\circ\text{C}$ solution of (S)-2-amino-3-methylbutanol, L-valinol, (26 mg, 0.25 mmol) in CH_2Cl_2 (10 mL) and NEt_3 (52 μ L, 0.71 mmol). The solution was allowed to slowly warm to room temperature and then it was washed with H_2O (50 mL) and extracted with CH_2Cl_2 (2 \times 25 mL). The combined organic layers were washed with brine (25 mL), dried over Na_2SO_4 , filtered and evaporated to dryness *in vacuo*. Purification by flash chromatography (SiO_2 , 5% methanol in CH_2Cl_2) yielded 69 mg (80%) of **2.7** as a white solid. M.p. = 42–45 $^\circ\text{C}$. ^1H NMR (CDCl_3 , 500 MHz) δ 7.31 (s, 2H), 6.54 (d, J = 9 Hz, 2H), 3.78–3.85 (m, 2H), 3.73 (d, J = 4 Hz, 4H), 3.14 (br s, 2H), 2.05 (s, 6H), 1.84–2.94 (m, 4H), 0.98 (d, J = 7 Hz, 6H), 0.95 (d, J = 7 Hz, 6H). ^{13}C NMR (CDCl_3 , 125 MHz) δ

161.5, 146.7, 137.0, 128.0, 125.1, 63.0, 57.4, 29.2, 19.5, 19.2, 14.8 (11 of 14 found). FT-IR (KBr-cast): 3332, 2964, 2876, 1639, 1630, 1556, 1275, 1194, 1141, 1126, 1084, 1041, 987, 902, 748 cm^{-1} . LRMS (MALDI) $m/z = 627 [M+1]^+$. $[\alpha]_D^{20} = -48^\circ$ ($c = 2.1 \times 10^{-3}$ in CH_2Cl_2).



Synthesis of C5 bis(oxazoline) DTE 2.2o. A solution of **2.7** (420 mg, 0.7 mmol) in anhydrous CH_2Cl_2 (50 mL) at 0 °C was treated with thionyl chloride (SOCl_2) (339 mg, 2.9 mmol) and the reaction was stirred at this temperature for 2 h. The solution was allowed to slowly warm to room temperature at which point a saturated aqueous solution of NaHCO_3 (40 mL) was added and the mixture was stirred for 1 h. The organic layer was washed with H_2O (2 \times 40 mL), dried over Na_2SO_4 , filtered and evaporated to dryness *in vacuo*. Purification by flash chromatography (SiO_2 , 20% EtOAc in hexanes) yielded 320 mg (81%) of **2.2o** as a white solid. M.p. = 117–120 °C. ^1H NMR (CD_2Cl_2 , 400 MHz) δ 7.50 (s, 2H), 4.40 (dd, $J = 8, 9$ Hz, 2H), 4.10 (t, $J = 8$ Hz, 2H), 3.98-4.05 (m, 2H), 1.93 (s, 6H), 1.74-1.83 (m, 2H), 1.00 (d, $J = 7$ Hz, 6H), 0.90 (d, $J = 7$ Hz, 6H). ^{13}C NMR (CD_2Cl_2 , 100 MHz) δ 159.6, 148.1, 131.2, 131.1, 126.9, 74.9, 72.9, 34.8, 20.6, 20.0, 16.4. (11 of 14 found). FT-IR (KBr-cast): 3424, 2962, 2932, 2874, 1656, 1650, 1644, 1468, 1356, 1274, 1193, 1119, 1065, 1033, 986, 949, 894, 744 cm^{-1} . LRMS (CI) $m/z = 591 [M+1]^+$. $[\alpha]_D^{20} = -53^\circ$ ($c = 0.8 \times 10^{-3}$ in CH_2Cl_2).



Synthesis of the *ring-closed* isomer 2.2c. A solution of compound **2.2o** (1.0 mg, 1.7×10^{-3} mmol) in CD_2Cl_2 (0.75 mL) was placed in a 5-mm NMR tube and irradiated with 313-nm light for 5 min yielding a solution of the photostationary state containing 87% of the *ring-closed* **2.2c** as a mixture of diastereoisomers according to the ^1H NMR spectrum. The remaining 13% was assigned to the *ring-open* isomer **2.2o**. The ring-closed isomers were not purified or isolated. ^1H NMR (CD_2Cl_2 , 500 MHz) δ 6.70 (s, 2H), 4.39-4.43 (m, 2H), 4.01-4.12 (m, 4H), 2.18 (s, 3H), 2.16 (s, 3H), 1.74-1.82 (m, 2H), 0.99 (d, $J = 6.5$ Hz, 6H), 0.89 (dd, $J = 3, 7$ Hz, 6H).

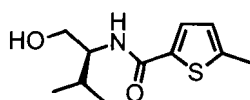
Metal complexation study of 2.2o with copper(I). A CD_2Cl_2 solution of *ring-open* isomer **2.2o** (1.3×10^{-2} M) was prepared by dissolving **2.2o** (7.6 mg, 1.3×10^{-2} mmol) in CD_2Cl_2 (1 mL) in a volumetric flask. Similarly, a 1.3×10^{-2} M solution of $\text{Cu}(\text{CH}_3\text{CN})_4\text{PF}_6$ was prepared by dissolving (24.7 mg, 6.6×10^{-2} mmol) in CD_2Cl_2 (5 mL) in a volumetric flask. A solution of **2.2o** (0.5 mL, 6.4×10^{-3} mmol) in an NMR tube was treated with aliquots ($5 \times 100 \mu\text{L}$) of the $\text{Cu}(\text{CH}_3\text{CN})_4\text{PF}_6$ solution until 1 molar equiv. was added ($500 \mu\text{L}$, 6.7×10^{-3} mmol).

Ring closure of 2.2o in the presence of copper(I). A solution of **2.2o** (7.9 mg, 1.3×10^{-2} mmol) in CH_2Cl_2 (1 mL) was treated with $\text{CuOTf} \cdot 1/2\text{C}_6\text{H}_6$ (6.1 mg, 1.2

$\times 10^{-2}$ mmol) and stirred for 20 min, at which point the solution was irradiated for 15 min with 313-nm light. Then, 3 drops of NH_4OH were added to the solution and the mixture was stirred for 10 min. The solvent was washed with water (2 mL) and the organic layer was dried with anhydrous Na_2SO_4 , at which point the solvent was evaporated *in vacuo*. The extent of ring-closure was determined to be 42% by ^1H NMR spectroscopy. The diastereoisomeric ratio could be determined from the ^1H NMR signals at 2.18 and 2.16 ppm taken on the crude sample. No attempt was made to isolate and characterize the pure diastereoisomers.

Catalytic experiments using 2.2o as ligand. In a typical reaction, the oxazoline ligand **2.2o** (7.6 mg, 1.29×10^{-2} mmol) was dissolved in CH_2Cl_2 (1 mL) and $\text{CuOTf} \cdot 1/2\text{C}_6\text{H}_6$ (5.5 mg, 1.09×10^{-2} mmol, 10 mol%) was added. The solution was cooled to 0 °C in an ice bath and stirred for 30 min at which time an excess of styrene (100 μL , 0.87 mmol) was added. After stirring for an additional 30 min, ethyldiazoacetate (10 μL , 0.07 mmol) in CH_2Cl_2 (1 mL) was added using a syringe pump over 6 h while maintaining the solution at 0 °C. The solution was stirred overnight at 25 °C, then filtered through a small plug (SiO_2 , CH_2Cl_2). The excess styrene was removed by gradient flash chromatography (SiO_2 , 100% hexanes to 1:1 hexanes/EtOAc). Both the *cis* and the *trans* enantiomeric mixtures were analyzed by chiral HPLC using a CHIRACEL-OD chiral column (0.5 mL \cdot min $^{-1}$, 95:5 hexanes/2-propanol). Detection was adjusted at 220 nm, which is a maximum in the absorption spectrum of the *trans* diastereoisomers. A solution of *trans* enantiomers gave two peaks separated in their retention times

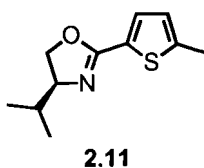
by 3.7 min. The *cis* isomers were only separated by 0.4 min and were not baseline separated. It was however possible to distinguish both maxima and by deconvoluting the data using the software (Breeze™) provided with the HPLC, the separate peak areas were obtained.



2.10

Synthesis of (S)-N-(1-hydroxy-3-methylbutan-2-yl)-5-methylthiophene-2-carboxamide (2.10). A suspension of compound **2.9** (2.5 g, 23 mmol) in anhydrous DMF (250 μ L) and anhydrous CH_2Cl_2 (50 mL) was treated dropwise with a solution of oxalyl chloride (57 mL, 2 M in CH_2Cl_2 , 114 mmol) under an N_2 atmosphere over 5 min at 0 $^\circ\text{C}$, then the cooling bath was removed and the reaction mixture was slowly warmed to room temperature and stirred there for 16 h, at which point it was evaporated to dryness *in vacuo* and dried under high vacuum (10 mm Hg) for 2 h. The crude acid chloride was taken up in anhydrous CH_2Cl_2 (20 mL) and was added dropwise over 30 min to a 0 $^\circ\text{C}$ solution of (S)-2-amino-3-methylbutanol, L-valinol, (1.8 g, 17 mmol) in CH_2Cl_2 (100 mL) and NEt_3 (14 mL, 102 mmol). The solution was allowed to slowly warm to room temperature. Then it was washed with H_2O (50 mL) and extracted with CH_2Cl_2 (2 \times 25 mL). The combined organic layers were washed with brine (25 mL), dried over Na_2SO_4 , filtered and evaporated to dryness *in vacuo*. Purification by flash chromatography (SiO_2 , 10% methanol in CH_2Cl_2) yielded 2.2 g (43%) of **2.10** as a yellow oil. M.p. oil. ^1H NMR (CDCl_3 , 500 MHz) δ 7.33 (d, J = 3.5 Hz, 1H), 6.71 (d, J = 3.5 Hz, 1H), 6.19 (d, J = 8 Hz, 1H), 3.83-3.88 (m, 1H), 3.72-3.79 (m, 2H),

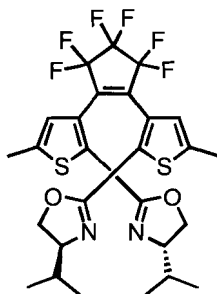
2.49 (s, 3H), 1.94-2.01 (m, 1H), 1.00 (d, $J = 7$ Hz, 3H), 0.98 (d, $J = 7$ Hz, 3H). ^{13}C NMR (CDCl_3 , 125 MHz) δ 162.8, 145.4, 136.0, 128.5, 126.0, 63.8, 57.5, 29.2, 19.6, 18.9, 15.6. FT-IR (KBr-cast): 3325, 2960, 2873, 1639, 1626, 1552, 1463, 1316, 1124, 1079, 809, 746 cm^{-1} . LRMS (CI) $m/z = 228$ $[\text{M}+1]^+$. $[\alpha]_D^{20} = -52^\circ$ ($c = 3.5 \times 10^{-3}$ in CH_2Cl_2).



Synthesis of (S)-4-isopropyl-2-(5-methylthiophen-2-yl)-4,5-dihydrooxazole

(2.11). A solution of compound **2.10** (2.0 g, 9 mmol) in anhydrous CH_2Cl_2 (50 mL) and anhydrous NEt_3 (2.5 mL, 18 mmol) was treated with methanesulfonyl chloride (MsCl) (0.8 mL, 11 mmol) at 0 °C over 30 min. The solution was allowed to warm to room temperature and was further stirred for 3 h, at which point the solution was evaporated to dryness *in vacuo*. The crude was taken up in methanol (50 mL) to which was added KOH (2.5 g, 44 mmol), followed by stirring for 15 h at room temperature, at which point the solution was evaporated *in vacuo*. Purification by flash chromatography (SiO_2 , 33% EtOAc in hexanes) yielded 1.5 g (81%) of **2.11** as clear colourless crystals. M.p. = 42–44 °C. ^1H NMR (CDCl_3 , 500 MHz) δ 7.37 (d, $J = 3$ Hz, 1H), 6.71 (d, $J = 3$ Hz, 1H), 4.35 (dd, $J = 8, 9$ Hz, 1H), 4.03-4.11 (m, 2H), 2.50 (s, 3H), 1.81-1.88 (m, 1H), 1.00 (d, $J = 7$ Hz, 3H), 0.90 (d, $J = 7$ Hz, 3H). ^{13}C NMR (CDCl_3 , 125 MHz) δ 159.0, 144.7, 130.3, 127.9, 125.9, 72.6, 70.2, 32.7, 19.0, 17.9, 15.5. FT-IR (KBr-cast): 3440,

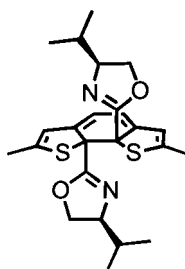
2954, 2893, 2868, 1649, 1644, 1478, 1354, 1315, 1259, 1223, 1068, 1026, 1012, 947, 804 cm^{-1} . LRMS (CI) $m/z = 210$ $[\text{M}+1]^+$. $[\alpha]_D^{20} = -61^\circ$ (1.2×10^{-3} in CH_2Cl_2).



2.3o

Synthesis of C2 bis(oxazoline) DTE 2.3o. A solution of **2.11** (500 mg, 2.6 mmol) in anhydrous THF (25 mL) was treated dropwise with *n*-butyllithium (1.1 mL, 2.5 M in hexanes, 2.8 mmol) over 5 min at -78°C under an N_2 atmosphere. The resulting solution was stirred at this temperature for 30 min then quickly treated with octafluorocyclopentene (170 μL , 1.3 mmol) in one portion using a gas-tight syringe cooled with dry ice. After stirring at this temperature for 1 h, the cooling bath was removed and the reaction was allowed to slowly warm to room temperature and stirred there for 1 h, at which time it was quenched with saturated aqueous NH_4Cl (20 mL). The aqueous layer was separated and extracted with EtOAc (2 \times 20 mL). The combined organic layers were dried over Na_2SO_4 , filtered and evaporated to dryness *in vacuo*. Purification by flash chromatography (SiO_2 , 20% EtOAc in hexanes) followed by crystallization from hexanes yielded 160 mg (46%) of **2.3o** as clear colourless crystals. M.p. = $151\text{--}153^\circ\text{C}$. ^1H NMR (CDCl_3 , 400 MHz) δ 6.63 (s, 2H), 4.28 (dd, $J = 8, 8$ Hz, 2H), 3.99 (t, $J = 8$ Hz, 2H), 3.92 (m, 2H), 2.43 (s, 6H), 1.74 (m, 1H), 0.97 (d, $J = 7$ Hz, 6H), 0.87 (d, $J = 7$ Hz, 6H). ^{13}C NMR (CD_2Cl_2 , 125 MHz) δ 157.5, 143.9,

128.9, 128.2, 127.7, 73.2, 71.0, 33.3, 18.9, 18.6, 15.5 (11 of 14 found). FT-IR (KBr-cast): 3426, 2963, 2929, 2878, 1645, 1480, 1401, 1269, 1186, 1119, 1059, 968, 863, 738, 620 cm^{-1} . LRMS (CI) $m/z = 591$ $[\text{M}+1]^+$. Anal. calcd. for $\text{C}_{27}\text{H}_{28}\text{F}_6\text{N}_2\text{O}_2\text{S}_2$: C, 54.90; H, 4.78; N, 4.74. Found: C, 54.69; H, 4.73; N, 4.55. $[\alpha]_D^{20} = +26^\circ$ ($c = 3.7 \times 10^{-3}$ in CH_2Cl_2).



2.3c + diastereoisomer

Synthesis of the *ring-closed* 2.3c diastereoisomers. A solution of compound **2.3o** (1.8 mg, 3.1×10^{-3} mmol) in CD_2Cl_2 (1.0 mL) was placed in a 5-mm NMR tube and irradiated with 313-nm light for 5 min yielding a solution of the photostationary state containing 59% of the *ring-closed* isomer **2.3c** according to the ^1H NMR spectrum. The remaining 41% was assigned to the *ring-open* isomer **2.3o**. One of the *ring-closed* diastereoisomers could be purified up to 97% by centrifugal chromatography (SiO_2 , 5% MeOH in CH_2Cl_2) with the remainder 3% assigned to the *ring-open* isomer. ^1H NMR (CD_2Cl_2 , 500 MHz) δ 6.05 (s, 2H), 4.23 (dd, $J = 8.5, 10$ Hz, 2H), 3.98 (dd, $J = 8, 8.5$ Hz, 2H), 3.85-3.90 (m, 2H), 2.16 (s, 6 H), 1.63-1.70 (m, 2H), 0.86 (d, $J = 6.5$ Hz, 6H), 0.83 (d, $J = 6.5$ Hz, 6H).

Metal complexation study of 2.3o with copper(I). A CD_2Cl_2 solution of *ring-open* isomer **2.3o** (1.4×10^{-2} M) was prepared by dissolving compound **2.3o** (8.1

mg, 1.4×10^{-2} mmol) in CD_2Cl_2 (1 mL) in a volumetric flask. Half of the solution of **2.3o** (0.5 mL, 6.9×10^{-3} mmol), in an NMR tube, was treated with aliquots ($5 \times 100 \mu\text{L}$) of $\text{Cu}(\text{CH}_3\text{CN})_4\text{PF}_6$ solution, the same copper(I) solution (1.3×10^{-2} M) used for **2.2o**, until 1 molar equiv. was added ($500 \mu\text{L}$, 6.7×10^{-3} mmol).

Ring closure of 2.3o in the presence of copper(I). A solution of compound **2.3o** (7.7 mg, 1.3×10^{-2} mmol) in CH_2Cl_2 (1 mL) and CH_3CN ($50 \mu\text{L}$) was treated with $\text{CuOTf} \cdot 1/2\text{C}_6\text{H}_6$ (6.1 mg, 12.1×10^{-3} mmol) and stirred for 20 min, at which point the solution was irradiated for 15 min with 313-nm light. Then, 3 drops of NH_4OH were added to the solution and the mixture was stirred for 10 min. The solvent was washed with water (2 mL) and the organic layer was dried with anhydrous Na_2SO_4 , at which point the solvent was evaporated *in vacuo*. The extent of ring-closure was determined to be 5% by ^1H NMR spectroscopy. The diastereoisomeric ratio could be determined from the ^1H NMR signals at 6.06 and 6.10 ppm taken on the crude sample. No attempt was made to isolate and characterize the pure diastereoisomers.

Catalytic experiments using compound 2.3o as a ligand. Using the same methodology described above for compound **2.2o**, the oxazoline ligand **2.3o** (7.6 mg, 1.3×10^{-2} mmol) was dissolved in CH_2Cl_2 (1 mL) and $\text{CuOTf} \cdot 1/2\text{C}_6\text{H}_6$ (5.5 mg, 1.1×10^{-2} mmol, 10 mol%) was added. The solution was cooled to in an ice bath and stirred for 30 min at which time an excess of styrene ($100 \mu\text{L}$, 0.87 mmol) was added. After stirring for an additional 30 min, ethyldiazoacetate ($10 \mu\text{L}$, 0.07 mmol) in CH_2Cl_2 (1 mL) was added using a syringe pump over 6 h while maintaining the solution at 0°C . The solution was stirred overnight at 25

°C, then filtered through a small plug (SiO₂, CH₂Cl₂). The excess styrene was removed by gradient flash chromatography (SiO₂, 100% hexanes to 1:1 hexanes/EtOAc). The amount of catalyst could be lowered to 1 mol% with respect to the ethyldiazoacetate to produce 120 mg (63%) of the cyclopropanated products as a mixture of stereoisomers after workup and isolation by centrifugal chromatography (2% EtOAc in hexanes).

3 Synthesis and Coordination Chemistry of a Photoswitchable Bis(phosphine) Ligand

The research presented in this chapter was reproduced in part with permission “*Inorganic Chemistry*, Copyright 2005 American Chemical Society” from: Sud, D.; McDonald, R.; Branda, N. R. “Synthesis and Coordination Chemistry of a Photoswitchable Bis(phosphine) Ligand” *Inorg. Chem.* **2005**, *44*, 5960-5962.

3.1 Dithienylethene ligands

Because metal-coordination complexes provide their own assortment of photophysical and electrochemical characteristics and because the metal centers' properties are highly sensitive to the steric and electronic nature of their associated ligands,⁴³ developing tunable coordination complexes by combining a switching ligand with a metal ion will advance the use of coordination compounds in optoelectronics as well as in chemical reactivity and metal catalysis. In this regard, the DTE backbone could be integrated into the design of photoregulated catalysts and reagents because it exhibits dramatic steric and electronic differences between two interconverting isomers. Metals bound to ligands made from this architecture would experience significant variations.

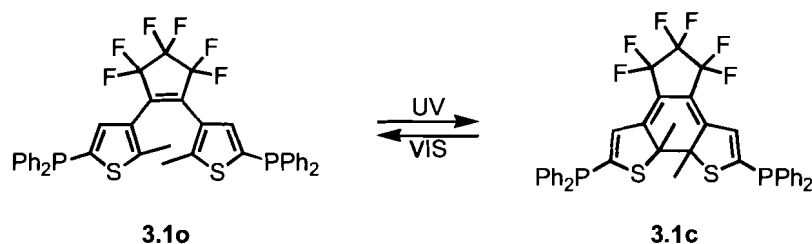
Several reports have described the use of DTE derivatives in which nitrogen ligands (pyridine, bipyridine, and phenanthroline) were used to construct metal complexes and coordination polymers.⁴⁴⁻⁵¹ The previous chapter described

how a bis(oxazoline) DTE ligand could be used to regulate the outcome of a catalytic reaction based on the geometry of the complex formed in solution. However, there are no examples of photoresponsive DTE derivatives decorated with the tertiary phosphorous family of ligands, which is one of the most ubiquitous in coordination chemistry. These ligands boast dramatic and versatile changes in properties based on the fine-tuning of the electronic and steric framework of the groups attached to the phosphorous atom.⁵² The steric and electronic properties of a tertiary phosphine can dramatically influence a metal center and lead to marked changes in reactivity.⁵³⁻⁵⁶

This chapter describes the synthesis of a photoswitchable tertiary phosphorous compound and some derivatives to investigate the effects of photochemistry on the electronic properties of the phosphorous atom.

3.2 Triarylphosphine DTE derivative

The structural changes resulting from the light-induced isomerization of a phosphine-substituted DTE are depicted in Equation 3.2.1.



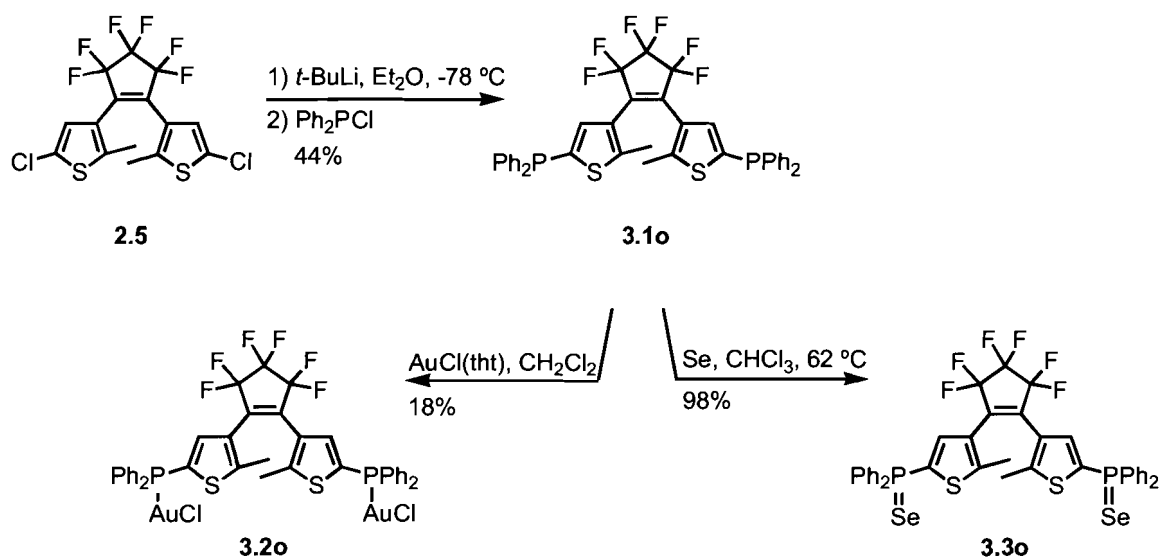
Equation 3.2.1 A triaryl phosphine DTE derivative **3.1o** can be isomerized with UV light into its corresponding *ring-closed* isomer **3.1c**. The *ring-open* isomer **3.1o** can be regenerated with visible wavelengths of light.

UV-light irradiation on the *ring-open* isomer **3.1o** would produce the *ring-closed* isomer **3.1c**. Visible wavelengths of light can in turn be used to regenerate

the *ring-open* isomer **3.1o**. This bis(phosphine) ligand could be used either as a reagent or as a ligand, in which case it could influence the reactivity of a metal complex due to the electronic differences between both isomeric forms. The two phosphines are electronically insulated in the *ring-open* isomer **3.1o**, while they are electronically conjugated through the extended conjugation backbone of the *ring-closed* form **3.1c**.

3.3 Synthesis of DTE diphenylphosphine derivatives

The bis(phosphine) DTE **3.1o** and its corresponding derivatives could be easily prepared in a few steps from the previously reported 1,2-bis(5'-chloro-2'-methylthien-3'-yl)perfluorocyclopent-1-ene **2.5** as shown in Scheme 3.3.1.



Scheme 3.3.1 Synthesis of bis(diphenylphosphine) **3.1o**, gold chloride complex **3.2o** and selenide **3.3o** derivatives.

Compound **3.1o** was prepared by quenching the lithium salt of compound **2.5**, generated by lithium halogen exchange using *n*-buthyllithium, with chlorodiphenylphosphine⁵⁷ in 44% yield. The gold chloride derivative **3.2o** was

prepared in one step by mixing gold tetrahydrothiophene (Au(tht))⁵⁸ and compound **3.1o**, in 18% yield, to investigate the effects of coordination chemistry on the photochromism. The phosphine selenide **3.3o** derivative was prepared in high yield (98%) by refluxing compound **3.1o** with selenium powder in chloroform⁵⁹ to examine the electronic differences between the two photoisomers.

3.3.1 Photochromism of bis(phosphine) DTE 3.1o

The photochromism of compound **3.1o** was best monitored using UV-VIS spectroscopy to follow the absorption changes accompanying the light-induced isomerization between the *ring-open* isomer **3.1o** and the *ring-closed* isomer **3.1c**, as illustrated in Figure 3.3.1.

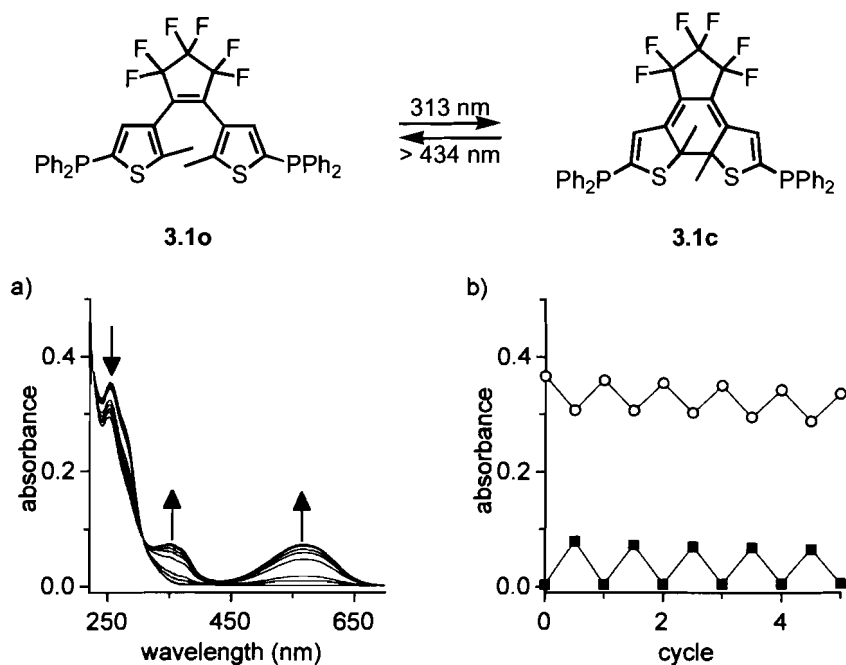


Figure 3.3.1 Changes in the UV-VIS absorption spectra of a 9.9×10^{-6} M solution of bis(diphenylphosphine) **3.1o** in CH₃CN upon irradiation with 313-nm light. (a) Total irradiation periods are 0, 5, 10, 30, 45, 60, 75 and 90 sec. (b) Modulated absorbance at 253 nm (○) and 570 nm (■) during alternate irradiation of with 313-nm light for 90 sec, then > 434 nm for 120 sec.

Irradiation with 313-nm light, using a hand-held TLC lamp, resulted in an immediate decrease of the high-energy absorption bands ($\lambda_{\text{max}} = 253 \text{ nm}$) and a corresponding increase in the low energy absorptions ($\lambda_{\text{max}} = 570 \text{ nm}$), resulting in the appearance of a deep purple colour from a colourless solution. Irradiation of the solution for longer than 90 sec did not result in any additional change in the absorption spectrum indicating that a photostationary state had been reached. Bleaching the solution with light of greater than 434 nm from a 150-W tungsten source, passed through a cutoff filter to remove the higher energy light, regenerated the original spectrum of **3.1o**. A series of ring-closures followed by ring-openings resulted in a decrease of 18% in the absorption for both isomers after 4-5 cycles indicative of degradation (Figure 3.3.1b). This decrease could be

due to oxidative degradation on either the thiophene or the phosphine, or photodegradation from the ring-closing reaction.

The photochemical interconversion between the *ring-open* isomer **3.1o** and the *ring-closed* isomer **3.1c** was also monitored by ^1H NMR spectroscopy. Irradiation of a CD_2Cl_2 solution of **3.1o** (4.4×10^{-3} M) with 313-nm light resulted in the appearance of a new set of signals for **3.1c**, including a singlet at 2.06 ppm, while the corresponding thiophene-C2 methyl singlet was at 1.94 ppm for **3.1o**, as illustrated in Figure 3.3.2.

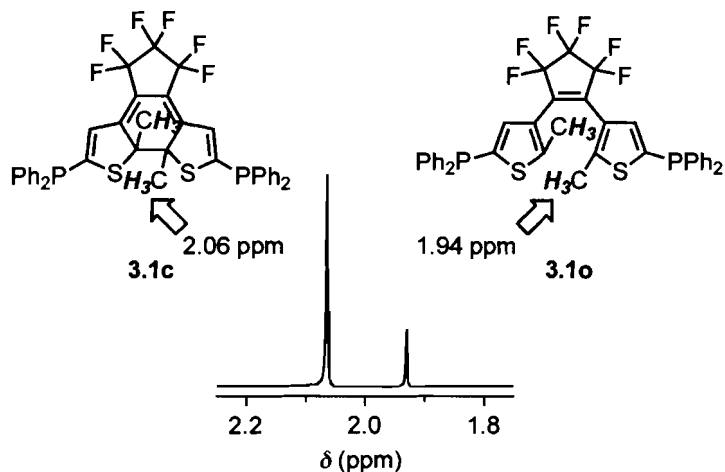
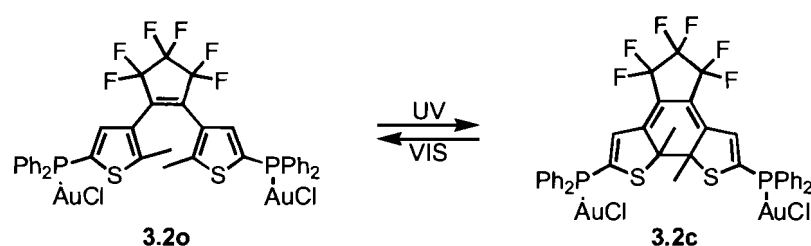


Figure 3.3.2 Selected region in the ^1H NMR spectrum obtained after irradiation of a CD_2Cl_2 solution of **3.1o** (4.4×10^{-3} M) with 313-nm light, highlighting the thiophene-C2 methyl singlet used in determining the extent of photoconversion.

When additional irradiation of the solution with 313-nm light resulted in no further changes in the relative integration of the area under the peaks assigned to compounds **3.1o** and **3.1c**, the photostationary state was determined to be a mixture of 80% of *ring-closed* isomer **3.1c** with the remaining 20% assigned to the *ring-open* isomer **3.1o**.

3.4 Bis(phosphine) DTE gold complex 3.2o

Binding a DTE to a metal center could have dramatic effects on the photoswitching properties of a DTE derivative. Indeed, as seen in the previous chapter, in one instance a bis(oxazoline) ligand in a metal-complex only displayed limited photochromism. The coordination chemistry of the bis(phosphine) DTE ligand **3.1o** was typified by the preparation of the air-stable gold chloride complex **3.2o**, shown in Equation 3.4.1.



Equation 3.4.1 Diphenylphosphine gold chloride DTE **3.2o** can be converted into the *ring-closed* isomer **3.2c** using UV light. Irradiation of the *ring-closed* isomer **3.2c** with visible wavelengths of light regenerates the *ring-open* isomer **3.2o**.

Using UV light, the *ring-open* **3.2o** isomerizes into the *ring-closed* **3.2c**. Irradiation with visible wavelengths of light regenerates the *ring-open* isomer **3.2o**.

3.4.1 Crystal structure of complex 3.2o

Confirmation of the structure of complex **3.2o** was provided by X-ray crystallography. Single crystals suitable for X-ray analysis were grown by slowly evaporating a solution of the complex **3.2o** in a mixture of CH_2Cl_2 and hexanes. The structure of the complex in the single crystal is shown in Figure 3.4.1.

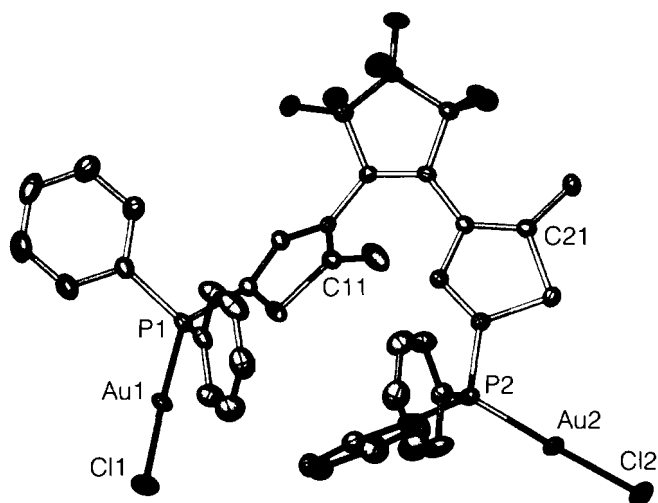


Figure 3.4.1 Molecular structure of complex **3.2o**. Ellipsoids are shown at the 20% probability level. The hydrogen atoms were omitted for clarity.

In the crystal, the gold complex was locked into a non-photochromic conformation, which was an expected outcome considering the large changes in the geometrical structure accompanying the photoinduced reaction. The ring-closing reaction could not have taken place with the restricted movement in a tightly packed crystal. Additionally, the photochromism depended on the conformation of the molecule in the lattice. As discussed in the *Introduction*, only the antiparallel conformation is productive towards photoisomerization, whereas the parallel conformation is not. This means that the molecules should be packed in an antiparallel geometry to maintain photochromic activity in the crystal structure. The crystal structure of **3.2o** demonstrated that the molecules existed in a distorted parallel conformation, and that the distance between the reactive carbons (labelled C11-C21 in Figure 3.4.1.) was too large⁶⁰ for the photocyclization to occur in the single crystal (4.78 Å). This finding was verified by the fact that irradiating a single crystal of **3.2o** with 313-nm light for 30 min resulted in no observable change in the colour of the crystal. Unlike this example,

there are a few DTE derivatives where the photochromism is maintained in a single-crystal lattice, and it was reported that the distance between the reactive carbons (C2 carbon on both thiophene rings) should be less than 4 Å.¹⁸

The coordination geometry around the gold atom was linear (P1-Au1-Cl1 and P2-Au2-Cl2 in Figure 3.4.2) with bond angles of 178°. The inter- and intramolecular distance between gold atoms indicated that there was no gold-gold bond, as shown for other (diphenylphosphino)thiophene gold(I) complexes.⁵⁸

3.4.2 Photochromism of bis(phosphine) DTE gold complex 3.2o

The photochemistry of complex **3.2o** was monitored by UV-VIS absorption spectroscopy. Irradiation of a CH₂Cl₂ or CH₃CN solution of **3.2o** with 313-nm light, using a hand-held TLC lamp, induced an immediate colour change (colourless to purple) and the appearance of an absorption peak ($\lambda_{\text{max}} = 565$ nm) in the UV-VIS spectrum (Figure 3.4.2a).

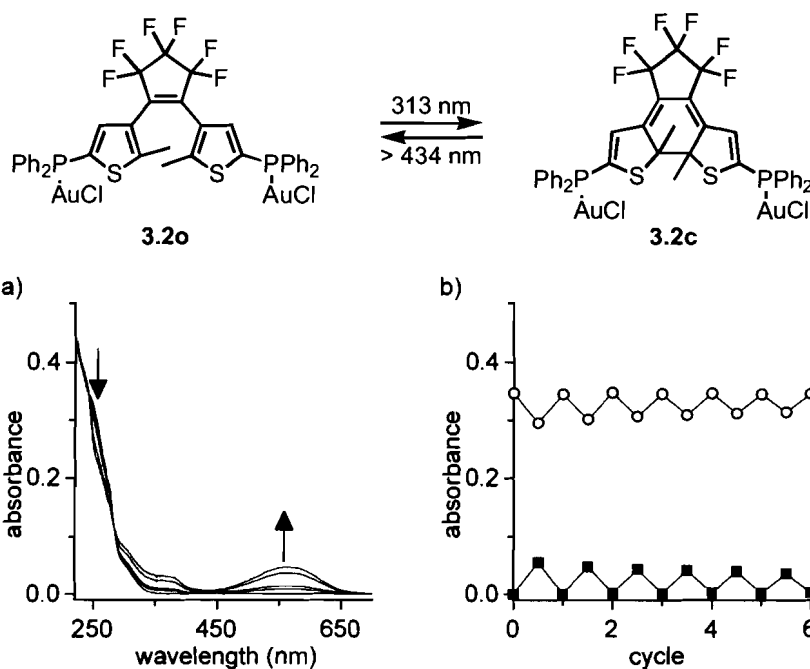


Figure 3.4.2 Changes in the UV-VIS absorption spectra of a 9.6×10^{-6} M solution of bis(diphenylphosphine) gold chloride **3.2o** in CH_3CN upon irradiation with 313-nm light. (a) Total irradiation periods are 0, 5, 10, 30, and 60 sec. (b) Modulated absorbance at 246 nm (○) and 565 nm (■) during alternate irradiation with 313-nm light for 20 sec, then > 434 nm for 30 sec.

A photostationary state was reached after 1 min irradiation of a CH_3CN solution of **3.2o** (9.6×10^{-3} M), as indicated by the absence of change in the absorption spectrum following further irradiation with the same light source. The original absorption spectrum could be regenerated following irradiation with filtered light of greater than 434 nm. Cycling could be performed, but degradation occurred, as indicated by the 35% decrease in the absorption spectrum of the *ring-closed* isomer **3.2c** after six cycles (Figure 3.4.2b).

The photochemical interconversion between the *ring-open* isomer **3.2o** and the *ring-closed* isomer **3.2c** was also monitored by ^1H NMR spectroscopy. Irradiation of a CD_2Cl_2 solution of **3.2o** (2.1×10^{-3} M) with 313-nm light resulted in the appearance of a new set of signals for **3.2c** including a singlet at 2.11 ppm,

while the corresponding thiophene-C2 methyl singlet was at 2.07 ppm for **3.2o**, as illustrated in Figure 3.4.3.

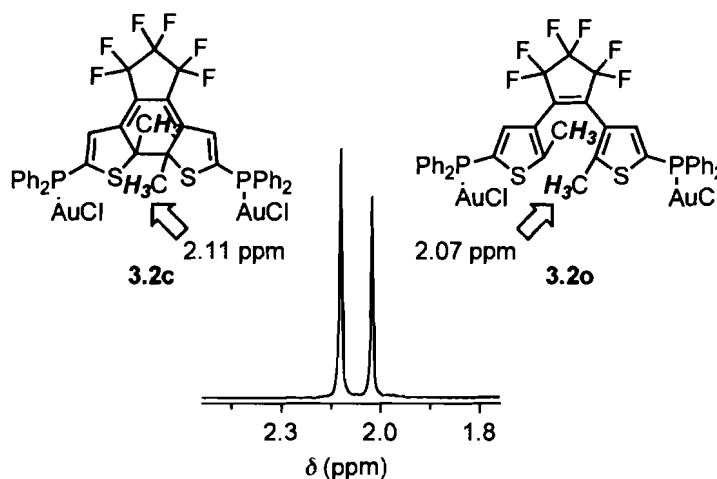


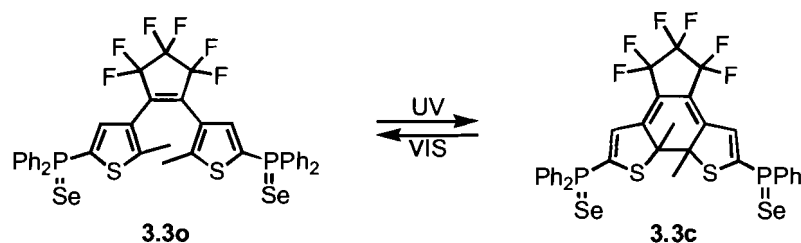
Figure 3.4.3 Selected region in the ^1H NMR spectrum obtained after irradiation of a CD_2Cl_2 solution of **3.2o** (2.1×10^{-3} M) with 313-nm light, highlighting the thiophene-C2 methyl singlet used in determining the extent of photoconversion.

When additional irradiation of the solution with 313-nm light resulted in no further changes in the relative integration between the signals assigned to **3.2o** and **3.2c**, the photostationary state was determined to be a mixture of 60% of *ring-closed* isomer **3.2c**, with the remaining 40% assigned to the *ring-open* isomer **3.2o**.

3.5 Bis(phosphine) DTE selenide 3.3o

Previous reports indicated that measuring the $^1J(^{77}\text{Se}-^{31}\text{P})$ spin-spin coupling constants could be used to quantify the electron-withdrawing properties of phosphine derivatives.^{59,61} The magnitude of $^1J(^{77}\text{Se}-^{31}\text{P})$ depends upon the nature of the organic substituents on phosphorus, electron-withdrawing groups causing an increase of the coupling constant, from the increase in the s character of the lone pair, whereas electron-donating and bulky groups cause the coupling

to decrease. Therefore, the bis(phosphine) selenide **3.3o**, illustrated in Equation 3.5.1, was prepared to investigate the electronic changes resulting from the backbone photoisomerization.



Equation 3.5.1 Diphenylphosphine selenide DTE **3.3o** is converted to the *ring-closed* isomer **3.3c** with UV light. Visible wavelengths of light regenerate the *ring-open* isomer **3.3o**.

The *ring-open* isomer of the bis(phosphine) selenide DTE **3.3o** could be converted to the *ring-closed* isomer **3.3c** using UV light (Equation 3.5.1). The *ring-open* isomer could be regenerated using visible light.

3.5.1 Photochromism of bis(phosphine) selenide **3.3o**

The photochromic conversion of **3.3o**, using UV light producing a purple colour, was best monitored by UV-VIS spectroscopy (Figure 3.5.1a).

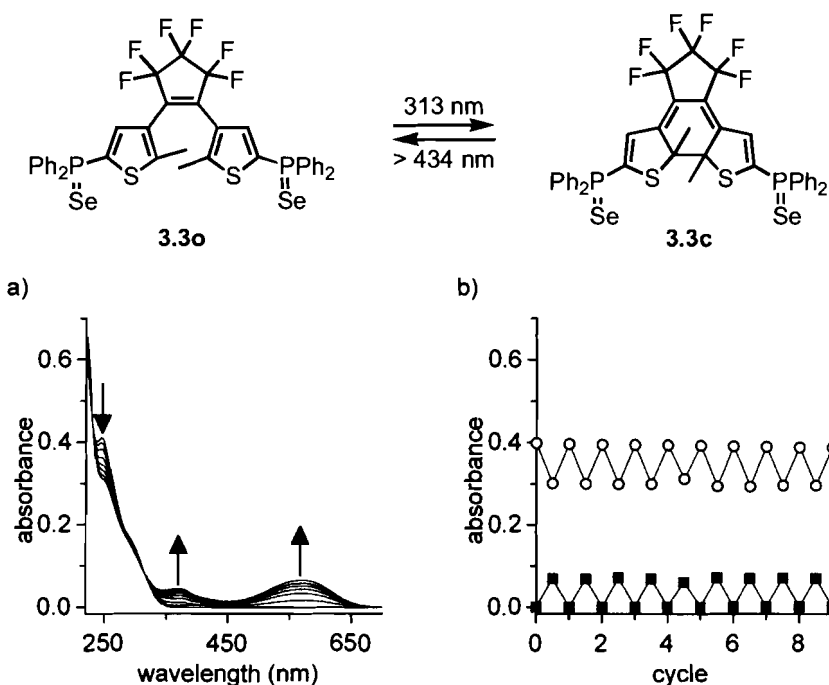


Figure 3.5.1 Changes in the UV-VIS absorption spectra of a 5.4×10^{-6} M solution of bis(diphenylphosphine) selenide **3.3o** in CH_3CN upon irradiation with 313-nm light. (a) Total irradiation periods are 0, 10, 20, 30, 40, 50 and 60 sec. (b) Modulated absorbance at 245 nm (○) and 574 nm (■) during alternate irradiation of with 313-nm light for 60 sec, then > 434 nm for 60 sec.

Irradiation of a CH_3CN solution of the *ring-open* isomer **3.3o** with 313-nm light resulted in immediate colour changes due to the growth of an absorption peak ($\lambda_{\text{max}} = 574$ nm) for the *ring-closed* isomer **3.3c**, which was accompanied with a decrease in the high-energy absorptions ($\lambda_{\text{max}} = 245$ nm). Irradiation with filtered light greater than 434 nm regenerated the original absorption spectrum. Cycling between compounds **3.3o** and **3.3c** demonstrated that there was no significant decrease in the absorbance values of either isomer, indicative of no degradation (Figure 3.5.1b).

The photochemical interconversion between the *ring-open* isomer **3.3o** and the *ring-closed* isomer **3.3c** was then monitored by ^1H NMR spectroscopy. Irradiation of a CDCl_3 solution of compound **3.3o** (2.2×10^{-3} M) with 313-nm light

resulted in the appearance of a new set of signals for compound **3.3c** including a singlet at 2.10 ppm, while the corresponding thiophene-C2 methyl singlet was at 2.02 ppm for compound **3.3o**, as illustrated in Figure 3.5.2.

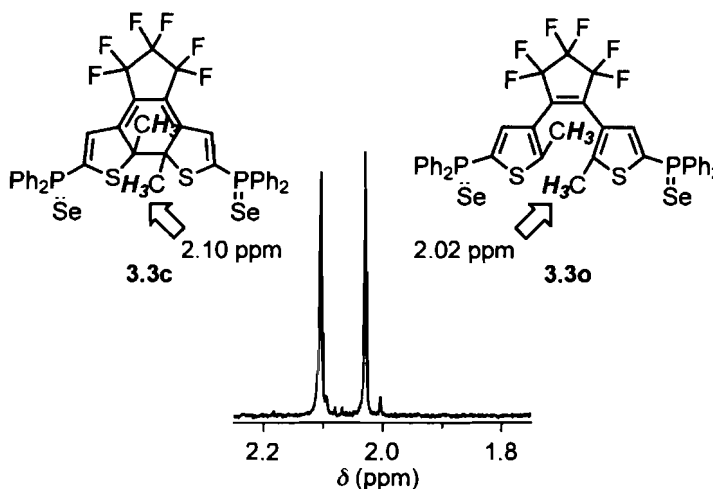


Figure 3.5.2 Selected region in the ^1H NMR spectrum obtained after irradiation of a CDCl_3 solution of compound **3.3o** (2.2×10^{-3} M) with 313-nm light, highlighting the thiophene-C2 methyl singlet used in determining the extent of photoconversion.

When additional irradiation of the solution with 313-nm light resulted in no further changes in the relative integration between the signals assigned to compounds **3.3o** and **3.3c**, the photostationary state was determined to be a mixture of 55% of *ring-closed* isomer **3.3c** with the remaining 45% assigned to the *ring-open* isomer **3.3o**.

3.5.2 Electronic effects of the backbone conjugation differences

The signals in the ^{31}P NMR signals were different for the two isomers and appeared at 22.4 and 27.0 ppm for compounds **3.3o** and **3.3c**, respectively. What was more indicative of the electronic differences affecting the nucleophilicity of the lone pair on each of the phosphorous atoms were the

coupling constants $^1J(^{77}\text{Se}-^{31}\text{P})$, which were 744 and 756 Hz for compounds **3.3o** and **3.3c**, respectively, as shown in Figure 3.5.3.

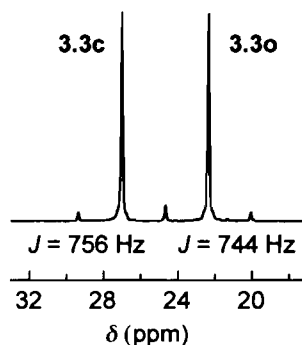


Figure 3.5.3 ^{31}P NMR of a photostationary state CDCl_3 solution of compounds **3.3o** and **3.3c** generated using 313-nm light where the coupling constants are indicated below the corresponding resonance signal peak. The central peak is a coincidental overlap of the splitting of both peaks.

This difference in coupling constants indicated that the *ring-closed* isomer of the parent bis(phosphine), **3.1c**, was a weaker nucleophile than the *ring-open* isomer **3.1o**. This difference could be attributed to the increased electron-withdrawing properties of the molecular backbone in compound **3.1c**.²³ The difference in the $^{77}\text{Se}-^{31}\text{P}$ coupling constants for compounds **3.3o** and **3.3c** could be compared to previously reported compounds, shown in Table 3.5.1.

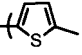
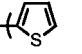
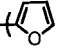
$R\text{-PPh}_2$	$R\text{-PPh}_2$	$^{31}\text{P NMR } \delta \text{ /ppm}$	$R\text{-P(Se)Ph}_2$	$J(^{77}\text{Se}\text{-}^{31}\text{P}) \text{ /Hz}$
$R = \text{Ph}$	(1) ⁵⁹	- 4.7	35.9	732
$R = $ 	(2) ⁵⁹	- 21.9	19.3	733
$R = $ 	(3) ⁵⁹	- 19.3	20.6	743
$R = $ 	(4) ⁵⁹	- 26.6	16.9	754
<i>Ring-open 3.1o</i>	(5)	- 18.7	22.4	744
<i>Ring-closed 3.1c</i>	(6)	- 8.3	27.0	756

Table 3.5.1 ^{31}P NMR characterizations for a series of phosphine selenide derivatives.

The parent compound, triphenyl phosphine in entry (1), was included in Table 3.5.1 to provide a comparison measure for other entries. The 2-methylthien-5-yl (2) was included since it is a good control for the substitution of one phenyl with a methylthiophene, as that present in compound **3.1o**. The magnitude of the change in electron-withdrawing strength is equivalent to a 2-thienyl (3), for the *ring-open* isomer (5), being replaced by a 2-furyl (4) substituent, for the *ring-closed* isomer (6); a change that could lead to significant differences in reactivity. There are no direct correlations with electron-withdrawing strength of substituents in the ^{31}P signals since there are other factors affecting the ^{31}P chemical shift, namely, the bond angles at the phosphorus and the effect of π -bonding between the phosphorus and its substituents.⁶¹

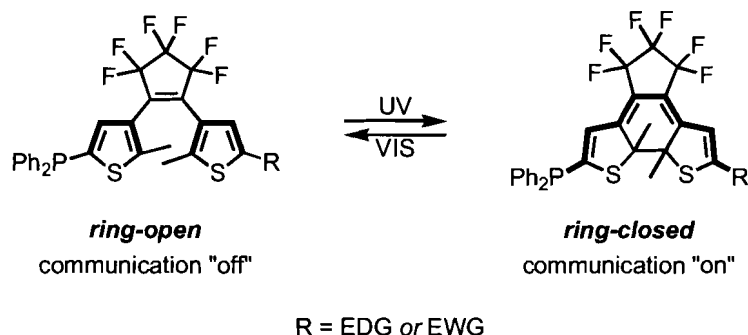
3.6 Conclusion

In this chapter the preparation and characterization of the first reversible photoswitching bis(phosphine) ligand was described. Through illustrative examples, the coordination chemistry and the electron-withdrawing differences

between the two photoisomers were demonstrated. While this new ligand showed potential for applications in catalysis, the gold chloride derivative displayed moderate photoconversion (60%) and limited photochromic performance due to degradation when cycled between the two photoisomers. However, the phosphine selenide derivative did have limited photoconversion (55%), no degradation was observed upon cycling perhaps as a result of protecting the phosphine from photooxidative degradation. These findings indicated that the metal could significantly impact the photochromic performance of DTE-metal complexes.

3.7 Future work

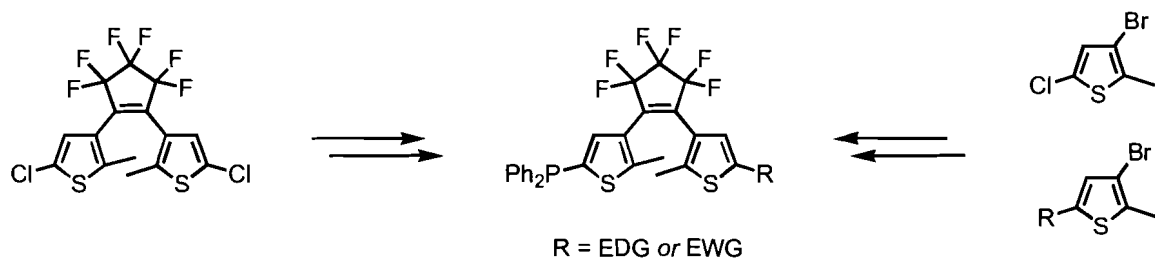
This chapter introduced the new bis(diphenylphosphine) ligand/reagent to modulate reactivity. Synthetic modifications of the bis(diphenylphosphine) DTE could afford larger electronic communication differences between the two isomers. For instance, since the conjugated backbone extends from both C5 positions on the thiophenes, electron-withdrawing groups (EWG) or electron-donating groups (EDG) could be appended on one of the C5 position to affect the phosphine on the opposite thiophene in the *ring-closed* isomer, as shown in Equation 3.7.1.



Equation 3.7.1 Electronic communication between a diphenyl phosphine and an electron-donating group (EDG) or electron-withdrawing group (EWG) can be turned "on" using UV light or "off" using light of visible wavelengths. The conjugation is highlighted in both structures in bold.

Electronic communication could be switched "on" by using UV light and turned "off" using visible light, as shown in bold in the structures in Equation 3.7.1. The sterics around the phosphine and the electronic differences could also be fine-tuned by choosing phosphine substituents other than phenyl groups, providing large reactivity differences between the *ring-open* isomer and the *ring-closer* isomer.

Different derivatives could be prepared by installing the phosphine and the EWG/EDG in the appropriate order, depending on their relative stabilities to the synthetic conditions required, as shown in Scheme 3.7.1.

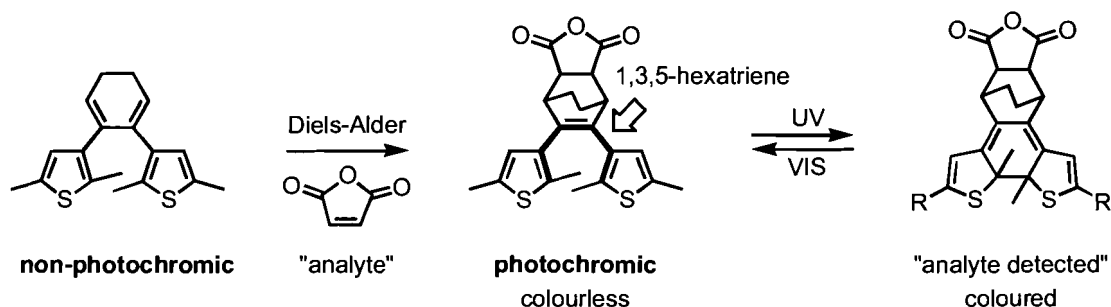


Scheme 3.7.1 Two different synthetic routes for the phosphine derivatives starting either from a preassembled DTE or from derivatized thiophene groups.

Synthesis could begin from a preassembled DTE to which the phosphine and 'R' groups would be sequentially attached. Alternatively, the DTE could be

assembled from functionalized thiophene derivatives. The selenide derivation would then allow quantitative evaluation of the electron-withdrawing character of all photoisomers.

Another completely different usage of the phosphine **3.10** would be to monitor reaction progress. If a *ring-open* DTE were “locked” in a non-photochromic conformation such that irradiation with any wavelength caused no colour change, then a colour change would be induced only when the additional “unlocking” reaction was present. The concept of reactivity-gating DTE photochromism has already been reported by Lemieux *et al.* for the Diels-Alder reaction,⁶² where a Diels-Alder adduct was photochromic but the precursor was not. Hence, the reactivity-gated photochromism of DTE could be used in dosimetry applications for the sensing of dienophiles, as illustrated in Equation 3.7.2.

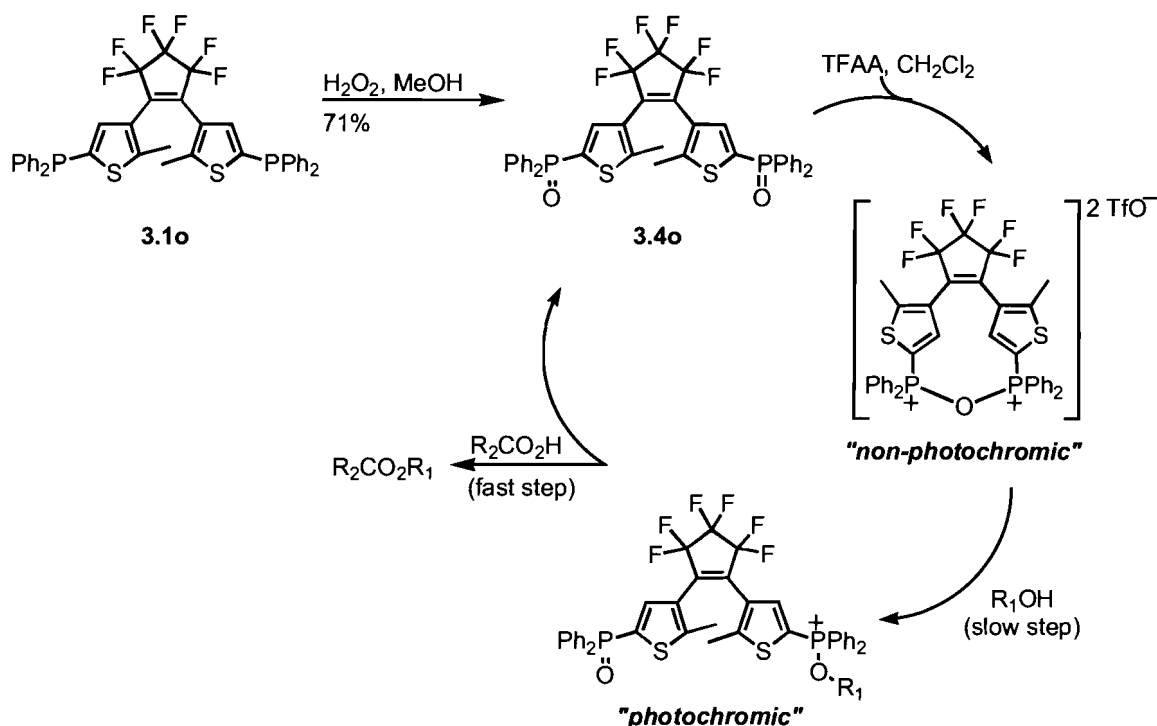


Equation 3.7.2 The reactivity-gated photochromism is based on the Diels-Alder reaction of a non-photochromic diene precursor with a dienophile “analyte” creating a colourless DTE containing a 1,3,5-hexatriene (bold), and thus generating a photochromic Diels-Alder adduct. UV light is then used to generate the coloured isomer, indicating that the analyte was detected.

A dienophile reacting with the non-photochromic precursor, generated the hexatriene-containing (bold) DTE architecture, which became photochromic and could be converted to a coloured isomer with UV light. The ring-closing reaction

was thus gated by an initial Diels-Alder reaction. Alternatively, the photochromic reaction could be used to monitor the progress of the Diels-Alder reaction by following the increasing amount of coloured product by UV-VIS absorption spectroscopy.

The bis(phosphine) ligand could be used to monitor the reaction progress of the Hendrickson reaction,^{63,64} which provides a useful procedure with mild conditions for the esterification of primary alcohols as an alternative to the harsher conditions of the Mitsunobu reaction.^{65,66} In this case, a DTE "POP" (phosphine-oxygen-phosphine) reagent would be used, as illustrated in Scheme 3.7.2.



Scheme 3.7.2 The POP reagent, prepared in two steps from compound **3.1o**, should be locked in a non-photochromic parallel conformation. The reaction with a primary alcohol is the slow step, which “unlocks” the photochromism followed by the esterification, which is the fast step. The reactivity gated photochromism of a DTE could be used to monitor the progress of the esterification reaction.

The phosphine oxide derivative **3.4o** was obtained by mixing compound **3.1o** with H_2O_2 in methanol in 71% yield and provided the oxidative side-product expected from reactions using compound **3.1**. Alternatively, compound **3.4o** could be used as the starting material for the “POP” reagent. After reaction of the bis(phosphine oxide) DTE **3.4o** with trifluoromethanesulfonic anhydride (TFAA),⁶⁴ it was proposed that the cyclic “POP” configuration would position the thiophene groups in a geometry unproductive towards the ring-closing isomerization reaction. The slow step, involving the reaction with a primary alcohol,⁶⁶ would “unlock” the DTE and be followed by the rapid esterification with a carboxylic acid reagent. The ring-closing reaction could be used to monitor the slow step of the reaction, and thus the corresponding absorbance of the *ring-closed* isomer could

be correlated to the extent of the reaction with an increasing absorbance value in the visible range for an increasing “unlocking” of the DTE. Preliminary experiments indicated that the photochromic performance of the system was not affected at all by the addition of one equivalent or an excess of TFAA in the absence of an alcohol. The same photoconversion as for the free phosphine oxide was measured for the proposed cyclic compound using ^1H NMR spectroscopy, and therefore the anticipated reaction monitoring did not work. A dimer or polymer could also have formed instead where the photochromism would not be locked. Further investigation is required to determine the nature of the “POP” reagent formed *in situ*.

3.8 Experimental

3.8.1 General

All solvents used for synthesis and characterization were dried and degassed by passing them through steel columns containing activated alumina under nitrogen using an MBraun solvent purification system. Solvents for NMR analysis (Cambridge Isotope Laboratories) were used as received. All reagents were purchased from Aldrich with the exception of Au(tht) which was provided by Prof. Danny Leznoff (SFU, Dept. of Chemistry).

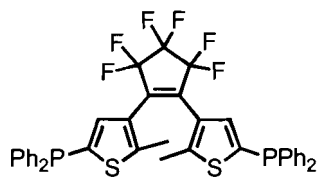
3.8.2 Methods

^1H NMR, ^{31}P NMR and ^{13}C NMR characterizations were performed on a Bruker AMX 400 instrument with a 5 mm inverse probe operating at 400.13 MHz for ^1H NMR, 161.98 MHz for ^{31}P NMR and 100.6 MHz for ^{13}C NMR; a Varian 400

MercuryPlus instrument with a 5 mm ATB probe equipped with a shielded gradient operating at 400.10 MHz for ^1H NMR and 100.60 MHz for ^{13}C NMR; a Varian Inova 500 instrument with a 5 mm inverse probe equipped with a shielded gradient operating at 499.8 MHz for ^1H NMR and 125.7 MHz for ^{13}C NMR; or a Bruker Avance II 600 with a 5 mm QNP cryoprobe operating at 150.90 MHz for ^{13}C NMR and 242.9 MHz for ^{31}P NMR with a WALTZ-16 composite pulse decoupling of ^1H used for all ^{13}C NMR and ^{31}P NMR spectra. Chemical shifts (δ) are reported in parts per million relative to tetramethylsilane using the residual solvent peak as a reference standard. Coupling constants (J) are reported in Hertz. FT-IR spectroscopy was performed using a Nicolet Nexus 670 instrument. UV-VIS absorption spectroscopy was performed using a Varian Cary 300 Bio spectrophotometer. Low resolution mass spectrometry (LRMS) measurements were performed using a HP5985 mass spectrometer with isobutane as the chemical ionization source, a Varian 4000 GC/MS/MS with electron impact operating at 10 mamp as the ionization source or chemical ionization (CI) with methanol or a PerSeptive Biosystems Voyager-DE Biospectrometry Workstation MALDI spectrometer using a 2,4-dihydroxybenzoic acid matrix. Melting points were measured using a Fisher-Johns melting point apparatus. X-ray diffraction studies were performed on a Bruker PLATFORM/SMART 1000CCD. Flash chromatography was performed using silica gel 60 (230–400 mesh) from Silicycle Inc. Centrifugal chromatography was performed using a Harrison Research Inc. Chromatotron, model 8924 using TLC grade 7749 silica gel from Merck. Standard hand-held lamps used for visualizing TLC plates (Spectroline E-

series, 470 mW/cm²) were used to carry out the ring-closing reactions at 313 nm. The ring-opening reactions were carried out using the light of a 150-W tungsten source or of a 300-W halogen photo optic lamp source that was passed through a 434-nm cutoff filter to eliminate higher energy light. Microanalyses were performed on a Carlo Erba Model 1106 CHN analyser.

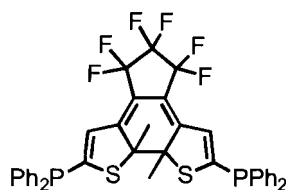
3.8.3 Syntheses and experiments



3.1o

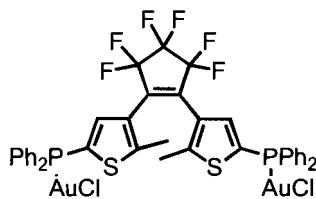
Synthesis of 1,2-bis(5'-(diphenylphosphino)-2'-methylthien-3'-yl)perfluorocyclopent-1-ene (3.1o). Using a known procedure to prepare phosphinothiophene ligands,⁵⁷ a solution 1,2-bis(5'-chloro-2'-methylthien-3'-yl)hexafluorocyclopentene **2.5** (250 mg, 0.57 mmol) in anhydrous Et₂O (50 mL) cooled to -78 °C was treated drop-wise with *t*-butyllithium (0.94 mL, 1.7 M in pentane, 1.6 mmol) under an N₂ atmosphere. The reaction mixture was stirred at this temperature for 1 h at which time it was treated with PPh₂Cl (226 μL, 1.3 mmol) in one portion *via* a syringe. After the cold bath was removed and the reaction was slowly warmed to room temperature, it was stirred for 14 h. The solution was concentrated to dryness *in vacuo*. The crude product was dissolved in CH₂Cl₂ (5 mL) and was purified by passing it through a small plug (SiO₂, CH₂Cl₂). The product was further purified by flash chromatography (SiO₂, 15% CH₂Cl₂ in hexanes) yielding 170 mg (44%) of **3.1o** as white crystals after

recrystallization from ethanol. M.p. = 154–157 °C. ^1H NMR (500 MHz, CD_2Cl_2) δ 7.30–7.40 (m, 20H), 7.27 (d, J = 6 Hz, 2H), 1.94 (s, 6H). ^{13}C NMR (100 MHz, CD_2Cl_2) δ 137.4 (d, J = 9 Hz), 136.3, 136.0, 133.0 (d, J = 20 Hz), 129.2, 128.7, 128.6, 14.6 (8 of 12 carbons found). ^{31}P NMR (162 MHz, CD_2Cl_2) δ –18.7 (s). FT-IR (KBr-cast) 3438, 3071, 3051, 2917, 2852, 1957, 1886, 1809, 1429, 1274, 1185, 1114, 1088, 972, 747, 695, 496 cm^{-1} . LRMS (MALDI) m/z = 736 $[\text{M}]^+$. Anal. Calcd for $\text{C}_{39}\text{H}_{28}\text{P}_2\text{F}_6\text{S}_2$: C, 63.58; H, 3.83. Found: C, 63.25; H, 3.61.



3.1c

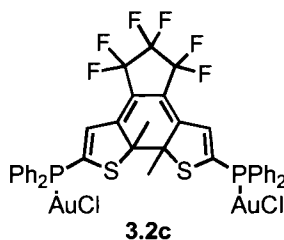
Photochemical synthesis of the *ring-closed* isomer 3.1c. A solution of compound **3.1o** (1.6 mg, 2.2×10^{-3} mmol) in CD_2Cl_2 (0.5 mL) was irradiated with 313-nm light for 10 min yielding a solution containing 80% of compound **3.1c** at the photostationary state as determined by ^1H NMR analysis. The remaining 20% was assigned to *ring-open* isomer **3.1o**. ^1H NMR (500 MHz, CD_2Cl_2) δ 7.37–7.52 (m, 20H), 6.20 (d, J = 4 Hz, 2H), 2.06 (s, 6H). ^{31}P NMR (162 MHz, CD_2Cl_2) δ –8.3 (s).



3.2o

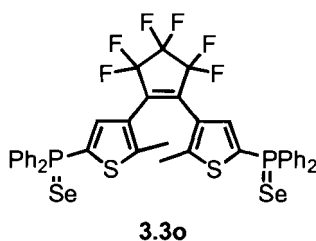
Synthesis of 1,2-bis(5'-((chlorogold)diphenylphosphino)-2'-methylthien-3'-yl)hexafluorocyclopentene 3.2o. Following previously reported preparation of

gold complexes of phosphinothiophene ligands,⁵⁸ a solution of AuCl(tht) (44 mg, 0.14 mmol) in CH₂Cl₂ (10 mL) was treated drop-wise with a solution of compound **3.1o** (50 mg, 0.07 mmol) in CH₂Cl₂ (5 mL) at 25 °C. After stirring at this temperature for 14 h, the solution was evaporated to dryness *in vacuo*. The product was purified by flash chromatography (SiO₂, 25% CH₂Cl₂ in hexanes) yielding 15 mg (18%) of air-stable crystals of complex **3.2o** suitable for X-ray structural analysis after crystallization from hexanes and CH₂Cl₂. M.p. = 217 °C (dec.) ¹H NMR (500 MHz, CD₂Cl₂) δ 7.48-7.64 (m, 20H), 7.27 (d, *J* = 9 Hz, 2H), 2.07 (s, 6H). ¹³C NMR (150 MHz, CDCl₃) δ 151.2 (d, *J* = 3.3 Hz), 138.9 (d, *J* = 12.2 Hz), 133.4 (d, *J* = 14.4 Hz), 132.6 (d, *J* = 2.6 Hz), 129.5 (d, *J* = 12.3 Hz), 128.8 (d, *J* = 65.0 Hz), 128.6 (d, *J* = 63.5 Hz), 126.7 (d, *J* = 12.0 Hz), 14.928. (9 of 12 found) ³¹P NMR (162 MHz, CDCl₃) δ 19.8. FT-IR (KBr-cast) 1478, 1436, 1341, 1227, 1204, 1139, 1101, 986, 746, 692, 537, 524, 502, 491 cm⁻¹.



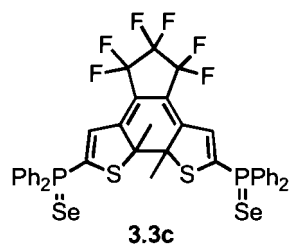
Photochemical synthesis of ring-closed isomer 3.2c. A solution of complex **3.2o** (2.5 mg, 2.1 × 10⁻³ mmol) in CD₂Cl₂ (1.0 mL) was irradiated with 313-nm light for 10 min yielding a solution containing 60% of complex **3.2c** at the photostationary state as determined by ¹H NMR analysis. The remaining 40% was assigned to *ring-open* isomer **3.2o**. ¹H NMR (400 MHz, CD₂Cl₂): δ 7.40-7.80 (m, 20H), 6.45 (d, *J* = 10 Hz, 2H), 2.11 (s, 6H).

X-ray crystallography: 1,2-bis(5-((chlorogold)diphenylphosphino)-2-methylthien-3-yl)hexafluorocyclopentene 3.2o. Crystals of complex **3.2o** were grown by slowly evaporating a solution of complex **3.2o** in 50% CH₂Cl₂ in hexanes. Crystal dimensions (mm) 0.47 × 0.38 × 0.33, triclinic. The crystal structure was solved using direct methods (*SHELXS-86*) and refined by full-matrix least squares on *F*² (*SHELXL-93*). Details about the crystal structure are provided in the *Appendix*.

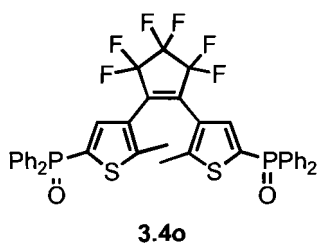


Synthesis of 1,2-bis(5'-(diphenylphosphinoselenide)-2'-methylthien-3'-yl)hexafluorocyclopentene 3.3o. Following a known procedure to prepare phosphine selenides,^{59,61} a solution of compound **3.1o** (50 mg, 0.07 mmol) in CHCl₃ (5 mL) was treated with selenium (43 mg, 0.55 mmol) in one portion. The resulting solution was heated at reflux (62 °C) for 4 h, when the heating source was removed and the reaction mixture was slowly cooled to room temperature. After stirring at this temperature for 30 min, the reaction mixture was filtered through a plug (SiO₂, CHCl₃) yielding 60 mg (98%) of compound **3.3o** as a yellowish solid. M.p. = 100-105 °C. ¹H NMR (500 MHz, CDCl₃) δ 7.68-7.74 (m, 8H), 7.48-7.56 (m, 4H), 7.42-7.48 (m, 8H), 7.23 (d, *J* = 9 Hz, 2H), 2.02 (s, 6H). ¹³C NMR (100 MHz, CDCl₃) δ 136.8 (d, *J* = 9 Hz), 133.8 (d, *J* = 83 Hz), 132.1 (d, *J* = 3 Hz), 132.0 (d, *J* = 11 Hz), 131.3, 128.7 (d, *J* = 13 Hz), 126.2 (d, *J* = 13 Hz), 14.7 (8 of 12 carbons found). ³¹P NMR (162 MHz, CDCl₃) δ 22.4 (d, ¹*J*⁷⁷Se-³¹P =

744 Hz). FT-IR (KBr-cast) 1436, 1334, 1269, 1191, 1141, 1100, 1061, 998, 983 cm^{-1} . LRMS (MALDI) $m/z = 895$ $[\text{M}]^+$. Anal. Calcd. for $\text{C}_{39}\text{H}_{28}\text{S}_2\text{F}_6\text{P}_2\text{Se}_2$: C, 52.36; H, 3.15. Found: C, 52.50; H, 3.37.



Photochemical synthesis of ring-closed isomer 3.3c. A solution of compound **3.3o** (1.0 mg, 1.1×10^{-3} mmol) in CDCl_3 (0.5 mL) was irradiated with 313-nm light for 3 min yielding a solution containing 55% of compound **3.3c** at the photostationary state as determined by ^1H NMR analysis. The remaining 45% was assigned to *ring-open* isomer **3.3o**. ^1H NMR (500 MHz, CDCl_3) δ 7.40-7.90 (m, 20H), 6.64 (d, $J = 11$ Hz, 2H), 2.10 (s, 6H). ^{31}P NMR (162 MHz, CD_2Cl_2) δ 27.03 (d, $^1J^{77}\text{Se}-^{31}\text{P} = 756$ Hz).



Synthesis of 1,2-bis(5'-(diphenylphosphino)-2'-methylthien-3'-yl)hexafluorocyclopentene 3.4o. A solution of compound **3.1o** (50 mg, 0.07 mmol) in methanol (50 mL) was treated with 30% aqueous H_2O_2 (10 mL) in one portion. The resulting solution was stirred at 25 $^\circ\text{C}$ for 2 h, at which point it was quenched with a 10% Na_2SO_3 aqueous solution (20 mL). The mixture was extracted with Et_2O (3×30 mL), dried with Na_2SO_4 and evaporated to dryness *in*

vacuo. The crude was purified by flash chromatography (SiO₂, EtOAc) yielding 37 mg (71%) of compound **3.4o** as a clear solid. M.p. = 158-160 °C. ¹H NMR (500 MHz, CD₂Cl₂) δ 7.62-7.66 (m, 8H), 7.57-7.61 (m, 4H), 7.49 (dt, *J* = 3.5, 7.5 Hz, 8H), 7.25 (d, *J* = 8 Hz, 2H), 2.01 (s, 6H). ¹³C NMR (150 MHz, CDCl₃) δ 150.1 (d, *J* = 3.5 Hz), 136.4 (d, *J* = 9.2 Hz), 133.3 (d, *J* = 108.5 Hz), 132.6 (d, *J* = 2.3 Hz), 132.4, 131.6 (d, *J* = 10.5 Hz), 128.7 (d, *J* = 12.6 Hz), 126.1 (d, *J* = 12.9 Hz), 14.7 (9 of 12 carbons found). ³¹P NMR (243 MHz, CDCl₃) δ 21.0. FT-IR (KBr-cast) 1539, 1435, 1384, 1325, 1276, 1192, 1119, 1104, 1064, 982, 897, 887, 756, 740, 725, 694, 635, 626, 537, 527 cm⁻¹. LRMS (MALDI) *m/z* = 769 [M]⁺.

Photochemical synthesis of ring-closed isomer 3.4c. A solution of compound **3.4o** (1.0 mg, 1.3 × 10⁻³ mmol) in CDCl₃ (0.5 mL) was irradiated with 313-nm light for 4 min yielding a solution containing 59% of compound **3.4c** at the photostationary state as determined by ¹H NMR analysis. The remaining 41% was assigned to *ring-open* isomer **3.4o**. ¹H NMR (500 MHz, CDCl₃): δ 7.47-7.76 (m, 20H), 6.69 (d, *J* = 9 Hz, 2H), 2.10 (s, 6H).

4 Creating a Reactive Eneidyne by Using Visible Light: Photocontrol of the Bergman Cyclization

The research presented in this chapter was published as a communication: Sud, D.; Wigglesworth, T. J.; Branda, N. R. "Creating a Reactive Eneidyne by Using Visible Light: Photocontrol of the Bergman Cyclization" *Angew. Chem. Int. Ed.* **2007**, *46*, 8017-8019.

4.1 Generating more reactive structures with light

The potential role of integrating light with chemical reactivity is especially significant in modern therapeutic technologies. Light could be used to trigger the rearrangement of a molecular architecture to activate "masked" chemotherapeutic agents that are broadly toxic, have severe side effects and cannot be administered in their "unmasked" forms.⁶⁷ One example that would benefit from such photocontrol is the well-known Bergman cyclization of the eneidyne architecture. This reaction requires the presence of a precise arrangement of π -bonds for the reaction to proceed.^{68,69} Eneidyne-containing compounds are known for their potent anticancer activity, but they are considered too toxic because they are not tumor specific,^{70,71} both healthy and tumor cells are affected. Photoregulating the presence/absence of the eneidyne moiety would provide spatial and temporal control over the activity of potentially useful drugs. A selection of eneidyne-containing natural products are illustrated below in Figure 4.1.1.

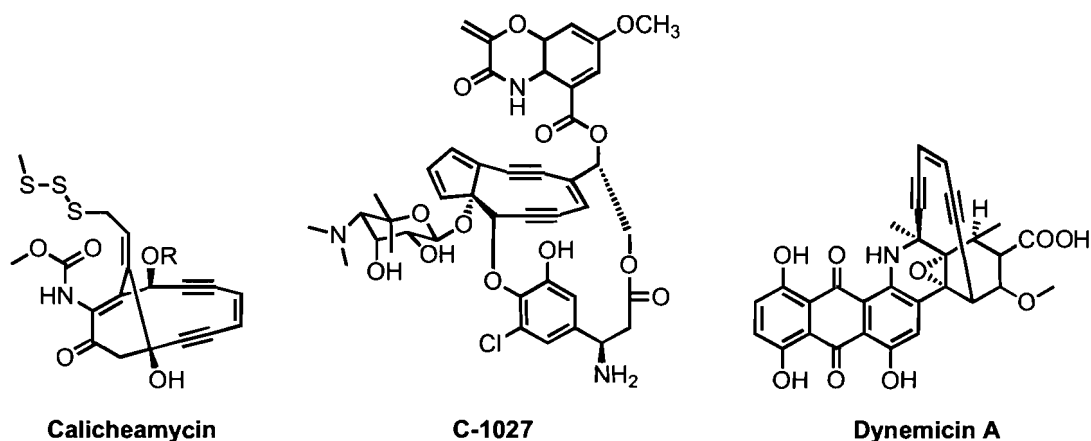
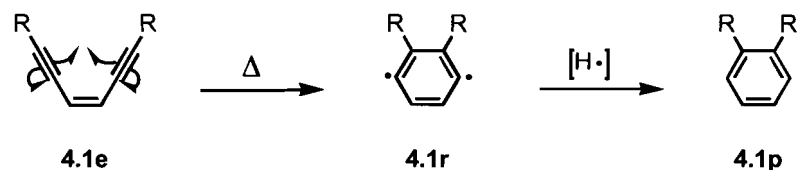


Figure 4.1.1 Natural products containing enediyne moieties.

Enediyne-containing compounds derive their activity from the thermally generated benzenoid diradical, which has been found to cleave double stranded DNA eventually leading to cell apoptosis.^{70,71} The Bergman cyclization of an enediyne is shown in Scheme 4.1.1.



Scheme 4.1.1 The Bergman cyclization of an enediyne **4.1e** is a thermal process that produces a benzenoid diradical **4.1r**, which can be trapped with a radical hydrogen source to afford the cyclized product **4.1p**.

An enediyne, **4.1e**, can thermally cyclize to a benzenoid diradical **4.1r**, that can in turn be trapped with a hydrogen radical source to give **4.1p**. The activation temperature is dependent on the distance between the two alkynes, the ring-strain and electronic effects of substituents on the enediyne,⁷¹⁻⁷³ as shown in Figure 4.1.2.

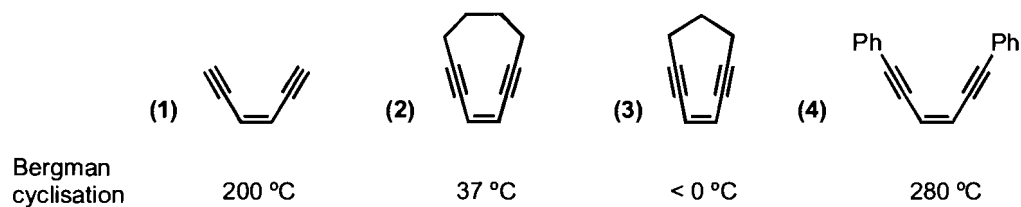


Figure 4.1.2 Examples of enediynes and their respective cyclization temperatures.

The simple enediyne unit in entry **(1)** cyclizes at 200 °C, while the 10-membered **(2)** and 9-membered **(3)** cycles react at 37 °C and less than 0 °C, respectively.⁷¹ For comparison, entry **(4)** indicates that the phenyl derivative of an enediyne has an increased cyclization temperature (280 °C).⁷⁴

4.1.1 Previous systems used for controlling an enediyne with light

There are a few other research groups that have attempted regulating enediynes using light. The first set of examples, shown in Figure 4.1.3, light was used to alter the ring-strain of cyclic enediynes, thereby affecting the activation temperature of the Bergman cyclization.

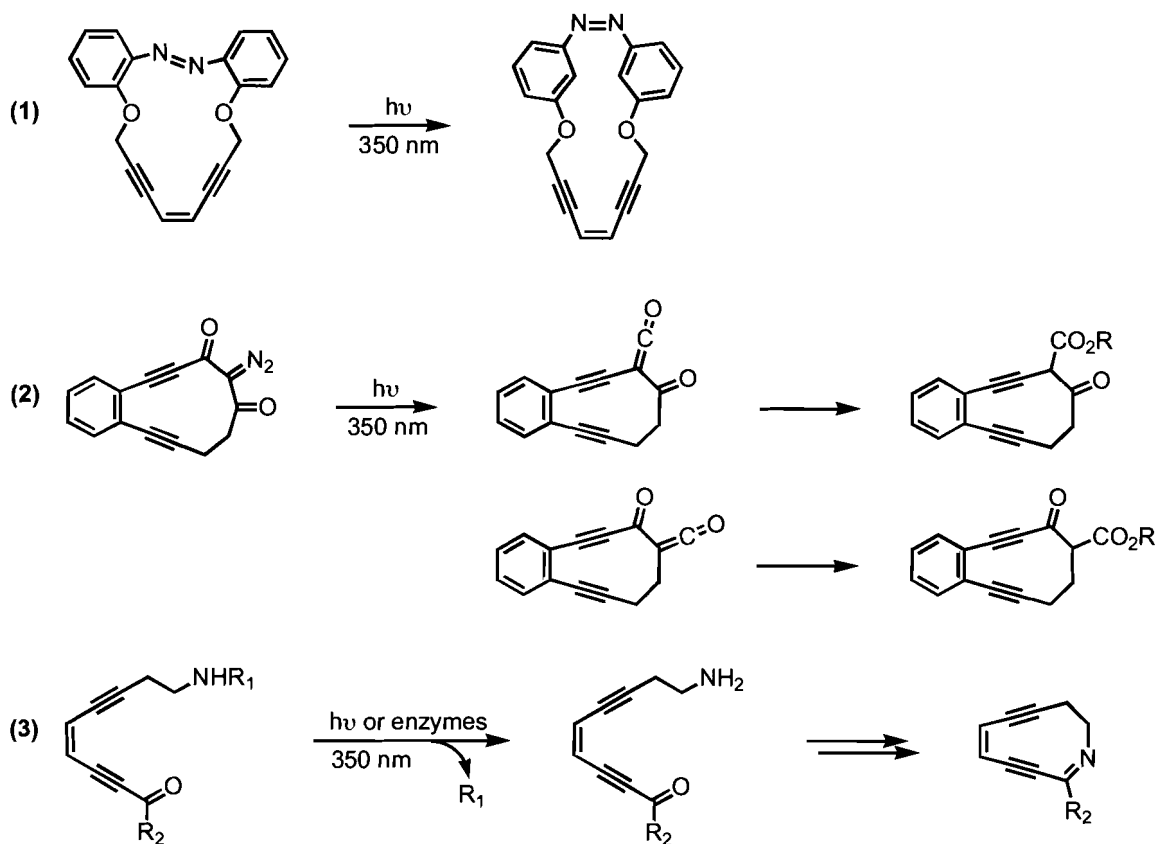


Figure 4.1.3 Literature examples where light induces a change in the ring strain of an enediyne macrocycle.

Entry **(1)** in Figure 4.1.3, by M. Kar, *et al.*,⁷⁵ took advantage of the geometrical changes accompanying the photoisomerization of an azobenzene to change the Bergman cyclization temperature. In this system, a UV light induced *trans*→*cis* isomerization decreased the activation temperature by as much as 30 °C by bringing the two alkynes into closer proximity. A major drawback of this strategy that has not been addressed is the fact that the photoisomerization of azobenzene derivatives is thermally reversible,¹⁰ thus this system would have conflicting thermal cyclization and *cis*→*trans* isomerization. Other examples showed permanent reactivity changes and made use of light-induced bond rearrangements, or photocleavage. Entry **(2)** of Figure 4.1.3 is a compound,

designed by G. V. Karpov *et al.*,⁷⁶ that took advantage of a light-induced Wolff rearrangement to reduce its activation temperature by around 100 °C. While rather complex, entry **(3)**, designed by A. Basak *et al.*,⁷⁷ is an example of how UV light was used to release a protecting group that initiated a subsequent ring-formation cyclization event to reduce the activation temperature of the enediyne to biologically relevant temperatures (37 °C).

An alternative approach to control the activation temperature of enediynes is to photochemically generate an enediyne motif from an inactive precursor, some examples of which are described in Figure 4.1.4.

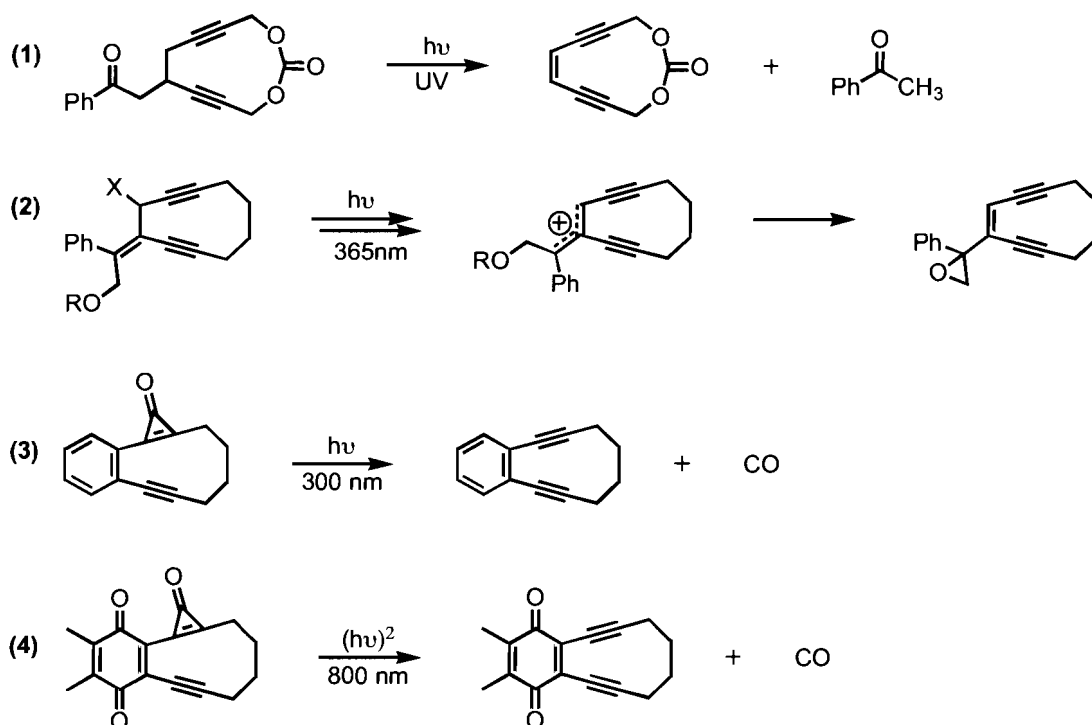


Figure 4.1.4 Literature examples that generate the enediyne substructure from a thermally stable precursor.

In entry **(1)** in Figure 4.1.4, by J. M. Nuss *et al.*,⁷⁸ an enediyne was created by a Norrish Type II reaction, using UV light, which afforded a double bond

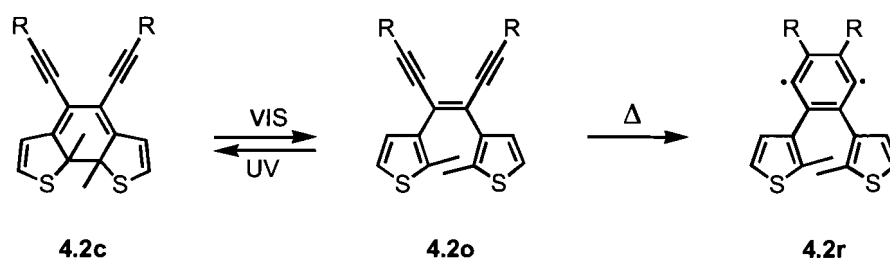
between two alkynes. In entry **(2)**, Y. Tachi *et al.*⁷⁹ generated an enediyne following side group cleavage induced by extended (4-8 h) UV-light irradiation, leading to alkene isomerization. The next two entries in Figure 4.1.4, **(3)** and **(4)**, by A. Poloukhine *et al.*^{80,81} took advantage of the light-induced release of carbon monoxide from cyclopropanone, generating an alkyne. For entry **(4)**, two-photon photolysis lead to the decarbonylation of the cyclopropanone.⁸¹ All the examples in Figure 4.1.4 generated an undesired side product.

The examples summarized above in Figures 4.1.3 and 4.1.4 describe all the systems published to date. All but the last example used UV light, which is harmful to cell cultures and has poor tissue penetration,^{82,83} to either generate an enediyne or lower its activation temperature by creating ring-strain. In practice, the phototherapeutic window is 650-950 nm, where light can penetrate deeper into tissue with less damage to cells. In the last example, **(4)** by Poloukhine *et al.*, the authors claimed that two-photon reactions are a viable solution to replace UV-light irradiation. However, the high intensity lasers required for two photon reactions can also be harmful to cell cultures.^{84,85}

4.1.2 Design for the control of a Bergman cyclization with DTE

The ring-closing isomerization of DTEs requires UV light, while the ring-opening reaction requires visible wavelengths of light. The hexatriene moiety, responsible for the photoisomerization of DTEs, experiences π -bond rearrangements, which can be designed to modulate the presence/absence of reactive groups, as seen in the *Introduction* chapter. A new photocontrollable system in which the thermal Bergman cyclization would follow the visible light

induced ring-opening isomerization is described here to address the wavelength-based limitations of biological applications, as depicted in the Scheme 4.1.2.



Scheme 4.1.2 An enediyne **4.2o** is generated using visible light from compound **4.2c** by taking advantage of the photoisomerization of a DTE. The enediyne could then undergo a Bergman cyclization to yield the benzenoid diradical **4.2r**.

By integrating the hexatriene and enediyne structures into a single architecture (**4.2o**), a molecular system that uses visible light to control the Bergman cyclization reaction has been designed. Only the *ring-open* isomer **4.2o** contains the enediyne motif needed to undergo spontaneous cyclization and yield the active diradical **4.2r**, which is the chemical species responsible for the high antitumor activity previously mentioned in this chapter. UV light triggers the photocyclization reaction of the hexatriene in **4.2o** and converts it to its *ring-closed* counterpart **4.2c**. This photochemical reaction rearranges the π -system and delocalizes it along the rigid backbone formed during the ring-closing reaction. The consequence is the removal of the enediyne architecture necessary for the compound to undergo spontaneous conversion to the diradical, making the *ring-closed* isomer **4.2c** “inactive”. Visible light can be used to “activate” the system by triggering the ring-opening reaction, regenerating the enediyne in compound **4.2o**. That this system is activated with visible light, which has the potential to penetrate deeper tissue with less damage to surrounding

tissue than the more commonly used UV light, is a particularly significant feature and adds to the appeal of the system.

This chapter describes how two DTE-enediyne compounds, shown in Figure 4.1.5, were prepared.

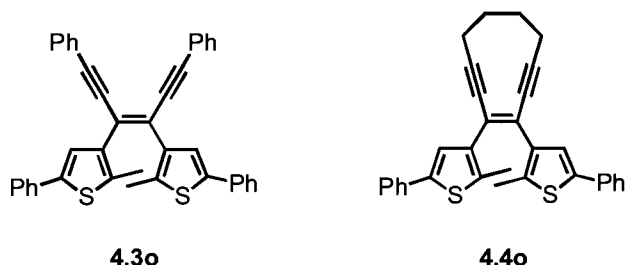


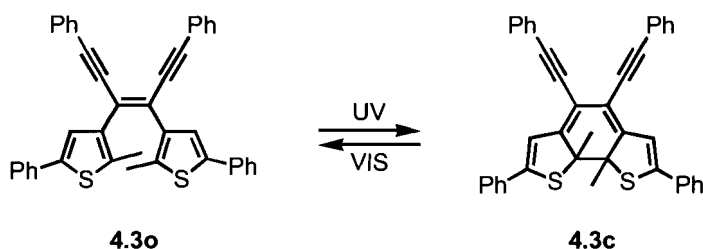
Figure 4.1.5 DTE enediyne derivatives, prepared and analyzed.

The phenyl-substituted derivative **4.3o** was prepared because its thermal stability provided a good control for the photochromic activity of this new enediyne DTE architecture. The 10-membered ring derivative **4.4o** provided a thermally sensitive enediyne, in which the Bergman cyclization could potentially be studied at biological temperatures. As stated before, cyclic enediynes with 10-membered rings are often biologically active and thermally cyclize at 37 °C.⁷¹ Using derivative **4.4o**, photoregulation of the presence/absence of an enediyne moiety was demonstrated to be essential for the cyclization to take place.

4.2 Phenyl-substituted enediyne DTE 4.3o

Since the photochromism of DTEs can be greatly affected by synthetic changes to the backbone, it was necessary to prepare an enediyne that would be stable at ambient conditions (20-25 °C) in order to separately study the backbone modification effects on the photochromic performance. Previously published⁸⁶

synthetic procedures to prepare *cis* phenyl-substituted enediynes and the need for a thermally stable model enediyne DTE resulted in **4.3o** being the first molecule to be prepared. The light-induced isomerization of **4.3o** is depicted in Equation 4.2.1.

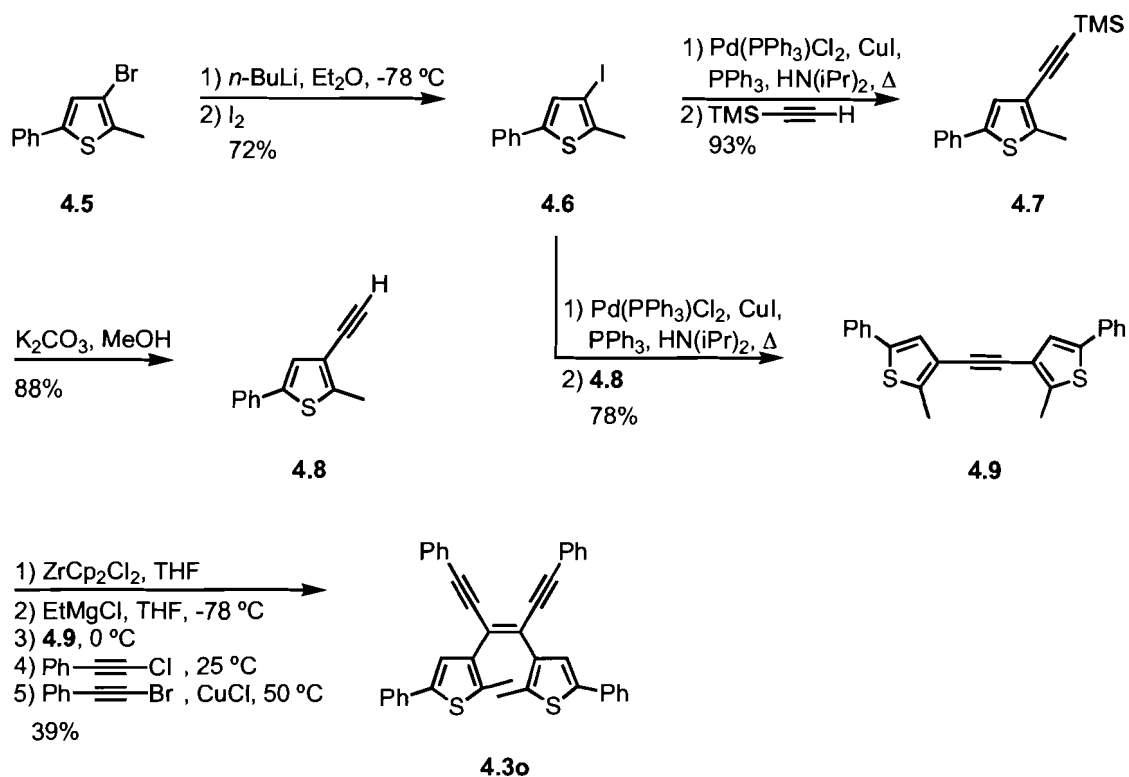


Equation 4.2.1 Phenyl-substituted enediyne DTE derivative **4.3o** can isomerize with UV light into its corresponding *ring-closed* isomer **4.3c**. The *ring-open* isomer **4.3o** can be regenerated with visible wavelengths of light.

UV light is used to ring-close compounds **4.3o** into **4.3c**, effectively removing the enediyne. Visible light can in turn be used to regenerate the *ring-open* isomer **4.3o**, which is the only isomer containing an enediyne.

4.2.1 Synthesis of the phenyl-substituted enediyne DTE **4.3o**

Both enediyne derivatives could be prepared from an alkylzirconation reaction, which installs two alkynes *cis* to one another on an alkyne substrate (**4.9**), yielding an enediyne in one step.⁸⁶ The complete synthetic route used to prepare the phenyl enediyne is shown in Scheme 4.2.1.



Scheme 4.2.1 Synthesis of the phenyl-substituted enediyne DTE **4.3o**.

The first step of the synthesis converted the known 3-bromo-2-methyl-5-phenylthiophene **4.5**,⁸⁷ into its corresponding iodide, compound **4.6**, in order for it to undergo a more facile palladium-catalyzed Sonogashira coupling reaction with TMS-acetylene to produce compound **4.7**. After removing the trimethylsilyl protecting group with potassium carbonate (K_2CO_3) and methanol, alkynylthiophene **4.8** could be re-subjected to the Sonogashira coupling with the same iodothiophene compound **4.6**, generating alkyne-linked bis(thiophene) **4.9**. This was where the syntheses of the different enediyne DTE derivatives **4.2o** stemmed from. The enediyne portion of compound **4.3o** was installed by reacting with halogenated phenylacetylenes using a one-pot alkylzirconation reaction.⁸⁶ This multi-step reaction ensured that the two alkyne groups were appropriately

positioned *cis* to each other, so that the enediynes could eventually undergo the Bergman cyclization reaction.

4.2.2 Photochromism of the phenyl-substituted enediyne DTE 4.3o

The hexatriene in compound **4.3o** was very sensitive to UV light, and irradiation of solutions of compound **4.3o** with 365-nm light immediately triggered significant optical changes. The photo-induced cyclization was best monitored using UV-VIS absorption spectroscopy (Figure 4.2.1a), where there was an obvious decrease in high-energy absorptions and an accompanying appearance of absorption bands in the lower energy regions ($\lambda_{\text{max}} = 573$ and 393 nm) of the spectra when a benzene solution of compound **4.3o** was irradiated with 365-nm light. These trends are typical for DTE derivatives, and accounted for the change in colour of the solutions from colourless to purple due to the creation of the linearly conjugated pathway in the *ring-closed* form.

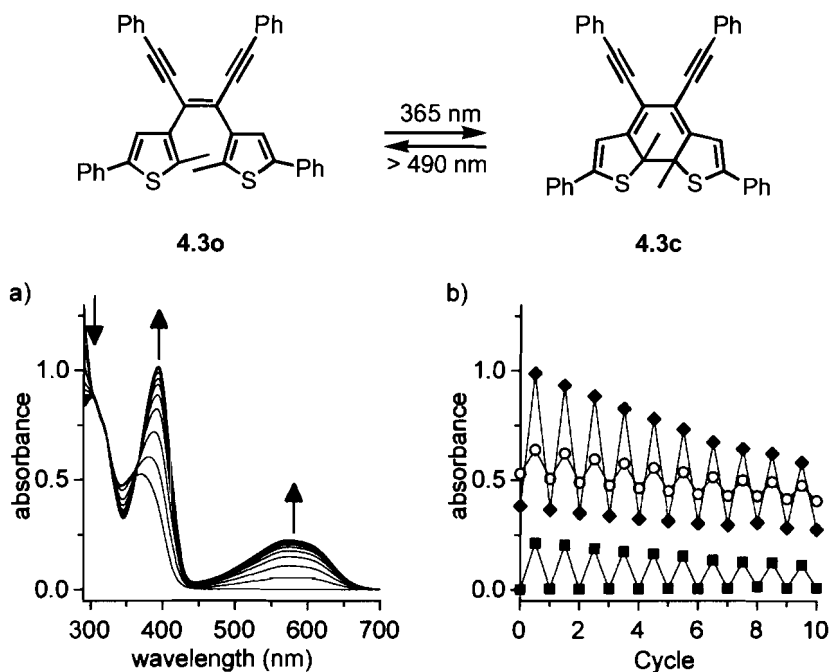


Figure 4.2.1 Changes in the UV-VIS absorption spectra of a 2.65×10^{-5} M solution of enediyne **4.3o** in C₆H₆ upon irradiation with 365-nm light. (a) Total irradiation periods are 0, 10, 20, 30, 40, 50, 60, 70, 80 and 90 sec. (b) Modulated absorbance at 369 nm (○), 393 nm (◆) and 575 nm (■) during alternate irradiation of with 365-nm light for 90 sec, then > 490 nm for 90 sec.

The *ring*-closed isomer was stable at ambient temperature as long as it was kept in the dark. Irradiation of the coloured solution with visible light (greater than 490 nm) converted the *ring*-closed isomer **4.3c** back to compound **4.3o** and regenerated the original absorption spectrum. Repetitive cycling of the isomerization reaction resulted in slow degradation. The effect is shown in Figure 4.2.1b where 30% of the original absorption value was lost after ten consecutive ring-closing/ring-opening cycles. The side products of the photodegradation are often uncharacterizable and could not be isolated for this specific compound. However, since this compound was designed as a drug, only one event of phototriggering is necessary. In this case, the ring-opening reaction was the triggering event and was quantitative. Previous literature reports indicated that side products arose from the ring-closing reaction.^{88,89}

The photochemical interconversion between the *ring-open* isomer **4.3o** and the *ring-closed* isomer **4.3c** was also monitored by ^1H NMR spectroscopy. Irradiation of a C_6D_6 solution of compound **4.3o** (3.8×10^{-3} M) with 365-nm light resulted in the appearance of a new set of signals for compound **4.3c** including a singlet at 2.38 ppm, while the corresponding thiophene-C5 methyl singlet was at 2.20 ppm for compound **4.3o**, as illustrated in Figure 4.2.2.

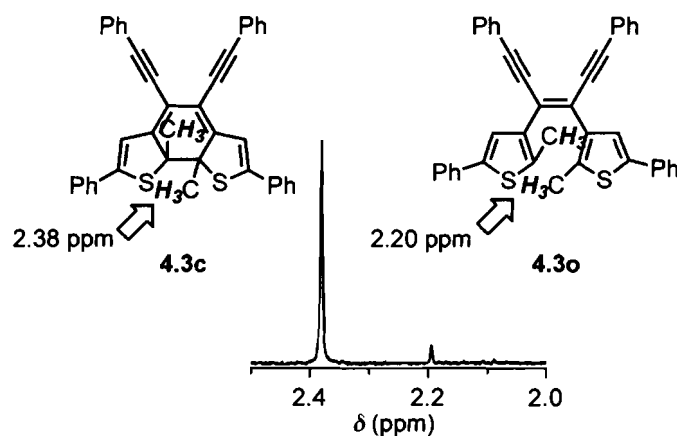


Figure 4.2.2 Selected region in the ^1H NMR spectrum obtained after irradiation of a C_6D_6 solution of compound **4.3o** (3.8×10^{-3} M) with 313-nm light, highlighting the thiophene-C5 methyl singlet used in determining the extent of photoconversion.

When additional irradiation of the solution with 365-nm light resulted in no further changes in the relative integration between the signals assigned to compounds **4.3o** and **4.3c**, the photostationary state was determined to be a mixture of 92% of *ring-closed* isomer **4.3c**, with the remaining 8% assigned to the *ring-open* isomer **4.3o**.

4.2.3 Thermal studies of the phenyl-substituted enediyne DTE **4.3o**

One of the quickest ways to estimate the Bergman cyclization temperature is to perform a differential scanning calorimetry (DSC) experiment. In this technique, the heat flux (power) to a sample pan and a reference pan is

monitored against temperature, while the temperature of the sample is varied. This technique gives information about exothermic and endothermic processes occurring in the sample. When the sample absorbs or gives off heat, the instrument measures the amount of energy needed to keep the reference pan at the same temperature. It is this differential energy that gives rise to peaks in a DSC thermograph.

The thermal reactivity of compound **4.3o** was expected to happen at elevated temperatures, when considering the phenyl-substituted enediyne (**4**) in Figure 4.1.2. During the DSC experiment performed, an exothermic peak could indicate that the diradical was formed due to the resulting polymerization/degradation that released heat.^{90,91} A first DSC trace using compound **4.3o** (broken line) displayed an exothermic peak starting at around 175 °C, as shown in Figure 4.2.3.

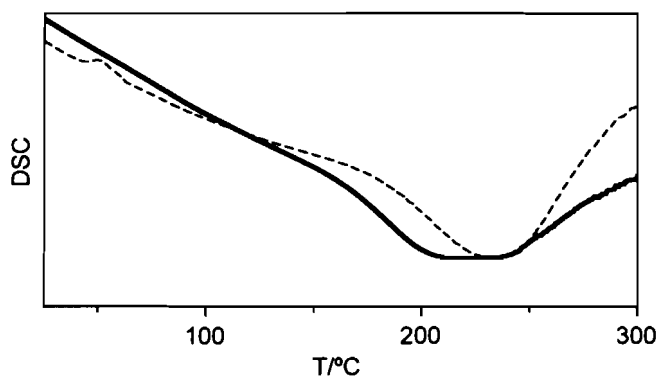


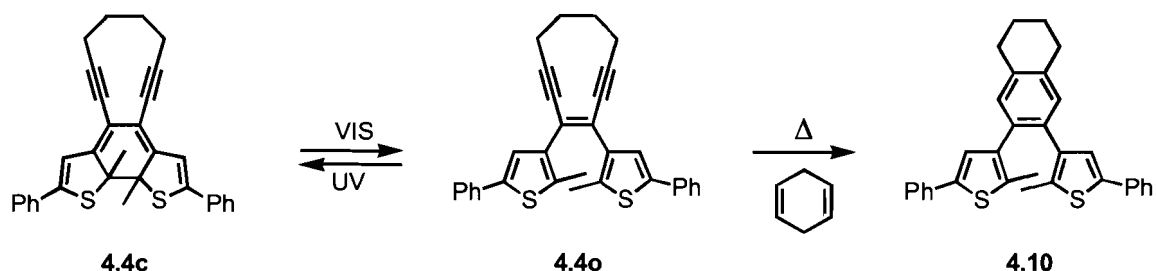
Figure 4.2.3 DSC thermograph with a heating rate of 10 °C/min for *ring-open* isomer **4.3o** (broken line) and *ring-closed* isomer **4.3c** (bold line) phenyl-substituted enediyne

A sample of pure *ring-closed* isomer **4.3c** was then prepared by purification by HPLC from a photostationary mixture of compounds **4.3o** and **4.3c**, generated using 365-nm light. The DSC trace of compound **4.3c** (bold line)

appeared to be slightly different to that of the *ring-open* isomer **4.3o**. However, since the Bergman cyclization occurred at such an elevated temperature, one could not rule out the thermal degradation of either the *ring-open* or the *ring-closed* isomer by other pathways, thus explaining the difficulty in clearly observing the differences between both forms. A derivative with a lower cyclization temperature had to be prepared next.

4.3 10-membered ring enediyne DTE **4.4o**

Now that the photochromism of a DTE enediyne system was confirmed, the 10-membered carbocycle was installed to facilitate a lower temperature Bergman cyclization, which could be monitored by the formation of the cyclized product, as shown in Scheme 4.3.1.

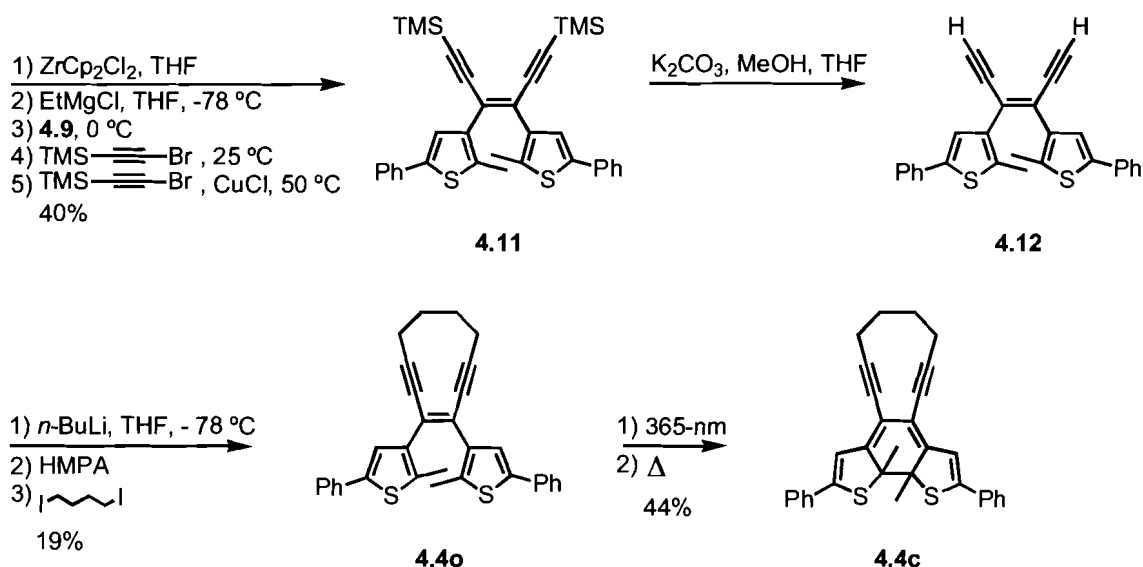


Scheme 4.3.1 Visible light isomerizes the *ring-closed* **4.4c** into the *ring-open* isomer **4.4o**, which thermally forms the benzenoid diradical that can be trapped, using a radical quencher, as the cyclized product **4.10**.

Compound **4.4o** should undergo the Bergman cyclization at significantly lower temperatures than that of the phenyl-substituted derivative **4.3o**. Irradiation with UV light removes the enediyne, making compound **4.4c** stable under the cyclization conditions. Quenching the diradical formed thermally by the Bergman cyclization from compound **4.4o**, using a hydrogen radical source such as 1,4-cyclohexadiene, generates the product **4.10**.

4.3.1 Synthesis of the 10-membered ring enediyne DTE 4.4o

Compound **4.4o** was synthesized using a similar route to that described above (Scheme 4.2.1) for the phenyl-substituted enediyne DTE **4.3o**. Using the alkyne-linked bis(thiophene) **4.9**, a *cis* enediyne terminated with trimethylsilyl (TMS) protecting groups was prepared following the one-pot alkylzirconation described previously, using brominated TMS-acetylene.⁸⁶ The 10-membered ring was formed by first deprotecting the TMS-acetylenes in compound **4.11** with potassium carbonate in methanol/THF to give compound **4.12**, and then quenching the dianion generated using strong base (*n*-butyllithium) with 1,4-diodobutane, as illustrated in Scheme 4.3.2.

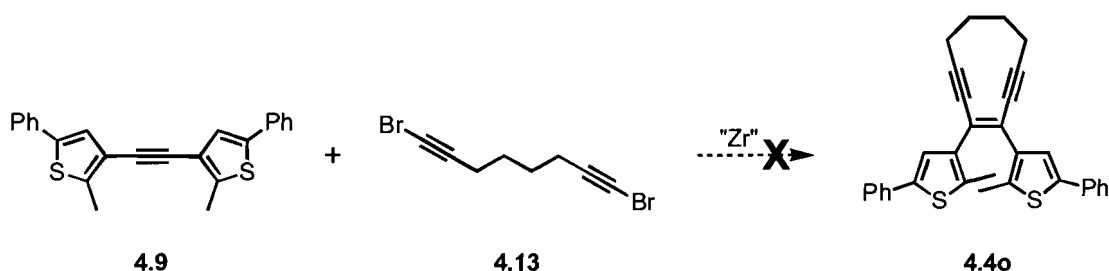


Scheme 4.3.2 Synthesis of the 10-membered ring enediyne DTE **4.4o** and its corresponding *ring-closed* isomer **4.4c**.

When compound **4.4o** was irradiated with 365-nm light, compound **4.4c** was formed, according to ^1H NMR spectroscopy. The first indication of the difference in thermal reactivity between isomers **4.4o** and **4.4c** was that when a mixture of them, generated using 365-nm light, was heated to $75\text{ }^\circ\text{C}$, only the

ring-open isomer **4.4o** degraded, as confirmed by a disappearance of its ^1H NMR resonance signals. The remaining *ring-closed* isomer **4.4c** could be purified from the mixture by flash chromatography and was isolated in 44% yield.

In another attempt to synthesize compound **4.4o**, a halogenated bis(alkyne) **4.13** was used for the alkylzirconation coupling reaction to prepare the 10-membered ring in one pot from compound **4.9**, as shown in Scheme 4.3.3, but proved to be unsuccessful.



Scheme 4.3.3 Unsuccessful synthetic route to make the compound **4.4o** in one pot from compound **4.9** using bis(alkyne) **4.13**.

If the two alkyne coupling reactions would have happened sequentially, the 10-membered ring product would have been prepared all in one pot from compound **4.9**. ^1H NMR analysis of the crude reaction mixture indicated that the major components were the starting materials.

4.3.2 Photochromism of the 10-membered ring enediyne DTE **4.4o**

As seen for compound **4.3o**, a colour change resulted from irradiation of a benzene solution of compound **4.4o** with 365-nm light. These colour changes were characterized by UV-VIS absorption spectroscopy (Figure 4.3.1a), which showed that there was a clear decrease in high-energy absorptions ($\lambda_{\text{max}} = 301$ nm) and an accompanying appearance of absorption bands in the lower-energy

regions ($\lambda_{\max} = 373 \text{ nm}$ and 550 nm) of the spectrum following irradiation with 365-nm light.

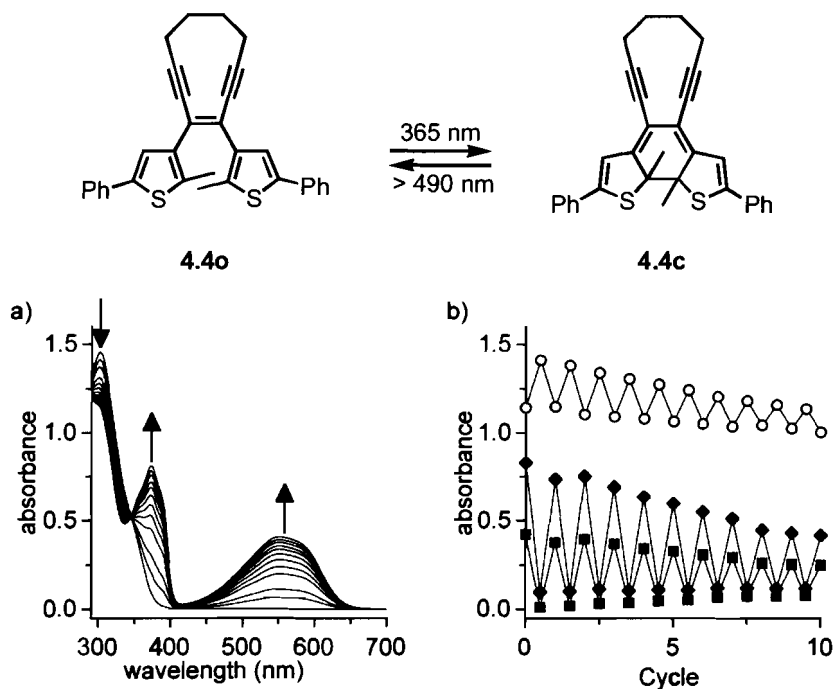


Figure 4.3.1 Changes in the UV-VIS absorption spectra of a $8.22 \times 10^{-5} \text{ M}$ solution of enediyne **4.4o** in C_6H_6 upon irradiation with 365-nm light. (a) Total irradiation periods are for 10 sec intervals until 120 sec is reached. (b) Modulated absorbance at 301 nm (○), 373 nm (◆) and 550 nm (■) during alternate irradiation of with 365-nm light for 120 sec, then > 490 nm for 90 sec.

Repetitive cycling of the isomerization reaction resulted in degradation. The effect was shown in Figure 4.3.1b where 40% of the original absorption value was lost after 10 consecutive ring-closing/ring-opening cycles, similarly to what was observed for compound **4.3o**. As mentioned before, since the ring-opening reaction is a triggering event, it only needs to occur a single time and the importance of the cycling performance of compound **4.4o** is minimal.

The photochemical interconversion between the *ring-open* isomer **4.4o** and the *ring-closed* isomer **4.4c** was also monitored by ^1H NMR spectroscopy. Irradiation of a C_6D_6 solution of compound **4.4o** ($2.1 \times 10^{-2} \text{ M}$) with 365-nm light

resulted in the appearance of a new set of signals for compound **4.4c**, including a singlet at 6.91 ppm, while the corresponding thiophene proton singlet was at 7.22 ppm for compound **4.4o**, as illustrated in Figure 4.3.2.

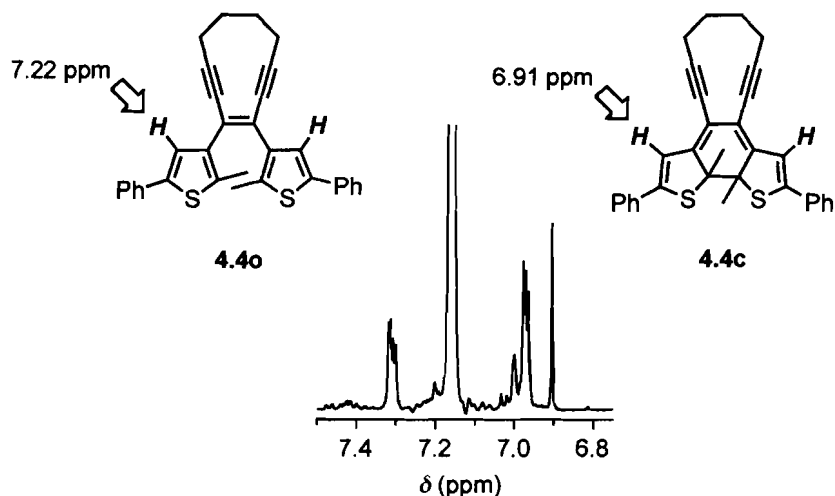


Figure 4.3.2 Selected region in the ¹H NMR spectrum obtained after irradiation of a C₆D₆ solution of compound **4.4o** (2.1×10^{-2} M) with 313-nm light, highlighting the thiophene proton singlet used in determining the extent of photoconversion.

When additional irradiation of the solution with 365-nm light resulted in no further changes in the relative integration between the signals assigned to compounds **4.4o** and **4.4c**, the photostationary state was determined to be a mixture of 82% of *ring-closed* isomer **4.4c** with the remaining 18% assigned to the *ring-open* isomer **4.4o**.

4.3.3 Thermal studies of the 10-membered ring enediyne DTE **4.4o**

The Bergman cyclization was monitored by NMR spectroscopy, rather than by DSC, because the reaction occurred at lower temperatures and could be performed in deuterated solvents. Such a treatment could provide greater insight into the mechanistic details of the reaction. The formation of the reactive diradical of the *ring-open* isomer **4.4o** in C₆D₆, heated to 75 °C, could be probed by ¹H

NMR spectroscopy with 1,4-cyclohexadiene as a radical trapping agent, used in large excess to prevent side product formation and to provide *pseudo* first order kinetics.⁹² The temperature of 75 °C was determined from preliminary studies at 40, 60 and 80 °C indicating that the reaction only occurred in higher temperature range. A thermally stable internal standard, *p*-nitroanisole, was used to normalize the integration values of compounds **4.4o** and **4.10**. This internal standard was chosen because its ¹H NMR signals in the aromatic and aliphatic region were not overlapping with the *ring-open* **4.4o**, *ring-closed* **4.4c** or the cyclized **4.10** compounds as shown in Figure 4.3.3.

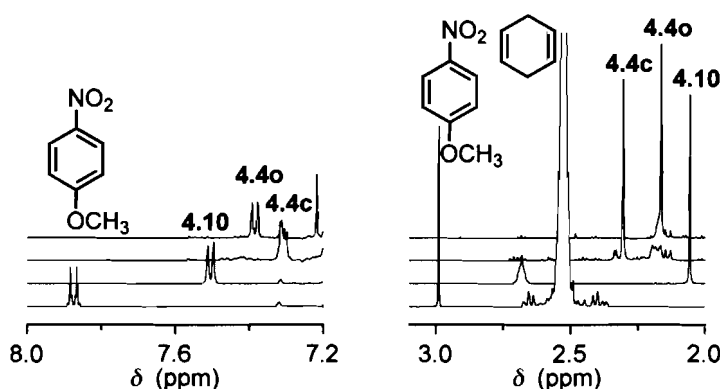


Figure 4.3.3 Selected ¹H NMR signals in C₆D₆ for *p*-nitroanisole, 1,4-cyclohexadiene, *ring-open* isomer **4.4o**, *ring-closed* isomer **4.4c** and cyclized product **4.10** as monitored for the thermal reaction progress.

The integration of the area under the peaks for both in the aromatic and the aliphatic region was possible. However, due to some peak overlap and side-product formation, only the thiophene-methyl peaks, between 2.0 and 2.4 ppm, were used for further data analysis. When heated to 75 °C, the integration values of compound **4.4o** showed a pattern of exponential decay that also correlated to the appearance of the cyclized product **4.10** as illustrated in Figure 4.3.4.

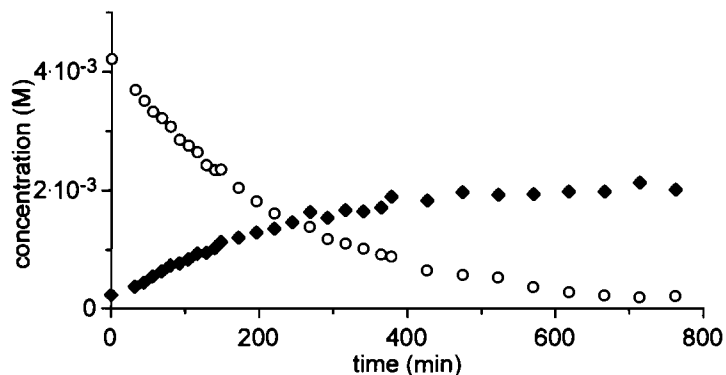


Figure 4.3.4 Concentration of the *ring-open* isomer **4.4o** (○) and the cyclized product **4.10** (◆) obtained by integration, normalized against the internal standard in thermal study in C_6D_6 . Initial concentrations were of 4.2×10^{-3} M for **4.4o**, of 1.9×10^{-3} M for *p*-nitroanisole and of 2.8×10^{-1} M for 1,4-cyclohexadiene.

The trapping of the thermal cyclization of compound **4.4o** afforded compound **4.10** in 30% yield when performed on a larger scale. In contrast, the *ring-closed* isomer did not show any signs of degradation when heated to 75 °C for 13 h.

The following describes the kinetics of the Bergman cyclization reaction. In order to compare all reaction rates and to verify the first-order nature of the decay or appearance of the *ring-open* **4.4o** and Bergman product **4.10**, respectively, equations need to be introduced. The first order kinetic expression, Equation 4.3.1, was used to determine the apparent rate of decay of compounds **4.4o** and of **4.4c**.

$$C = C_0 e^{-k_{eff}t}$$

Equation 4.3.1 First-order rate equation.

$$\ln(C/C_0) = \ln C - \ln C_0 = -k_{eff}t$$

Equation 4.3.2 Normalized rate equation.

$$\ln\left(\frac{P_\infty}{P_\infty - C}\right) = k_{eff}t$$

Equation 4.3.3 Apparent rate of product formation.

Equation 4.3.2 allowed normalization of all concentrations with respect to the initial concentrations for the *ring-open* **4.4o** and *ring-closed* **4.4c** isomers, since both reactions were not performed at the same concentration. This manipulation had no effect on the rate constant ($-k_{eff}$), but rather changed the y-axis intercept for both to be “0”. Equation 4.3.3, where P_∞ is the concentration of product **4.10** at time $t = \infty$ and C is the concentration of product **4.10** at time t , was used to determine the apparent rate of formation,⁹² assuming that a minimal amount of side product was formed due to the presence of an excess of 1,4-cyclohexadiene. Figure 4.3.5 illustrates the changes in concentration over time.

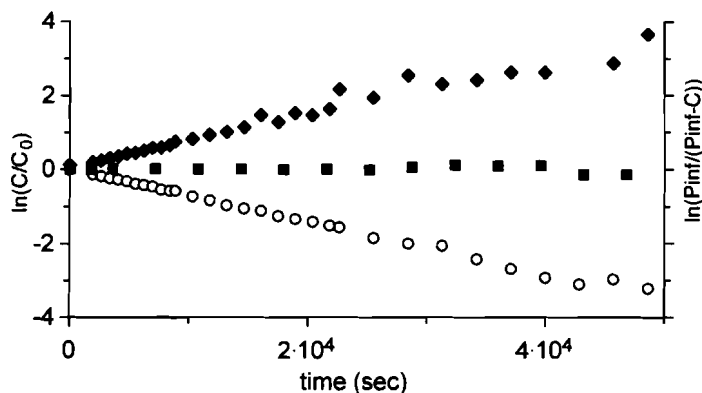


Figure 4.3.5 Changes in concentration of *ring-open* isomer **4.4o** (○) (4.2×10^{-3} M), *ring-closed* isomer **4.4c** (■) (2.4×10^{-3} M) and cyclized product **4.10** (◆).

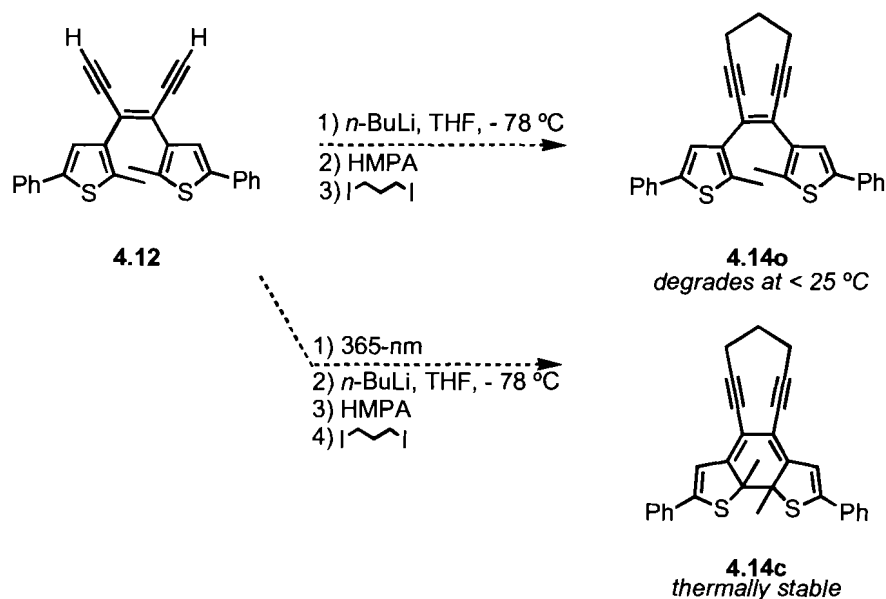
The Bergman cyclization reaction followed pseudo first-order kinetics (Figure 4.3.5) with apparent rates being $k = 7.0 \times 10^{-5} \text{ sec}^{-1}$ for the disappearance of compound **4.4o** and $k = 7.0 \times 10^{-5} \text{ sec}^{-1}$ for the formation of compound **4.10**. Conversely, the *ring-closed* isomer **4.4c** showed significant thermal stability, with an apparent rate of decay of $k = 7.0 \times 10^{-7} \text{ sec}^{-1}$, 100 times slower decay than that of its *ring-open* counterpart, if it could be considered to be decaying following first-order kinetics. Another notable observation was that no single detectable side product was formed from compound **4.4c**, even in the presence of the radical trapping agent, indicating that the degradation reaction probably did not go through a well-defined radical intermediate. This last observation is of particular significance in the case where these compounds would be used as a drug, implying that the ring-closed isomer might degrade, but would not form the aforementioned active diradical species responsible for DNA damage.

4.4 Conclusion

The initial design for light-triggerable enediyne DTE derivatives was based on the visible light isomerization of the *ring-closed* isomers into the *ring-open* isomers, with their accompanying π -bond rearrangements. The photochromism of the enediyne DTE system was demonstrated using a thermally stable phenyl-substituted enediyne DTE **4.3o**, while a thermally reactive 10-membered ring enediyne DTE **4.4o** was prepared as well. A significant difference in reactivity was demonstrated between either isomers of the 10-membered enediyne DTE, compound **4.4o** thermally cyclizing while compound **4.4c** was thermally stable, providing an unprecedented example of generating an enediyne using visible light. The active *ring-open* isomer **4.4o**, created using visible light (wavelengths greater than 490-nm) from its corresponding unreactive *ring-closed* isomer **4.4c**, showed first-order degradation kinetics at 75 °C. Since the activation temperature for the Bergman cyclization in compound **4.4o** is too high for biological applications, a lower temperature derivative is still needed.

4.5 Future work

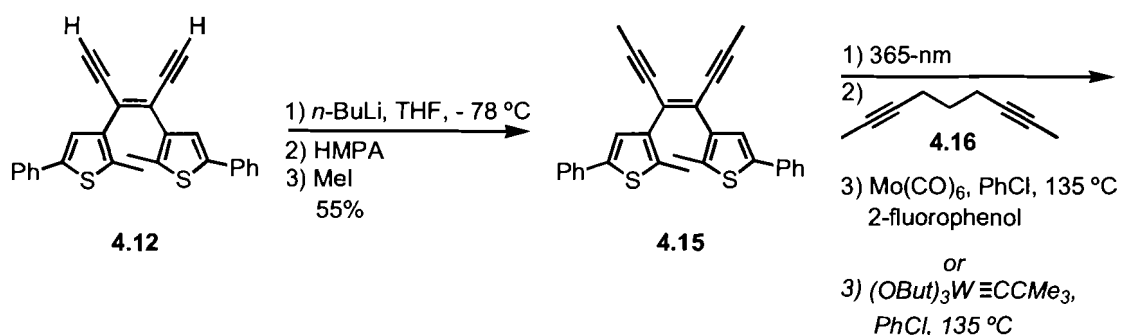
Preliminary attempts were made at synthesizing a 9-membered ring derivative **4.14c**, which should have significantly lower activation temperatures⁷¹ because of its increased ring strain, as shown in Scheme 4.5.1.



Scheme 4.5.1 Unsuccessful synthetic route to make the *ring-closed* isomer of a 9-membered ring enediyne DTE **4.14c** by quenching the lithiated product of **4.12** with diiodopropane.

The lithiation quenching approach with 1,3-diiodopropane, analogous to the method used to prepare compound **4.4o**, proved to be unsuccessful after several attempts. This was anticipated in view of the low yielding reaction to produce **4.4o**. The low reactivity of alkynyl nucleophiles⁹³ and the high level of strain in a 9-membered ring severely limited this reaction. One important synthetic issue is that if the product has lower than room temperature reactivity, it would be impossible to isolate it by conventional methods at room temperature. It is due to this limitation that the synthesis was attempted from the photostationary state of compound **4.12**, and is represented by compound **4.14c** (Scheme 4.5.1) if the product were to be isolated. All of the *ring-open* isomer product, compound **4.14o**, would degrade thermally by forming a diradical, while the *ring-closed* isomer could be purified. The solutions of compound **4.12** were irradiated with 365-nm light for 1 h prior to adding the other reagents in all experiments attempted.

Another potentially promising route involves alkyne metathesis,⁹⁴ and two of the commercially available catalysts are molybdenum carbonyl ($\text{Mo}(\text{CO})_6$)⁹⁵ and Schrock's alkyne metathesis catalyst $[(\text{OtBu})_3\text{W}\equiv\text{CMe}_3]$,⁹⁶ both shown in Scheme 4.5.2.



Scheme 4.5.2 Alkyne metathesis route starting with methyl-terminated enediyne DTE **4.15**.

Terminal alkynes cannot be used in alkyne metathesis,⁹⁶ and the methyl terminated derivatives are most commonly used since the side-product, 2-butyne, can be easily removed by evaporation from the reaction mixture, *in vacuo* or N_2 purge, pushing the reaction equilibrium towards the products.⁹⁷ Both methyl-terminated acetylenes, compounds **4.15** and **4.16**, were prepared and the two different alkyne metathesis catalysts were tried, but neither produced measurable amounts of compound **4.14c**. Alkyne metathesis conditions are only used to make ring sizes of 12 atoms or greater, because the newly formed alkyne does not tolerate a large amount of ring strain⁹⁸ and homodimeric products are usually formed instead of the expected macrocycle. A more extensive tuning of the reaction conditions is required in order to yield any of the desired products.

In the event that a lower temperature enediyne DTE derivative were to be prepared, it would have to possess adequate compatibility with biological matrices to be useful in a practical setting. Enediyne-containing natural products typically have 3 functional domains: 1) the “warhead”, which is the enediyne itself and has the potential to damage biological material (DNA, proteins) in its presence upon formation of the benzenoid diradical; 2) the “trigger”, which upon activation will make the “warhead” reactive at biological temperatures; and 3) a “delivery system”, which is a DNA-binding group that positions the enediyne-drug in close proximity of its intended target.^{71,99} Since the enediyne DTE derivatives have both the “trigger” and the “warhead”, the remaining modification to a functional DTE-based enediyne would be a DNA-targeting group. While the use of light for drug activation does decrease the need for high sensitivity site-targeting, the drug would still need to be triggered in the presence of DNA to inflict a maximal amount of damage. Also, drugs need to be soluble in biological matrices to be useful. Both of these two requirements would necessitate synthetic modifications of the DTE enediyne derivatives, with some suggestions illustrated in Figure 4.5.1.

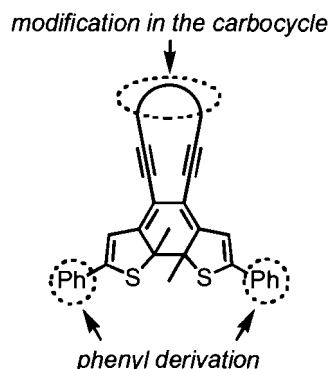


Figure 4.5.1 Possible modification sites on an enediyne DTE derivative for DNA targeting and biologically soluble groups.

Many useful derivatives are accessible either through modification of the carbocycle or derivation of the phenyl groups on the thiophene, as shown in Figure 4.5.1. Typical “delivery” groups include intercalators, such as naphthalene, anthraquinone and anthracene derivatives, which position the molecule in the minor groove of DNA and oligosaccharide chains with shape-selective association with DNA. The oligosaccharides are of particular appeal since they would also address the solubility issue, thus solving both design features.

4.6 Experimental

4.6.1 General

All solvents used for synthesis and characterization were dried and degassed by passing them through steel columns containing activated alumina under nitrogen using an MBraun solvent purification system. Solvents for NMR analysis (Cambridge Isotope Laboratories) were used as received. All reagents were purchased from Aldrich with the exception of (trimethylsilyl)acetylene, which was purchased from Alfa Aesar, and $\text{Pd}(\text{PPh}_3)_4$, Cp_2ZrCl_2 , $\text{Mo}(\text{CO})_6$ and

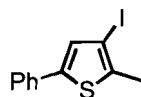
(*tert*-Bu)₃W≡CMe₃ which were purchased from Strem. The starting material 3,5-dibromo-2-methylthiophene³⁵ was prepared according to the literature procedure.

4.6.2 Methods

¹H NMR and ¹³C NMR characterizations were performed on a Bruker AMX 400 instrument with a 5 mm inverse probe operating at 400.13 MHz for ¹H NMR and 100.6 MHz for ¹³C NMR; a Varian 400 MercuryPlus instrument with a 5 mm ATB probe equipped with a shielded gradient operating at 400.10 MHz for ¹H NMR and 100.60 MHz for ¹³C NMR; a Varian Inova 500 instrument with a 5 mm inverse probe equipped with a shielded gradient operating at 499.8 MHz for ¹H NMR and 125.7 MHz for ¹³C NMR; or a Bruker Avance II 600 with a 5 mm QNP cryoprobe operating at 150.90 MHz for ¹³C NMR with a WALTZ-16 composite pulse decoupling of ¹H used for all ¹³C NMR. Chemical shifts (δ) are reported in parts per million relative to tetramethylsilane using the residual solvent peak as a reference standard. Coupling constants (*J*) are reported in Hertz. FT-IR spectroscopy was performed using a Nicolet Nexus 670 instrument. UV-VIS absorption spectroscopy was performed using a Varian Cary 300 Bio spectrophotometer. Low resolution mass spectrometry (LRMS) measurements were performed using a HP5985 mass spectrometer with isobutane as the chemical ionization source, a Varian 4000 GC/MS/MS with electron impact operating at 10 mamp as the ionization source or chemical ionization (CI) with methanol or a PerSeptive Biosystems Voyager-DE Biospectrometry Workstation MALDI spectrometer using a 2,4-dihydroxybenzoic acid matrix. Melting points were measured using a Fisher-Johns melting point apparatus. Flash

chromatography was performed using silica gel 60 (230–400 mesh) from Silicycle Inc. Centrifugal chromatography was performed using a Harrison Research Inc. Chromatotron, model 8924 using TLC grade 7749 silica gel from Merck. HPLC analyses were performed using a Waters 1515 HPLC pump connected in series with a Waters 2487 Absorbance detector and equipped with a Waters μ Porasil normal phase analytical size column or, for purifications, a Waters μ Porasil normal phase semi-preparation size column. Standard hand-held lamps used for visualizing TLC plates (Spectroline E-series, 470 mW/cm²) were used to carry out the ring-closing reactions at 365 nm. The ring-opening reactions were carried out using the light of a 150-W tungsten source or a 300-W halogen photo-optic light source that was passed through a 490-nm cutoff filter to eliminate higher-energy light. Microanalyses were performed on a Carlo Erba Model 1106 CHN analyser.

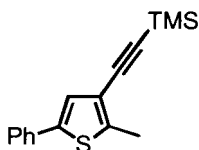
4.7 Syntheses and experiments



4.6

Synthesis of 3-iodo-2-methyl-5-phenylthiophene (4.6). A solution of compound **4.5** (2.0 g, 7.9 mmol) in anhydrous Et₂O (50 mL) was treated dropwise with *n*-butyllithium (3.8 mL, 2.5 M in hexanes, 9.5 mmol) over 5 min at –78 °C under an N₂ atmosphere. The resulting solution was stirred at this temperature for 30 min then quickly treated with a solution of I₂ (2.0 g, 8.7 mmol) in anhydrous Et₂O (20 mL) using a cannula. After stirring at this temperature for 1 h, the cooling bath was removed and the reaction was allowed to slowly warm to room

temperature and stirred there for 18 h, at which time it was quenched with saturated aqueous solution of NH_4Cl (25 mL). The aqueous layer was separated and extracted with Et_2O (3 \times 50 mL). The combined organic layers were then washed with 20% $\text{Na}_2\text{S}_2\text{O}_3 \cdot 5\text{H}_2\text{O}$ (100 mL), to quench the excess iodine, and then brine (1 \times 50 mL), dried over Na_2SO_4 , filtered and evaporated to dryness *in vacuo*. Purification by flash chromatography (SiO_2 , hexanes) yielded 1.7 g (72%) of compound **4.6** as off-white coloured crystals. M.p. = 64–66 °C. ^1H NMR (CDCl_3 , 500 MHz) δ 7.51 (d, J = 7.2 Hz, 2H), 7.36 (t, J = 7.2 Hz, 2H), 7.28 (d, J = 7.2 Hz, 1H), 7.16 (s, 1H) 2.44 (s, 3H). ^{13}C NMR (CDCl_3 , 100 MHz) δ 142.7, 138.0, 133.4, 130.3, 128.9, 127.7, 125.4, 81.1, 18.0. FT-IR (KBr-cast): 1499, 1442, 1328, 1155, 1073, 1032, 1008, 830, 792, 758, 709, 689, 591, 463 cm^{-1} . LRMS (EI) m/z = 300 $[\text{M}]^+$. Anal. Calcd. For $\text{C}_{11}\text{H}_9\text{Si}$: C, 44.02; H, 3.02. Found: C, 44.33; H, 3.16.

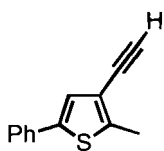


4.7

Synthesis of trimethyl(2-(2'-methyl-5'-phenylthiophen-3'-yl)ethynyl)silane

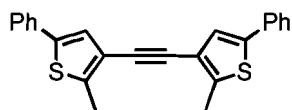
(4.7). A solution of compound **4.6** (700 mg, 2.3 mmol) in anhydrous N,N -diisopropylamine ($\text{HN}(i\text{Pr})_2$) (50 mL) was treated with dichlorobis(triphenylphosphine)palladium(II) ($\text{Pd}[\text{PPh}_3]_2\text{Cl}_2$) 10 mg, 0.014 mmol), triphenylphosphine (PPh_3) (4 mg, 0.015 mmol) and copper(I) iodide (3 mg, 0.016 mmol). The resulting solution was treated with an excess of trimethylsilylacetylene (3.25 mL, 23.3 mmol) under an N_2 atmosphere and heated

at 70 °C for 18 h, at which time it was filtered while hot and evaporated to dryness *in vacuo*. Purification by flash chromatography (SiO₂, hexanes) yielded 590 mg (93%) of compound **4.7** as an off white coloured solid. M.p. = 50–53 °C. ¹H NMR (CDCl₃, 500 MHz) δ 7.51 (d, *J* = 8.0 Hz, 2H), 7.35 (d, *J* = 8.0 Hz, 2H), 7.26 (m, 1H), 2.53 (s, 3H), 0.26 (s, 9H). ¹³C NMR (CDCl₃, 100 MHz) δ 144.1, 139.9, 133.7, 128.7, 127.3, 125.4, 125.1, 120.7, 99.5, 96.4, 14.5, 0.0. FT-IR (KBr-cast): 2965, 2150, 1248, 1098, 897, 837, 751, 684 cm⁻¹. LRMS (EI) *m/z* = 270 [M]⁺. Anal. Calcd. For C₁₆H₁₈SSi: C, 71.05; H, 6.71. Found: C, 71.04; H, 6.85.



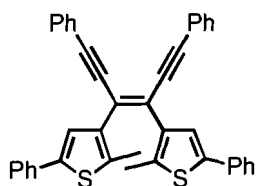
4.8

Synthesis of 3-ethynyl-2-methyl-5-phenylthiophene (4.8). A solution of compound **4.7** (600 mg, 2.2 mmol) and K₂CO₃ (338 mg, 2.4 mmol) in methanol (25 mL) was stirred at room temperature for 1 h. The resulting suspension was evaporated to dryness *in vacuo*. The crude product was taken up in water (50 mL) and extracted with Et₂O (3 × 50 mL). The combined organic layers were dried with Na₂SO₄, filtered and evaporated to dryness *in vacuo*. Purification by flash chromatography (SiO₂, hexanes) yielded 387 mg (88%) of compound **4.8** as an off-white coloured solid, which was then used directly in the next reaction. ¹H NMR (CDCl₃, 400 MHz) δ 7.52 (d, *J* = 7.2 Hz, 2H), 7.36 (t, *J* = 7.2 Hz, 2H), 7.27-7.29 (m, 1H), 7.19 (s, 3H), 3.20 (s, 1H), 2.55 (s, 3H). LRMS (EI) *m/z* = 198 [M]⁺.



4.9

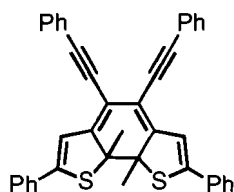
Synthesis of 1,2-bis(2'-methyl-5'-phenylthiophen-3'-yl)ethyne (4.9). A solution of compound **4.6** (395 mg, 1.3 mmol) in anhydrous N,N-diisopropylamine (50 mL), was treated with Pd(PPh₃)₂Cl₂ (10 mg, 0.014 mmol), PPh₃ (4 mg, 0.015 mmol) and copper(I) iodide (3 mg, 0.016 mmol). The resulting solution was treated with compound **4.8** (389 mg, 2.0 mmol) under an N₂ atmosphere and heated at 70 °C for 18 h, at which time it was evaporated to dryness *in vacuo*. Purification by flash chromatography (SiO₂, hexanes) yielded 380 mg (78%) of compound **4.9** as a pale yellow solid. M.p. = 177–180 °C. ¹H NMR (CDCl₃, 500 MHz) δ 7.56 (d, *J* = 7.5 Hz, 4H), 7.38 (t, *J* = 7.5 Hz, 4H), 7.29 (d, *J* = 6.5 Hz, 2H), 7.25 (s, 2H), 2.61 (s, 6H). ¹³C NMR (CDCl₃, 100 MHz) δ 142.5, 140.3, 133.8, 128.9, 127.5, 125.5, 125.1, 120.8, 86.2, 14.7. FT-IR (KBr-cast): 1499, 1426, 1092, 901, 832, 751, 685 cm⁻¹. LRMS (EI) *m/z* = 370 [M]⁺. Anal. Calcd. For C₂₄H₁₈S₂: C, 77.80; H, 4.90. Found: C, 77.95; H, 4.85.



4.3o

Synthesis of (Z)-1,6-bis(phenyl)-3,4-bis-(2'-methyl-5'-phenyl-thiophen-3'-yl)hex-3-en-1,5-diyne (4.3o). Following a procedure for the synthesis of *cis* enediynes,⁸⁶ a solution of Cp₂ZrCl₂ (494 mg, 1.7 mmol) in THF (12.5 mL) was treated with EtMgCl (1.7 mL, 2.0 M THF solution, 3.4 mmol) at -78 °C. The

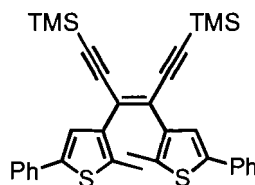
reaction mixture was stirred for 1 h at the same temperature, at which time, compound **4.9** (500 mg, 1.4 mmol) was added. After warming to 0 °C and stirring at this temperature for 90 min, 1-(2-chloroethynyl)benzene (184 mg, 1.4 mmol) was added. The reaction was allowed to warm to room temperature and stirred there for 30 min followed by heating at 50 °C for 2 h. The reaction mixture was treated with 1-(2-bromoethynyl)benzene (326 mg, 1.7 mmol) and CuCl (13 mg, 0.13 mmol) stirred at 50 °C for 18 h. The reaction mixture was evaporated to dryness *in vacuo* and purification by flash chromatography (SiO₂, 10% CH₂Cl₂ in hexanes) yielding 300 mg (39%) of compound **4.3o** as a green crystalline solid. M.p. = 70–75 °C. ¹H NMR (CDCl₃, 500 MHz) δ 7.58-7.55 (m, 4H), 7.44 (d, *J* = 7.0 Hz, 4H), 7.38-7.36 (m, 6H), 7.32 (t, *J* = 7.0 Hz, 4H), 7.23 (t, *J* = 7.5 Hz, 2H), 7.01 (s, 2H), 2.33 (s, 6H). ¹³C NMR (CDCl₃, 100 MHz) δ 139.9, 137.5, 135.0, 134.2, 131.7, 128.8, 128.6, 128.4, 127.2, 125.6, 125.0, 124.8, 123.4, 96.9, 90.5, 14.5. FT-IR (KBr-cast): 1597, 1486, 1441, 1069, 1027, 947, 911, 841, 758, 688, 530, 489, 466 cm⁻¹. LRMS: (MALDI) *m/z* = 573 [M+1]⁺. Anal. Calcd. For C₄₀H₂₈S₂: C, 83.88; H, 4.93. Found: C, 83.79; H, 5.03.



4.3c

Photochemical synthesis of the ring-closed isomer 4.3c. A solution of compound **4.3o** (2 mg, 3 × 10⁻³ mmol) in C₆D₆ (0.8 mL) was placed in a 5-mm NMR tube and irradiated with 365-nm light for 5 min yielding a solution of the photostationary state containing 92% of the *ring-closed* isomer **4.3c** according to

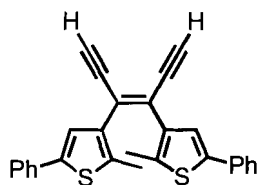
the ^1H NMR spectrum. The remaining 8% was assigned to the *ring-open* isomer **4.3o**. The *ring-closed* isomer **4.3c** could be purified by semi-preparatory HPLC (0.05% EtOAc in hexanes). ^1H NMR (C_6D_6 , 500 MHz) δ 7.62 (d, $J = 7.5$ Hz, 4 H), 7.39-7.41 (m, 4 H), 7.07 (s, 2 H), 6.93-7.02 (m, 12 H), 2.38 (s, 6 H).



4.11

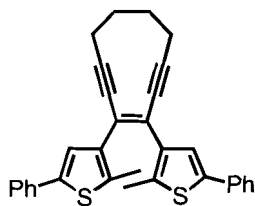
Synthesis of (Z)-1,6-bis(trimethylsilyl)-3,4-bis-(2'-methyl-5'-phenylthiophen-3'-yl)-hex-3-en-1,5-diyne (4.11). A solution of Cp_2ZrCl_2 (494 mg, 1.7 mmol) in THF (25 mL) was treated with EtMgCl (1.7 mL, 2.0 M THF solution, 3.4 mmol) at -78 °C. After stirring for 90 min at the same temperature, the reaction mixture was treated with compound **4.9** (500 mg, 1.4 mmol) and warmed to 0 °C. After stirring for 2 h, the reaction was treated with (2-bromoethynyl)trimethylsilane (250 mg, 1.4 mmol) and stirred at room temperature for 30 min, followed by heating at 50 °C for 1 h. The reaction was treated with (2-bromoethynyl)trimethylsilane (250 mg, 1.4 mmol) and CuCl (13 mg, 0.13 mmol) and stirred at 50 °C for 3 h. The heating source was removed, reaction was allowed to cool to room temperature and stirred there for 16 h, at which time it was quenched with NH_4Cl (25 mL) and extracted with EtOAc (3 \times 50 mL). The combined organic layers were dried with Na_2SO_4 , filtered and evaporated to dryness *in vacuo*. Purification by flash chromatography (SiO_2 , 10–50% CH_2Cl_2 in hexanes) followed by centrifugal chromatography (SiO_2 , 10% CH_2Cl_2 in hexanes) and crystallization from $\text{MeOH}/\text{CH}_2\text{Cl}_2$ yielded 340 mg (45%) of compound **4.11** as colourless needles.

M.p. = 178–180 °C. ^1H NMR (CDCl_3 , 500 MHz) δ 7.37 (d, J = 7.5 Hz, 4H), 7.30 (t, J = 7.5 Hz, 4H), 7.23-7.20 (m, 2H), 6.83 (s, 2H), 2.23 (s, 6H), 0.27 (s, 18H). ^{13}C NMR (CDCl_3 , 100 MHz) δ 139.6, 137.6, 134.5, 134.1, 128.8, 127.2, 125.7, 125.5, 124.7, 104.6, 102.5, 14.4, 0.0. FT-IR (KBr-cast): 3448, 2958, 2143, 1249, 847, 756, 691 cm^{-1} . LRMS (EI) m/z = 565 $[\text{M}]^+$. Anal. Calcd. For $\text{C}_{34}\text{H}_{36}\text{S}_2\text{Si}_2$: C, 72.28; H, 6.42. Found: C, 72.19; H, 6.55.



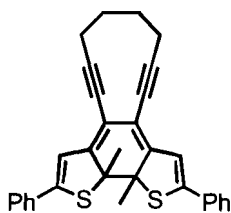
4.12

Synthesis of (Z)-3,4-bis(2'-methyl-5'-phenylthiophen-3'-yl)hex-3-en-1,5-diyne (4.12). A solution of compound **4.11** (250 mg, 0.44 mmol) and potassium carbonate (K_2CO_3) (306 mg, 2.2 mmol) in methanol (50 mL) and THF (50 mL) was stirred at room temperature for 1 h. The resulting suspension was evaporated to dryness *in vacuo*. Purification by flash chromatography (SiO_2 , 25% CH_2Cl_2 in hexanes) yielded compound **4.12**, which was used directly in the next reaction. ^1H NMR (CDCl_3 , 400 MHz) δ 7.41 (d, J = 8.0 Hz, 4H), 7.31 (t, J = 7.7 Hz, 4H), 7.20-7.25 (m, 2H), 6.93 (s, 2H), 3.57 (s, 2H), 2.20 (s, 6H). ^{13}C NMR (CDCl_3 , 100 MHz) δ 140.1, 137.6, 134.1, 133.9, 128.8, 127.3, 125.5, 125.4, 124.3, 84.4, 83.4, 14.4.



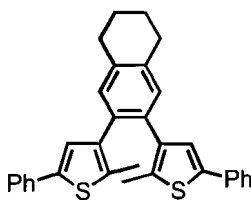
4.4o

Synthesis of (Z)-3,4-bis(2'-methyl-5'-phenylthiophen-3'-yl)cyclodeca-3-en-1,5-diyne (4.4o). A solution of compound **4.12** (0.44 mmol) in anhydrous THF (50 mL) was treated dropwise with *n*-butyllithium (0.44 mL, 2.5 M in hexanes, 1.1 mmol) over a 5-min period at -78 °C under an N_2 atmosphere. After stirring at this temperature for 30 min, HMPA (2 mL) was added and the resulting suspension was stirred for 30 min, at which time 1,4-diiodobutane (53 μ L, 124 mg, 0.4 mmol) was added dropwise. The cooling bath was removed and the reaction was allowed to slowly warm to room temperature and the reaction was stirred there for 16 h. The crude reaction mixture was evaporated to dryness *in vacuo*. Purification by flash chromatography (SiO₂, 10% CH₂Cl₂ in hexanes) afforded 40 mg (19% for two steps) of compound **4.4o**. M.p. = 65–70 °C. ¹H NMR (C₆D₆, 500 MHz) δ 7.39 (d, *J* = 7 Hz, 4H), 7.22 (s, 2H), 6.99 (t, *J* = 7.5 Hz, 4H), 6.92 (m, 2H), 2.15-2.20 (m, 10H), 1.59-1.65 (m, 4H). ¹³C NMR (CDCl₃, 150 MHz) δ 139.8, 137.0, 134.3, 134.2, 128.8, 127.1, 125.5, 124.5, 100.9, 85.3, 29.0, 21.8, 14.5. FT-IR (KBr-cast): 3446, 3059, 2918, 2854, 2195, 1600, 1502, 1444, 1073, 756, 691, 483 cm⁻¹. LRMS: (MALDI) *m/z* = 474 [M]⁺.



4.4c

Synthesis of the *ring-closed* isomer 4.4c. A solution of compound **4.4o** (8.0 mg, 0.017 mmol) in C₆D₆ (0.8 mL) was placed in a 5-mm NMR tube and irradiated with 365-nm light for 50 min yielding a solution of the photostationary state containing 82% of the *ring-closed* isomer **4.4c** according to the ¹H NMR spectrum. The remaining 18% was assigned to the *ring-open* isomer **4.4o**. This mixture was heated at 75 °C for 23 h using an oil bath to thermally decompose the remaining *ring-open* isomer **4.4o**. The solution was evaporated to dryness *in vacuo* and purified by centrifugal chromatography (SiO₂, 5% CH₂Cl₂ in hexanes) yielding 3.5 mg of compound **4.4c** (44%). M.p. = 130 °C (dec.). ¹H NMR (C₆D₆, 500 MHz) δ 7.31 (dd, *J* = 4, 8 Hz, 4H), 6.96-7.01 (m, 6H), 6.91 (s, 2H), 2.31 (s, 6H), 2.11-2.22 (m, 4H), 1.55 (br s, 4H). ¹³C NMR (C₆D₆, 150 MHz) δ 150.7, 149.9, 134.2, 129.1, 128.7, 126.8, 117.9, 115.5, 101.4, 81.4, 65.1, 28.4, 27.0, 21.9. FT-IR (KBr-cast): 3420, 2923, 2854, 1638, 1486, 1444, 1075, 756, 687, 469 cm⁻¹. LRMS: (MALDI) *m/z* = 474 [M]⁺.



4.10

Synthesis of 1,2-bis(2'-methyl-5'-phenylthiophen-3'-yl)-5,6,7,8-tetrahydronaphthalene (4.10). A solution of compound **4.4o** (10 mg, 21 mmol) in C_6D_6 (5 mL) in a Wheaton vial was treated with (199 μ l) 1,4-cyclohexadiene. The solution was heated with constant stirring in an oil bath at 75 °C for 19 h. The crude reaction mixture was evaporated to dryness *in vacuo*. Purification by flash chromatography (SiO_2 , 25% CH_2Cl_2 in hexanes) afforded 3 mg (30%) of compound **4.10** as a light yellow solid. M.p. = 75–80 °C. 1H NMR (C_6D_6 , 500 MHz) δ 7.51 (d, J = 7.5 Hz, 4H), 7.13 (s, 2H), 7.11 (s, 2H), 7.06 (t, J = 7.5 Hz, 4H), 6.95-6.99 (m, 2H), 2.68 (br s, 4H), 2.06 (s, 6H), 1.64 (br s, 4H). ^{13}C NMR (C_6D_6 , 150 MHz) δ 140.0, 139.8, 136.3, 135.1, 134.9, 133.8, 131.5, 129.1, 127.2, 126.6, 125.8, 29.4, 23.6, 14.0. FT-IR (KBr-cast): 3446, 2955, 2917, 2849, 1634, 1473, 1463, 1389, 1366, 1230, 730, 719, 478 cm^{-1} . LRMS: (EI) m/z = 476 $[M]^+$.

Reaction kinetics of the Bergman cyclization of compound 4.4o. A benzene solution of *ring-open* isomer **4.4o** (8.4×10^{-3} M) was prepared by dissolving compound **4.4o** (20.0 mg, 4.2×10^{-2} mmol) in C_6D_6 (5 mL) in a volumetric flask. Similarly, a 1.9×10^{-2} M solution of an internal standard was prepared by dissolving *p*-nitroanisole (28.4 mg, 1.9×10^{-1} mmol) in C_6D_6 (10 mL) in a volumetric flask. Using *p*-nitroanisole as an internal standard (0.3 mL, 5.6×10^{-3} mmol), a solution of compound **4.4o** (0.3 mL, 2.5×10^{-3} mmol) in an NMR tube

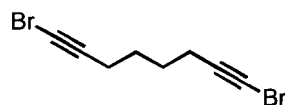
was treated with 1,4-cyclohexadiene (26 μL , 2.8×10^{-2} mmol), at which point the solution was frozen with liquid N_2 and degassed under high vacuum. The reaction mixture was heated to 75 $^\circ\text{C}$ and the reaction progress was monitored using a Varian Inova 500 instrument working at 499.8 MHz over a 14-h period.

Reaction kinetics for the consumption of compound 4.4o and formation of compound 4.10 (data processing). The area under the peaks observed in the ^1H NMR spectrum corresponding to ring-open isomer **4.4o** and product **4.10** were integrated and their values were normalized against those for the internal standard (*p*-nitroanisole). These values were converted to concentration by setting time $t = 0$ sec to the initial concentration of compound **4.4o**. Apparent reaction rates were determined by fitting the data, assuming *pseudo*-first order kinetic conditions. To plot the data of compound **4.4o** presented in Figure 4.3.5, the values of $\ln(C_0)$ were subtracted from each data point. The effective rate of formation⁹² of compound **4.10** was calculated by fitting the data to $\ln[P_\infty/(P_\infty - C)]$ where P_∞ is the concentration of compound **4.10** when the reaction is completed.

Reaction kinetics of the Bergman cyclisation of the ring-closed isomer 4.4c. A benzene solution of compound **4.4c** (3.2×10^{-3} M) was prepared by dissolving compound **4.4c** (3.0 mg, 6.3×10^{-3} mmol) in C_6D_6 (2 mL) in a volumetric flask. The internal standard solution, *p*-nitroanisole 1.9×10^{-2} M in C_6D_6 (the same one as described above) was added. Using *p*-nitroanisole as an internal standard (0.15 mL, 2.7×10^{-3} mmol), a solution of compound **4.4c** (0.50 mL, 1.6×10^{-3} mmol). The NMR tube was placed in a preheated oil bath at 75 $^\circ\text{C}$ and removed at different time intervals for ^1H NMR analysis. After 7 h, 1,4-

cyclohexadiene (26 μL , 2.8×10^{-2} mmol) was added and the NMR tube was further heated and removed at intervals for ^1H NMR analysis until a total time of 13 h was reached.

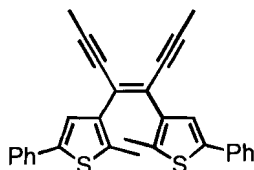
Reaction kinetics for the consumption of compound 4.4c. As described above for compound 4.4o, the area under the peaks in the ^1H NMR spectrum corresponding to *ring-closed* isomer 4.4c were integrated and their value were normalized against those for the *p*-nitroanisole internal standard. These values were converted to concentration by setting time $t = 0$ sec to the initial concentration of compound 4.4c. Apparent reaction rates were determined by fitting the data, assuming *pseudo*-first order kinetic conditions. To plot the data of compound 4.4c presented in Figure 4.3.5, $\ln(C_0)$ was subtracted from each data point.



4.13

Synthesis of 1,8-dibromoocta-1,7-diyne (4.13). To a solution of octa-1,7-diyne (2.5 mL, 19 mmol) in acetone (50 mL) was added *N*-bromosuccinimide (NBS) (7.4 g, 41.4 mmol) and AgNO_3 (0.6 g, 3.8 mmol) and the mixture was stirred overnight at 25 $^\circ\text{C}$. The reaction was washed with water (30 mL) and extracted with Et_2O (3×50 mL). The organic layer was washed with brine (50 mL), dried with Na_2SO_4 , and the solvent was evaporated *in vacuo*. The crude product was purified by column chromatography (SiO_2 , hexanes) to yield a clear oil (3.4 g, 67%). ^1H NMR (CDCl_3 , 500 MHz) δ 2.20-2.28 (m, 4H), 1.59-1.64 (m, 4H). ^{13}C

NMR (CDCl₃, 100 MHz) δ 79.69, 38.1, 27.2, 19.1. FT-IR (KBr-cast): 2946, 2864, 2837, 2218, 1459, 1429, 1328, 1051, 738 cm⁻¹. LRMS: (CI) m/z = 265.9 [M+2]⁺.
Anal. Calcd. For C₈H₈Br₂: C, 36.40; H, 3.05 Found: C, 36.47; H, 3.11.



4.15

Synthesis of (Z)-4,5-bis(2'-methyl-5'-phenylthiophen-3'-yl)oct-4-en-2,7-diyne (4.15). A solution of compound **4.12** (0.81 mmol) in anhydrous THF (50 mL) was treated dropwise with *n*-butyllithium (1.0 mL, 2.5 M in hexanes, 2.5 mmol) over a 5-min period at -78 °C under an N₂ atmosphere. After stirring at this temperature for 30 min, methyl iodide (MeI) (157 μ L, 2.5 mmol) was added dropwise. The cooling bath was removed and the reaction was allowed to slowly warm to room temperature and the reaction was stirred there for 16 h. The crude reaction mixture was evaporated to dryness *in vacuo*. Purification by flash chromatography (SiO₂, 25% CH₂Cl₂ in hexanes) afforded 200 mg (55%) of compound **4.15**. M.p. = 130-135 °C. ¹H NMR (CDCl₃, 500 MHz) δ 7.42 (d, *J* = 7.5 Hz, 4H), 7.31 (t, *J* = 7.5 Hz, 4H), 6.22 (m, 2H), 6.91 (s, 2H), 2.18 (s, 6H), 2.16 (s, 6H). ¹³C NMR (CDCl₃, 150 MHz) δ 139.6, 136.7, 135.6, 134.3, 128.8, 127.1, 125.5, 124.8, 124.6, 92.9, 80.4, 14.3, 5.1. FT-IR (KBr-cast): 1631, 1435, 1384, 1269, 1190, 1099, 998, 982, 760, 725, 692, 563 cm⁻¹. LRMS: (CI) m/z = 448 [M]⁺.

5 Conclusions

Photochemistry provides a promising approach for the modulation of chemical reactivity due to the fast response and the absorption-dependence of photochemical processes. Photochromic compounds undergo reversible isomerization reactions with light between two distinct forms with different physicochemical properties, but very few reports have demonstrated their application in photoregulating reactivity. The modulation of chemical reactivity with light could significantly impact both synthesis and drug delivery by increasing reaction efficiency and decreasing unwanted side-reactions. Photochromic systems such as azobenzenes have been used in previous examples attempting to control reactivity. However, dithienylethenes are better suited for controlling reactivity reversibly due to their well-behaved photochromism (reversible and predictable) and their increased thermal stability for both isomers. Dithienylethenes exhibit significant differences between the *ring-open* and *ring-closed* isomers. Namely, there are changes in 1) the sterics; 2) the electronic communication along the backbone; and 3) in the π -bond arrangement between the two photoisomers. In this thesis, systems were specifically designed to harness these three changes for the application of modulating chemical reactivity.

The initial approach took into consideration the large structural flexibility changes accompanying the ring-closing/ring-opening isomerization reactions.

The *ring-open* isomer of the DTE has conformational flexibility from the relatively free rotation about σ -bonds. The UV-light induced rigidified tricyclic backbone in the *ring-closed* isomer prevents such movement. With these flexibility differences in mind, two bis(oxazoline) DTE ligands were designed for their ability to chelate to a metal center. In their flexible *ring-open* form, metal-binding groups could converge towards each other forming a bidentate metal-binding pocket, while in the rigid *ring-closed* isomer, metal binding groups were held in a divergent geometry where the metal-binding pocket was not favourable towards bidentate complexation. The differences in the metal binding were monitored by comparing the stereoselectivity in the product distribution from an asymmetric catalytic reaction requiring a bidentate ligand. In one instance, the absence of stereoselectivity using a C5 bis(oxazoline) DTE, **2.2o**, suggested that the expected bidentate complex was not formed even with the *ring-open* isomer. Alternatively, a C2 bis(oxazoline) DTE having different metal-binding possibilities, **2.3o** afforded stereoselectivity in the product distribution of the cyclopropanation of styrene with ethyldiazoacetate in its *ring-open* form. The *ring-closed* isomer showed reduced stereoselectivity under the same reaction conditions, which confirmed that there was a significant difference in the metal-complex geometry. The ring-opening reaction was even shown to be possible *in situ*, thus clearly demonstrating that the stereoselectivity could be controlled with light. However, the ring-closing reaction was compromised in the complex, perhaps because the DTE was tightly bound in a geometry unproductive towards the photocyclization. The chapter highlighted that subtle changes in the DTE structure could have

large effects in the metal-complex assembly, which in turn could result in differences in the reaction products. It was also shown that DTE ligand metal-complexes could be subject to limited photochromism.

The second system discussed was a bis(phosphine) DTE **3.1o**, which provided a new versatile photoresponsive ligand/reagent for catalysis and chemical processes. The differences in electronic communication between the two isomers directly influenced the electron-withdrawing properties of the phosphine; the *ring-closed* isomer being more electron-withdrawing than the corresponding *ring-open* isomer due to the extended conjugated backbone as demonstrated with the selenide derivative **3.3o**. The photochromism of the bis(phosphine) DTE was maintained in a metal complex, as shown with the gold chloride derivative **3.2o**. Initial attempts at using a “POP” Hendrickson derivative of the bis(phosphine) DTE in a reactivity-gated photochromism esterification reaction proved unsuccessful since the “POP” reagent was too labile and did not prevent the photochromic reaction from taking place. This system demonstrated how metals bound to DTE ligands could alter the photostationary state of the DTE. In addition, limitations to the design of reaction monitoring were discovered by the fact that the proposed geometry-locked compound was found to be labile and retained its photochromic activity even in the absence of the proposed analyte.

In the final approach, the localized π -bond arrangement differences between the *ring-open* and *ring-closed* isomers of DTEs were applied to Bergman cyclization activation. An enediyne appended on a DTE was effectively

“unmasked” only in the *ring-open* isomer, whereas, it was “masked” in the *ring-closed* isomer. The major advantage of this new system is that the activation step required visible light, which is less damaging to biological systems and can penetrate deeper into tissue than the more commonly used UV light. Two enediyne DTE derivatives were prepared and proved that while the photochromism was still possible, the thermal Bergman cyclization could only proceed from the *ring-open* isomer. In the case of the *ring-closed* isomer **4.4c**, activation with visible light provided the enediyne **4.4o**, which could then cyclize at 75 °C. This represents an unprecedented example of activation of a potential antitumor compound with visible light. Before a system based on these findings can become practical, much work remains to be done, including 1) improving the synthetic yield, 2) decreasing the activation temperature to body temperature (37 °C) by structural modifications, and 3) functionalizing the compound to insure biological compatibility.

Overall, this thesis has demonstrated three different approaches to modulating reactivity using dithienylethene derivatives opening promising avenues for further research into regulating chemical processes.

6 Appendix

6.1 NMR Characterization of new compounds from *Chapter 2*

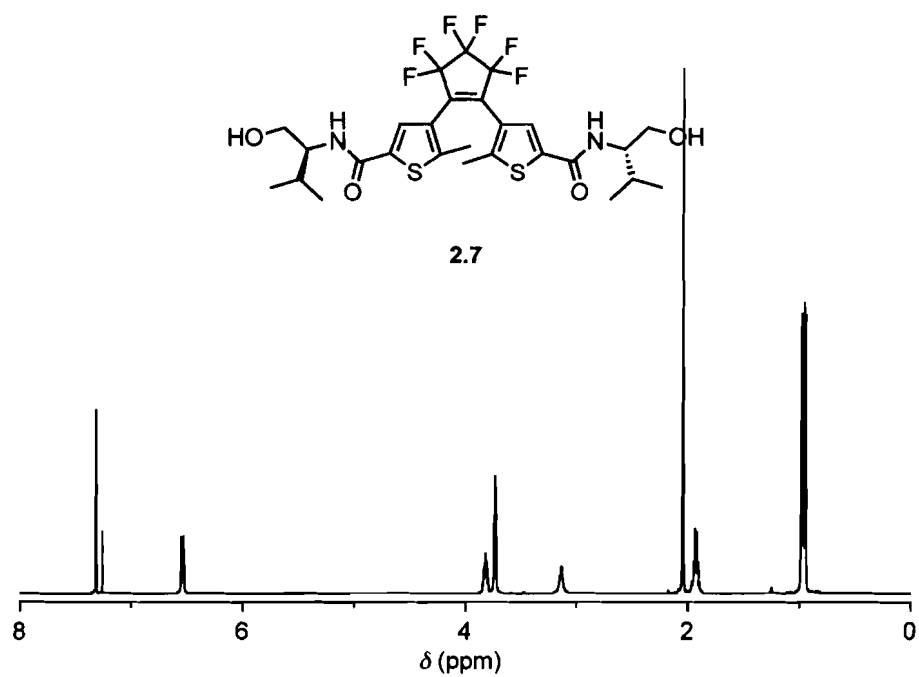


Figure 6.1.1 ¹H NMR (500 MHz) spectrum of compound 2.7 in CDCl₃.

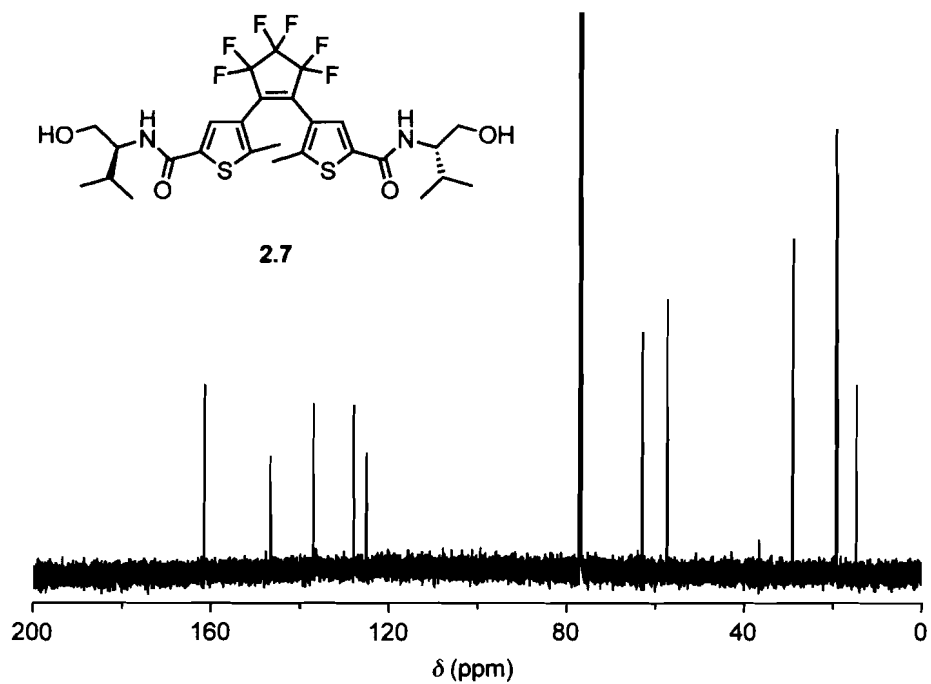


Figure 6.1.2 ^{13}C NMR (125 MHz) spectrum of compound **2.7** in CDCl_3 .

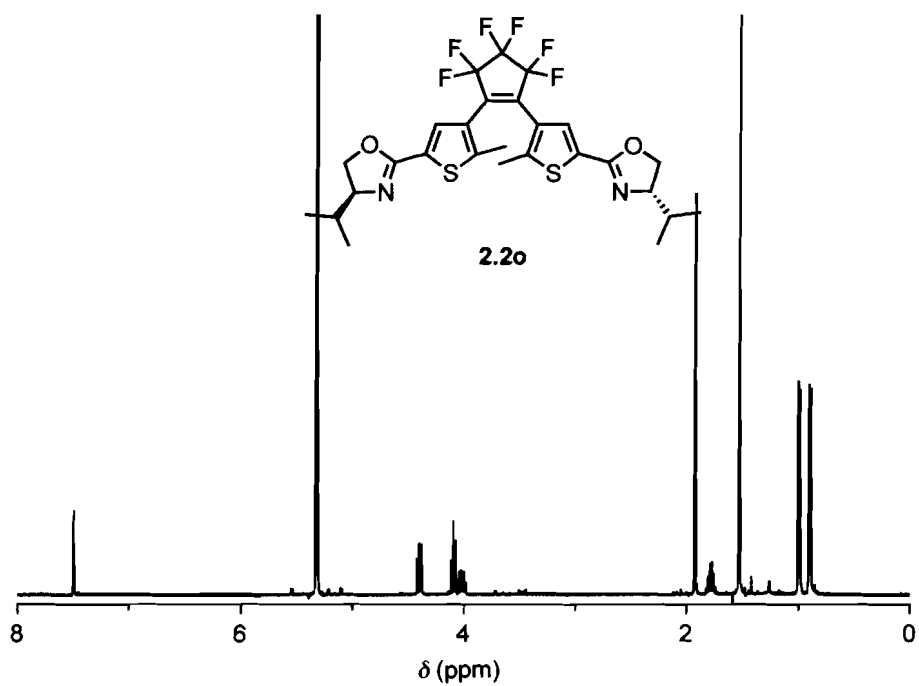


Figure 6.1.3 ^1H NMR (400 MHz) spectrum of compound **2.2o** in CD_2Cl_2 .

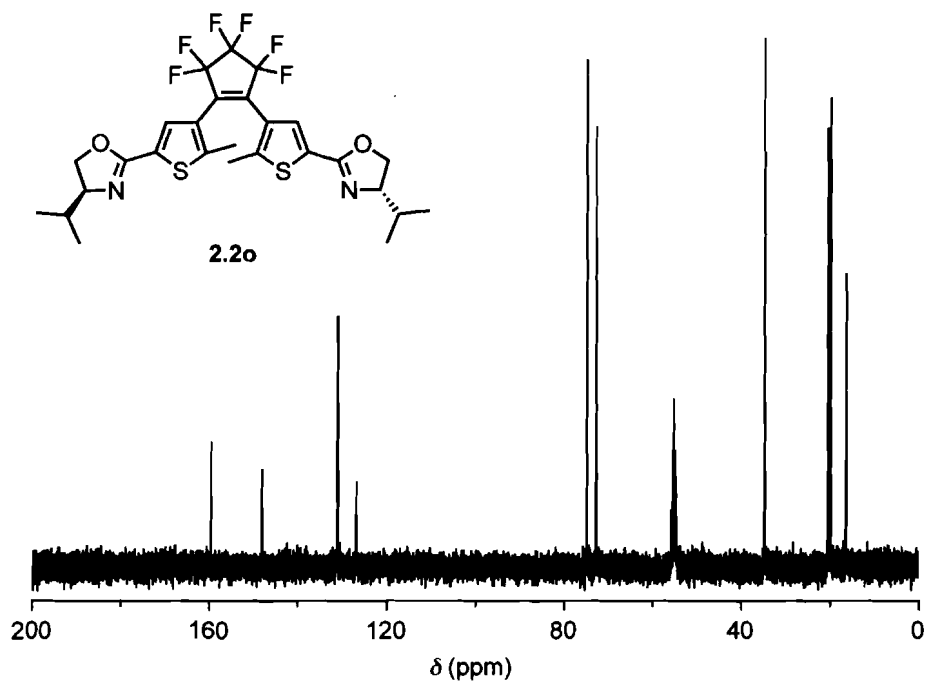


Figure 6.1.4 ^{13}C NMR (100 MHz) spectrum of compound **2.2o** in CD_2Cl_2 .

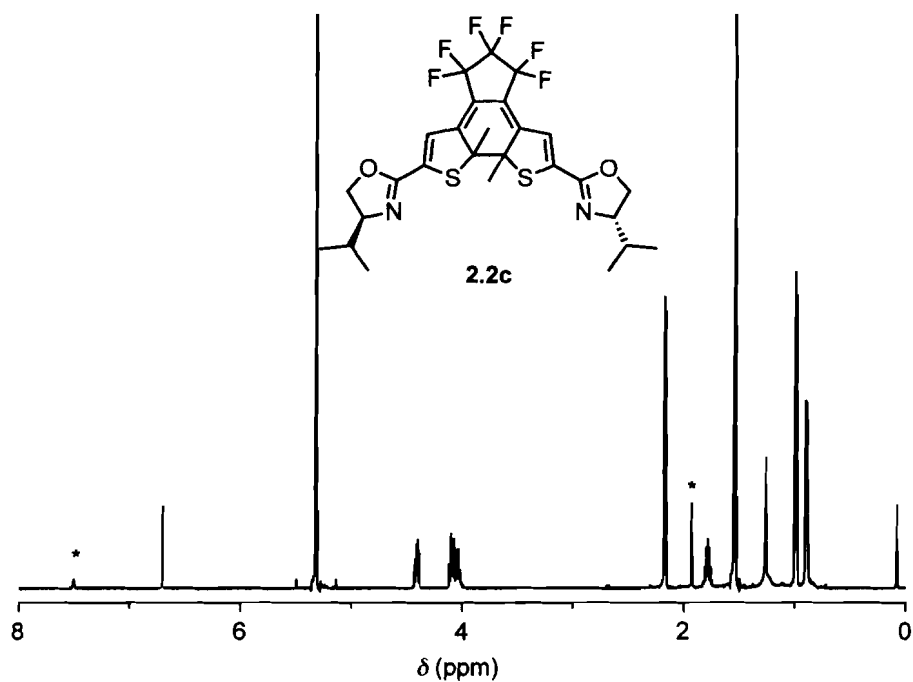


Figure 6.1.5 ^1H NMR (500 MHz) spectrum in CD_2Cl_2 of compound **2.2c** after 5 min irradiation with 313-nm light containing 87% compound **2.2c** and 13% compound **2.2o**, highlighted (*) by the C2 methyl and thienyl peaks.

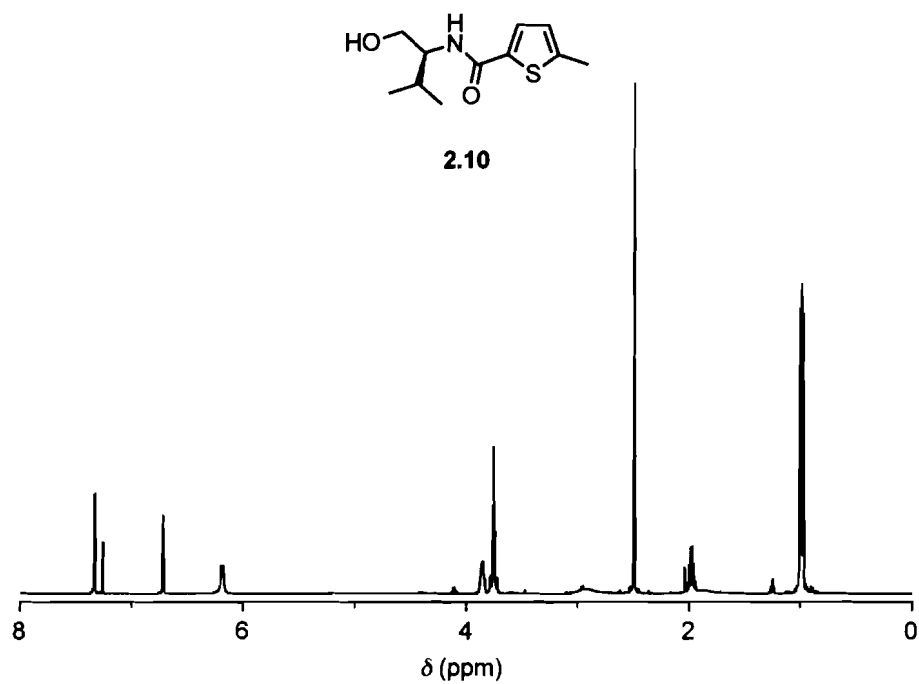


Figure 6.1.6 ^1H NMR (500 MHz) spectrum of compound **2.10** in CDCl_3 .

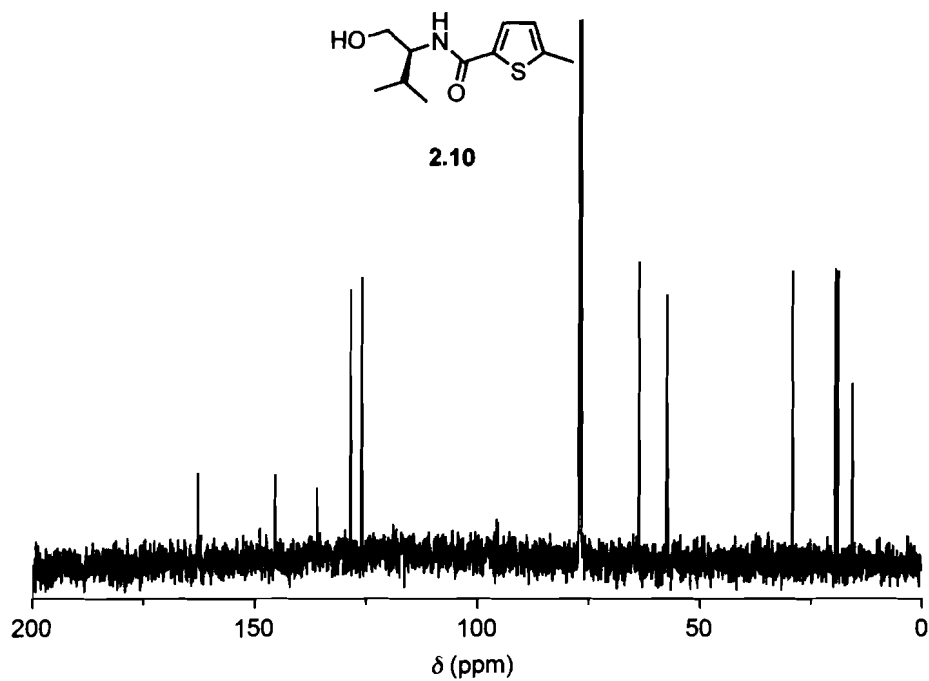


Figure 6.1.7 ^{13}C NMR (125 MHz) spectrum of compound **2.10** in CDCl_3 .

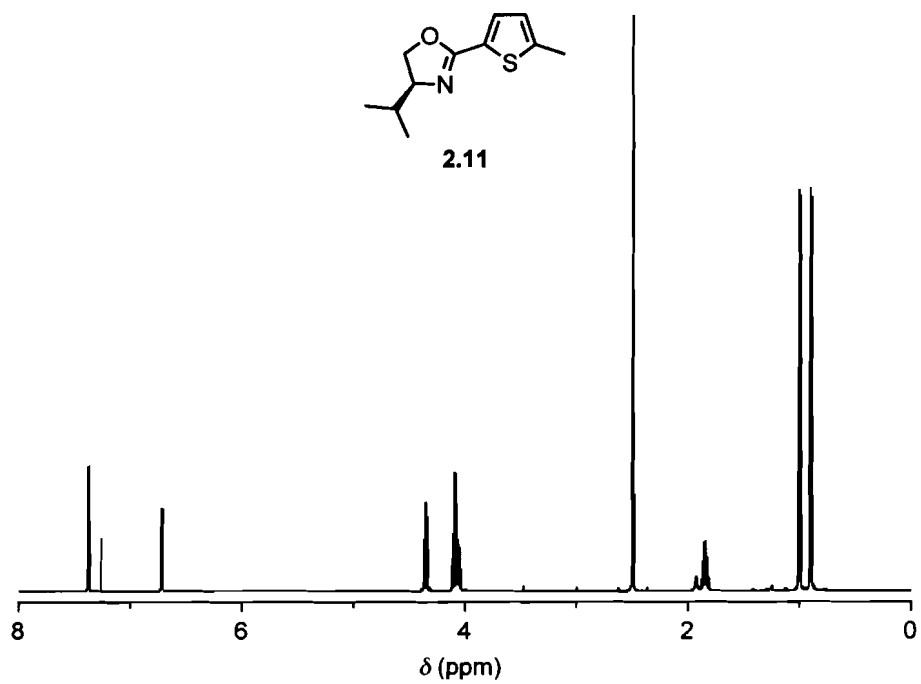


Figure 6.1.8 ¹H NMR (500 MHz) spectrum of compound 2.11 in CDCl₃.

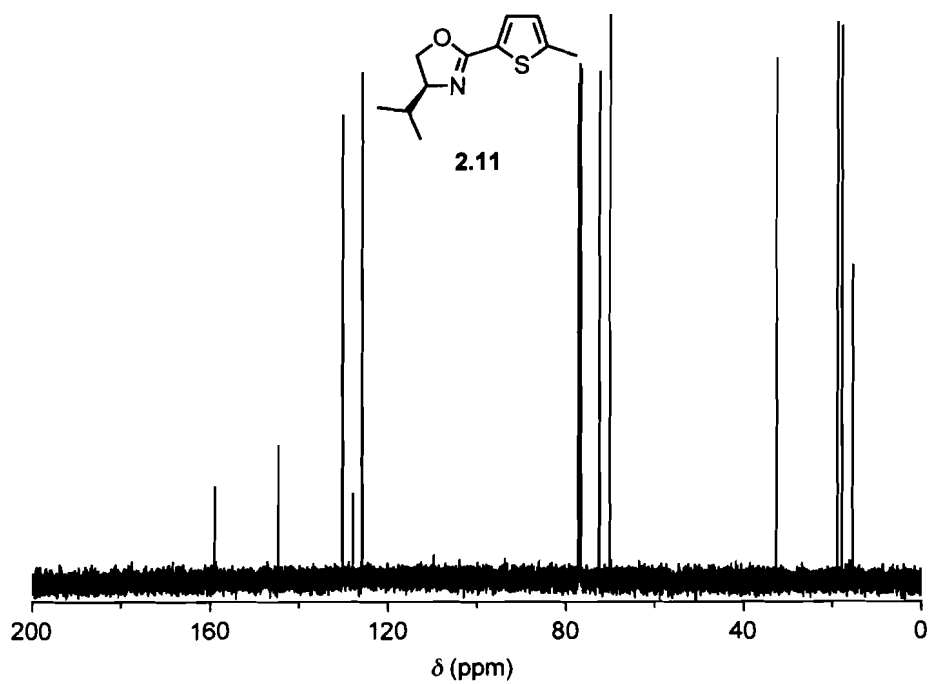


Figure 6.1.9 ¹³C NMR (125 MHz) spectrum of compound 2.11 in CDCl₃.

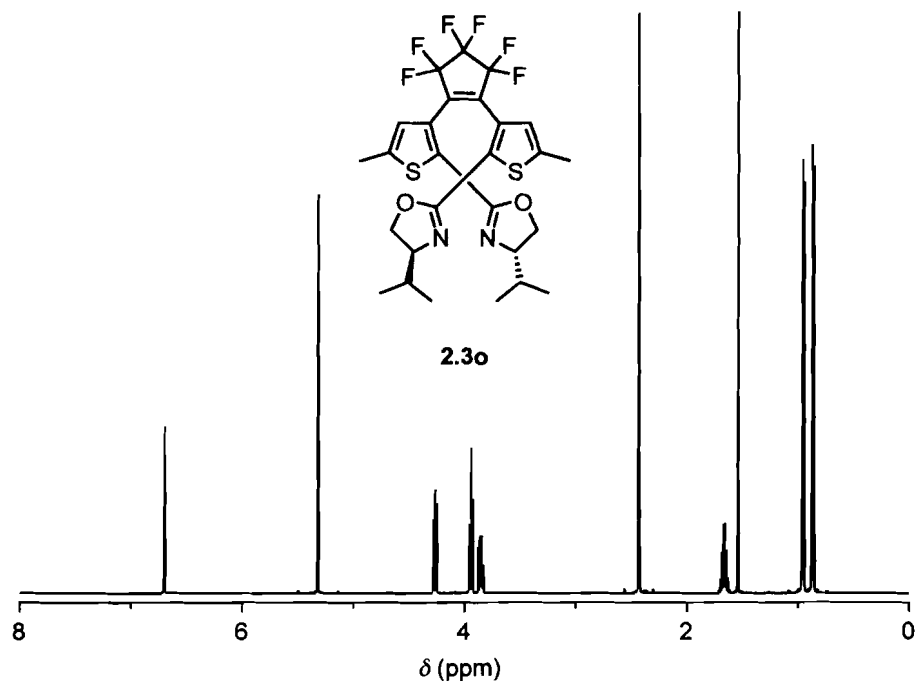


Figure 6.1.10 ^1H NMR (500 MHz) spectrum of compound **2.3o** in CD_2Cl_2 .

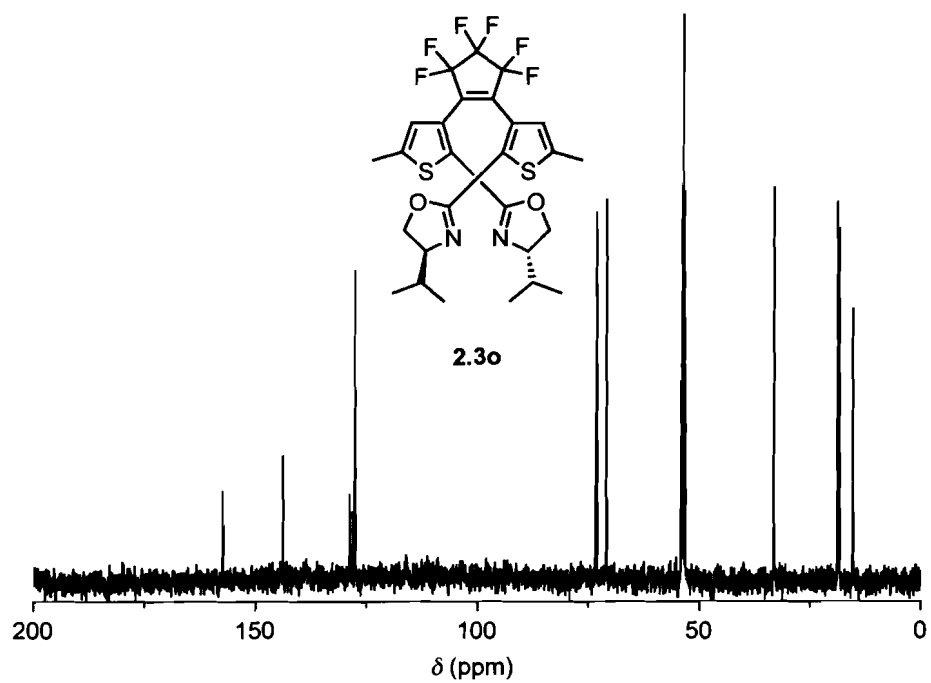


Figure 6.1.11 ^{13}C NMR (125 MHz) spectrum of compound **2.3o** in CD_2Cl_2 .

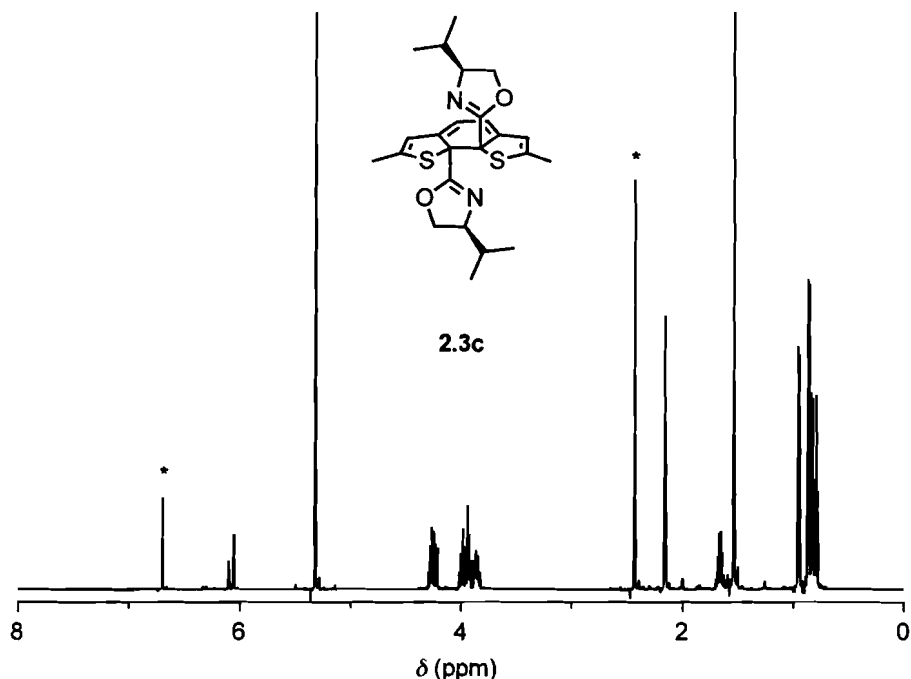
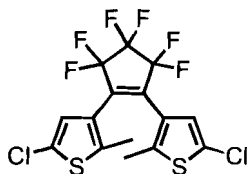


Figure 6.1.12 ^1H NMR (500 MHz) spectrum in CD_2Cl_2 of compound **2.3c** after 5 min irradiation with 313-nm light containing 59% compound **2.3c** and 41% compound **2.3o**, highlighted (*) by the C5 methyl and thienyl peaks.

6.2 Synthesis and characterization of previously known compounds for *Chapter 2*



2.5

Synthesis of 1,2-bis(5'-chloro-2'-methylthiophen-3'-yl)perfluorocyclopent-1-ene (2.5).³⁵ A solution of 3-bromo-2-methyl-5-chlorothiophene **2.4** (1.0 g, 4.7 mmol) in anhydrous Et_2O (25 mL) was treated dropwise with *n*-butyllithium (2.3 mL, 2.5 M in hexanes, 5.7 mmol) over 5 min at $-78\text{ }^\circ\text{C}$ under an N_2 atmosphere. The resulting solution was stirred at this temperature for 30 min then quickly treated with perfluorocyclopentene (317 μL , 2.4 mmol) in one portion. After stirring at this temperature for 1 h, the cooling bath was removed and the

reaction was allowed to slowly warm to room temperature and stirred there for 1 h, at which time it was quenched with saturated aqueous NH_4Cl (25 mL). The aqueous layer was separated and extracted with Et_2O (3 \times 50 mL). The combined organic layers were dried over Na_2SO_4 , filtered and evaporated to dryness *in vacuo*. Purification by flash chromatography (SiO_2 , hexanes) followed by crystallization from hexanes yielded 0.4 g (46%) of compound **2.5** as clear colourless crystals. M.p. = 146–150 °C. ^1H NMR (CDCl_3 , 500 MHz) δ 6.88 (s, 2H), 1.89 (s, 6H). ^{13}C NMR (CDCl_3 , 125 MHz): δ 140.5, 128.0, 125.5, 124.0, 115.8, 110.8, 14.4 (7 of 8 found). LRMS (CI) m/z = 438 $[\text{M}+1]^+$.

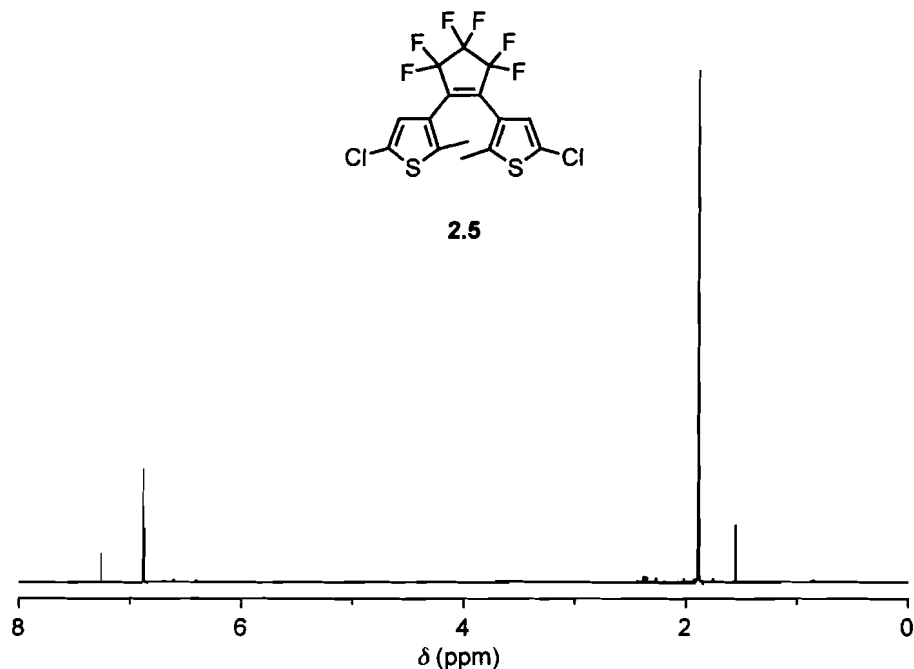
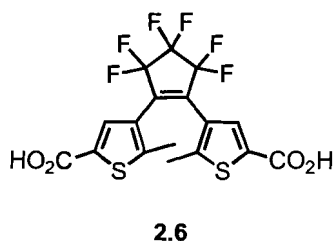
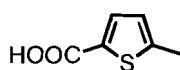
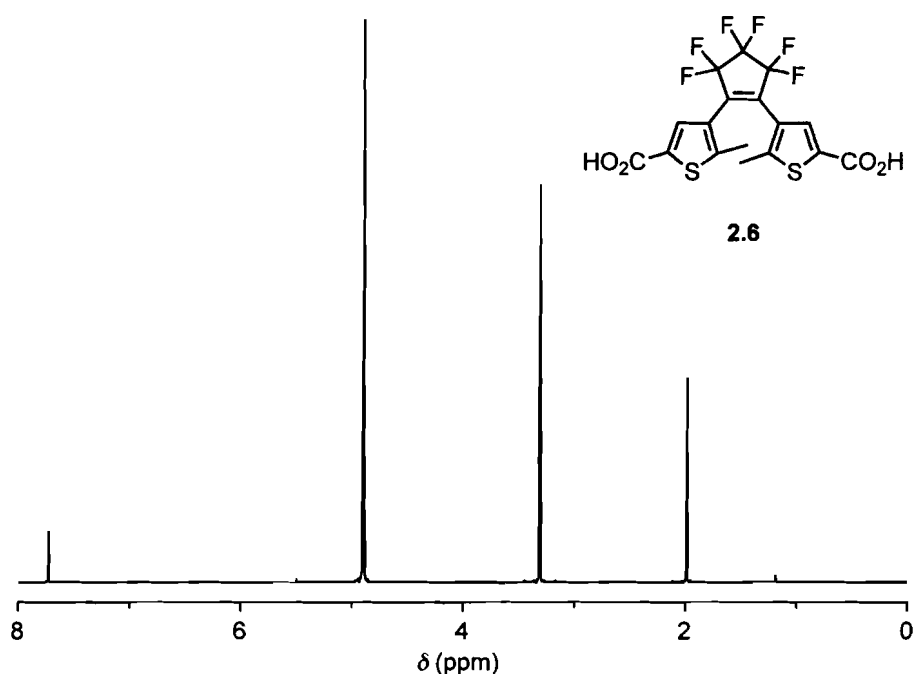


Figure 6.2.1 ^1H NMR (500 MHz) spectrum of compound **2.5** in CDCl_3 .



Synthesis of 1,2-bis (5'-carboxy-2'-methylthiophen-3'-yl)perfluorocyclopent-1-ene (2.6).¹⁰⁰ A solution of compound **2.5** (500 mg, 1.1 mmol) in anhydrous Et_2O (25 mL) was treated dropwise with *t*-butyllithium (1.7 mL, 1.7 M in pentane, 2.9 mmol) over 5 min at $-78\text{ }^\circ\text{C}$ under an N_2 atmosphere. The resulting solution was stirred at this temperature for 30 min, then the cooling bath was removed and dry CO_2 gas was bubbled through the solution for 30 min, at which time it was quenched with an aqueous HCl solution (25 mL, 1 M). The aqueous layer was separated and extracted with Et_2O (3 \times 50 mL). The combined organic layers were extracted with aqueous 5% NaOH solution (3 \times 40

mL). The basic aqueous layer was acidified with conc. HCl and extracted with Et₂O (3 × 50 mL). The combined organic layers were dried over Na₂SO₄, filtered and evaporated to dryness *in vacuo*. Purification by flash chromatography (SiO₂, 1% AcOH, 3% methanol in CH₂Cl₂) yielded 200 mg (38%) of compound **2.6** as a white solid. M.p. = 255–260 °C (dec.). ¹H NMR (CD₃OD, 400 MHz) δ 7.72 (s, 2H), 1.98 (s, 6H). FT-IR (KBr-cast): 3358, 3083, 2978, 1886, 1691, 1500, 1475, 1270 cm⁻¹.



2.9

Synthesis of the commercially available 5-methylthiophene-2-carboxylic acid (2.9).¹⁰¹ A solution of 2-bromo-5-methylthiophene, compound **2.8**, (5.0 g, 28 mmol) in anhydrous Et₂O (100 mL) was treated dropwise with *n*-butyllithium

(12.4 mL, 2.5 M in hexanes, 31 mmol) over 5 min at -78 °C under an N₂ atmosphere. The resulting solution was stirred at this temperature for 30 min, at which time the cooling bath was removed and dry CO₂ gas was bubbled through the solution for 30 min. The reaction was extracted with saturated aqueous NaHCO₃ (2 × 100 mL). The combined aqueous layers were acidified with conc. HCl and extracted with Et₂O (3 × 50 mL), dried over Na₂SO₄, filtered and evaporated to dryness *in vacuo*. Purification by flash chromatography (SiO₂, 1% AcOH, 7% CH₃OH in CH₂Cl₂) yielded 2.9 g (94%) of compound **2.9** as a light yellow crystals. M.p. = 120–125 °C. (135-138 °C)¹⁰¹ ¹H NMR (CDCl₃, 500 MHz) δ 11.44 (br s), 7.71 (d, *J* = 4 Hz, 1H), 6.81 (d, *J* = 4 Hz, 1H), 2.55 (s, 3H).

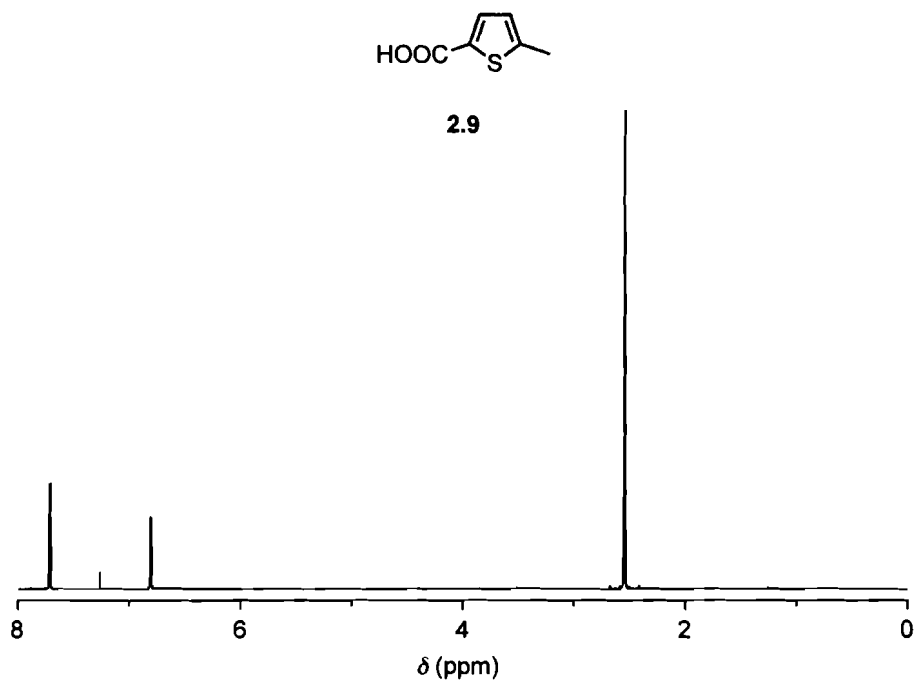


Figure 6.2.3 ^1H NMR (500 MHz) spectrum of compound **2.9** in CDCl_3 .

6.3 Characterization of new compounds from *Chapter 3*

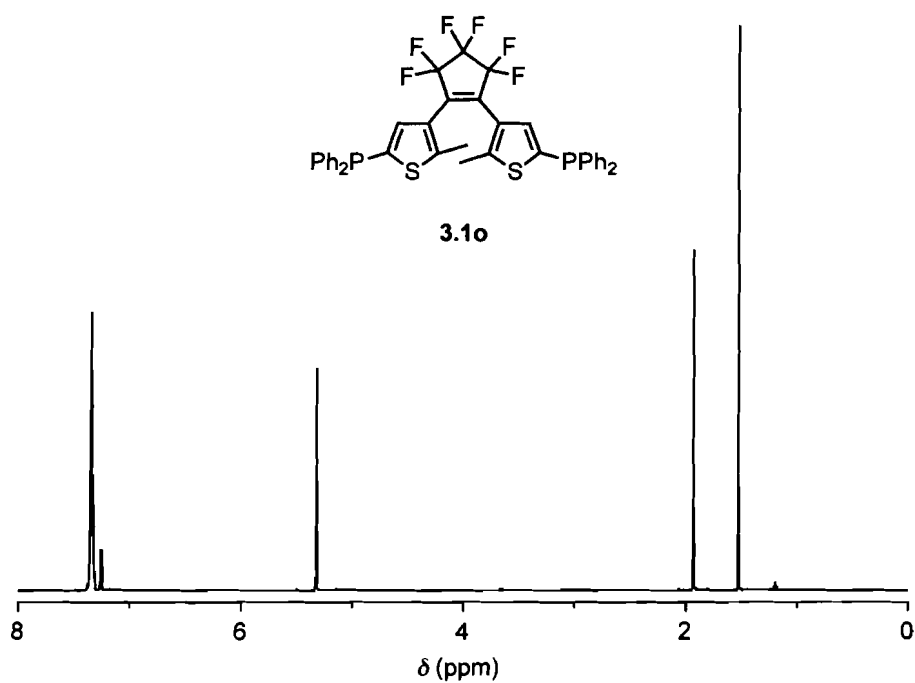


Figure 6.3.1 ^1H NMR (500 MHz) spectrum of compound **3.1o** in CD_2Cl_2 .

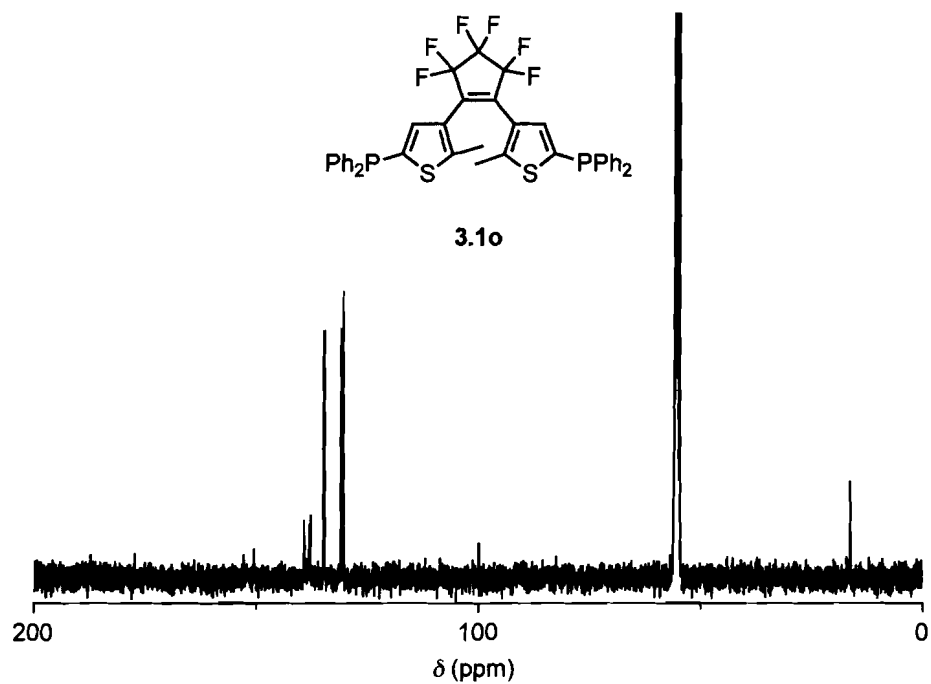


Figure 6.3.2 ^{13}C NMR (100 MHz) spectrum of compound **3.1o** in CD_2Cl_2 .

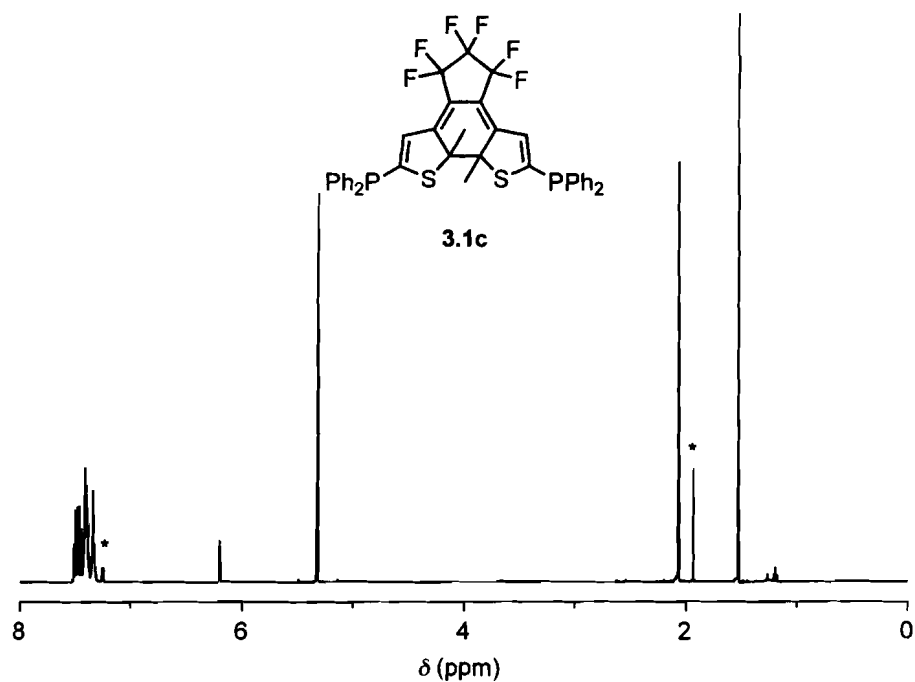


Figure 6.3.3 ^1H NMR (500 MHz) spectrum in CD_2Cl_2 of compound **3.1c** after 10 min irradiation with 313-nm light containing 80% compound **3.1c** and 20% compound **3.1o**, highlighted (*) by the C2 methyl and thienyl peaks.

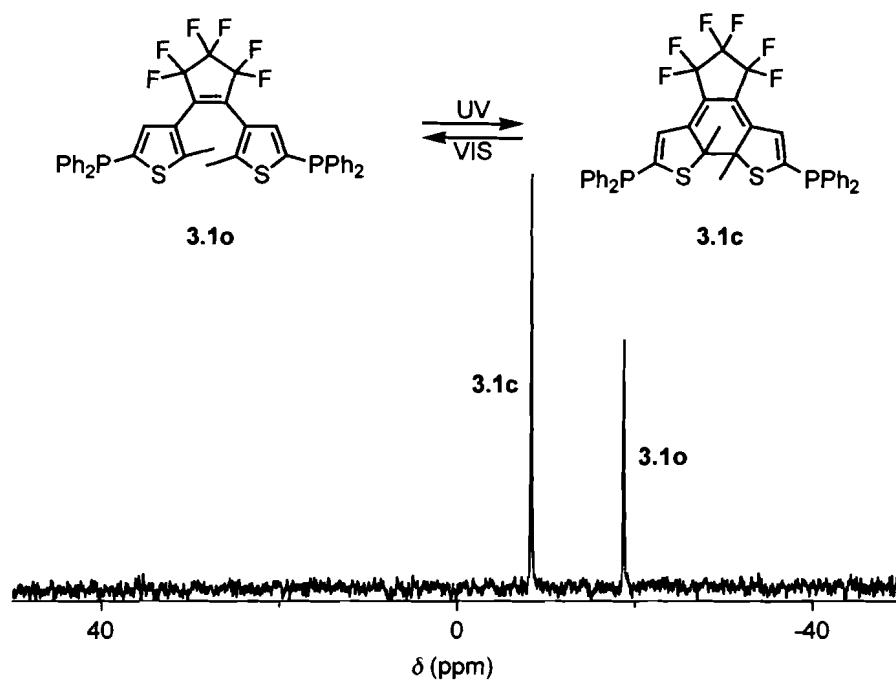


Figure 6.3.4 ^{31}P NMR (162 MHz) spectrum in CD_2Cl_2 of a mixture of compound **3.1o** and compound **3.1c** generated with 313-nm light.

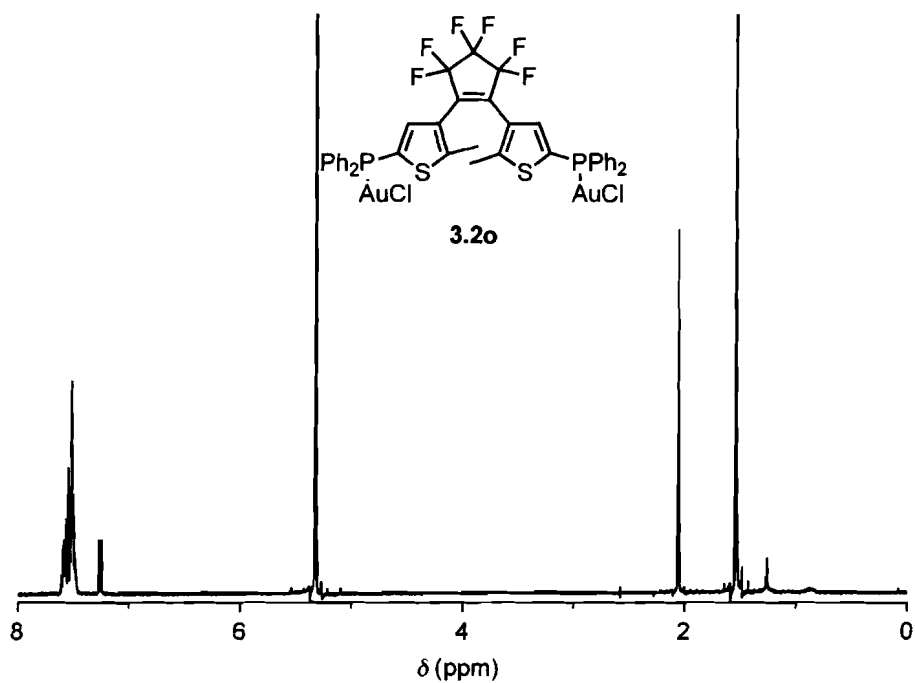


Figure 6.3.5 ^1H NMR (500 MHz) spectrum of compound **3.2o** in CD_2Cl_2 .

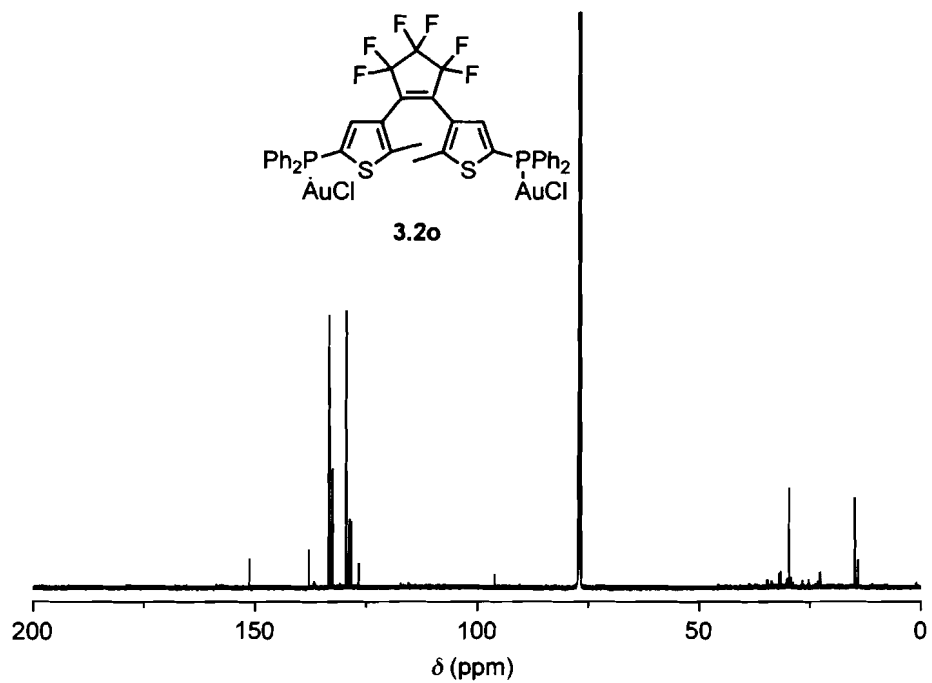


Figure 6.3.6 ^{13}C NMR (150 MHz) spectrum of compound **3.2o** in CDCl_3 .

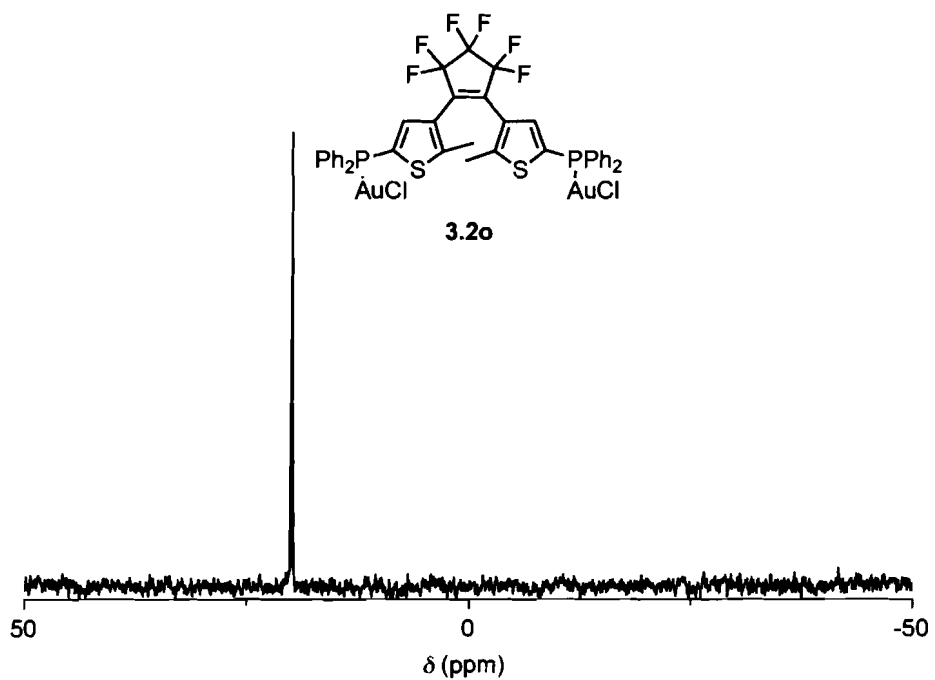


Figure 6.3.7 ^{31}P NMR (162 MHz) spectrum of compound **3.2o** in CDCl_3 .

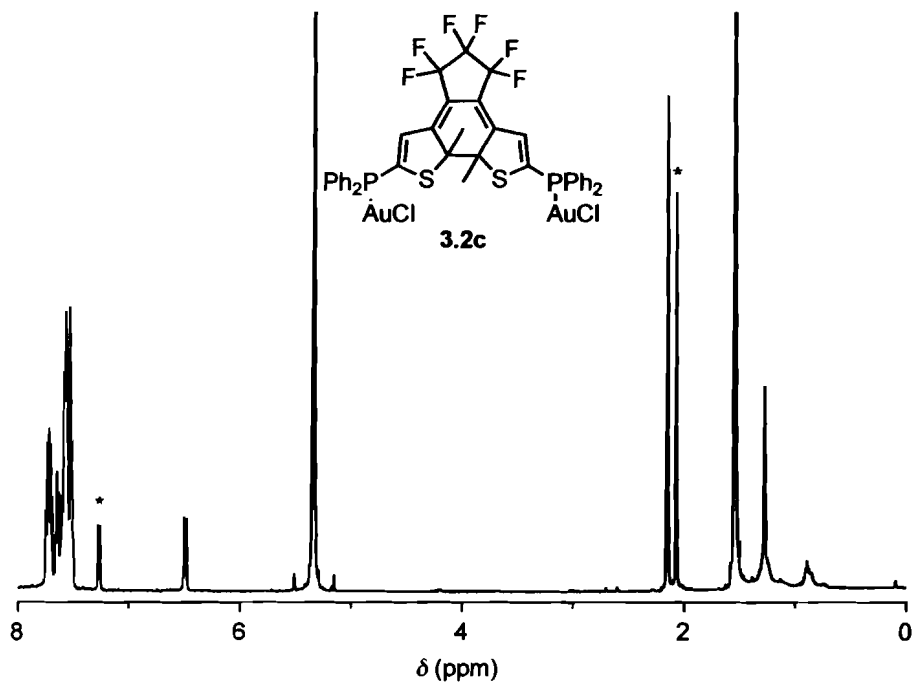


Figure 6.3.8 ^1H NMR (400 MHz) spectrum in CD_2Cl_2 of compound **3.2c** after 10 min irradiation with 313-nm light containing 60% compound **3.2c** and 40% compound **3.2o**, highlighted (*) by the C2 methyl and thienyl peaks.

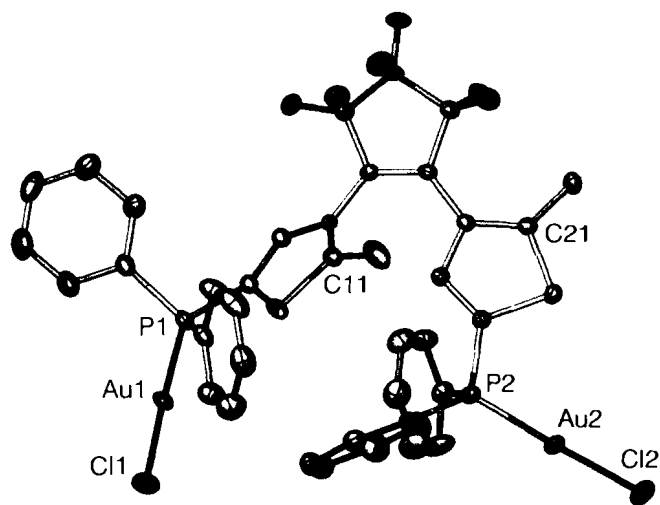


Figure 6.3.9. Molecular structure of complex **3.2o**. Thermal ellipsoids are shown at 20% probability. The hydrogen atoms are omitted for clarity.

Formula	$C_{39}H_{28}Au_2Cl_2F_6P_2S_2$
Mol wt	1201.51
<i>T</i> (K)	193
Space group	$P\bar{1}$ (No. 2)
<i>a</i> (Å)	9.7100(6)
<i>b</i> (Å)	10.2317(6)
<i>c</i> (Å)	20.4590(12)
α (deg)	83.1693(9)
β (deg)	76.9049(8)
γ (deg)	84.1473(9)
<i>V</i> (Å ³)	1959.8(2)
ρ_c (g cm ⁻³)	2.036
<i>Z</i>	2
μ (mm ⁻¹)	7.860
$R_1 [F_0^2 \geq 2\sigma(F_0^2)]$	0.0214
$wR_2 [F_0^2 \geq -3\sigma(F_0^2)]$	0.0542

Table 6.3.1 Crystallographic data for complex **3.2o**.

	Distances, Å
Au(1)-Au(2)	8.9954(4)
Au(1)-P(1)	2.2291(8)
Au(1)-Cl(1)	1.717(3)
P(1)-C(14)	1.795(3)
P(1)-C(31)	1.820(4)
P(1)-C(41)	1.818(4)
C(11)-C(21)	4.776(4)
	Angles, °
Cl(1)-Au(1)-P(1)	177.68(3)
Au(1)-P(1)-C(14)	109.56(11)
Au(1)-P(1)-C(31)	113.87(12)
Au(1)-P(1)-C(41)	115.51(11)
P(1)-C(14)-S(1)	118.66(18)
P(1)-C(14)-C(13)	130.7(3)

Table 6.3.2 Selected bond lengths and angles for complex **3.2o**.

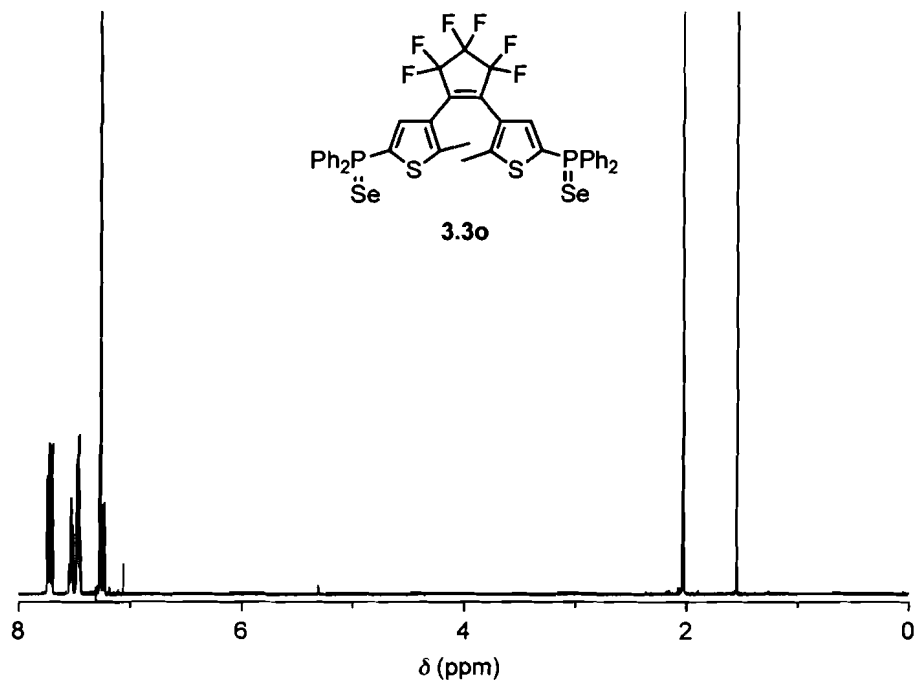


Figure 6.3.10 ^1H NMR spectrum (500 MHz) of compound **3.3o** in CDCl_3 .

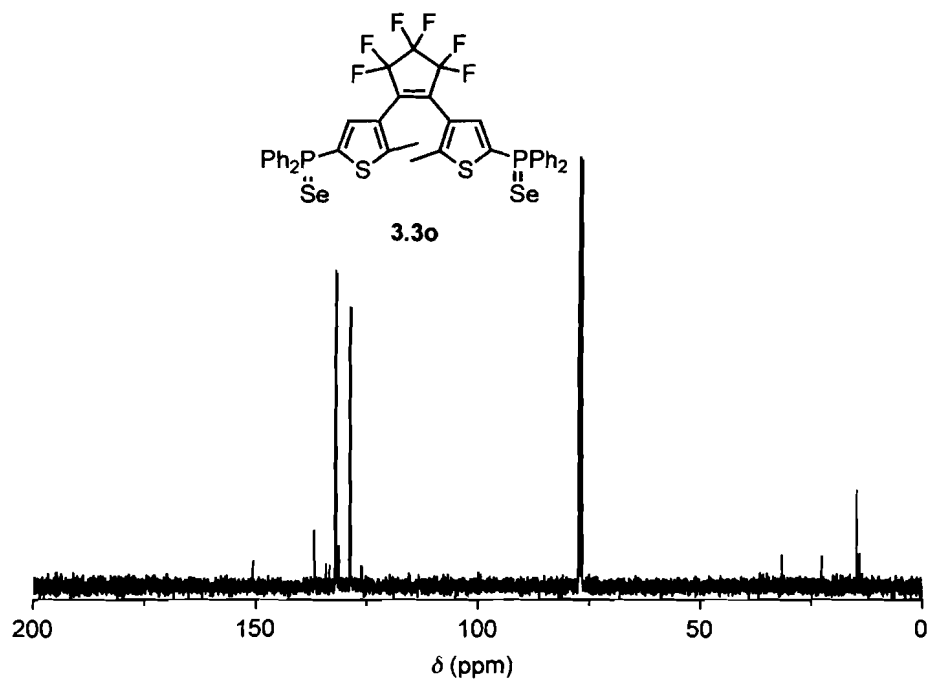


Figure 6.3.11 ^{13}C NMR (100 MHz) spectrum of compound **3.3o** in CDCl_3 .

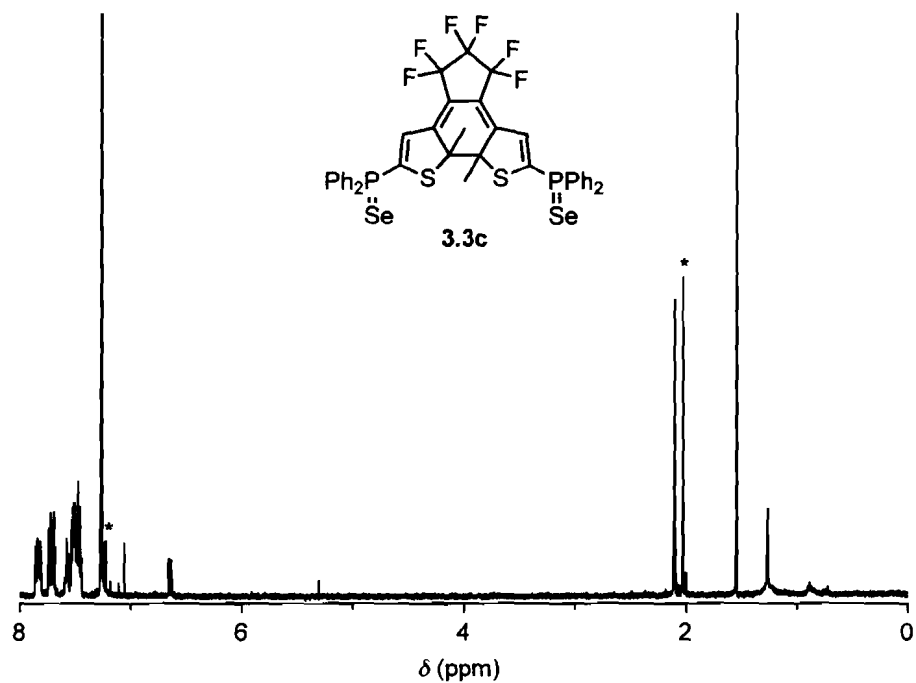


Figure 6.3.12 ^1H NMR (500 MHz) spectrum in CDCl_3 of compound **3.3c** after 3 min irradiation with 313-nm light containing 55% compound **3.3c** and 45% compound **3.3o**, highlighted (*) by the C2 methyl and thienyl peaks.

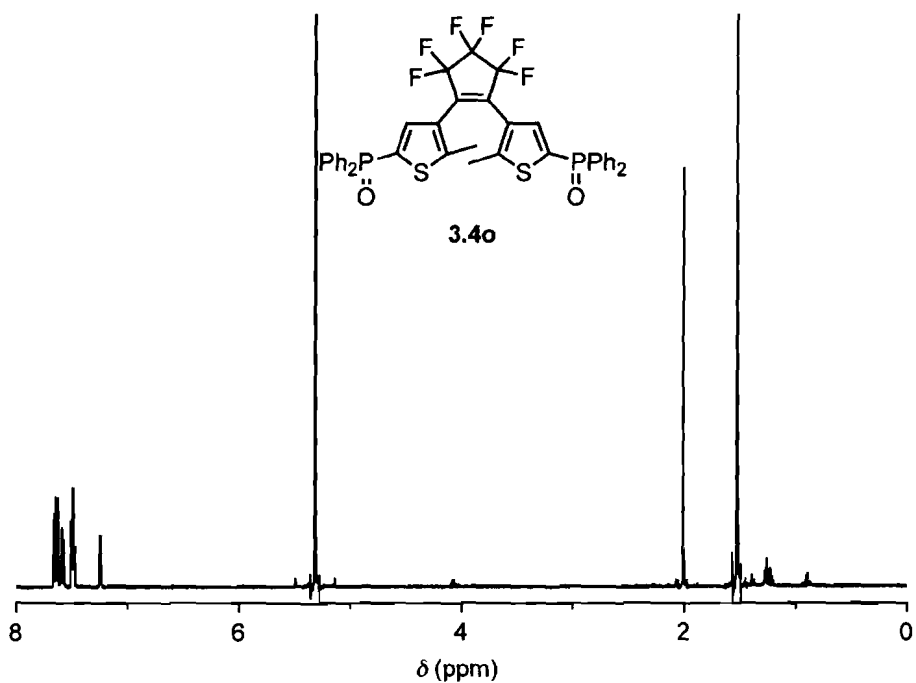


Figure 6.3.13 ^1H NMR (500 MHz) spectrum of compound **3.4o** in CD_2Cl_2 .

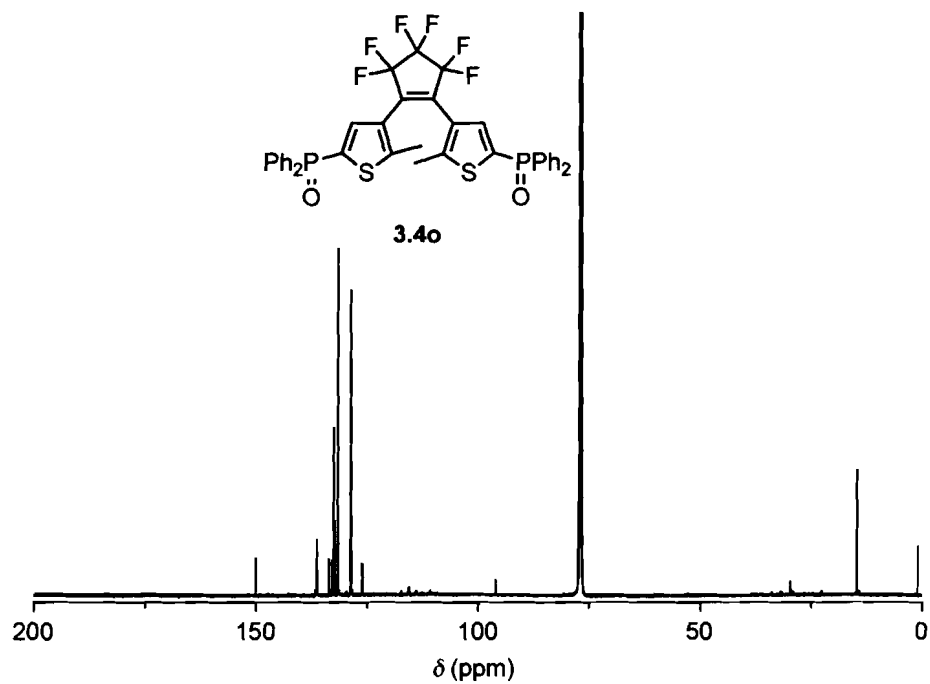


Figure 6.3.14 ¹³C NMR (150 MHz) spectrum of compound 3.4o in CDCl₃.

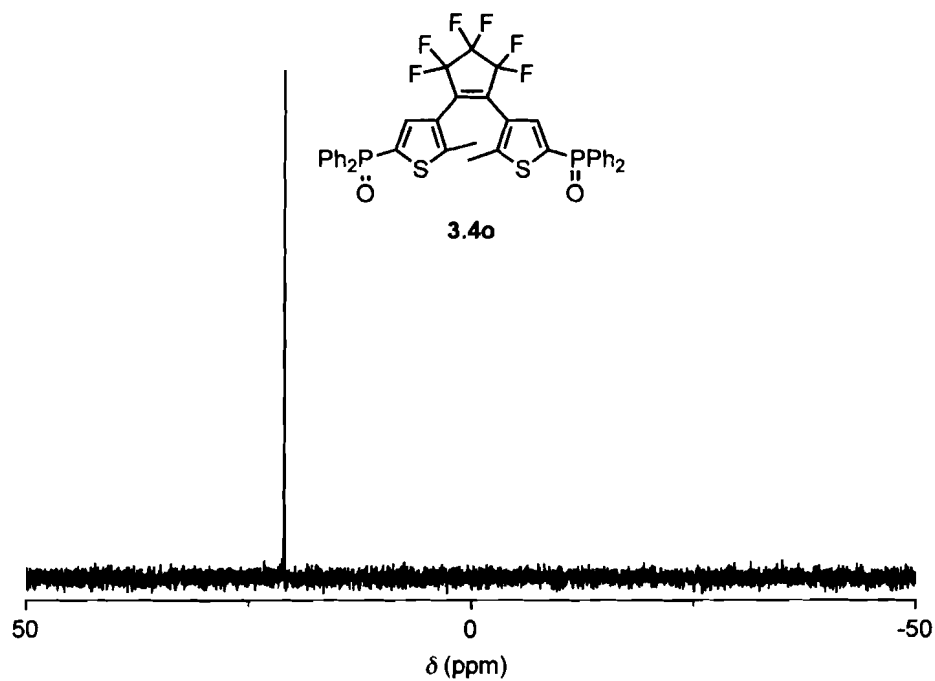


Figure 6.3.15 ³¹P NMR (243 MHz) spectrum of compound 3.4o in CDCl₃.

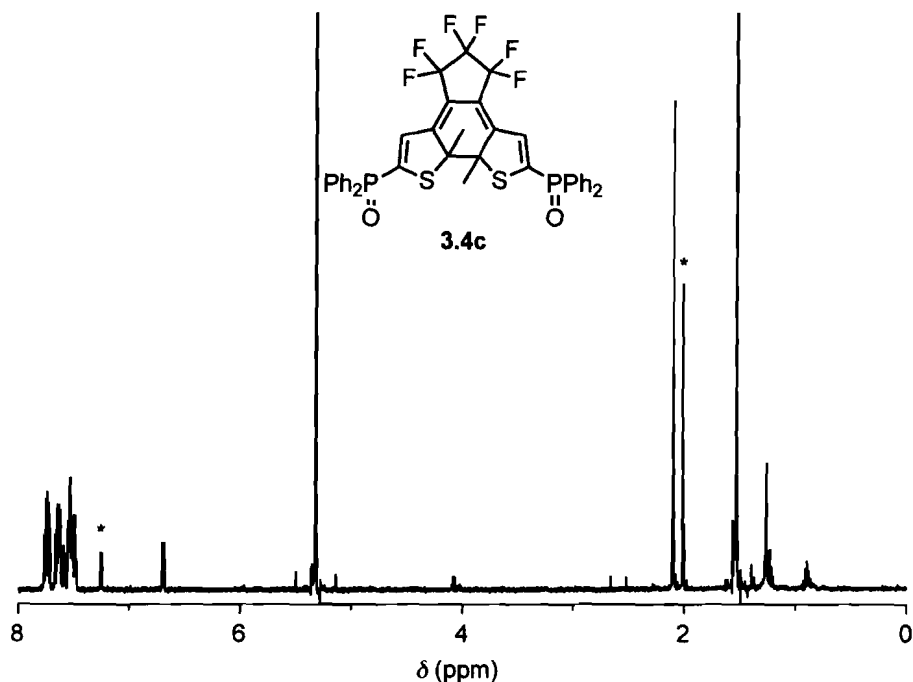
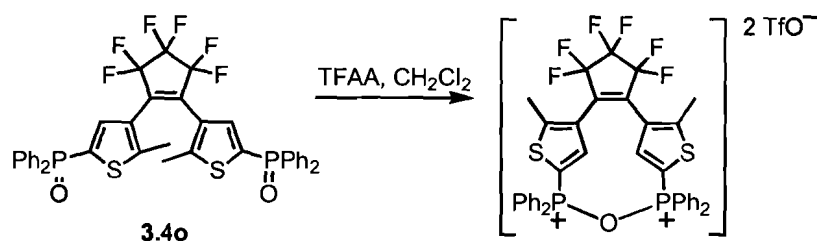


Figure 6.3.16 ^1H NMR (500 MHz) spectrum in CD_2Cl_2 of compound **3.4c** after 3 min irradiation with 313-nm light containing 59% compound **3.4c** and 41% compound **3.4o**, highlighted (*) by the C2 methyl and thienyl peaks.

6.3.1 Future work experiments from Chapter 3



Preparation of the DTE “POP” reagent. A CD_2Cl_2 solution of *ring-open* isomer **3.4o** (1.9×10^{-3} M) was prepared by dissolving compound **3.4o** (7.3 mg, 9.5×10^{-3} mmol) in CD_2Cl_2 (5 mL) in a volumetric flask. The solution of compound **3.4o** (0.6 mL, 1.1×10^{-3} mmol), in an NMR tube, was treated with aliquots ($2 \times 25 \mu\text{L}$) of a (2.3×10^{-2} M) trifluoromethanesulfonic anhydride (TFAA) in CD_2Cl_2 solution, ($19 \mu\text{L}$, 0.11 mmol) in CD_2Cl_2 (5 mL), until 1 equiv. was added ($50 \mu\text{L}$, 1.1×10^{-3}

mmol). After mixing the resulting solution for 10 min by shaking the NMR tube, it was irradiated for 2 min with 313-nm light.

6.4 NMR characterization of new compounds from *Chapter 4*

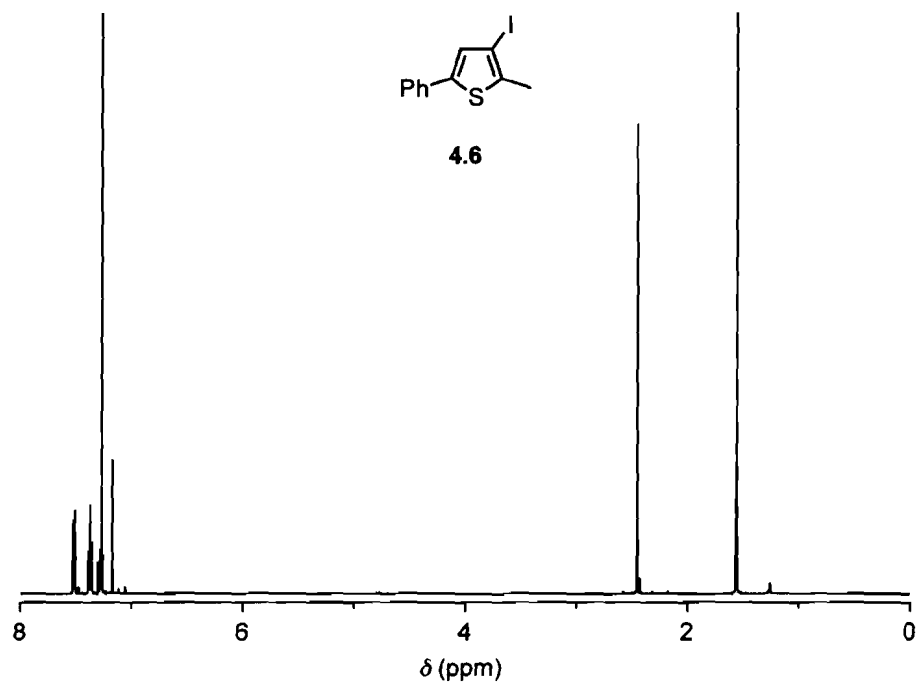


Figure 6.4.1 ¹H NMR (500 MHz) spectrum of compound 4.6 in CDCl₃.

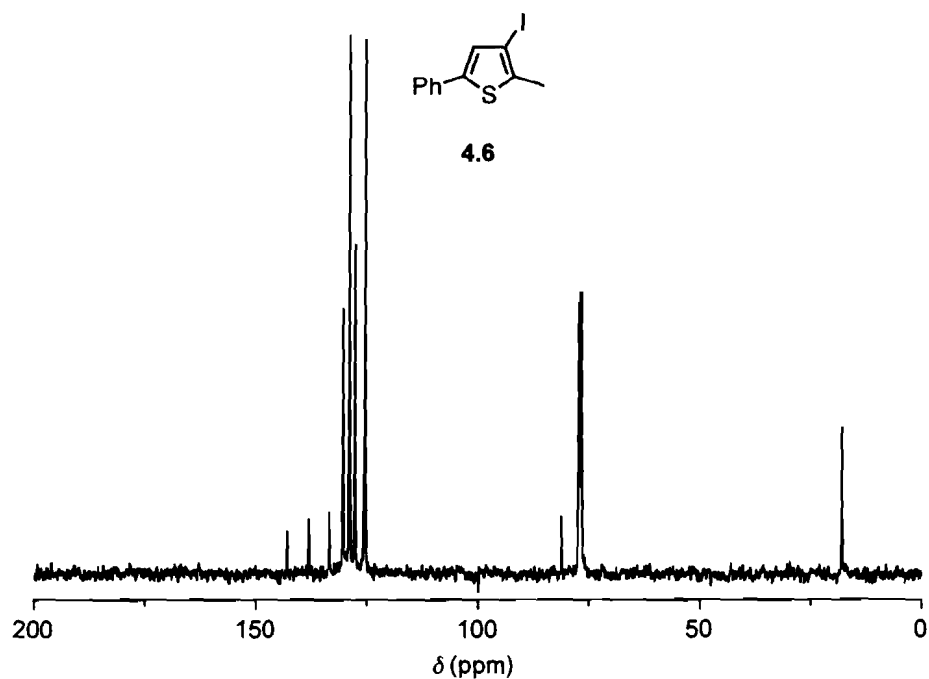


Figure 6.4.2 ¹³C NMR (100 MHz) spectrum of compound 4.6 in CDCl₃.

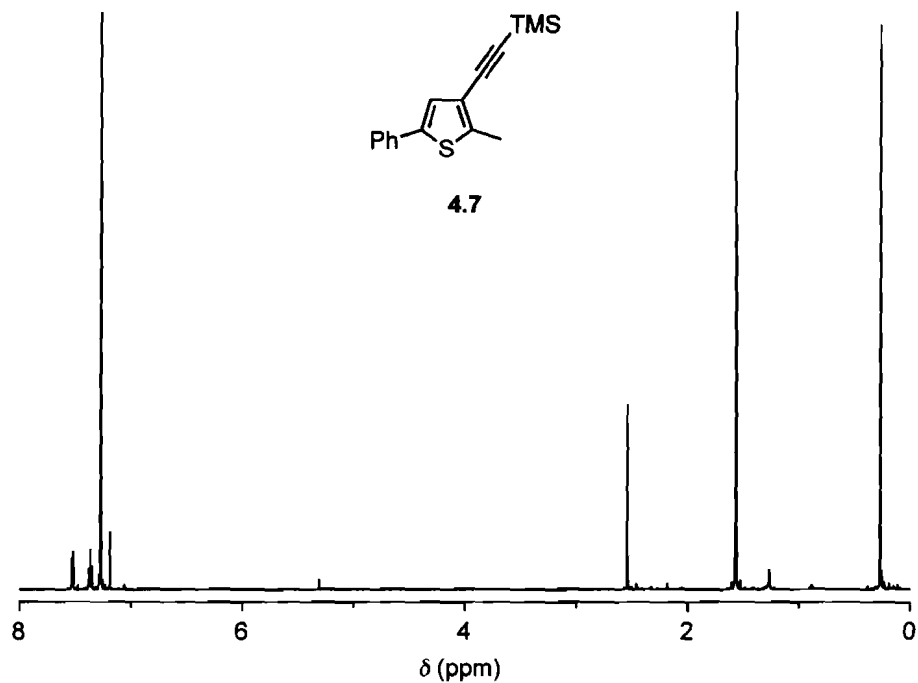


Figure 6.4.3 ¹H NMR (500 MHz) spectrum of compound 4.7 in CDCl₃.

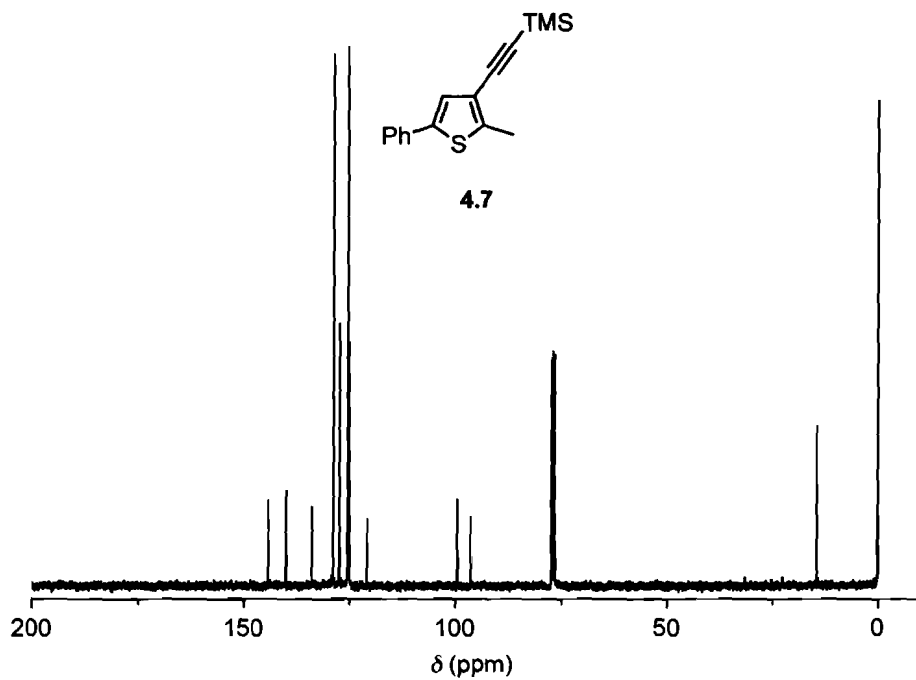


Figure 6.4.4 ¹H NMR (100 MHz) spectrum of compound 4.7 in CDCl₃.

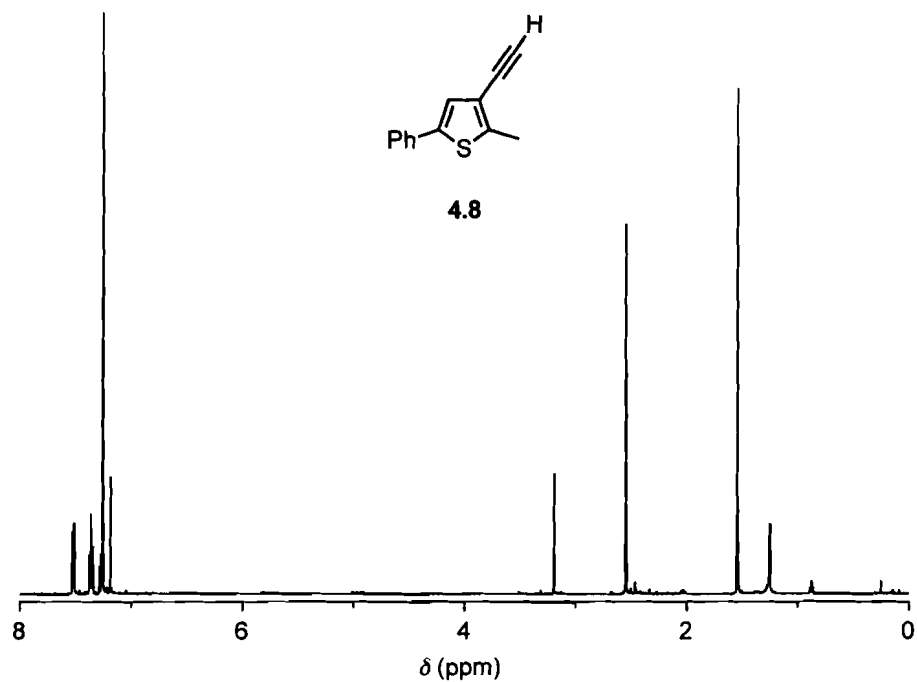


Figure 6.4.5 ^1H NMR (400 MHz) spectrum of compound 4.8 in CDCl_3 .

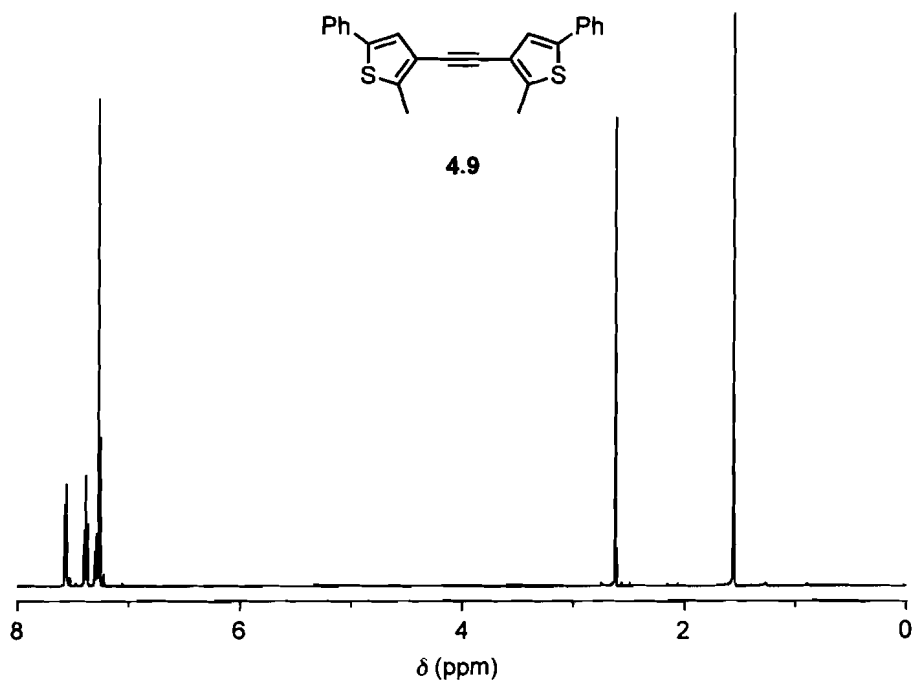


Figure 6.4.6 ^1H NMR (500 MHz) spectrum of compound 4.9 in CDCl_3 .

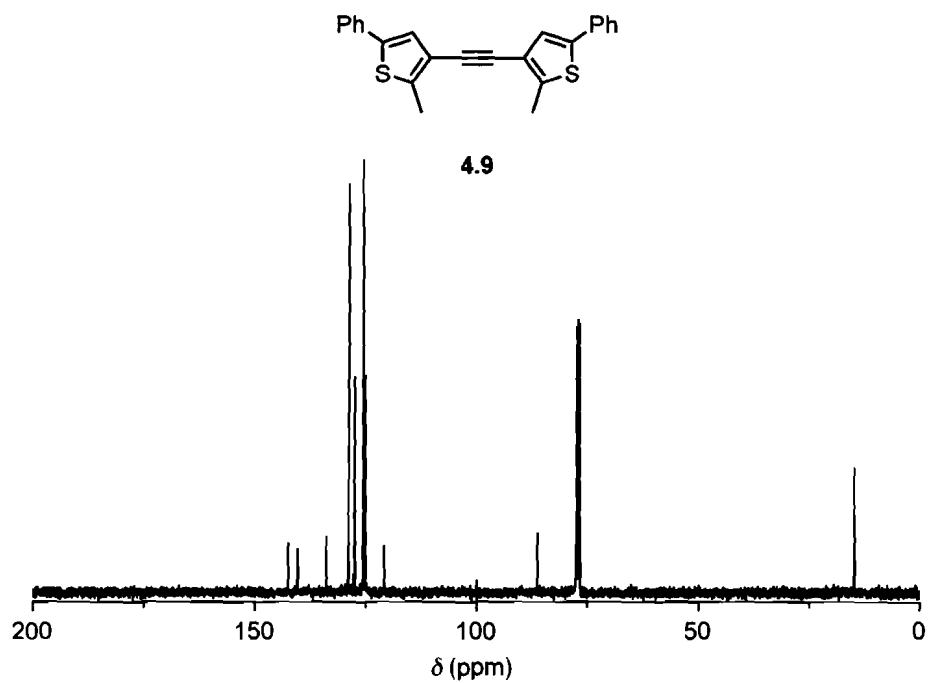


Figure 6.4.7 ¹³C NMR (100 MHz) spectrum of compound 4.9 in CDCl₃.

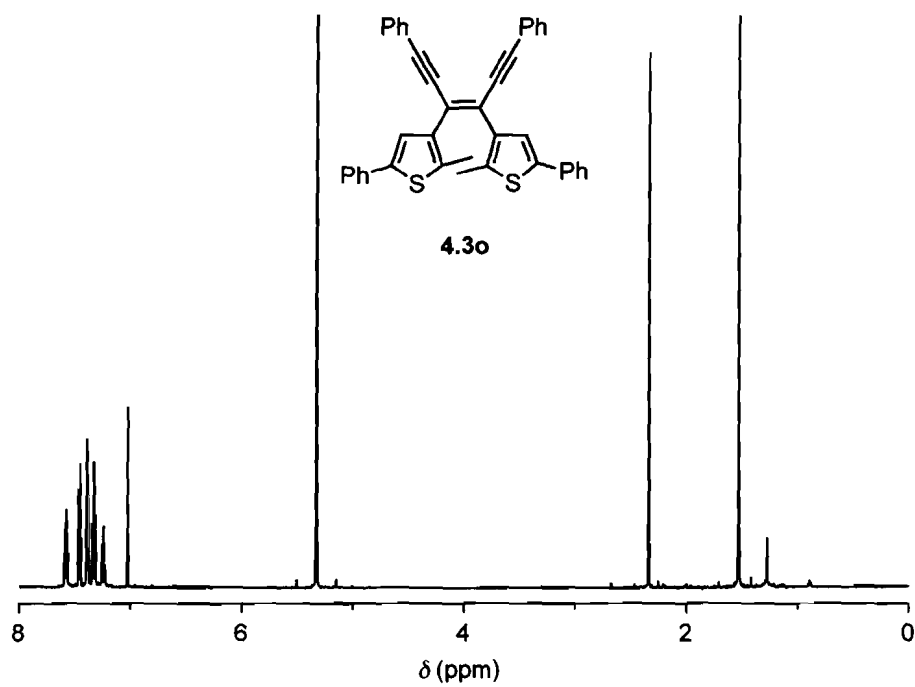


Figure 6.4.8 ¹H NMR (500 MHz) spectrum of compound 4.3o in CD₂Cl₂.

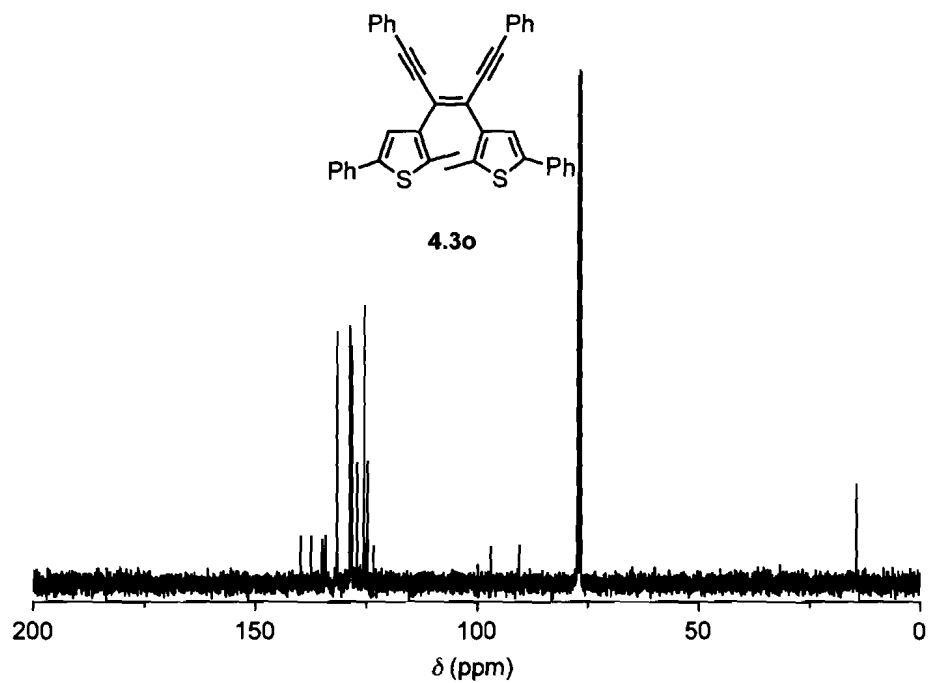


Figure 6.4.9 ^{13}C NMR (100 MHz) spectrum of compound **4.3o** in CDCl_3 .

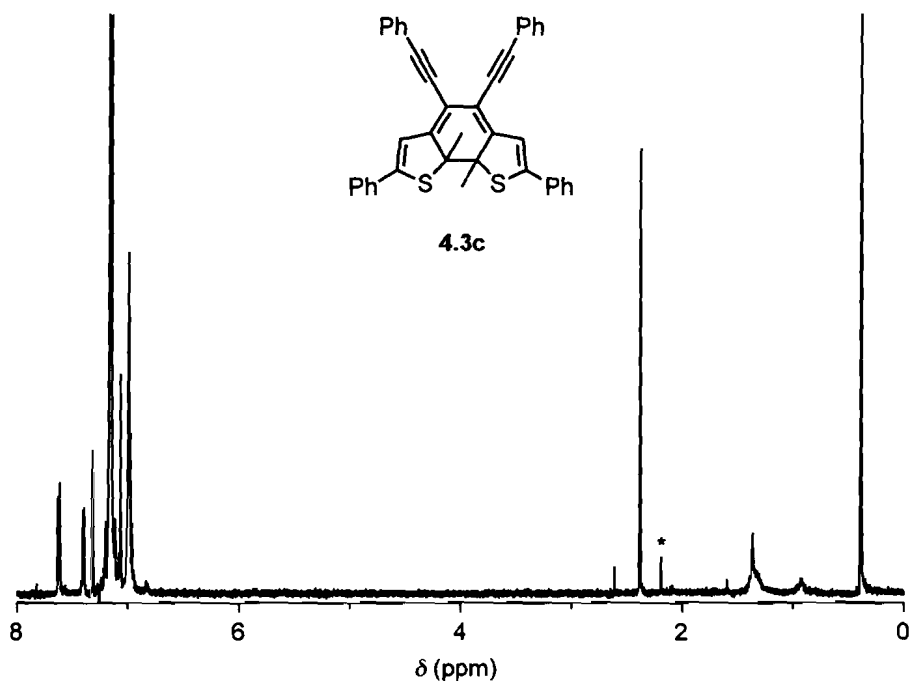


Figure 6.4.10 ^1H NMR (500 MHz) spectrum in C_6D_6 of compound **4.3o** after 4 min irradiation with 313-nm light containing 92% compound **4.3c** and 8% compound **4.3o**, highlighted (*) by the C2 methyl peak.

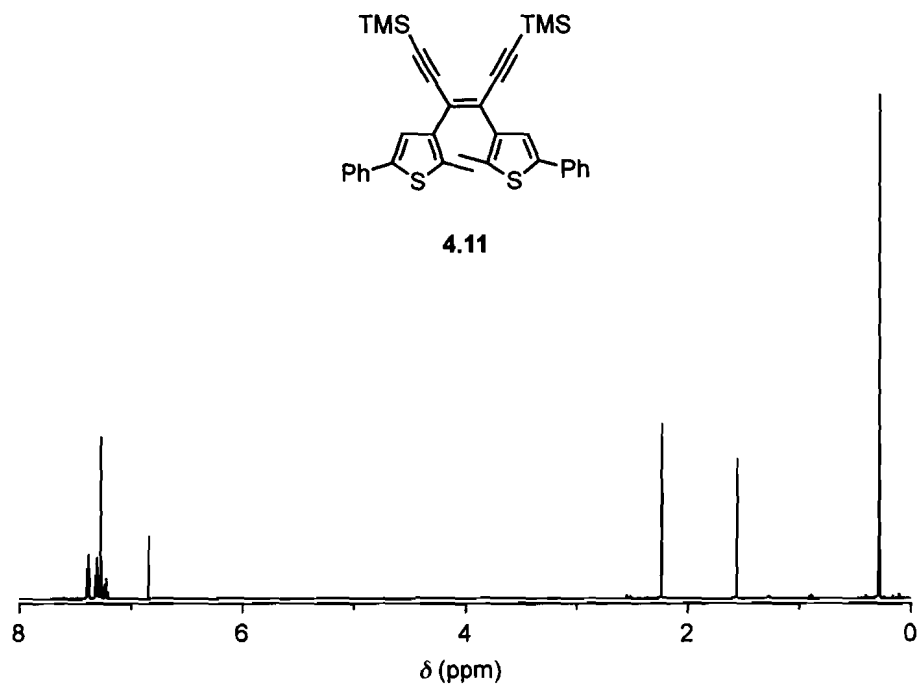


Figure 6.4.11 ^1H NMR (500 MHz) spectrum of compound **4.11** in CDCl_3 .

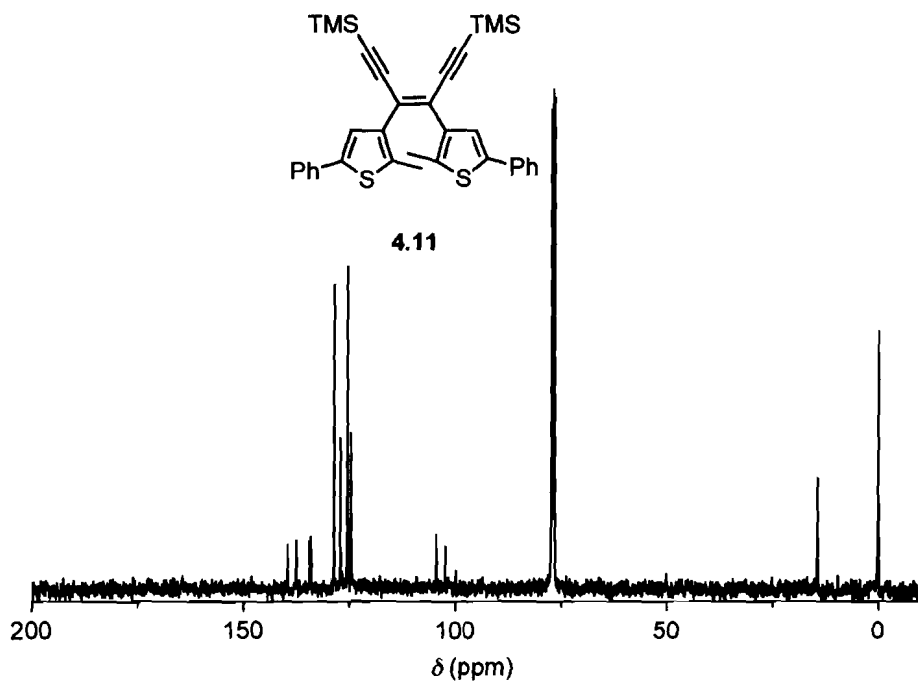


Figure 6.4.12 ^{13}C NMR (100 MHz) spectrum of compound **4.11** in CDCl_3 .

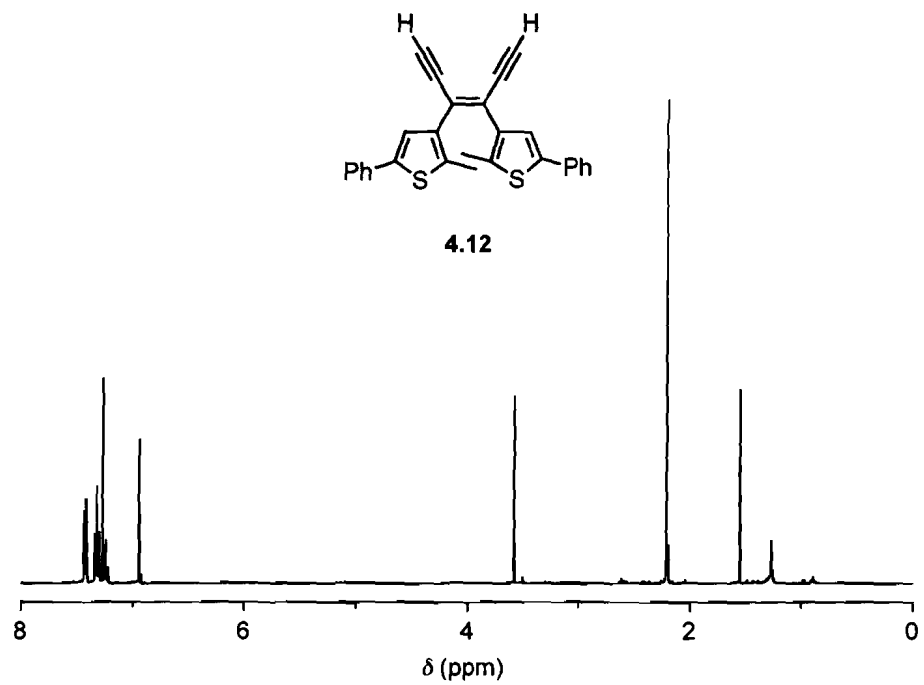


Figure 6.4.13 ^1H NMR (400 MHz) spectrum of compound 4.12 in CDCl_3 .

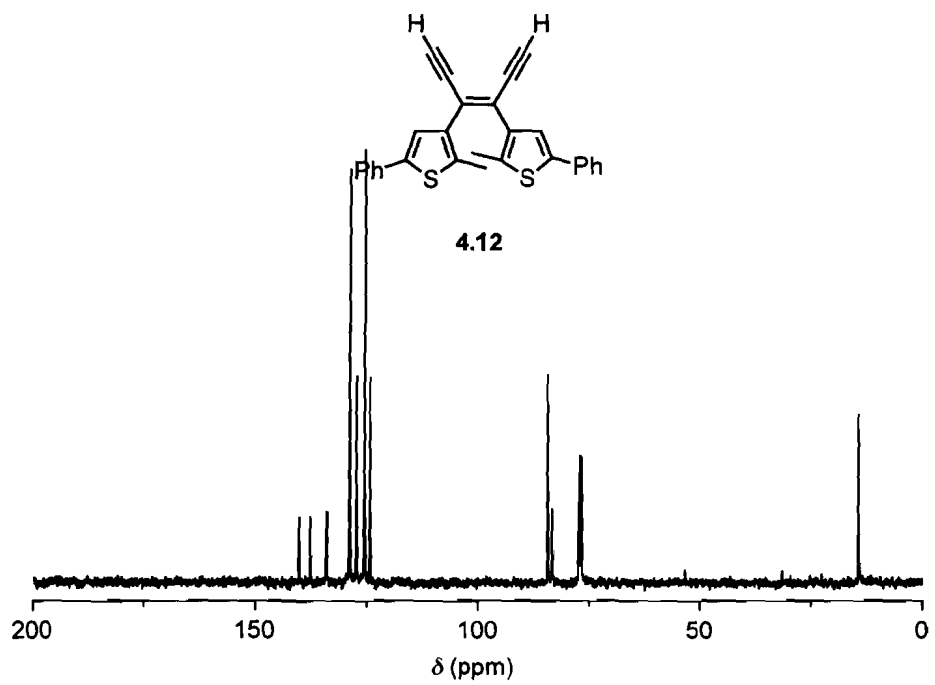


Figure 6.4.14 ^{13}C NMR (100 MHz) spectrum of compound 4.12 in CDCl_3 .

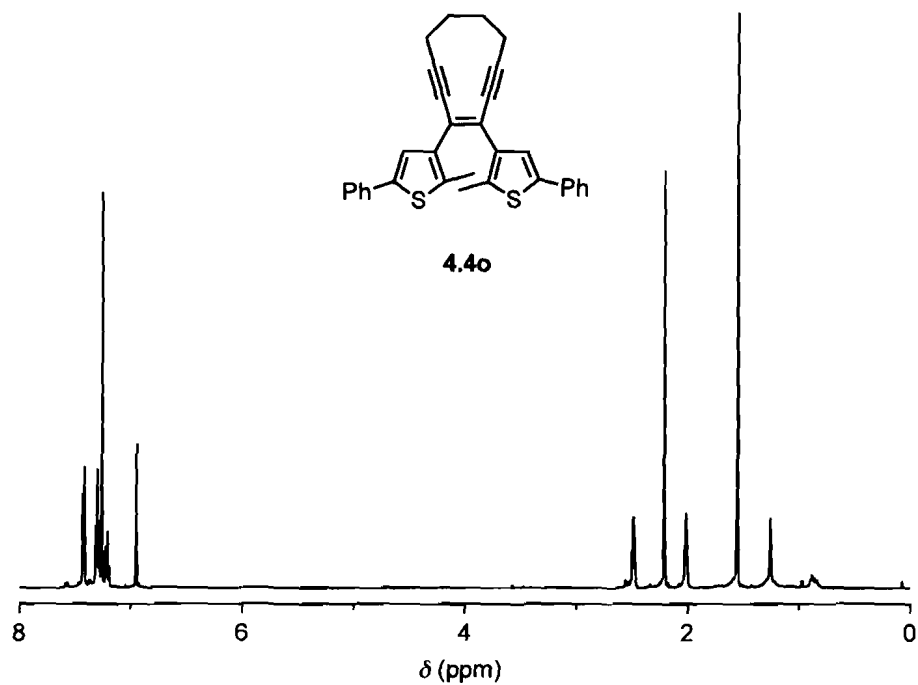


Figure 6.4.15 ^1H NMR (500 MHz) spectrum of compound **4.4o** in CDCl_3 .

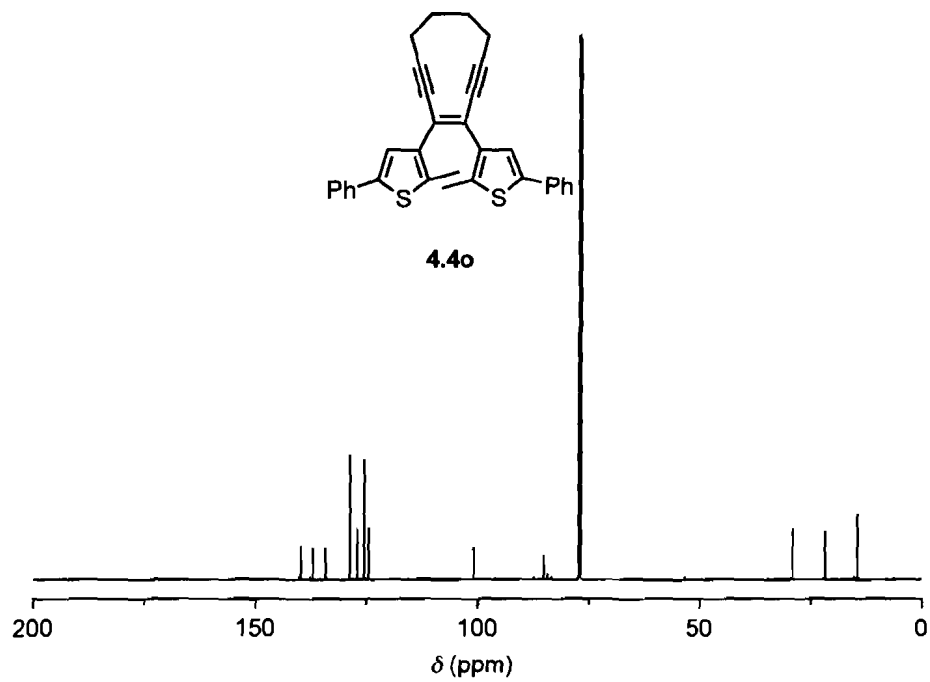


Figure 6.4.16 ^{13}C NMR (150 MHz) spectrum of compound **4.4o** in CDCl_3 .

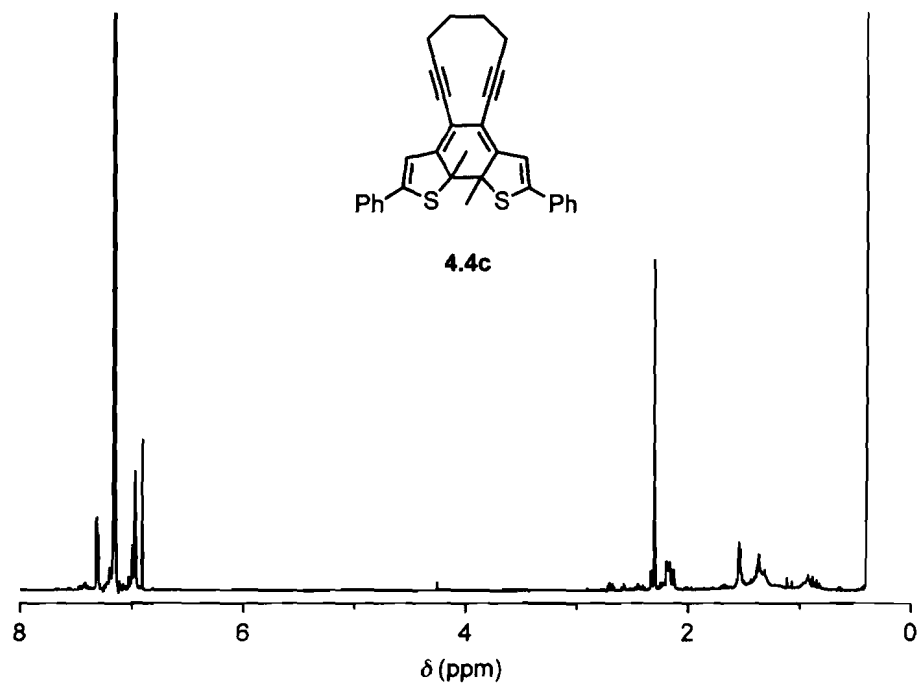


Figure 6.4.17 ^1H NMR (500 MHz) spectrum of compound 4.4c in C_6D_6 .

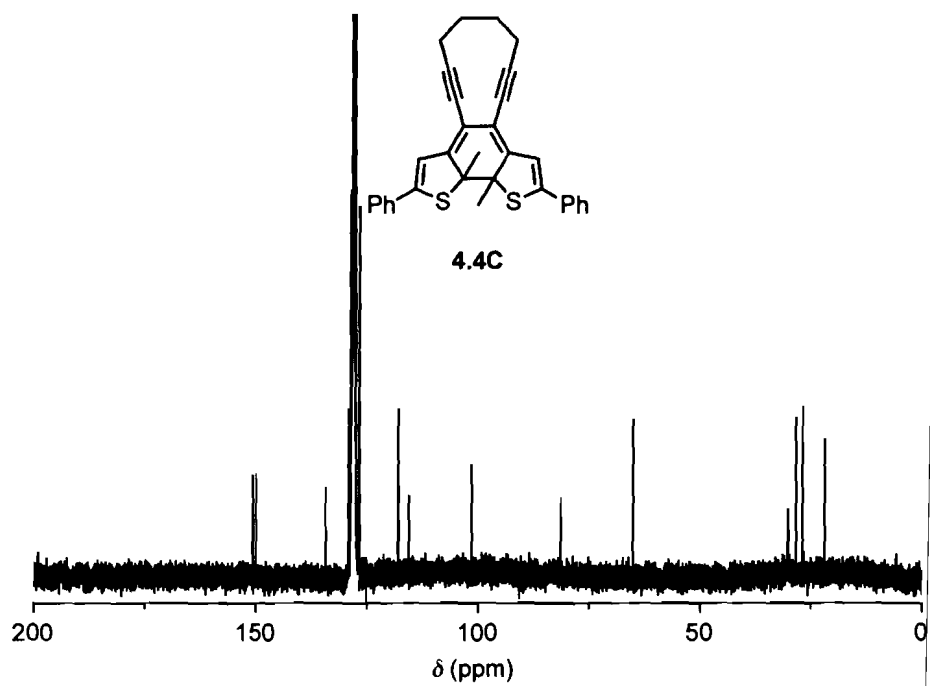


Figure 6.4.18 ^{13}C NMR (150 MHz) spectrum of compound 4.4c in C_6D_6 .

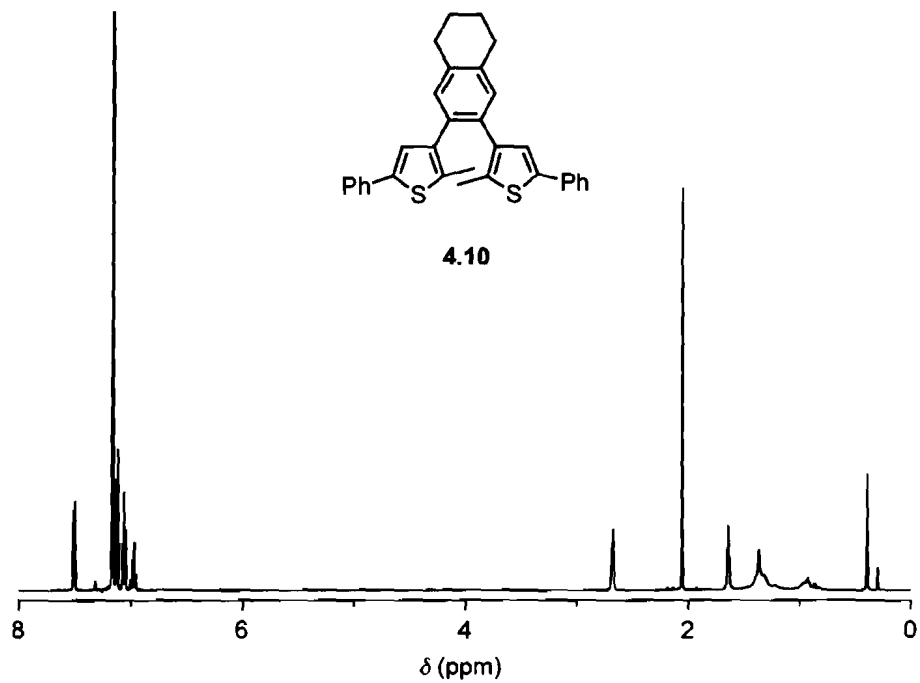


Figure 6.4.19 ^1H NMR (500 MHz) spectrum of compound 4.10 in C_6D_6 .

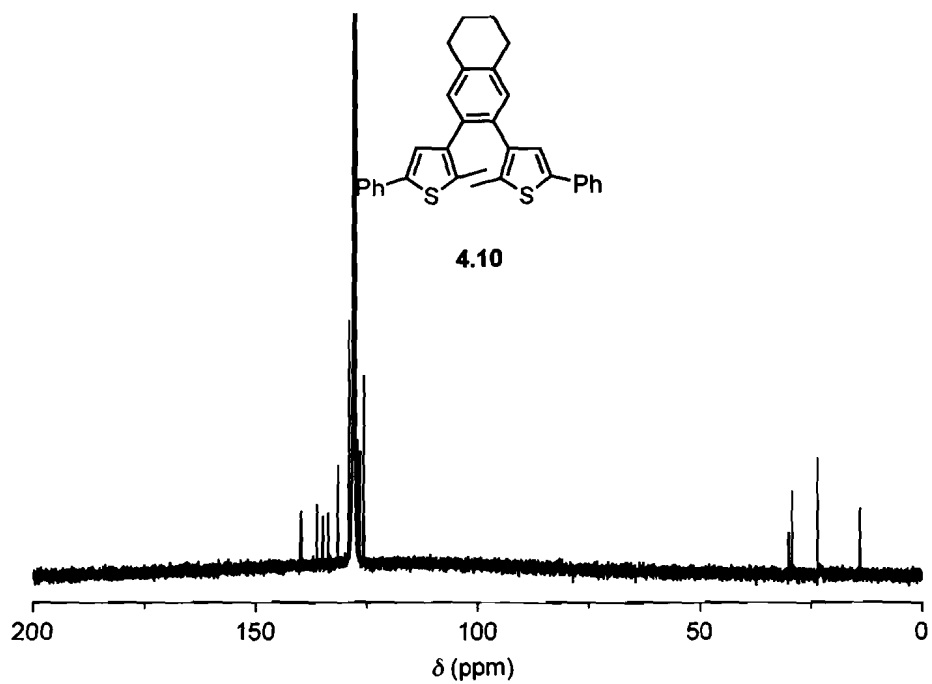


Figure 6.4.20 ^{13}C NMR (150 MHz) spectrum of compound 4.10 in C_6D_6 .

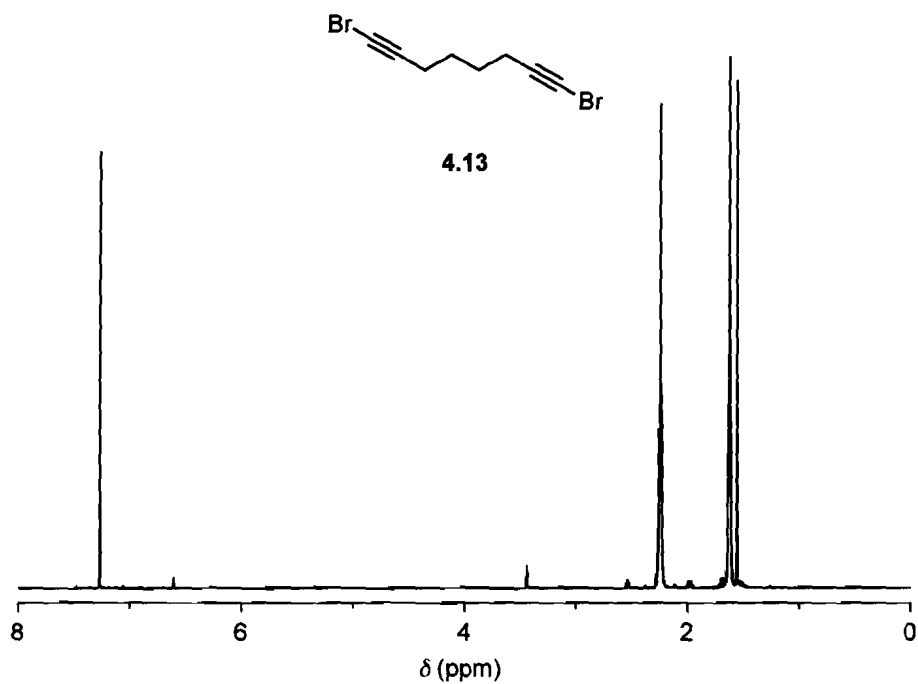


Figure 6.4.21 ¹H NMR (500 MHz) spectrum of compound 4.13 in CDCl₃.

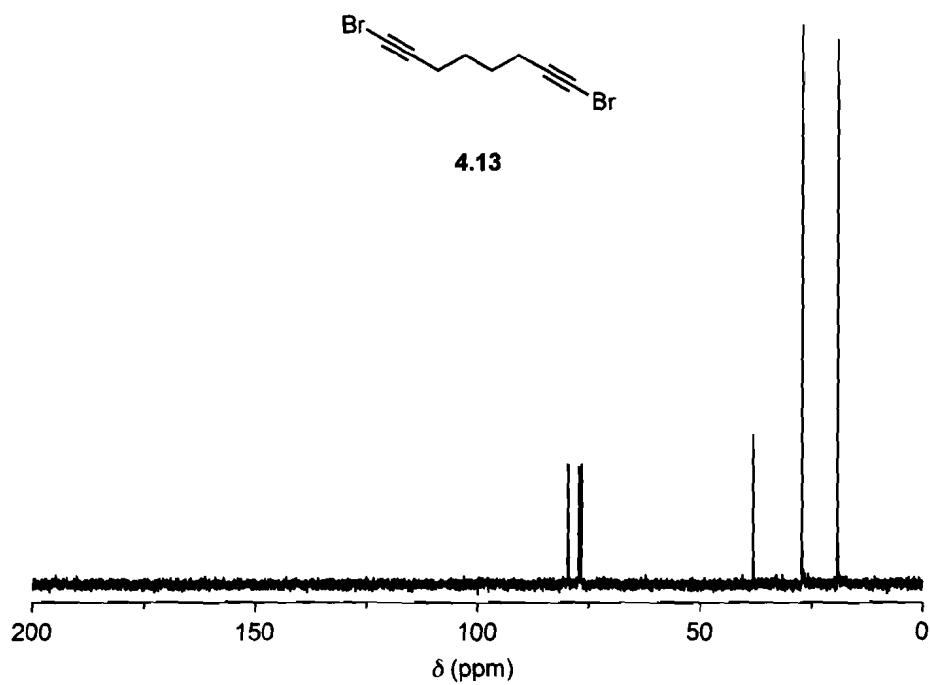


Figure 6.4.22 ¹³C NMR (100 MHz) spectrum of compound 4.13 in CDCl₃.

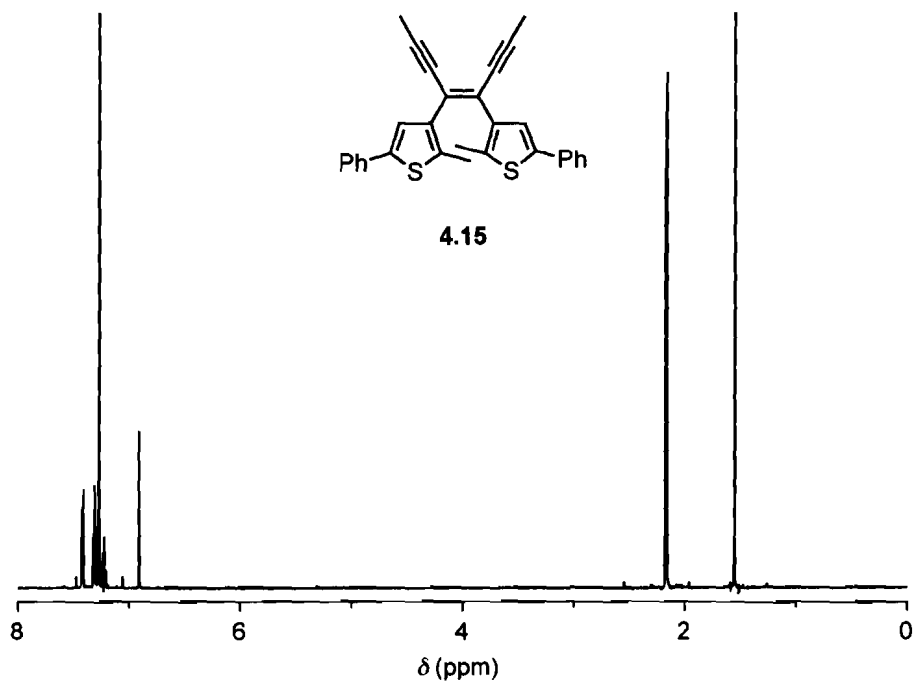


Figure 6.4.23 ^1H NMR (500 MHz) spectrum of compound **4.15** in CDCl_3 .

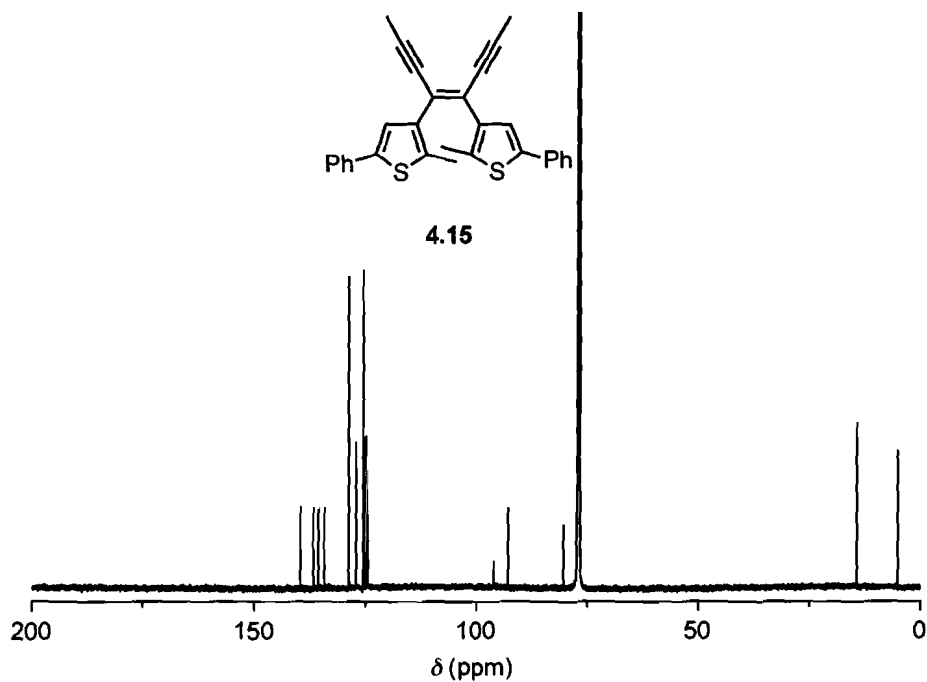
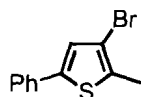


Figure 6.4.24 ^{13}C NMR (150 MHz) spectrum of compound **4.15** in CDCl_3 .

6.5 Synthesis and characterization of previously known compounds and unsuccessful reactions in *Chapter 4*



4.5

Synthesis of 3-bromo-2-methyl-5-phenylthiophene (4.5).⁸⁷ A two-phase mixture containing toluene (100 mL), aqueous Na₂CO₃ (100 mL, 2 M) and 3,5-dibromo-2-methylthiophene (15.0 g, 58.6 mmol) was deoxygenated by bubbling N₂ through it for 60 min. This mixture was treated with a solution of phenylboronic acid (7.15 g, 58.6 mmol) in EtOH (50 mL) and the reaction was bubbled with N₂ for an additional 30 min, at which time Pd(PPh₃)₄ (0.6 g, 0.5 mmol) was added in one portion. The reaction was heated at reflux for 16 h under an N₂ atmosphere. The heat source was removed and the reaction was allowed to cool to room temperature. The mixture was extracted with Et₂O (3 × 100 mL). The combined organic layers were extracted with brine (100 mL), dried using Na₂SO₄, filtered and evaporated to dryness *in vacuo*. Purification by flash chromatography (SiO₂, hexanes) yielded 11.1 g (75%) compound **4.5** as a white solid. M.p. = 71–72 °C. (72–73 °C)⁸⁷ ¹H NMR (CDCl₃, 400 MHz) δ 7.51 (d, *J* = 8 Hz, 2H), 7.37 (t, *J* = 8 Hz, 2H), 7.28–7.30 (m, 1H), 7.10 (s, 1H), 2.42 (s, 3H).

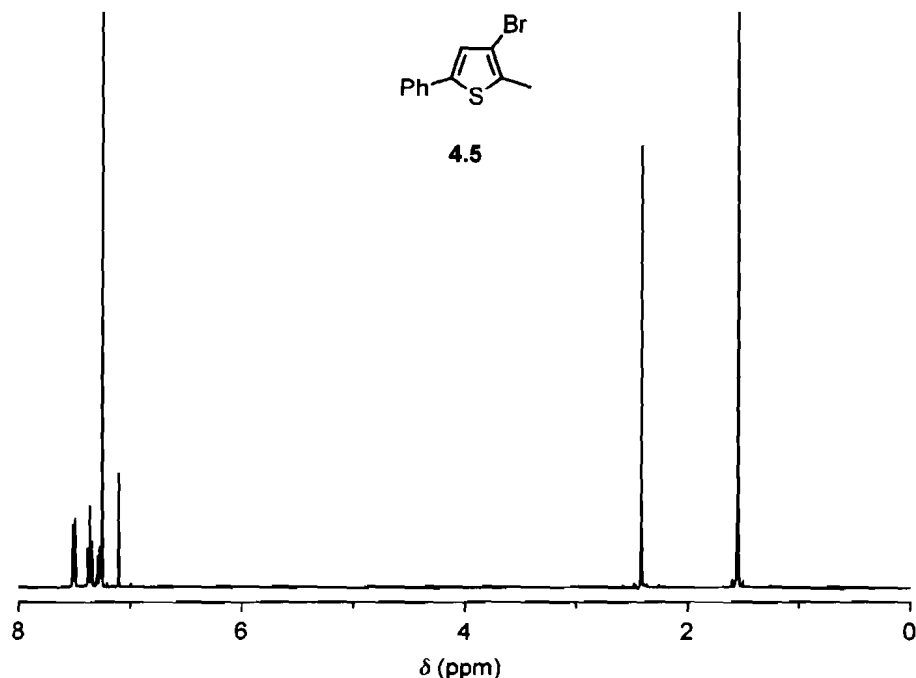
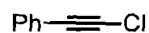


Figure 6.5.1 ^1H NMR (400 MHz) spectrum of compound **4.5** in CDCl_3 .



Synthesis of 1-(2-chloroethynyl)benzene.⁸⁶ A solution of phenylacetylene (2.0 g, 19.6 mmol) in THF (40 mL) was treated dropwise with *n*-butyllithium (8.0 mL, 2.5 M in hexanes, 21.5 mmol) over 5 min at $-78\text{ }^\circ\text{C}$ under an N_2 atmosphere. The resulting suspension was stirred at this temperature for 30 min, at which time a solution of *N*-chlorosuccinimide (2.87 g, 21.5 mmol) in THF (20 mL) was added in rapidly through a cannula. After stirring at this temperature for 1 h, the cooling bath was removed and the reaction was allowed to slowly warm to room temperature and stirred there for 18 h. The reaction was quenched with saturated NH_4Cl (25 mL), the aqueous layer was separated and extracted with Et_2O (3×50 mL). The combined organic layers were dried with Na_2SO_4 , filtered and evaporated to dryness *in vacuo*. Purification by flash chromatography (SiO_2 ,

hexanes) yielded 1.94 g (73%) of 1-(2-chloroethynyl)benzene as a clear oil. ^1H NMR (CDCl_3 , 400 MHz) δ 7.44 (dd, $J = 6, 1$ Hz, 2H), 7.30-7.34 (m, 3H).

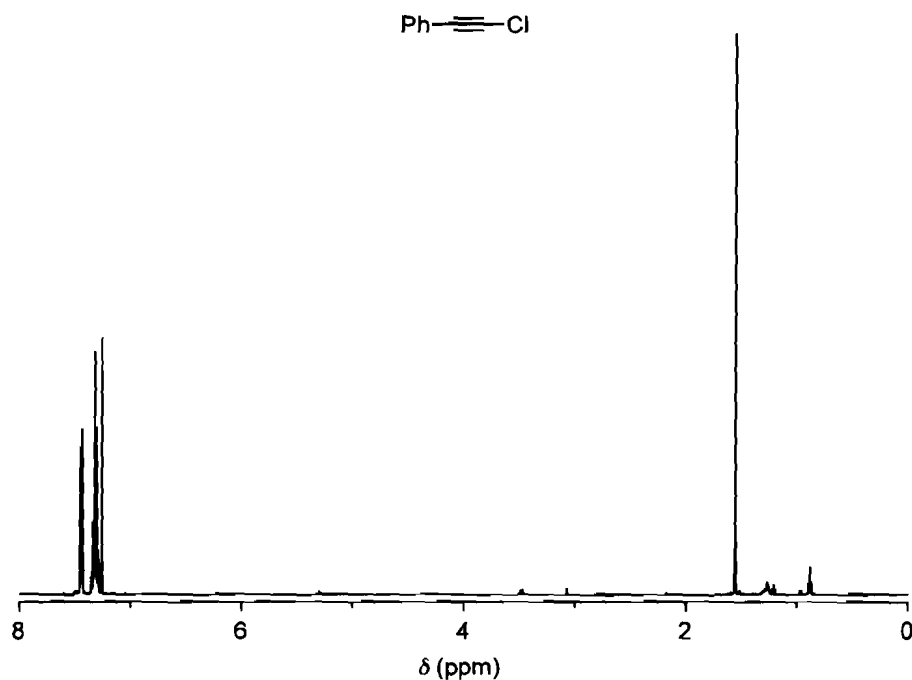


Figure 6.5.2 ^1H NMR (400 MHz) spectrum of 1-(2-chloroethynyl)benzene in CDCl_3 .



Synthesis of 1-(2-bromoethynyl)benzene.¹⁰² A solution of NaOBr was prepared by mixing a solution of NaOH (5.9 g, 150 mmol) in H_2O (25 mL) with Br_2 (4.7 g, 29 mmol) at 0 °C. To this solution was added phenylacetylene (5.0 g, 49 mmol) dropwise at 0 °C and after the addition, the reaction mixture was allowed to warm and was stirred at 25 °C for 4 h. Then the reaction mixture was extracted with Et_2O (3 \times 50 mL) and the organic layer was dried with Na_2SO_4 and evaporated to dryness *in vacuo*. Purification by flash chromatography (SiO_2 , hexanes) yielded 4.2 g of 1-(2-bromoethynyl)benzene as an orange-yellow oil. (44 %). ^1H NMR (CDCl_3 , 400 MHz) δ 7.45 (dd, $J = 8, 2$ Hz, 2H), 7.30-7.34 (m, 3H).

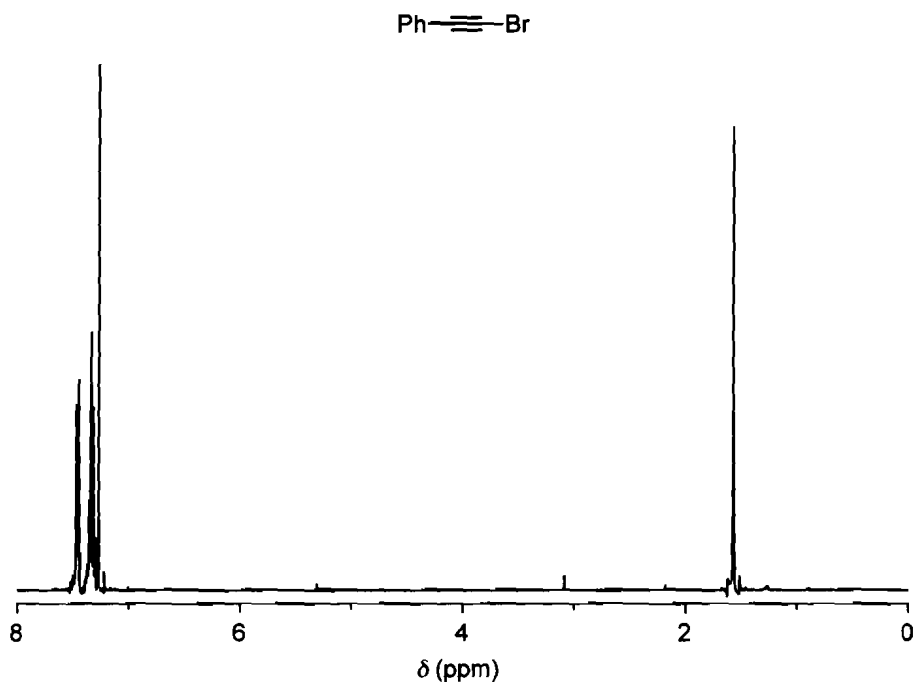
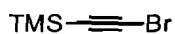


Figure 6.5.3 ^1H NMR (400 MHz) spectrum of 1-(2-bromoethynyl)benzene in CDCl_3 .



Synthesis of 1-(2-bromoethynyl)trimethylsilane.¹⁰² To a solution of trimethylsilylacetylene (15.0 g, 153 mmol) in acetone (200 mL) was added N-bromosuccinimide (NBS) (27.0 g, 152 mmol) and AgNO_3 (2.4 g, 14 mmol) and the mixture was stirred at 25 °C for 18 h. Purification by distillation at 760 mmHg yielded 5.7 g of 1-(2-bromoethynyl)trimethylsilane (21%). B.p. = 760 mmHg, 110–115 °C. ^1H NMR (CDCl_3 , 400 MHz) δ 0.19 (s, 9H). ^{13}C NMR (CDCl_3 , 100 MHz) δ 87.0, 61.4, -0.26.

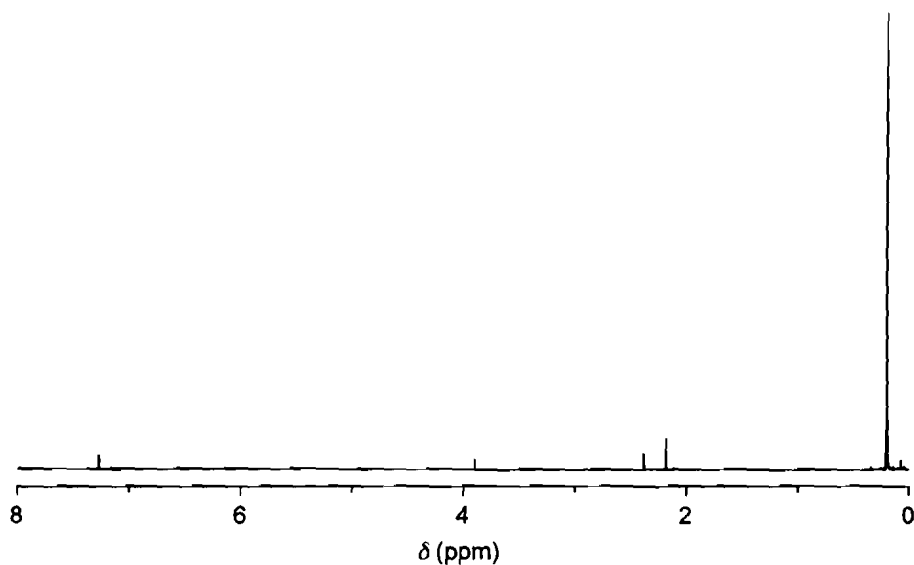
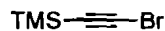
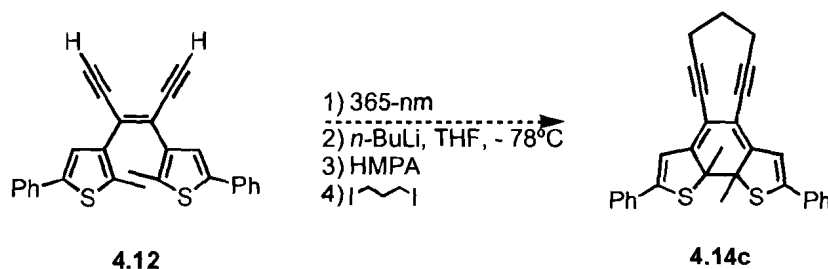


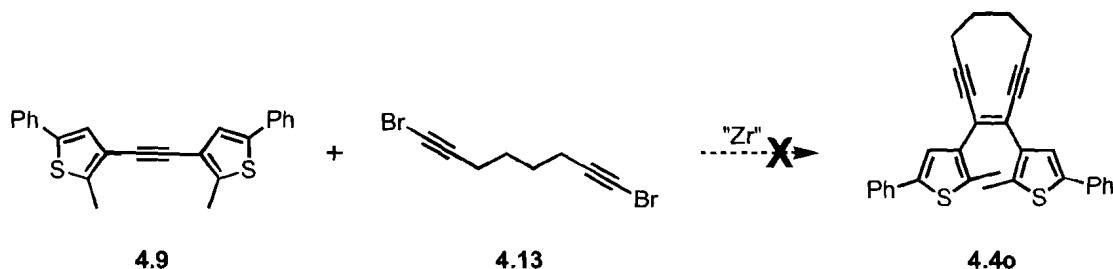
Figure 6.5.4 ^1H NMR (400 MHz) spectrum of 1-(2-bromoethynyl)trimethylsilane in CDCl_3 .

6.5.1 Future work experiments from Chapter 4

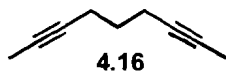


Attempted synthesis of compound 4.14c. A solution of compound **4.12** (0.20 mmol) in anhydrous THF (25 mL) was irradiated with 365-nm light for 1 h, at which point it was treated dropwise with *n*-butyllithium (0.20 mL, 2.5 M in hexanes, 0.51 mmol) over a 5-min period at -78°C under an N_2 atmosphere. After stirring at this temperature for 30 min, HMPA (1 mL) was added and the resulting suspension was stirred for 30 min, at which time 1,4-diiopropane (18 μL , 0.15 mmol) was added dropwise. The cooling bath and the reaction was allowed to slowly warm to room temperature and the reaction was stirred there for 16 h.

The crude reaction mixture was evaporated to dryness *in vacuo*. Purification by flash chromatography (SiO₂, 10% CH₂Cl₂ in hexanes) afforded only starting material **4.12**. Crude ¹H NMR did not indicate the presence of any product formation. The major peaks were attributed to the starting material. Purification by flash chromatography did not yield a measurable amount of photochromic product.



Attempted synthesis of compound 4.4o using compound 4.13. A solution of Cp₂ZrCl₂ (494 mg, 1.69 mmol) in THF (12.5 mL) was treated with EtMgCl (1.7 mL, 2.0 M THF solution, 3.4 mmol) at -78 °C. The reaction mixture was stirred for 1 h at the same temperature, at which time, compound **4.9** (500 mg, 1.4 mmol) was added. After warming to 0 °C and stirring at this temperature for 90 min, compound **4.13** (356 mg, 1.4 mmol) was added. The reaction was allowed to warm to room temperature and stirred there for 30 min followed by heating at 50 °C for 2 h. The reaction mixture was treated CuCl (13 mg, 0.13 mmol) stirred at 50 °C for 18 h. The reaction mixture was evaporated to dryness *in vacuo* and a crude ¹H NMR did not indicate the presence of compound **4.4o**. The major peaks were attributed to the starting materials. Purification by flash chromatography did not yield a measurable amount of a photochromic product.



Synthesis 2,7-nonadiyne (4.16).¹⁰³ A solution of 1,6-heptadiyne (1.0 g, 10.2 mmol) in anhydrous THF (50 mL) was treated dropwise with *n*-butyllithium (9.0 mL, 2.5 M in hexanes, 22.4 mmol) over a 5-min period at -78 °C under an N_2 atmosphere. After stirring at this temperature for 30 min, methyl iodide (MeI) (1.40 mL, 22.4 mmol) was added dropwise. The cooling bath and the reaction was allowed to slowly warm to room temperature and the reaction was stirred there for 16 h. The crude reaction mixture was evaporated to dryness *in vacuo*. Purification by flash chromatography (SiO_2 , 25% CH_2Cl_2 in hexanes) afforded 1.0 g (82%) of compound **4.16**. 1H NMR ($CDCl_3$, 500 MHz) δ 2.22-2.27 (m, 4H), 1.79 (t, $J = 2.5$ Hz, 6H), 1.62-1.68 (m, 2H).

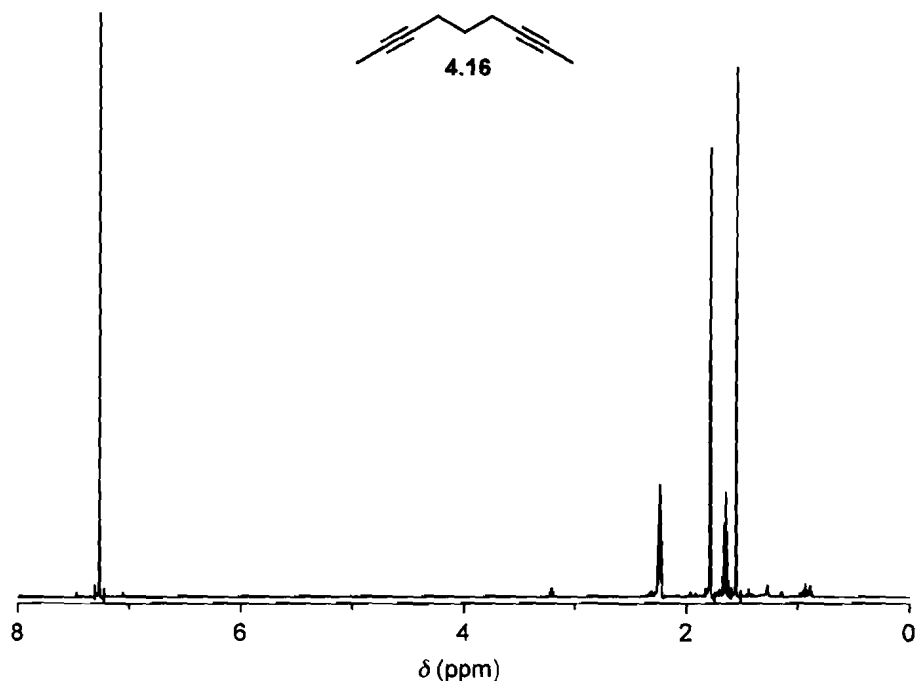
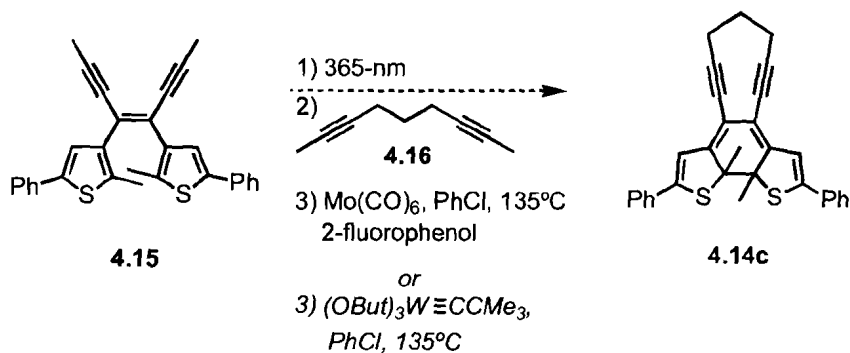


Figure 6.5.5 ^1H NMR (500 MHz) spectrum of compound **4.16** in CDCl_3 .



Attempted alkyne metathesis of compound 4.14c with $\text{Mo}(\text{CO})_6$. A solution of compound **4.15** (50 mg, 0.11 mmol) in benzene (250 mL) was irradiated with 365-nm light for 90 min, at which point the solvent was evaporated *in vacuo*. The crude compound **4.15** was taken up in chlorobenzene (PhCl) to which compound **4.16** (13 mg, 0.11 mmol) and 2-fluorophenol (12.5 mg, 0.11 mmol) were added. Molybdenum carbonyl ($\text{Mo}(\text{CO})_6$) (2.9 mg, 0.01 mmol) was added to the mixture which was then heated to reflux (135 °C) under a N_2 atmosphere for 14 h. Crude ^1H NMR analysis of the crude reaction mixture indicated that no major product

was formed. The major peaks were attributed to the starting material. Purification by flash chromatography did not yield a measurable amount of photochromic product.

Attempted alkyne metathesis with $(OtBu)_3W=CMe_3$. A solution of compound **4.15** (50 mg, 0.11 mmol) in benzene (250 mL) was irradiated with 365-nm light for 90 min, at which point the solvent was evaporated *in vacuo*. The crude compound **4.15** was taken up in chlorobenzene (PhCl) to which compound **4.16** (13 mg, 0.11 mmol) and 2-fluorophenol (12.5 mg, 0.11 mmol) were added. Shrock's alkyne metathesis catalyst $(OtBu)_3W\equiv CMe_3$ (4.2 mg, 0.01 mmol) was added to the mixture which was then heated to reflux (135 °C) under a N_2 atmosphere for 14 h. Crude 1H NMR analysis of the crude reaction mixture indicated that no major product was formed. The major peaks were attributed to the starting material. Purification by flash chromatography did not yield a measurable amount of photochromic product.

Reference List

1. *Essentials of Molecular Photochemistry*, Gilbert, A.; Baggott, J. ed.; CRC Press: Boca Raton, 1991.
2. *Photochromism: Molecules and Systems*, Durr, H.; Bouas-Laurent, H. eds.; Elsevier Science B. V.: Amsterdam, 2003.
3. *Organic Photochromic and Thermochromic Compounds*, Crano, J. C.; Guglielmetti, R. J. eds.; Plenum Press: New York, 1999; Vol. 1.
4. *Molecular Switches*, Feringa, B. L. ed; Wiley-VCH: Weinheim, 2001.
5. Ueno, A.; Takahashi, K.; Osa, T. *J. Chem. Soc. Chem. Commun.* **1980**, 837.
6. Ueno, A.; Takahashi, K.; Osa, T. *J. Chem. Soc. Chem. Commun.* **1981**, 94.
7. Würthner, F.; Rebek, J. *J. Chem. Soc. Perkin Trans. 2* **1995**, 1727.
8. Würthner, F.; Rebek, J. *Angew. Chem. Int. Edit.* **1995**, 34, 446.
9. Cacciapaglia, R.; Di Stefano, S.; Mandolini, L. *J. Am. Chem. Soc.* **2003**, 125, 2224.
10. Rau, H. in *Photochromism: Molecules and Systems*, Durr, H.; Bouas-Laurent, H. eds.; Elsevier Science B. V.: Amsterdam, 2003; pp 165-192.
11. Irie, M. in *Molecular Switches*, Feringa, B. L. ed; Wiley-VCH: Weinheim, 2001; pp 37-60.
12. Irie, M. in *Organic Photochromic and Thermochromic Compounds*, Crano, J. C.; Guglielmetti, R. J. eds.; Plenum Press: New York, 1999; Vol. 1, pp 207-221.
13. Irie, M. *Chem. Rev.* **2000**, 100, 1685.
14. Kawai, S. H.; Gilat, S. L.; Ponsinet, R.; Lehn, J. M. *Chem. Eur. J.* **1995**, 1, 285.
15. Tian, H.; Yang, S. *J. Chem. Soc. Rev.* **2004**, 33, 85.
16. Yokoyama, Y.; Kose, M. *J. Photochem. Photobiol. A Chem.* **2004**, 166, 9.
17. Irie, M.; Miyatake, O.; Uchida, K.; Eriguchi, T. *J. Am. Chem. Soc.* **1994**, 116, 9894.
18. Morimoto, M.; Irie, M. *Chem. Commun.* **2005**, 3895.

19. Takeshita, M.; Uchida, K.; Irie, M. *Chem. Commun.* **1996**, 1807.
20. Takeshita, M.; Irie, M. *J. Org. Chem.* **1998**, 63, 6643.
21. Kawai, S. H.; Gilat, S. L.; Lehn, J. M. *Eur. J. Org. Chem.* **1999**, 2359.
22. Odo, Y.; Matsuda, K.; Irie, M. *Chem. Eur. J.* **2006**, 12, 4283.
23. Samachetty, H. D.; Branda, N. R. *Chem. Commun.* **2005**, 2840.
24. Samachetty, H. D.; Branda, N. R. *Pure Appl. Chem.* **2006**, 78, 2351.
25. Lemieux, V.; Gauthier, S.; Branda, N. R. *Angew. Chem. Int. Edit.* **2006**, 45, 6820.
26. Murguly, E.; Norsten, T. B.; Branda, N. R. *Angew. Chem. Int. Edit.* **2001**, 40, 1752.
27. McManus, H. A.; Guiry, P. J. *Chem. Rev.* **2004**, 104, 4151.
28. Lowenthal, R. E.; Abiko, A.; Masamune, S. *Tetrahedron Lett.* **1990**, 31, 6005.
29. Muller, D.; Umbricht, G.; Weber, B.; Pfaltz, A. *Helv. Chim. Acta* **1991**, 74, 232.
30. Evans, D. A.; Woerpel, K. A.; Hinman, M. M.; Faul, M. M. *J. Am. Chem. Soc.* **1991**, 113, 726.
31. Pfaltz, A. *Acc. Chem. Res.* **1993**, 26, 339.
32. Bedekar, A. V.; Koroleva, E. B.; Andersson, P. G. *J. Org. Chem.* **1997**, 62, 2518.
33. Norsten, T. B., performed preliminary experiments where the obtained stereoselectivities could not be reproduced and were within the error range of the detector.
34. Norsten, T. B., *Methods to Control Molecular Structure and Function in Supramolecular Chemistry*, Ph.D. Thesis, University of Alberta, Edmonton, **2001**.
35. Lucas, L. N.; van Esch, J.; Kellogg, R. M.; Feringa, B. L. *Tetrahedron Lett.* **1999**, 40, 1775.
36. Tietze, L. F.; Lohmann, J. K. *Synlett* **2002**, 2083.
37. Shepperson, I.; Quici, S.; Pozzi, G.; Nicoletti, M.; O'Hagan, D. *Eur. J. Org. Chem.* **2004**, 4545.
38. Salomon, R. G.; Kochi, J. K. *J. Am. Chem. Soc.* **1973**, 95, 3300.

39. Sud, D.; Norsten, T. B.; Branda, N. R. *Angew. Chem. Int. Edit.* **2005**, *44*, 2019.
40. Carpenter, A. J.; Chadwick, D. J. *J. Chem. Soc. Perkin Trans. 1* **1985**, 173.
41. Denmark, S. E.; Nakajima, N.; Nicaise, O. J. C.; Faucher, A. M.; Edwards, J. P. *J. Org. Chem.* **1995**, *60*, 4884.
42. Corroborated with AM1 results obtained using *SpartanTM* where there was a slight difference in the energy between the two diastereoisomers as they approached the *ring-closed* isomer.
43. *Metals and Ligand Reactivity: An Introduction to the Organic Chemistry of Metal Complexes*, Constable, E. D. ed.; VCH Publishers: New York, 1995.
44. Yam, V. W. W.; Ko, C. C.; Zhu, N. Y. *J. Am. Chem. Soc.* **2004**, *126*, 12734.
45. Qin, B.; Yao, R. X.; Tian, H. *Inorg. Chim. Acta* **2004**, *357*, 3382.
46. Matsuda, K.; Takayama, K.; Irie, M. *Inorg. Chem.* **2004**, *43*, 482.
47. Matsuda, K.; Shinkai, Y.; Irie, M. *Inorg. Chem.* **2004**, *43*, 3774.
48. Jukes, R. T. F.; Adamo, V.; Hartl, F.; Belser, P.; De Cola, L. *Inorg. Chem.* **2004**, *43*, 2779.
49. Tian, H.; Qin, B.; Yao, R. X.; Zhao, X. L.; Yang, S. J. *Adv. Mater.* **2003**, *15*, 2104.
50. Qin, B.; Yao, R. X.; Zhao, X. L.; Tian, H. *Org. Biomol. Chem.* **2003**, *1*, 2187.
51. Fraysse, S.; Coudret, C.; Launay, J. P. *Eur. J. Inorg. Chem.* **2000**, 1581.
52. Dias, P. B.; Depiedade, M. E. M.; Simoes, J. A. M. *Coord. Chem. Rev.* **1994**, *135*, 737.
53. van Leeuwen, P.; Kamer, P. C. J.; Reek, J. N. H. *Pure Appl. Chem.* **1999**, *71*, 1443.
54. Freixa, Z.; van Leeuwen, P. *Dalton Trans.* **2003**, 1890.
55. Valentine, D. H.; Hillhouse, J. H. *Synthesis* **2003**, 317.
56. Valentine, D. H.; Hillhouse, J. H. *Synthesis* **2003**, 2437.
57. Field, J. S.; Haines, R. J.; Lakoba, E. I.; Sosabowski, M. H. *J. Chem. Soc. Perkin Trans. 1* **2001**, 3352.
58. Clot, O.; Akahori, Y.; Moorlag, C.; Leznoff, D. B.; Wolf, M. O.; Batchelor, R. J.; Patrick, B. O.; Ishii, M. *Inorg. Chem.* **2003**, *42*, 2704.
59. Chevykalova, M. N.; Manzhukova, L. F.; Artemova, N. V.; Luzikov, Y. N.; Nifant'ev, I. E.; Nifant'ev, E. E. *Russ. Chem. Bull.* **2003**, *52*, 78.

60. Kobatake, S.; Uchida, K.; Tsuchida, E.; Irie, M. *Chem. Commun.* **2002**, 2804.
61. Allen, D. W.; Taylor, B. F. *J. Chem. Soc. Dalton Trans.* **1982**, 51.
62. Lemieux, V.; Branda, N. R. *Org. Lett.* **2005**, 7, 2969.
63. Hendrickson, J. B.; Hussoin, M. S. *J. Org. Chem.* **1989**, 54, 1144.
64. Hendrickson, J. B.; Hussoin, M. S. *J. Org. Chem.* **1987**, 52, 4137.
65. Elson, K. E.; Jenkins, I. D.; Loughlin, W. A. *Org. Biomol. Chem.* **2003**, 1, 2958.
66. Elson, K. E.; Jenkins, I. D.; Loughlin, W. A. *Aust. J. Chem.* **2004**, 57, 371.
67. *Dynamic Studies in Biology: Phototriggers, Photoswitches and Caged Biomolecules*, Goeldner, M.; Givens, R. eds.; Wiley-VCH Verlag GmbH & Co. KGaA: Weinheim, 2005.
68. Jones, R. R.; Bergman, R. G. *J. Am. Chem. Soc.* **1972**, 94, 660.
69. Bergman, R. G. *Accounts Chem. Res.* **1973**, 6, 25.
70. Smith, A. L.; Nicolaou, K. C. *J. Med. Chem.* **1996**, 39, 2103.
71. Nicolaou, K. C.; Dai, W. M. *Angew. Chem. Int. Edit.* **1991**, 30, 1387.
72. Prall, M.; Wittkopp, A.; Fokin, A. A.; Schreiner, P. R. *J. Comput. Chem.* **2001**, 22, 1605.
73. Schreiner, P. R. *J. Am. Chem. Soc.* **1998**, 120, 4184.
74. Jones, G. B.; Plourde, G. W.; Wright, J. M. *Org. Lett.* **2000**, 2, 811.
75. Kar, M.; Basak, A.; Bhattacharjee, M. *Bioorg. Med. Chem. Lett.* **2005**, 15, 5392.
76. Karpov, G. V.; Popik, V. V. *J. Am. Chem. Soc.* **2007**, 129, 3792.
77. Basak, A.; Bdour, H. M.; Shain, J. C.; Mandal, S.; Rudra, K. R.; Nag, S. *Bioorg. Med. Chem. Lett.* **2000**, 10, 1321.
78. Nuss, J. M.; Murphy, M. M. *Tetrahedron Lett.* **1994**, 35, 37.
79. Tachi, Y.; Dai, W. M.; Tanabe, K.; Nishimoto, S. I. *Bioorg. Med. Chem.* **2006**, 14, 3199.
80. Poloukhine, A.; Popik, V. V. *Chem. Commun.* **2005**, 617.
81. Poloukhine, A.; Popik, V. V. *J. Org. Chem.* **2006**, 71, 7417.
82. Wilson, B. C.; Jeeves, W. P.; Lowe, D. M. *Photochem. Photobiol.* **1985**, 42, 153.

83. Henderson, B. W.; Dougherty, T. J. *Photochem. Photobiol.* **1992**, *55*, 145.
84. Dore, T. M. in *Dynamic Studies in Biology: Phototriggers, Photoswitches and Caged Biomolecules*, Goeldner, M.; Givens, R. eds.; Wiley-VCH Verlag CmbH & Co. KGaA: Weinheim, 2005, pp 435-460.
85. Hopt, A.; Neher, E. *Biophys. J.* **2001**, *80*, 2029.
86. Liu, Y. H.; Zhong, Z. Q.; Nakajima, K.; Takahashi, T. *J. Org. Chem.* **2002**, *67*, 7451.
87. Irie, M.; Lifka, T.; Kobatake, S.; Kato, N. *J. Am. Chem. Soc.* **2000**, *122*, 4871.
88. Irie, M.; Lifka, T.; Uchida, K.; Kobatake, S.; Shindo, Y. *Chem. Commun.* **1999**, 747.
89. Peters, A.; Branda, N. R. *Adv. Mater. Opt. Electron.* **2000**, *10*, 245.
90. Basak, A.; Mandal, S.; Bag, S. S. *Chem. Rev.* **2003**, *103*, 4077.
91. Rawat, D. S.; Zaleski, J. M. *Synlett* **2004**, 393.
92. Zeidan, T. A.; Kovalenko, S. V.; Manoharan, M.; Alabugin, I. V. *J. Org. Chem.* **2006**, *71*, 962.
93. Jones, G. B.; Wright, J. M.; Plourde, G. W.; Hynd, G.; Huber, R. S.; Mathews, J. E. *J. Am. Chem. Soc.* **2000**, *122*, 1937.
94. Fürstner, A.; Davies, P. W. *Chem. Commun.* **2005**, 2307.
95. Sashuk, V.; Ignatowska, J.; Grela, K. *J. Org. Chem.* **2004**, *69*, 7748.
96. Schrock, R. R. *Accounts Chem. Res.* **1986**, *19*, 342.
97. Kloppenburg, L.; Song, D.; Bunz, U. H. F. *J. Am. Chem. Soc.* **1998**, *120*, 7973.
98. Fürstner, A.; Mathes, C.; Lehmann, C. W. *Chem. Eur. J.* **2001**, *7*, 5299.
99. Jones, G. B.; Fouad, F. S. *Curr. Pharm. Design* **2002**, *8*, 2415.
100. Myles, A. J.; Branda, N. R. *Macromolecules* **2003**, *36*, 298.
101. Aldrich - Handbook of Fine Chemicals.
102. Jiang, M. X. W.; Rawat, M.; Wulff, W. D. *J. Am. Chem. Soc.* **2004**, *126*, 5970.
103. Han, Y.; Harlan, C. J.; Stoessel, P.; Frost, B. J.; Norton, J. R.; Miller, S.; Bridgewater, B.; Xu, Q. *Inorg. Chem.* **2001**, *40*, 2942.